Vibration of Rectangular and Skew Cantilever Plates

By M. V. BARTON,[1] AUSTIN, TEXAS

The Ritz method is used to determine approximate solutions for the frequencies and modes of vibration of uniform rectangular and skew cantilever plates. The functions used to represent the plate deflection correspond to those which define the normal modes of vibration of a uniform beam. Solutions are obtained for (*a*) uniform rectangular cantilever plates with cantilever span-to-breadth ratios of 1/2, 1, 2, and 5; (*b*) uniform skew cantilever plates with sides of equal length and skew angles of 15 deg, 30 deg, and 45 deg. Experimental values are presented and the correlation with analytical results discussed.

Nomenclature

The following nomenclature is used in the paper:

V = elastic strain energy of bending of a plate (in-lb)
T = kinetic energy of a plate (in-lb)
E = modulus of elasticity, psi
μ = Poisson's ratio
h = thickness of plate, in.
a, b = lateral dimensions of plate, in.
$D = Eh^3/12(1 - \mu^2)$ = bending stiffness of plate (lb-in.)
w = lateral deflection of plate, in.
x, y = rectangular co-ordinates
ξ, η = skew co-ordinates
θ = angle of skew
ρ = mass density of plate material, (lb sec^2/in.^{4})
f = frequency, cycles per second (cps)
$\omega = 2\pi f$ = angular frequency (radians per sec)
$\lambda = \omega^2 \rho h \frac{a^4 b}{D} \cos^4\theta$ = characteristic value
m, n; i, k; p, q = positive integers
A_{mn} = coefficient used in series representing deflections
ϕ_m = characteristic function for vibrating beam with one end fixed and one end free
ψ_n = characteristic function for vibrating beam with both ends free
β_m, γ_n; α_m, δ_n = parameters used in expressions for ϕ_m and ψ_n
E_{mi}, F_{nk}; H_{mi}, K_{nk}; L_{mi}, M_{nk}; P_{mi}, Q_{nk} = integrals defined by Equations [6]

Introduction

Exact solutions of the differential equation of a vibrating plate are known for the case of a rectangular plate simply supported at all edges and for a rectangular plate with two opposite edges simply supported and with any conditions at the other two edges (1, 2).[2] Approximate solutions have been obtained for plates with other edge conditions. The Ritz method (3), which, in effect, substitutes a variational problem for the usual characteristic value problem, has been used by Ritz to obtain the approximate solution for the frequencies and modes for a square plate with all four edges free. Recently, Young (4) applied this method to (*a*) a square plate clamped at all four edges, (*b*) a square plate clamped at two adjacent edges and free at the other two edges, and (*c*) a square plate clamped at one edge and free at the other three edges. Among other methods, Fung (5) uses the Ritz method to investigate the stresses and deflections of skew cantilever plates caused by lateral static loads. Approximate solutions have also been obtained for the frequencies and modes of a square cantilever plate by means of a set of finite-difference equations which are used in place of the Lagrange differential equation for the plate (6, 7). In this method it is necessary to solve a set of many simultaneous equations so that relaxation procedures or the use of an electric-analog computer (8) is sometimes advantageous.

The Ritz method is used in the present study of the frequencies and modes of vibration of cantilever plates. This study includes the results of the square cantilever plate made by Young and extends the investigation to rectangular cantilever plates with cantilever span to breadth ratios of 1/2, 2, and 5. In addition, a study is made of skew cantilever plates with sides of equal length and skew angles of 15 deg, 30 deg, and 45 deg.

The equations to be solved for the vibration of the uniform plates are set up in terms of oblique co-ordinates. The amount of computational labor is somewhat dependent upon the type of functions used to represent the plate deflections. The functions used in this study are combinations of the characteristic functions which define the normal modes of vibration of a uniform beam with one end fixed and the other end free, and for a uniform beam with both ends free.

Spot checks have been obtained experimentally for the frequencies of vibration and the nodal patterns of the uniform cantilever plates.

It should be emphasized that the analyses presented are for homogeneous elastic plates of uniform thickness corresponding to the ordinary theory of thin plates.

Ritz's Method

The maximum potential energy and kinetic energy for a uniform skew plate vibrating harmonically with amplitude $w(\xi, \eta)$ and

[1] Professor of Aeronautical Engineering, Research Engineer, Defense Research Laboratory, The University of Texas. Mem. ASME.

Contributed by the Applied Mechanics Division and presented at the Annual Meeting, New York, N. Y., November 26–December 1, 1950, of The American Society of Mechanical Engineers.

Discussion of this paper should be addressed to the Secretary, ASME, 29 West 39th Street, New York, N. Y., and will be accepted until July 10, 1951, for publication at a later date. Discussion received after the closing date will be returned.

Note: Statements and opinions advanced in papers are to be understood as individual expressions of their authors and not those of the Society. Manuscript received by the Applied Mechanics Division, March 16, 1950. Paper No. 50—A-12.

[2] Numbers in parentheses refer to the Bibliography at the end of the paper.

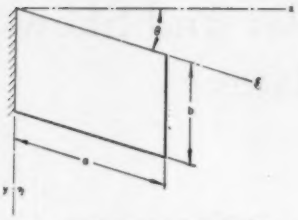

FIG. 1 CO-ORDINATE SYSTEM FOR PLATE

angular frequency ω in terms of the oblique co-ordinates indicated in Fig. 1, are

$$\left.\begin{aligned} V &= \frac{D}{2\cos\theta}\int\int\left\{\frac{1}{\cos^2\theta}\left[\frac{\partial^2 w}{\partial\xi^2} - 2\sin\theta\,\frac{\partial^2 w}{\partial\xi\partial\eta} + \frac{\partial^2 w}{\partial\eta^2}\right]^2 - 2(1-\mu)\left[\frac{\partial^2 w}{\partial\xi^2}\,\frac{\partial^2 w}{\partial\eta^2} - \left(\frac{\partial^2 w}{\partial\xi\partial\eta}\right)^2\right]\right\} d\xi d\eta \\ T &= \frac{1}{2}\rho h\,\omega^2\cos\theta\int\int w^2\,d\xi\,d\eta \end{aligned}\right\} \quad \ldots [1]$$

Equating the two energies, we have

$$\omega^2 = \frac{2}{\rho h\cos\theta}\,\frac{V}{\int\int w^2 d\xi\,d\eta} \quad \ldots [2]$$

The Ritz method consists of assuming a series of functions to represent the deflection w in which the coefficients of the series are adjusted to minimize Equation [2].

The functions chosen to represent the deflection will consist of two types, one to represent the variations in the ξ-direction and the other in the η-direction. Thus

$$w(\xi,\eta) = \sum_{m=1}^{p}\sum_{n=1}^{q} A_{mn}\phi_m(\xi)\,\psi_n(\eta) \quad \ldots [3]$$

The functions used are those corresponding to the characteristic functions for the normal modes of vibration of a beam fixed at one end and free at the other, and for a beam free at both ends. The use of these functions satisfies the conditions that the slope and deflection at one edge of the plate are zero, but since the functions correspond only to free end conditions for a beam, namely, $(d^2\phi)/(d\xi^2) = (d^3\phi)/(d\xi^3) = 0$ at one end and $(d^2\psi)/(d\eta^2) = (d^3\psi)/(d\eta^3) = 0$ at both ends, the plate boundary conditions for the three free edges are not satisfied.

The characteristic functions used are clamped-free

$$\left.\begin{aligned} \phi_m &= \cosh\beta_m\xi/a - \cos\beta_m\xi/a - \alpha_m(\sinh\beta_m\xi/a - \sin\beta_m\xi/a) \text{ for } m = 1, 2, 3\ldots, \\ &\text{and free-free} \\ \psi_1 &= 1 \\ \psi_2 &= \sqrt{3}(1 - 2\eta/b) \\ \psi_n &= \cosh\gamma_n\eta/b + \cos\gamma_n\eta/b - \delta_n(\sinh\gamma_n\eta/b + \sin\gamma_n\eta/b) \quad \text{for } n = 3, 4, 5\ldots \end{aligned}\right\} \quad \ldots [4]$$

The functions and their derivatives have been tabulated by Young and Felgar (10)

Substitution of the Functions [4] into Equation [2] and minimizing results in the following equation when the orthogonal properties of the functions are taken into account

$$\begin{aligned} &A_{ik}[\beta_i{}^4 b/a + \gamma_k{}^4(a/b)^3 - \lambda] \\ &+ \sum_{m=1}^{p}\sum_{n=1}^{q} A_{mn}\{[(\sin^2\theta + \mu\cos^2\theta)(E_{mi}F_{kn} + E_{im}F_{nk}) \\ &+ 2(1 + \sin^2\theta - \mu\cos^2\theta)H_{mi}K_{nk}]\,a/b - 2\sin\theta\,[(L_{mi}M_{kn} \\ &+ L_{im}M_{nk}) + (P_{mi}Q_{kn} + P_{im}Q_{nk})(a/b)^2]\} = 0 \quad \ldots [5] \end{aligned}$$

where

$$\left.\begin{aligned} \lambda &= \omega^2\rho h\,\frac{a^3 b}{D}\cos^4\theta \\ E_{mi} &= a\int_0^a \phi_m\frac{d^2\phi_i}{d\xi^2}\,d\xi \qquad E_{im} = a\int_0^a \phi_i\frac{d^2\phi_m}{d\xi^2}\,d\xi \\ F_{nk} &= b\int_0^b \psi_n\frac{d^2\psi_k}{d\eta^2}\,d\eta \qquad F_{kn} = b\int_0^b \psi_k\frac{d^2\psi_n}{d\eta^2}\,d\eta \\ H_{mi} &= a\int_0^a \frac{d\phi_m}{d\xi}\frac{d\phi_i}{d\xi}\,d\xi \qquad K_{nk} = b\int_0^b \frac{d\psi_n}{d\eta}\frac{d\psi_k}{d\eta}\,d\eta \\ L_{mi} &= a^2\int_0^a \frac{d\phi_m}{d\xi}\frac{d^2\phi_i}{d\xi^2}\,d\xi \qquad L_{im} = a^2\int_0^a \frac{d\phi_i}{d\xi}\frac{d^2\phi_m}{d\xi^2}\,d\xi \\ M_{nk} &= \int_0^b \psi_n\frac{d\psi_k}{d\eta}\,d\eta \qquad M_{kn} = \int_0^b \psi_k\frac{d\psi_n}{d\eta}\,d\eta \\ P_{mi} &= \int_0^a \phi_m\frac{d\phi_i}{d\xi}\,d\xi \qquad P_{im} = \int_0^a \phi_i\frac{d\phi_m}{d\xi}\,d\xi \\ Q_{nk} &= b^2\int_0^b \frac{d\psi_n}{d\eta}\frac{d^3\psi_k}{d\eta^3}\,d\eta \qquad Q_{kn} = b^3\int_0^b \frac{d\psi_k}{d\eta}\frac{d^3\psi_n}{d\eta^3}\,d\eta \end{aligned}\right\} \quad \ldots [6]$$

The values for the integrals, Equations [6], and the coefficients of Equation [5] for all the plates investigated are given in reference (11).

For each of the ik-combinations up to p and q, there will be an equation of the type of Equation [5]. The resulting set of equations are solved for the characteristic values λ from the condition that the determinant of the set must be zero. Since a considerable number of terms of the deflection series (up to eighteen) are used, an iteration procedure as indicated by Ritz (3, 4) is followed. Solving these equations determines the values of the characteristic λ's and the coefficients A_{mn} of the deflection series, so that the natural vibration frequencies of the plate and the modal configurations can be determined.

EVALUATIONS

Numerical evaluations have been made by the use of Equation [5] for the natural frequencies of vibration and the normal modes of several rectangular cantilever plates with various length-to-breadth ratios and for several skew cantilever plates with different angles of skew. In all cases a Poisson's ratio μ of 0.3 is used.

For the case of the rectangular plates $\theta = 0$ and evaluations have been made for cantilever span-to-breadth ratios of $a/b = 1/2, 1, 2$, and 5. An eighteen-term series for the deflection is used so that a set of eighteen equations for each a/b ratio result from substitution into Equation [5]. These equations have been solved by an iteration process for the frequencies and relative magnitude of the amplitude coefficients A_{mn} for the first three symmetrical modes and for the first two antisymmetrical modes. These values are given in Table 1.

The shape of each mode of vibration may be calculated from Equation [3] when the values of A_{mn} and the ϕ and ψ functions

TABLE 1 FREQUENCIES AND MODES OF VIBRATION OF RECTANGULAR CANTILEVER PLATE $\mu = 0.3$

First Mode

a/b	1/2	1	2	5
$\omega/\sqrt{D/\rho h a^4}$	3.508	3.494	3.472	3.450
A_{11}	1.0000	1.0000	1.0000	1.0000
A_{13}	-0.0151	-0.0089	-0.0029	-0.0004
A_{14}	-0.0028	-0.0008	-0.0002	0.0000
A_{22}	-0.0011	-0.0026	-0.0040	-0.0048
A_{23}	-0.0040	-0.0050	-0.0032	-0.0008
A_{25}	-0.0023	-0.0011	-0.0004	-0.0001
A_{31}	0.0001	+0.0001	-0.0003	-0.0010
A_{33}	-0.0005	-0.0014	-0.0015	-0.0005
A_{35}	-0.0008	-0.0006	-0.0003	-0.0001

Second Mode

a/b	1/2	1	2	5
$\omega/\sqrt{D/\rho h a^4}$	5.372	8.547	14.93	34.73
A_{12}	1.0000	1.0000	1.0000	1.0000
A_{14}	-0.0509	-0.0134	-0.0027	-0.0004
A_{16}	-0.0056	-0.0011	-0.0001	0.0000
A_{22}	0.0436	0.1212	0.2040	0.2555
A_{24}	0.0045	0.0044	0.0011	0.0001
A_{26}	0.0007	0.0006	0.0002	0.0000
A_{32}	-0.0012	-0.0020	0.0059	0.0235
A_{34}	-0.0014	-0.0013	-0.0005	-0.0001
A_{36}	-0.0010	-0.0006	-0.0002	0.0000

TABLE 1 (*continued*)

Third Mode

a/b	1/2	1	2	5
$\omega/\sqrt{D/\rho h a^4}$	21.96	21.44	21.61	21.52
A_{11}	0.0008	0.0053	0.0042	0.0048
A_{13}	-0.0465	0.2732	0.0346	0.0054
A_{15}	0.0725	0.0092	0.0029	0.0004
A_{21}	1.0000	1.0000	1.0000	1.0000
A_{23}	0.0271	0.0713	0.0206	0.0050
A_{25}	0.0196	0.0099	0.0024	0.0005
A_{31}	-0.0011	-0.0118	-0.0058	-0.0068
A_{33}	0.0001	0.0090	0.0010	-0.0009
A_{35}	0.0024	-0.0003	-0.0003	-0.0001

are known. The calculated nodal lines for five modes of the square plate where $a = b$ are shown in Table 1.

The variation of the natural frequencies with length-to-breadth ratios for the rectangular plate are given in Fig. 2. The test values which will be discussed later are shown as points on the same figure.

Evaluations are made of the first two frequencies and modes for the cantilever skew plate in which the length-to-breadth ratio is unity ($a = b$) and for angles of skew of $\theta = 15$ deg, 30 deg, and 45 deg. An eighteen-term series is again used to represent the deflection.

The values of the frequencies and the relative magnitude of the

TABLE 1 (*continued*)

Fourth Mode

a/b	1/2	1	2	5
$\omega/\sqrt{D/\rho h a^4}$	10.26	27.46	94.49	563.9
A_{11}	0.0155	0.0089	0.0034	0.0006
A_{13}	1.0000	1.0000	1.0000	1.0000
A_{15}	-0.0397	-0.0120	-0.0031	-0.0004
A_{21}	0.0459	-0.2865	-0.0389	-0.0065
A_{23}	0.1120	0.1986	0.2359	0.2469
A_{25}	0.0888	0.0099	0.0009	0.0001
A_{31}	-0.0091	-0.0451	0.1025	0.0104
A_{33}	0.0030	0.0125	0.0351	0.0381
A_{35}	-0.0018	-0.0023	-0.0003	-0.0002

Fifth Mode

a/b	1/2	1	2	5
$\omega/\sqrt{D/\rho h a^4}$	24.85	31.17	48.71	105.9
A_{12}	-0.0529	-0.1200	-0.2053	-0.2639
A_{14}	-0.1989	0.0627	0.0138	0.0016
A_{16}	0.0448	0.0081	0.0017	0.0002
A_{22}	1.0000	1.0000	1.0000	1.0000
A_{24}	-0.1069	-0.0388	-0.0168	-0.0028
A_{26}	0.0000	-0.0013	-0.0005	-0.0001
A_{32}	0.0262	0.0776	0.2222	0.3993
A_{34}	0.0003	0.0086	0.0048	0.0004
A_{36}	0.0040	0.0026	0.0012	0.0002

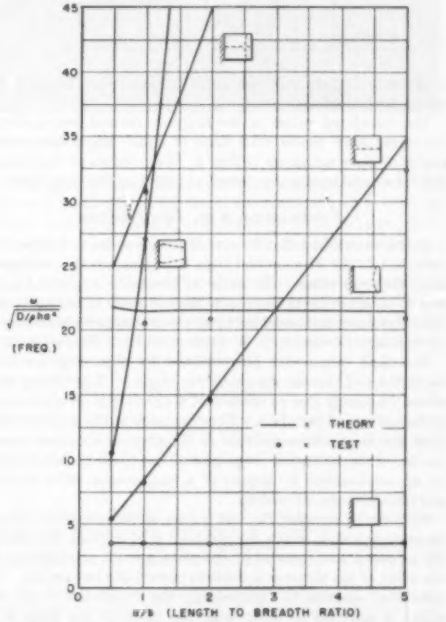

FIG. 2 FREQUENCIES OF VIBRATION OF RECTANGULAR CANTILEVER PLATES

TABLE 2 FREQUENCIES AND MODES FOR FIRST AND SECOND MODES OF VIBRATION OF SKEW CANTILEVER PLATES (a/b = 1; μ = 0.3)

ϕ	15°		30°		45°	
$\omega/b\sqrt{\rho h/D}$	3.601	8.872	3.961	10.190	4.824	13.75
A_{11}	1.0000	0.1162	1.0000	-0.2387	1.0000	0.3534
A_{12}	-0.1134	1.0000	-0.2288	1.0000	-0.3302	1.0000
A_{13}	-0.0041	-0.0721	0.0089	-0.1447	0.0231	-0.2173
A_{14}	+0.0007	-0.0145	-0.0006	+0.0179	0.0013	-0.0237
A_{15}	-0.0006	+0.0049	0.0001	-0.0093	0.0010	-0.0116
A_{21}	+0.2552	0.0862	-0.0139	0.1705	-0.0704	0.2683
A_{22}	-0.0223	0.1035	-0.0399	0.0489	-0.0488	-0.0411
A_{23}	-0.0016	-0.0184	0.0074	+0.0958	0.0197	-0.0990
A_{24}	-0.0015	0.0057	-0.0028	0.0103	-0.0038	0.0283
A_{25}	-0.0006	-0.0035	0.0002	+0.0049	0.0007	-0.0040
A_{31}	-0.0001	-0.0043	-0.0006	-0.0138	-0.0003	-0.0337
A_{32}	-0.0011	+0.0082	0.0010	-0.0254	0.0032	-0.0511
A_{33}	-0.0006	-0.0074	0.0017	+0.0048	0.0036	0.0027
A_{34}	-0.0003	-0.0005	-0.0008	0.0024	-0.0021	0.0074
A_{41}	+0.0005	0.0034	-0.0014	0.0057	-0.0021	0.0064
A_{42}	+0.0009	0.0032	-0.0010	0.0020	-0.0008	0.0046
A_{43}	-0.0001	-0.0020	0.0002	-0.0009	-0.0007	0.0039
A_{51}	0.0001	-0.0010	0.0002	-0.0026	0.0005	-0.0044
Node Lines						

coefficients A_{ms} are given in Table 2, along with diagrams indicating the nodal lines.

The calculated values of the first two natural frequencies for cantilever skew plates with sides of equal length and various angles of skew are given in Fig. 3. Test values of the frequencies for several modes are plotted as points on the same figure.

Correlation With Test Results

It is a known fact that the use of a finite series to represent the deflection in the Rits method leads to frequencies that are greater than the true values. In order to check the analytical results and to obtain some indication of the adequacy of the series used, the frequencies and nodal patterns are determined experimentally by technique devised by J. W. Dalley and E. A. Ripperger (12).

Resonant frequencies are obtained by observing the forced oscillations of the various cantilever plates. A pulsating air jet whose frequency can be controlled accurately is directed normal to the surface of the plate. The frequency of the air jet is varied until the maximum amplitude of the plate is obtained for each mode. This oscillation frequency of the plate is then recorded on an oscillograph by means of a combination of a strobotac and photoelectric cell pickup.

In order to compare the test values of the frequency with the theoretical values which do not take into account the effect of the air movement induced by the plate, a crude approximation of the effect of the air mass is made to correct the test values. This correction consists in determining the "equivalent" air mass which is assumed to move with the plate on the basis of the theory of the aerodynamic forces on an oscillating airfoil made by Theodorsen (13) and taking this equivalent air mass into ac-

TABLE 3 COMPARISON BETWEEN THEORETICAL AND TEST FREQUENCIES

ϕ	a/b	Mode	$\omega/\sqrt{D/\rho h a^4}$ Test	Corrected Test	Theoretical	Uncorrected % DIFF.	Corrected % DIFF
0	1/2	1	3.34	3.40	3.51	4.8	3.1
		2	5.38	5.43	5.37	-0.1	-0.8
		3	10.31		10.26	-0.8	
0	1	1	3.39	3.43	3.49	3.04	1.9
		2	8.26	8.32	8.55	3.32	2.7
		3	20.55		21.44	4.15	
		4	27.15		27.46	1.12	
		5	29.75		31.17	4.56	
0	2	1	3.36	3.42	3.49	3.1	1.4
		2	14.43	14.52	14.93	3.4	2.8
		3	20.86		21.26	1.9	
		4	46.90		48.71	0.5	
		5	93.99		94.49	1.7	
0	5	1	3.32	3.35	3.45	3.7	3.0
		2	20.88		21.52	3.0	
		3	32.40	32.41	34.73	6.7	6.7
		4	97.35		103.9	6.1	
15°	1	1	3.38	3.44	3.60	6.2	4.6
		2	8.63	8.68	8.87	2.7	2.1
		3	21.49				
		4	26.04				
		5	33.01				
30°	1	1	3.82	3.88	3.96	3.6	2.0
		2	9.23	9.33	10.19	9.4	8.4
		3	24.51				
		4	25.54				
		5	40.64				
45°	1	1	4.26	4.33	4.82	11.8	10.1
		2	11.07	11.21	13.75	19.5	18.5
		3	26.52				
		4	30.13				
		5	50.19				

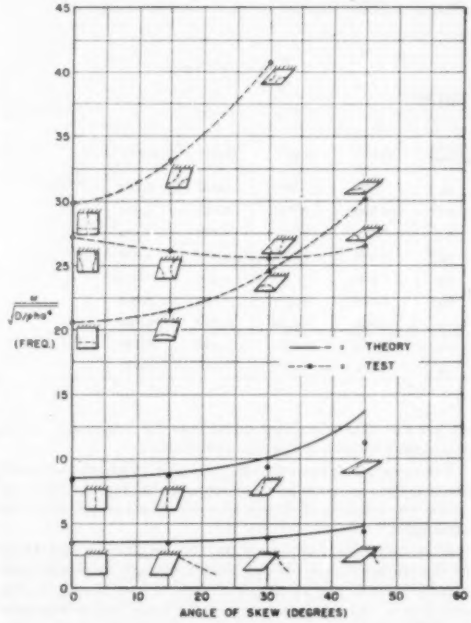

FIG. 3 FREQUENCIES OF VIBRATION OF SKEW CANTILEVER PLATES (a/b = 1)

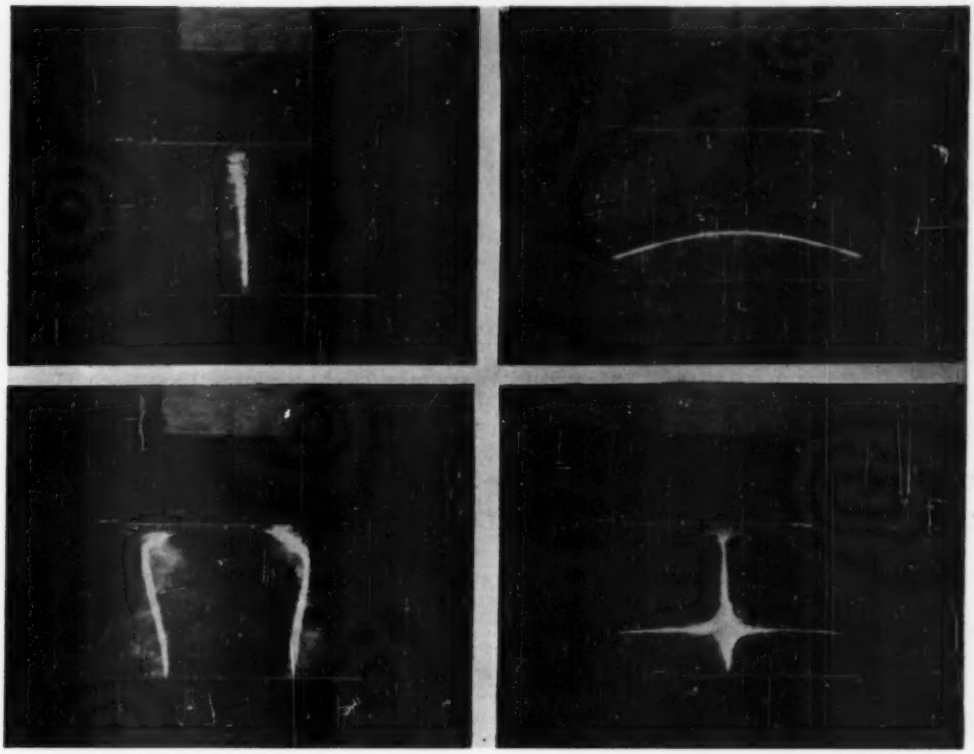

FIG. 4 NODE PATTERNS ON A SQUARE PLATE

count in adjusting the test values of the frequencies to vacuo. This type of correction has been applied only to the first and second modes of vibration.

A comparison of test and analytical frequencies is given in Table 3.

It is evident from the values given in Table 3 that, in general, the theoretical values of frequency are higher than the experimental ones as expected.

It is believed that the analytical results become less reliable as the angle of skew of the plate is increased. This trend seems to be substantiated by the test results.

The nodal lines for various modes are obtained by dusting soap powder on the plate while it is vibrating at a resonant frequency. This powder forms along the lines illustrated in Figs. 4 and 5. Fair agreement is obtained between the calculated nodal-line positions and the observed positions except for the 45-deg-skew plate.

DISCUSSION

It is apparent from this investigation that the number of terms which must be considered in the series representing the deflection increases with the number of modes to be determined and the angle of skew. The fundamental frequency for a square cantilever plate determined by the use of only the first term of the series representing the deflection is about 3 per cent higher than the frequency obtained by use of a nine-term series. On the other hand, although an eighteen-term series is used for the 45-deg-skew cantilever plate, the convergence of the iteration process is very slow, and the accuracy of the frequency obtained is very poor.

In general, it is believed that if the Ritz method is used, the series in terms of the characteristic beam functions assumed in this investigation are not suitable for practical application for the determination of first two frequencies of cantilever plates with skew angles greater than about 30 deg.

ACKNOWLEDGMENT

This work was carried out as a part of the program of the Defense Research Laboratory of The University of Texas and was sponsored by the Navy Department, Bureau of Ordnance.

BIBLIOGRAPHY

1 "Theory of Sound," by Lord Rayleigh, second American edition, Dover Publications, New York, N. Y., 1945.

2 "Vibration Problems in Engineering," by S. Timoshenko, second edition, D. Van Nostrand Company, Inc., New York, N. Y., 1937.

3 "Über eine neue Method zur Losung gewisser Varationsprobleme der Mathematische Physik," by W. Ritz, *Journal für reine und angewandte Mathematik*, vol. 135, 1909, pp. 1–61.

4 "Vibration of Rectangular Plates by the Ritz Method," by Dana Young (unpublished).

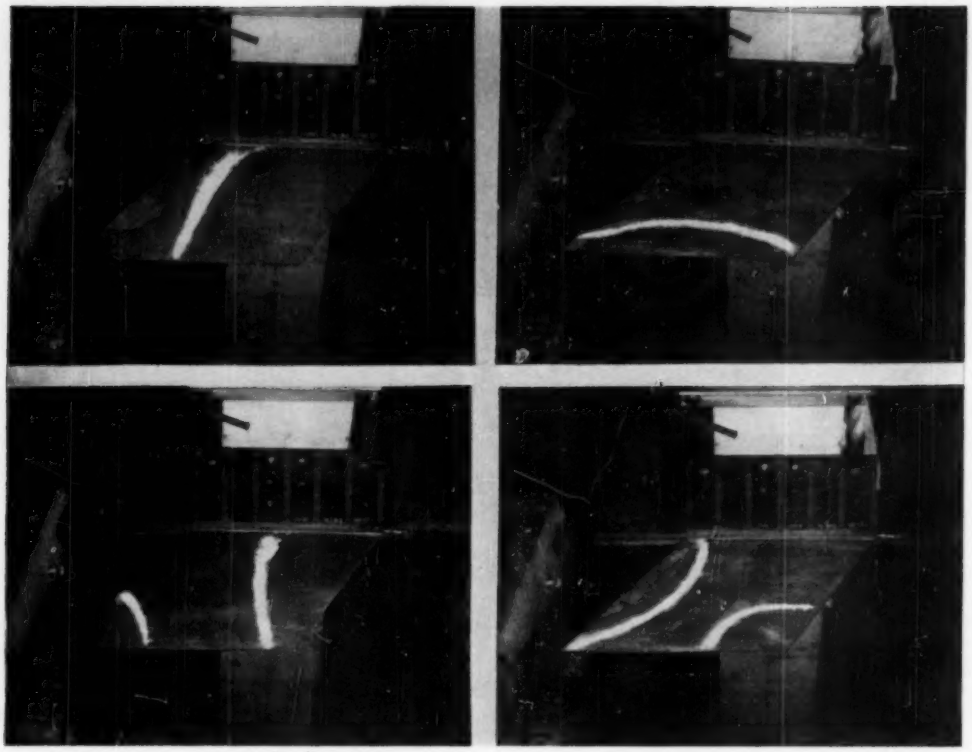

FIG. 5 NODE PATTERNS ON A 30-DEG-SKEW PLATE

5 "Theoretical and Experimental Effect of Sweep Upon the Stress and Deflection Distribution in Aircraft Wings of High Solidity. Part I—Elastostatic and Aeroelastic Problems Relating to Thin Wings of High-Speed Airplanes," by Yuan-Cheng Fung, AF Technical Report 5761, February, 1949.

6 "Finite Difference Equations for the Analysis of Thin Rectangular Plates With Combinations of Fixed and Free Edges," by M. V. Barton, Defense Research Laboratory, The University of Texas, DRL-175, CF-1005, August, 1948.

7 "Free Vibration Characteristics of Cantilever Plates," by M. V. Barton, Defense Research Laboratory, The University of Texas, DRL-212, CF-1258, May, 1949.

8 "Theoretical and Experimental Effect of Sweep Upon the Stress and Deflection Distribution in Aircraft Wings of High Solidity. Part IV—Application of the Electric Analogue Computer to the Elastic Plate Problem," by R. M. MacNeal, California Institute of Technology, Pasadena, Calif., June, 1949.

9 "Theory of Plates and Shells," by S. Timoshenko, McGraw-Hill Book Company, Inc., New York, N. Y., 1940.

10 "Table of Characteristic Functions Representing the Normal Modes of Vibration of a Beam," by Dana Young and R. P. Felgar, Jr., The University of Texas, Engineering Research Series, No. 4913, July, 1949.

11 "Vibration of Rectangular and Skew Cantilever Plates Representing Idealized Missile Fins," by M. V. Barton, Defense Research Laboratory, The University of Texas, DRL-222, CM-570, December, 1949.

12 "Experimental Values of Natural Frequencies for Skew and Rectangular Cantilever Plates," by J. W. Dalley and E. A. Ripperger, Defense Research Laboratory, The University of Texas, DRL-231, CF-1354, December, 1949.

13 "General Theory of Aerodynamic Instability and the Mechanism of Flutter," by T. Theodorsen, NACA Report 496, 1934.

Free Vibrations of a Pin-Ended Column With Constant Distance Between Pin Ends[1]

By DAVID BURGREEN,[2] BROOKLYN, N. Y.

In this paper a study is made of the free vibrations of a pin-ended column whose ends are pinned to points fixed in space. This imposes the condition of constant end distance instead of the usual theoretical assumption that the load on the column remains constant.[3] The differential equation of the system is nonlinear, and, with the assumptions that are made, is found to have an exact solution in terms of elliptic functions. Dependent upon the initial amplitude of deflection and the compressive load on the column, several types of vibrations are found to exist. The variation of frequency and wave form with the load-amplitude parameter is discussed. In particular, it is found that the frequency is dependent upon the amplitude of vibration, the effect of the amplitude of vibration becoming more pronounced as the Euler load is approached. For a column under the Euler load the classical theory gives the frequency of vibration as zero. The present theory shows that for finite amplitudes of vibration the frequency is not zero. Experimental results are presented, and a comparison of the theoretical and experimental frequencies and wave shapes is made.

Nomenclature

The following nomenclature is used in the paper:

- x = distance along column center line
- y = displacement of column center line
- t = time
- P_o = load on column when column is in straight position or $y = 0$
- P = load on column
- A = cross-sectional area
- L = length of column
- E = Young's modulus of elasticity
- a = initial amplitude of displacement of mid-point of column
- a_E = deflection of mid-point of column when column is under static Euler load
- d = depth of column
- r = radius of gyration
- I = moment of inertia
- ρ = mass density
- $P_E = \pi^2 EI/L^2$ = Euler load
- ω_o = circular frequency of vibration of a beam
- ω = circular frequency of vibration of a column under a static load P_o
- F = time function associated with the fundamental mode
- T = period of oscillation
- k^4 = amplitude parameter $= (Ea^2\pi^4)/(8\rho L^4)$
- $\beta = a/r$
- f_o = fundamental frequency of vibration of a beam in cycles per second ((cps)
- f = actual frequency of vibration of column in cycles per second (cps)
- cn = Jacobi cosine elliptic function
- dn = Jacobi delta cosine elliptic function

Introduction

The pin-ended rectangular column with pins attached to points fixed in space is shown in Fig. 1. The total shortening of the column is given by

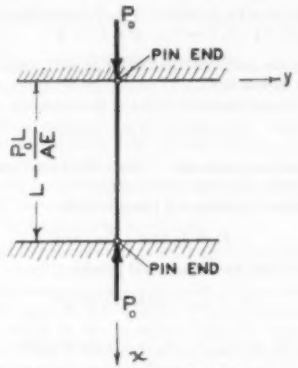

Fig. 1 Arrangement of Column

$$\Delta L = P_o L/AE = PL/AE + (1/2)\int_0^L (\partial y/\partial x)^2\, dx$$

or

$$P = P_o - (AE/2L)\int_0^L (\partial y/\partial x)^2 dx \quad \ldots\ldots [1]$$

Assume the deflected shape to be given by the half-sine wave $y = a\sin(\pi x/L)$. Setting this expression into Equation [1] gives

$$\Delta P = P_o - P = (a^2/4r^2)P_E \quad \ldots\ldots [2]$$

[1] This paper is based on a dissertation submitted in partial fulfillment of the requirements for the degree of Doctor of Philosophy in Applied Mechanics at the Polytechnic Institute of Brooklyn. The investigation was conducted as part of a project sponsored by the Office of Naval Research, U. S. Navy. After the completion of this manuscript a similar paper, entitled "The Effect of an Axial Force on the Vibration of Hinged Bars," by S. Woinowsky-Krieger was published in the March, 1950, issue of the Journal of Applied Mechanics, Trans. ASME, vol. 72, p. 35.

[2] Research Associate, Polytechnic Institute of Brooklyn. Now with Westinghouse Electric Corporation, Atomic Power Division, Pittsburgh, Pa.

[3] For a solution to the problem of a column vibrating under constant load see "Vibration Problems in Engineering," by S. Timoshenko, D. Van Nostrand Company, Inc., New York, N. Y., 1937, or "The Theory of Sound," by Lord Rayleigh, Macmillan and Company, Ltd., London, England, 1929.

Contributed by the Applied Mechanics Division and presented at the Annual Meeting, New York, N. Y., November 26–December 1, 1950, of The American Society of Mechanical Engineers.

Discussion of this paper should be addressed to the Secretary, ASME, 29 West 39th Street, New York, N. Y., and will be accepted until July 10, 1951, for publication at a later date. Discussion received after the closing date will be returned.

Note: Statements and opinions advanced in papers are to be understood as individual expressions of their authors and not those of the Society. Manuscript received by the Applied Mechanics Division, March 17, 1950. Paper No. 50—A-9.

For a rectangular column this load reduction becomes

$$\Delta P = (3a^2/d^2)P_E \quad \ldots\ldots [3]$$

Equation [3] indicates that deflections of the order of magnitude of the depth of the column cause large reductions in load. By the deflection of the mid-point of the column an amount equal to one quarter the depth, the load is reduced by about 0.19 P_E. With such a small deflection the curvature of the column can be calculated as y'', that is, $(y')^2$ can be neglected against unity in the denominator of the complete curvature expression. This means that even within the range of the classical linear theory, the deflections have a marked effect in altering the load on the column.

In the discussion that follows it is assumed that the column vibrates with small amplitude. As the load on the column depends upon the phase of vibration, the column will vibrate under a periodically varying load, the variations in the load being induced by the vibrations of the column.

Differential Equation

The differential equation governing the vibration of a column is[4]

$$EI(\partial^4 y/\partial x^4) + P(\partial^2 y/\partial x^2) + \rho A(\partial^2 y/\partial t^2) = 0 \quad \ldots\ldots [4]$$

The condition of constant distance between pin ends causes the load P to depend upon the deflection of the column and is given by Equation [1] as

$$P = P_o - (AE/2L)\int_o^L (\partial y/\partial x)^2 dx \quad \ldots\ldots [1]$$

To start the oscillations, the column is assumed to be initially deflected into a half-sine wave, $y = a\sin(\pi x/L)$.

The boundary conditions are

$$\left.\begin{array}{ll} y(0,t) = y''(o,t) = 0 & y(x,o) = a\sin(\pi x/L) \\ y(L,t) = y''(L,t) = 0 & \dot{y}(x,o) = 0 \end{array}\right\} \quad \ldots [5]$$

where the prime indicates differentiation with respect to x and the dot with respect to t.

The solution to Equations [1] and [4] is taken as

$$y(x,\ t) = a\ \sin(\pi x/L)F(t) \quad \ldots\ldots [6]$$

$F(t)$, hereafter designated as F, being the time function associated with the fundamental mode $a\sin(\pi x/L)$.

The boundary Conditions [5] require that

$$F(o) = 1 \quad \text{and} \quad \dot{F}(o) = 0 \quad \ldots\ldots [7]$$

Equation [6] set into Equation [1] yields

$$P = P_o - (AEa^2\pi^2/4L^2)F^2$$

or

$$P = P_o - (P_E - P_o)(2k^4/\omega^2)F^2 \quad \ldots\ldots [8]$$

where

$$2k^4 = (Ea^2\pi^4/4\rho L^4)$$

and

$$\omega^2 = (\pi^2/\rho AL^2)(P_E - P_o)$$

The dimensionless load-amplitude parameter ω^2/k^4 which is used in the text that follows is

$$\omega^2/k^4 = (8r^2/a^2)(1 - P_o/P_E)$$

Setting Equations [6] and [8] into Equation [4] and simplifying gives

$$\ddot{F} + \omega^2 F + 2k^4F^3 = 0 \quad \ldots\ldots [9]$$

Solution

Taking into account the boundary Conditions [7], the integral of Equation [9] is

$$t = (1/k^2)\int_1^F \frac{dF}{\{(1-F^2)[F^2 + 1 + (\omega^2/k^4)]\}^{1/2}} \quad \ldots [10]$$

The solution for the function F of this elliptic integral may appear in several different forms, depending upon the value of ω^2/k^4. It can be shown that solutions exist for all values of ω^2/k^4. They are classified as follows:

Type 1	$\omega^2/k^4 > -1$
Type 2	$-2 < \omega^2/k^4 < -1$
Type 3	$\omega^2/k^4 < -2$
Limiting Case 1	$\omega^2/k^4 = -1$
Limiting Case 2	$\omega^2/k^4 = -2$

Type 1 When $\omega^2/k^4 > -1$ the Integral [10] gives

$$F = cn[t(2k^4 + \omega^2)^{1/2},\ k^2/(2k^4 + \omega^2)^{1/2}] \quad \ldots\ldots [11]$$

The period of oscillation is

$$T = [4/(2k^4 + \omega^2)^{1/2}]\int_o^{\pi/2} \frac{d\varphi}{\{1 - [k^4/(2k^4 + \omega^2)]\sin^2\varphi\}^{1/2}} \quad \ldots\ldots [12]$$

and the load is

$$P = P_o - (P_E - P_o)(2k^4/\omega^2)cn^2[t(2k^4 + \omega^2)^{1/2},\ k^2/(2k^4 + \omega^2)^{1/2}] \quad \ldots\ldots [13]$$

Equation [11] shows that when $\omega^2/k^4 > -1$ the column always vibrates past the $y = 0$ position. When $\omega^2/k^4 > 0$, that is, when P_o is less than the Euler load, the frequency increases with amplitude of vibration. This is true, as well, in the range $-1 < \omega^2/k^4 < 0$. In this range, the significance of limiting ω^2/k^4 to small negative values should be noted. It implies that, when the straight-column load is greater than the Euler load, large initial deflections are required in order to cause the column to vibrate past the $y = 0$ position.

Limiting Case 1. For $\omega^2/k^4 = -1$ the Integral [10] gives

$$F = \operatorname{sech}(k^2t) \quad \ldots\ldots [14]$$

$$T \to \infty$$

and

$$P = P_o + 2(P_E - P_o)\operatorname{sech}^2(k^2t) \quad \ldots\ldots [15]$$

In this case the motion of the column is aperiodic, approaching the straight position asymptotically with time. It may be seen from Equation [15] that the Euler load is the arithmetic average of the straight-column load and the load on the column in its initially deflected position.

Type 2. When $-2 < \omega^2/k^4 < -1$ the Integral [10] yields

$$F = dn[k^2t,\ (\omega^2 + 2k^4)^{1/2}/k^2] \quad \ldots\ldots [16]$$

$$T = (2/k^2)\int_o^{\pi/2} \frac{d\varphi}{\{1 - [(\omega^2 + 2k^4)/k^4]\sin^2\varphi\}^{1/2}} \quad \ldots [17]$$

$$P = P_o - (P_E - P_o)(2k^4/\omega^2)dn^2[k^2t,\ (\omega^2 + 2k^4)^{1/2}/k^2] \quad \ldots [18]$$

As the delta cosine elliptic function is always positive (or always negative) the vibrations are confined to one side of the straight column position. This is reasonable as the limitation of ω^2/k^4 to larger negative values restricts the initial amplitude of

[4] "The Theory of Sound," by Lord Rayleigh, Macmillan and Company, Ltd., London, England, 1929.

deflection; and because of the smaller initial deflections the column does not gain sufficient momentum to bring it past the vertical position.

Limiting Case 2. When $\omega^2/k^4 = -2$ the column remains in its statically deflected position and

$$F = 1$$
$$T = \pi/k^2 \quad \ldots\ldots [19]$$
$$P = P_E$$

Equations [19] give the period of vibration of an arched pin-ended strut which is vibrating with small amplitude.

Type 3. For $\omega^2/k^4 < -2$ the solution of the Integral [10] gives

$$F = [(-\omega^2 - k^4)^{1/2}/k^2]dn \left\{ [(\omega^2 + k^4)/k^2] \left(t + \frac{T}{2} \right), \right.$$
$$\left. (\omega^2 + 2k^4)^{1/2}/(\omega^2 + k^4)^{1/2} \right\} \quad \ldots\ldots [20]$$

$$T = -k^2/(\omega^2 + k^4) \int_0^{\pi/2} \frac{d\varphi}{\{1 - [(\omega^2 + 2k^4)/(\omega^2 + k^4)]\sin^2\varphi\}^{1/2}} \quad \ldots\ldots [21]$$

$$P = P_o + [(P_E - P_o)\,2(\omega^2 + k^4)/\omega^2]dn^2 \left\{ [(\omega^2 + k^4)/k^2] \left(t + \frac{T}{2} \right), (\omega^2 + 2k^4)^{1/2}/(\omega^2 + k^4)^{1/2} \right\} \quad \ldots\ldots [22]$$

This type of motion is similar to Type 2 with the column vibrating on one side of the $y = 0$ position. In this case, however, the absolute value of the time function F is always greater than unity. Previously, F was limited to values less than unity. This means that for the range $\omega^2/k^4 > -2$ the column was set into motion by pulling it away from the $y = 0$ position, while for the range $\omega^2/k^4 < -2$ the column was pushed toward the $y = 0$ position and let vibrate.

Discussion

An examination of the results shows that they are compatible with the anticipated physical behavior of the column. Below the Euler load the column always vibrates past the $y = 0$ position, the cosine elliptic pattern of the vibration becoming more accentuated as the load is increased, or as the modulus $k^2/(2k^4 + \omega^2)^{1/2}$ is increased. When P_o is greater than the Euler load the column has a stationary bent position under the Euler load. From this position the column can be made to vibrate past the vertical position only if the initial amplitude of deflection is sufficiently large. It will then vibrate in a more severe cosine elliptic pattern with larger modulus. When $\omega^2/k^4 = -1$, the column load and deflection are so related as to cause the column to approach the vertical position asymptotically with time. If the initial displacement for a given P_o is decreased still further, bringing ω^2/k^4 into the range $-2 < \omega^2/k^4 < -1$, the column will vibrate on one side of the $y = 0$ position.

In Fig. 2 the variation of frequency with load for various amplitudes of oscillation is shown. The range of the loads is restricted to $P_o < P_E$, so that Equation [12] is represented by these curves. It can be seen that the frequencies are higher with larger amplitudes of vibration. The curve labeled $\beta = 0$ is the same as is obtained from the linear theory of a column vibrating under constant load.

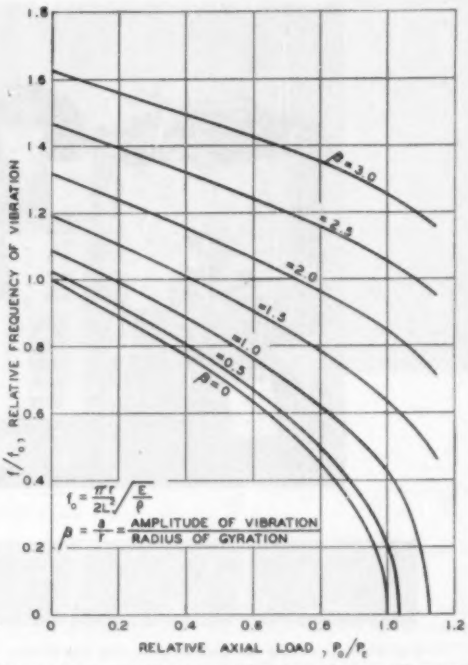

FIG. 2 VARIATION OF FREQUENCY WITH AXIAL LOAD FOR VARIOUS β

Experimental Results

The experimental arrangement is shown in Fig. 3. The jig in which the column rests is a heavy steel frame with a screw in the base for adjusting the end displacement. The test specimen is a steel column with a slenderness ratio of approximately 300. The hardened knife-edges of the column rest in hardened V-grooves which are attached to the frame and screw. A short description of the equipment and its operation, with reference to the numbers shown in Fig. 3, follows:

1 The steel frame and column, with two strain gages attached to the column at its mid-point, is shown.

2 The strain-gage bridge is composed of three dummy gages and one of the gages on the column. A carrier signal of 10 kc is fed into the bridge at two extreme terminals; the modulated output signal, which is caused by the vibrations of the column, is obtained at the other two terminals.

3 The Hewlett-Parkard oscillator, adjusted to 10 kc, furnishes the input to the bridge.

4 The Sola constant-voltage transformer furnishes a constant voltage to the oscilloscope.

5 The oscilloscope receives the modulated signal from the bridge. The 10-kc carrier wave is filtered out and the low-frequency signal of the vibrating column, after being amplified, is impressed across the horizontal plates of the oscilloscope. The sweep circuit is inactive.

6 The periscope transfers the image from the oscilloscope face to the camera.

7 The film-strip Fairchild camera takes the place of the sweep circuit and records the oscilloscope trace.

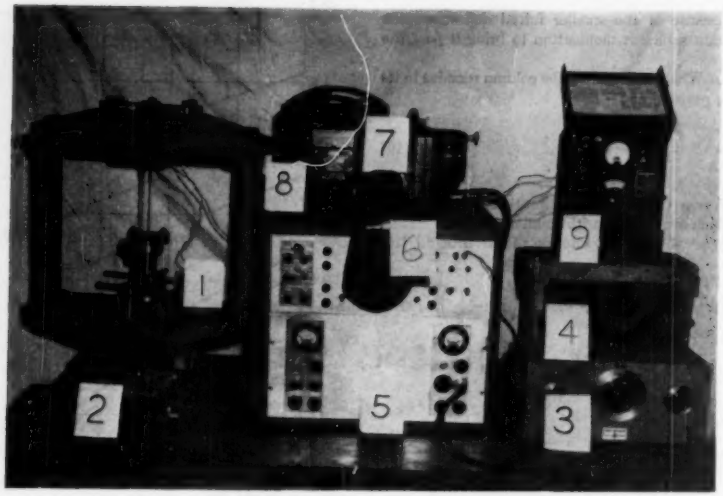

FIG. 3 TEST EQUIPMENT

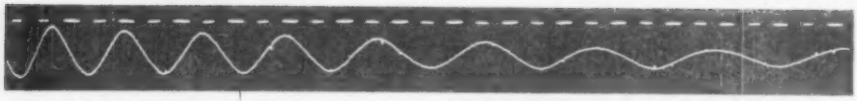

FIG. 4 OSCILLOGRAM SHOWING DECREASE IN FREQUENCY WITH DECREASING AMPLITUDE OF VIBRATION; $P_o = 0.95P_E$

8 The film-speed regulator controls the speed of the film in the camera.

9 The SR-4 strain indicator is used for calibration and for making static measurements.

In making calibrations of amplitude against oscilloscope deflection, the procedure was to deflect the mid-point of the column and measure the load reduction caused by this deflection with the SR-4 strain indicator. The amplitude of the half-sine wave that would give this load reduction was then considered to be the effective amplitude. The effective amplitude of deflection was then plotted against the observed deflection of the oscilloscope beam to give the amplitude calibration curve.

The test procedure follows:

The screw of the jig was adjusted to give the desired value of P_o, which was measured on the SR-4 strain indicator. The mid-point of the column was then deflected manually and released to set the column into vibration. During the vibration the oscilloscope trace was recorded on the film strip. A typical film strip of a test run is shown in Fig. 4. As the calibration of column amplitude against oscilloscope deflection is fairly linear, the variation of frequency with amplitude of vibration is clearly shown in Fig. 4.

Tests were run for several values of the compressive load P_o. In Fig. 5 the experimental values obtained from the film strips are plotted, together with the corresponding theoretical curves. It can be observed from the experimental data that there is a considerable increase in the frequency of vibration as the amplitude of vibration is increased, and that the agreement with the theoretical curves is fairly good. It should also be noted that the amplitude of vibration of the mid-point of the column is restricted to less than one third the depth of the column.

Several tests were run to check the theory of the vibration of an

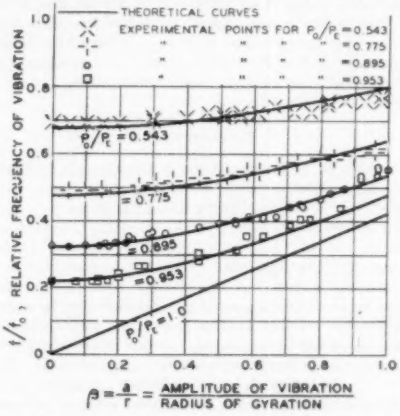

FIG. 5 TEST RESULTS SHOWING VARIATION OF FREQUENCY WITH AMPLITUDE OF VIBRATION FOR SEVERAL P_o/P_E

arched column under the static Euler load for vibrations of infinitesimally small amplitude. The period of vibration is given by Equations [19] and may be rewritten as

$$f/f_o = 0.7071a_E/r \quad \ldots\ldots\ldots\ldots\ldots\ldots [23]$$

The test results indicated that the frequency varied linearly with the static amplitude of deflection of the mid-point of the column a_E, as required by Equation [23]. The proportionality

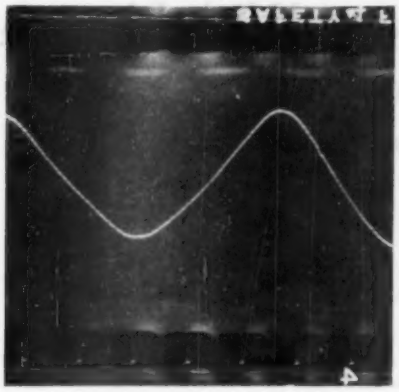

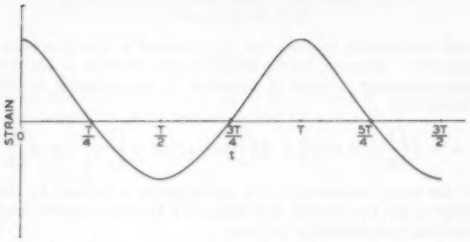

FIG. 6(a) STRAIN AT MID-POINT OF COLUMN FOR VIBRATIONS PAST $y = 0$ POSITION; $P_e = 1.2P_E$

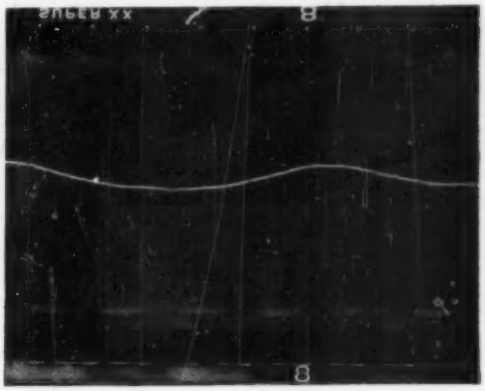

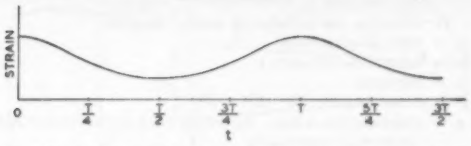

FIG. 6(b) STRAIN AT MID-POINT OF COLUMN FOR VIBRATIONS ON ONE SIDE OF $y = 0$ POSITION; $P_e = 1.2P_E$

factor differed, however, and was found to be approximately 0.5, giving

$$f/f_e = 0.5a_E/r \quad [24]$$

For $P_e > P_E$, the variation with time of the extreme fiber strain at the mid-point of the column was recorded for vibrations past the $y = 0$ position and on one side of the $y = 0$ position. These oscillograms are shown in Figs. 6(*a*) and 6(*b*), respectively, and a comparison with the computed theoretical wave shapes shows them to be in good agreement.

CONCLUSIONS

1 In stipulating that a pin-ended column vibrates with constant distance between its pin ends rather than under constant load, it is found that the frequency increases with amplitude of vibration and that higher frequencies of vibration are obtained than those predicted in the classical linear theory. This has been verified experimentally.

2 When the straight-column load is greater than the Euler load, the column may vibrate either past the vertical position or on one side of the vertical position depending upon the initial amplitude of deflection. This has been observed in experiment.

3 When the straight-column load is the Euler load the theoretical results indicate that the frequency varies linearly with the amplitude of vibration according to the relation

$$f/f_e = 0.4236a/r \quad [25]$$

An extrapolation of the results obtained in tests indicates that Equation [25] represents the actual conditions with satisfactory accuracy.

4 For an arched column under the Euler load the theoretical frequency for vibrations of infinitesimally small amplitude is given as

$$f/f_e = 0.7071a_E/r \quad [23]$$

where a_E is the static deflection of the mid-point of the column. Experimental results verify the linear relationship but give a proportionality factor of 0.5.

ACKNOWLEDGMENT

The author wishes to acknowledge the helpful advice and criticism received from Prof. N. J. Hoff of the Polytechnic Institute of Brooklyn during the preparation of this paper, and the assistance of Mr. Julian Sano in the experimental phase of the investigation.

Axially Symmetrical Plates With Linearly Varying Thickness

By H. D. CONWAY,[1] ITHACA, N. Y.

The most practical problem in the bending of symmetrically loaded circular plates of variable thickness is probably that in which the thickness decreases linearly with the distance from the center of the plate. A general solution of the small-deflection problem of such plates is given here in closed form for the special case when Poisson's ratio is 1/3. Numerical results are given for two particular examples, and these are compared with the results for corresponding plates of constant thickness.

Nomenclature

The following nomenclature is used in the paper:

- u = radial displacement
- ϕ = slope of middle surface
- h = thickness
- D = flexural rigidity $Eh^3/12(1-\nu^2)$
- ρ = dimensionless radius. Subscripts o and i refer to outer and inner radii, respectively
- Q = shearing force per unit circumferential length
- μ = density of material
- ω = angular velocity

Analysis

The differential equation governing the symmetrical bending of circular plates of variable thickness may be shown to be (1)[2]

$$D\frac{d}{dr}\left(\frac{d\phi}{dr}+\frac{\phi}{r}\right)+\frac{dD}{dr}\left(\frac{d\phi}{dr}+\nu\frac{\phi}{r}\right)=-Q \quad \ldots\ldots [1]$$

The differential equation for the radial deformation of a rotating disk of variable thickness is (2)

$$h\frac{d}{dr}\left(\frac{du}{dr}+\frac{u}{r}\right)+\frac{dh}{dr}\left(\frac{du}{dr}+\nu\frac{u}{r}\right)=-\frac{\mu\omega^2(1-\nu^2)rh}{E} \quad . [2]$$

By comparing Equations [1] and [2], it will be seen that, in so far as the complementary functions are concerned, the equations are analogous, the flexural rigidity D and slope ϕ in the plate-bending equation being replaced, respectively, by the thickness h and radial displacement u in the rotating disk. Timoshenko (3) attributes the discovery of this analogy to L. Föppl.

Introducing the dimensionless radius $\rho = r/a$ in Equations [1] and [2], we obtain, respectively

$$\frac{d^2\phi}{d\rho^2}+\left(\frac{1}{\rho}+\frac{1}{D}\frac{dD}{d\rho}\right)\frac{d\phi}{d\rho}+\left(\frac{\nu}{D}\frac{dD}{d\rho}-\frac{1}{\rho}\right)\frac{\phi}{\rho}=-\frac{Qa^2}{D} \quad . [3]$$

and

$$\frac{d^2u}{d\rho^2}+\left(\frac{1}{\rho}+\frac{1}{h}\frac{dh}{d\rho}\right)\frac{du}{d\rho}+\left(\frac{\nu}{h}\frac{dh}{d\rho}-\frac{1}{\rho}\right)\frac{u}{\rho}=-\frac{\mu\omega^2a^2(1-\nu^2)\rho}{E} \quad \ldots\ldots [4]$$

In a discussion of the problem of the rotating disk, Gran Olsson (4) assumed a thickness variation of the type

$$h = h_{max}(1-\rho)^m$$

and, substituting in Equation [4], obtained a hypergeometric equation. However, for the particular case where $m = 1/\nu$, the complementary function of Equation [4] is expressible in the closed form

$$u = A\left(\frac{1}{\rho}+m-1\right)+B\left(\frac{1}{\rho}[1-\rho]^{1-m}-\left[\frac{1}{\rho}-1+m\right]\right)$$

If the radial displacement u in this equation is replaced by the slope ϕ, and the variable flexural rigidity D in the plate-bending problem is expressible in the form

$$D = D_{max}(1-\rho)^m$$

where $m = 1/\nu$, the complementary function of Equation [3] is obtained.

Taking a value of Poisson's ratio of 1/3, and remembering that the flexural rigidity is proportional to the cube of the plate thickness, the variable thickness h in the plate-bending problem is

$$h = h_{max}(1-\rho)$$

The thickness variation is therefore linear, being greatest at the center of the plate. Plates whose thickness variation is expressible in the form $h = h_{max}\,\rho$ have been discussed in an earlier paper (5).

Thus, for $m = 1/\nu = 3$, Equation [3] may be rewritten in the form

$$\rho^2(1-\rho)^3\frac{d^2\phi}{d\rho^2}+\rho(1-4\rho)(1-\rho)^2\frac{d\phi}{d\rho}-(1-\rho)^2\phi=-\frac{Qa^2\rho^2}{D_{max}} \quad \ldots\ldots [5]$$

and the complementary function is

$$\phi = A\left[\frac{2\rho+1}{\rho}\right]+B\left[\frac{3\rho-2\rho^2}{(1-\rho)^2}\right] \quad \ldots\ldots [6]$$

The particular solution for any case of symmetrical loading and boundary conditions is then obtainable by the method of variation of parameters. However, if the plate is bent only by pure couples distributed along the inner and outer edges, the shearing force Q per unit length is zero, and Equation [6] furnishes the complete solution.

Consider, as an example, the uniformly loaded plate shown in Fig. 1, the dimensionless outer radius ρ_o being free and the inner radius ρ_i clamped. The shearing force Q per unit length is then

---

[1] Professor of Mechanics, Cornell University. Jun. ASME.

[2] Numbers in parentheses refer to the Bibliography at the end of the paper.

Contributed by the Applied Mechanics Division and presented at the Annual Meeting, New York, N. Y., November 26–December 1, 1950, of The American Society of Mechanical Engineers.

Discussion of this paper should be addressed to the Secretary, ASME, 29 West 39th Street, New York, N. Y., and will be accepted until July 10, 1951, for publication at a later date. Discussion received after the closing date will be returned.

Note: Statements and opinions advanced in papers are to be understood as individual expressions of their authors and not those of the Society. Manuscript received by the Applied Mechanics Division, March 17, 1950. Paper No. 50—A-6.

$$Q = \frac{a}{\rho}\int_{\rho}^{\rho_o} q\rho d\rho = \frac{qa}{2}\left(\frac{\rho_o^2}{\rho} - \rho\right)$$

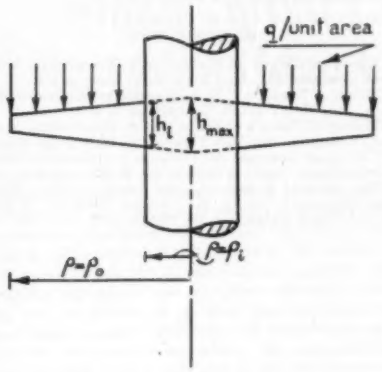

FIG. 1

With this value for Q and using the method of variation of parameters, the particular solution of Equation [5] is

$$\phi = \frac{qa^3}{2D_{max}}\left[\frac{(4\rho^3 + 15\rho^2 - 6\rho - 6)}{36\rho(1-\rho)^2} - \frac{\rho_o^2(2\rho^2 + \rho - 1)}{6\rho(1-\rho)^2} - \frac{(2\rho+1)(1+\rho_o^2)}{6\rho}\log(1-\rho) - \frac{(3-2\rho)\rho\rho_o^2}{6(1-\rho)^2}\log\rho\right]$$

and hence the complete solution is

$$\phi = A\left[\frac{2\rho+1}{\rho}\right] + B\left[\frac{3\rho - 2\rho^2}{(1-\rho)^2}\right] + \frac{qa^3}{2D_{max}}\left[\frac{(4\rho^3 + 15\rho^2 - 6\rho - 6)}{36\rho(1-\rho)^2} - \frac{\rho_o^2(2\rho^2 + \rho - 1)}{6\rho(1-\rho)^2} - \frac{(2\rho+1)(1+\rho_o^2)}{6\rho}\log(1-\rho) - \frac{(3-2\rho)\rho\rho_o^2}{6(1-\rho)^2}\log\rho\right] \quad \ldots\ldots [7]$$

The constants A and B are then determined from the fact that

$$\frac{d\phi}{d\rho} + \frac{\phi}{3\rho}$$

is zero at $\rho = \rho_o$, and that ϕ is zero at $\rho = \rho_i$.

For the particular case when $\rho_o = 2/3$ and $\rho_i = 1/6$, we obtain

$$A = 0.040144\,\frac{qa^3}{D_{max}};\quad B = -0.000474\,\frac{qa^3}{D_{max}}$$

Using these values, the distribution of radial and circumferential stresses at the extreme fiber has been calculated and is plotted in Fig. 2. As in the case of a corresponding plate having constant thickness, the maximum stress is radial and occurs at the clamped edge. In the present case, the maximum stress is

$$\sigma_{r(max)} = 3.130\,\frac{qr_o^2}{h_i^2}$$

where r_o is the outer radius. This stress is nearly 5 per cent greater than the stress

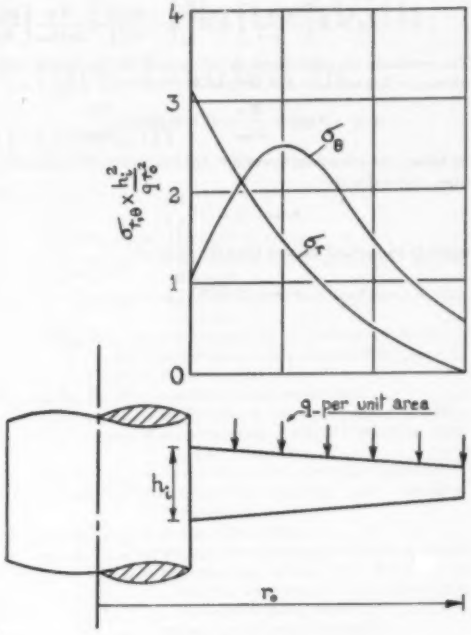

FIG. 2

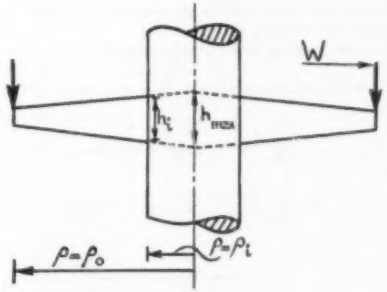

FIG. 3

$$\sigma_{r(max)} = 2.989\,\frac{qr_o^2}{h_i^2}$$

for a corresponding plate having constant thickness.

As a further example, the plate shown in Fig. 3 has been analyzed. The differential equation to be solved for this case is

$$\rho^2(1-\rho)^2\frac{d^2\phi}{d\rho^2} + \rho(1-4\rho)(1-\rho)^2\frac{d\phi}{d\rho} - (1-\rho)^2\phi = -\frac{Wa\rho}{2\pi D_{max}} \quad \ldots\ldots [8]$$

and the complete solution is

$$\phi = A\left[\frac{2\rho + 1}{\rho}\right] + B\left[\frac{3\rho - 2\rho^2}{(1-\rho)^2}\right] - \frac{Wa}{2\pi D_{max}}\left[\frac{2\rho^2 + \rho - 1}{6\rho(1-\rho)^2} + \frac{2\rho + 1}{6\rho}\log(1-\rho) + \frac{3\rho - 2\rho^2}{6(1-\rho)^2}\log\rho\right] \quad [9]$$

The constants are determined as before and, for the special case when $\rho_o = 2/3$ and $\rho_i = 1/6$, they are found to be

$$A = -0.03291\frac{Wa}{D_{max}}; \quad B = 0.02491\frac{Wa}{D_{max}}$$

As before, the maximum stress is radial and occurs at the clamped edge. Its value is

$$\sigma_{r(max)} = 1.717\frac{W}{h_i^2}$$

which is 14 per cent greater than the value of

$$\sigma_{r(max)} = 1.501\frac{W}{h_i^2}$$

for a corresponding plate of constant thickness.

BIBLIOGRAPHY

1 "Theory of Plates and Shells," by S. Timoshenko, McGraw-Hill Book Company, Inc., New York, N. Y., 1950, p. 283.

2 "Theory of Elasticity," by S. Timoshenko, McGraw-Hill Book Company, Inc., New York, N. Y., 1934, eq. k, p. 67.

3 "Theory of Plates and Shells," by S. Timoshenko, McGraw-Hill Book Company, Inc., New York, N. Y., 1940, p. 287 (footnote).

4 "Über einige Lösungen des Problems der rotierenden Scheibe," by R. Gran Olsson, *Ingenieur Archiv.*, vol. 8, 1937, pp. 270–275.

5 "The Bending of Symmetrically Loaded Circular Plates of Variable Thickness," by H. D. Conway, JOURNAL OF APPLIED MECHANICS, Trans. ASME, vol. 70, 1948, p. A-1.

Large-Deflection Theory for Plates With Small Initial Curvature Loaded in Edge Compression[1]

By J. M. COAN,[2] URBANA, ILL.

This investigation of the buckling of a simply supported, rectangular isotropic plate with small initial curvature was undertaken to evaluate current procedures for deducing the true (flat plate) critical load from the measured deflections and strains of a nominally flat plate. The boundary conditions are those that are usually met in test practice but which have not been satisfied by earlier studies, i.e., stress-free supported edges and uniformly displaced loaded edges. Previous solutions require a distribution of transverse stress along the supported edges sufficient to keep them straight and parallel at all times. However, in most test specimens, the freedom of the supported edges to distort in the plane of the plate measurably influences the behavior of the plate and the stress distribution within it. Levy's solution of von Kármán's "large deflection" equations is adapted by the author to yield the nonuniform edge displacements that are characteristic of stress-free supported edges. Limited experimental evidence tends to confirm the predictions of this analysis.

Nomenclature

The following nomenclature is used in the paper:

a = half-length of plate in x-direction
b = half-width of plate in y-direction
h = plate thickness
u, v, w = displacements of point in x, y, and z-directions, respectively
x, y, z = co-ordinates of a point; origin at center of plate (see Fig. 1)
E = Young's modulus
μ = Poisson's ratio, taken as 0.316 unless otherwise specified
D = flexural rigidity of plate, $\frac{Eh^3}{12(1-\mu^2)}$
p_x, p_y = average edge stresses (magnitude only)
p_z = normal pressure
p_{cr} = critical stress for flat square plate
p_x/p_{cr} = load ratio
P_x, P_y = total loads in plate
w, w_{mn} = total deflection, and coefficient in this function
$w_0, w_{0(mn)}$ = initial deflection, and coefficient in this function
$K_{mn}, K_{0(mn)}$ = nondimensional deflection coefficients
K_c = nondimensional net center deflection
$F, \Delta F$ = stress function
$b_{pq}, A_p, C_p, B_q, D_q$ = coefficients in stress function
c_{pq}, e_{pq} = coefficients in converted stress function
$b_{0(pq)}$ = stress-function coefficient resulting from initial deflection
$\sigma_x', \sigma_y', \tau_{xy}'$ = median-fiber (i.e., membrane) stresses
$\sigma_x'', \sigma_y'', \tau_{xy}''$ = extreme-fiber bending and shearing stresses
$\epsilon_x', \epsilon_y', \gamma_{xy}'$ = median-fiber strains
$\epsilon_x'', \epsilon_y'', \gamma_{xy}''$ = extreme-fiber bending and shearing strains
e_1, e_2 = extreme-fiber strains (in direction of loading) at center of plate on concave and convex sides, respectively
ϵ_{cr} = critical strain for flat square plate
$\nabla^4 = \frac{\partial^4}{\partial x^4} + 2\frac{\partial^4}{\partial x^2 \partial y^2} + \frac{\partial^4}{\partial y^4}$
m, n, r, s = subscripts in deflection and normal pressure functions, positive odd integers
p, q = subscripts in stress function, positive even integers
k, t = positive integer subscripts, odd or even

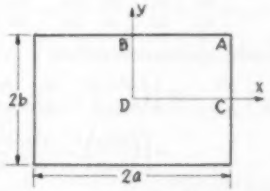

Fig. 1 Co-Ordinate System

Introduction

In a series of compression tests on flat plates, recently conducted at the Polytechnic Institute of Brooklyn, the loaded edges of each specimen were subjected to uniform compressive strain (by adjusting flexible loading strips) up to as much as 75 per cent of the critical load and were then uniformly displaced by the loading head as the test was continued to failure (1).[3] The supported edges were stress-free at all times and, therefore, at liberty to warp in the plane of the plate. Under such conditions of loading and support, nonuniform displacements could

[1] This paper is based on a thesis submitted by the author to the Polytechnic Institute of Brooklyn in partial fulfillment of the requirements for the degree of Doctor of Aeronautical Engineering.

[2] Associate Professor of Aeronautical Engineering, University of Illinois.

Contributed by the Applied Mechanics Division and presented at the Annual Meeting, New York, N. Y., November 26–December 1, 1950, of The American Society of Mechanical Engineers.

Discussion of this paper should be addressed to the Secretary, ASME, 29 West 39th Street, New York, N. Y., and will be accepted until July 10, 1951, for publication at a later date. Discussion received after the closing date will be returned.

Note: Statements and opinions advanced in papers are to be understood as individual expressions of their authors and not those of the Society. Manuscript received by the Applied Mechanics Division, June 24, 1949. Paper No. 50—A-2.

[3] Numbers in parentheses refer to the Bibliography at the end of the paper.

occur on all edges during the early stages of loading and did occur on the supported edges during the remainder of the test.

Feeling that these boundary conditions, particularly that of stress-free supported edges, would result in significantly different behavior from that predicted for the conventional (i.e., straight-edge) problem, an investigation was made to estimate their effects on available methods for determining the critical load. An additional objective was that of determining the corresponding stress distribution in the buckled plate when the critical load has not been too greatly exceeded.

The available solutions of von Kármán's large-deflection equations—notably those of Timoshenko, Marguerre, and Levy—correspond to undistorted edges. The solutions of Timoshenko (2*a*) and Marguerre (3) are approximate since each employed the energy method. Levy (4) has given an exact solution of von Kármán's equations which employs a double Fourier series for each of three functions, deflection, stress, and normal pressure. Levy's work has been extended (5) to include plates whose initial deviations from flatness are as much as 1/10 of the thickness. In the following treatment Levy's solution is further extended to allow for nonuniform edge displacements. The supported edges are considered stress-free while the loaded edges may be subjected to either uniform displacement, uniform stress, or uniform strain.

Large-Deflection Theory for Thin Plates With Small Initial Curvature

The fundamental differential equations governing the deformation of thin flat plates (2*b*) were derived by von Kármán from the joint requirements of compatible strains in the middle surface and equilibrium of forces normal to that surface. If the middle surface of a plate with small initial curvature is represented by the deflection function w_0, the median-fiber strains become

$$\left.\begin{aligned} \epsilon_x' &= \frac{\partial u}{\partial x} + \frac{1}{2}\left(\frac{\partial w}{\partial x}\right)^2 - \frac{1}{2}\left(\frac{\partial w_0}{\partial x}\right)^2, \\ \epsilon_y' &= \frac{\partial v}{\partial y} + \frac{1}{2}\left(\frac{\partial w}{\partial y}\right)^2 - \frac{1}{2}\left(\frac{\partial w_0}{\partial y}\right)^2, \\ \gamma'_{xy} &= \frac{\partial u}{\partial y} + \frac{\partial v}{\partial x} + \frac{\partial w}{\partial x}\frac{\partial w}{\partial y} - \frac{\partial w_0}{\partial x}\frac{\partial w_0}{\partial x} \end{aligned}\right\} \quad \ldots [1]$$

and the compatibility equation takes the form

$$\frac{\partial^4 F}{\partial x^4} + 2\frac{\partial^4 F}{\partial x^2 \partial y^2} + \frac{\partial^4 F}{\partial y^4} = E\left\{\left(\frac{\partial^2 w}{\partial x \partial y}\right)^2 - \frac{\partial^2 w}{\partial x^2}\frac{\partial^2 w}{\partial y^2} - \left[\left(\frac{\partial^2 w_0}{\partial x \partial y}\right)^2 - \frac{\partial^2 w_0}{\partial x^2}\frac{\partial^2 w_0}{\partial y^2}\right]\right\} \quad \ldots [2]$$

The equilibrium equation becomes

$$\frac{\partial^4 (w - w_0)}{\partial x^4} + 2\frac{\partial^4 (w - w_0)}{\partial x^2 \partial y^2} + \frac{\partial^4 (w - w_0)}{\partial y^4} = \frac{p_z}{D} + \frac{h}{D}\left[\frac{\partial^2 F}{\partial y^2}\frac{\partial^2 w}{\partial x^2} + \frac{\partial^2 F}{\partial x^2}\frac{\partial^2 w}{\partial y^2} - 2\frac{\partial^2 F}{\partial x \partial y}\frac{\partial^2 w}{\partial x \partial y}\right] \quad \ldots [3]$$

since the bending moments implicit in the left-hand member depend on the change in curvature, while the slopes implicit in the right-hand member depend only on the final deflected shape.

With the median-fiber stresses prescribed in the conventional manner

$$\sigma_x' = \frac{\partial^2 F}{\partial y^2}, \quad \sigma_y' = \frac{\partial^2 F}{\partial x^2}, \quad \tau_{xy}' = -\frac{\partial^2 F}{\partial x \partial y} \quad \ldots [4]$$

the median-fiber strains will be

$$\left.\begin{aligned} \epsilon_x' &= \frac{1}{E}\left(\frac{\partial^2 F}{\partial y^2} - \mu\frac{\partial^2 F}{\partial x^2}\right), \quad \epsilon_y' = \frac{1}{E}\left(\frac{\partial^2 F}{\partial x^2} - \mu\frac{\partial^2 F}{\partial y^2}\right), \\ \gamma_{xy}' &= -\frac{2(1+\mu)}{E}\frac{\partial^2 F}{\partial x \partial y} \end{aligned}\right\} \quad \ldots [5]$$

The extreme-fiber bending and shearing stresses, being functions of the change in curvature, become

$$\left.\begin{aligned} \sigma_x'' &= \pm\frac{Eh}{2(1-\mu^2)}\left[\frac{\partial^2 (w - w_0)}{\partial x^2} + \mu\frac{\partial^2 (w - w_0)}{\partial y^2}\right], \\ \sigma_y'' &= \pm\frac{Eh}{2(1-\mu^2)}\left[\frac{\partial^2 (w - w_0)}{\partial y^2} + \mu\frac{\partial^2 (w - w_0)}{\partial x^2}\right], \\ \tau_{xy}'' &= \pm\frac{Eh}{2(1+\mu)}\frac{\partial^2 (w - w_0)}{\partial x \partial y} \end{aligned}\right\} \quad \ldots [6]$$

Taking the origin of co-ordinates at the center of the plate to permit edge distortion, the initial deflected shape may be described by

$$w_0 = \sum_{m=1,3,}^{\infty}\sum_{n=1,3,}^{\infty} w_{0(mn)} \cos\frac{m\pi x}{2a}\cos\frac{n\pi y}{2b} \quad \ldots [7]$$

and the final deflected shape may be represented by

$$w = \sum_{m=1,3,}^{\infty}\sum_{n=1,3,}^{\infty} w_{mn} \cos\frac{m\pi x}{2a}\cos\frac{n\pi y}{2b} \quad \ldots [8]$$

Equation [2] is identically satisfied if the stress function is taken as

$$F = -\frac{p_x y^2}{2} - \frac{p_y x^2}{2} + \sum_{p=0,2,}^{\infty}\sum_{q=0,2,}^{\infty} (b_{pq} - b_{0(pq)}) \cos\frac{p\pi x}{2a}\cos\frac{q\pi y}{2b} \quad \ldots [9]$$

The amplitudes of the stress harmonics are obtained by inserting Equations [7], [8], and [9] into Equation [2], transforming the multiple products of odd sines and cosines that form in the right-hand member into simple products of even cosines, and then matching their coefficients with those of like cosine products in the left-hand member. The general stress coefficient for the flat plate is then found to be

$$b_{pq} = \frac{E}{4\left(p^2\frac{b}{a} + q^2\frac{a}{b}\right)^2}\sum_{n=1}^{9} B_n \quad \ldots [10]$$

where

$$B_1 = \sum_{k=1}^{p-1}\sum_{t=1}^{q-1} [kt(p-k)(q-t) - k^2(q-t)^2]\, w_{kt}\, w_{p-k,\,q-t}$$

if $q \neq 0$ and $p \neq 0$

and $B_1 = 0$ if $q = 0$ or $p = 0$

$$B_2 = -\sum_{k=1}^{\infty}\sum_{t=1}^{q-1} [kt(k+p)(q-t) + k^2(q-t)^2]\, w_{kt}\, w_{k+p,\,q-t}$$

if $q \neq 0$

and $B_2 = 0$ if $q = 0$

$$B_2 = -\sum_{k=1}^{\infty}\sum_{t=1}^{q-1}[(k+p)tk(q-t) + (k+p)^2(q-t)^2]\,w_{k+p,t}\,w_{k,q-t} \quad \text{if } q \neq 0 \text{ and } p \neq 0$$

and $B_2 = 0$ if $q = 0$ or $p = 0$

$$B_4 = -\sum_{k=1}^{p-1}\sum_{t=1}^{\infty}[kt(p-k)(t+q) + k^2(t+q)^2]\,w_{kt}\,w_{p-k,t+q} \quad \text{if } p \neq 0$$

and $B_4 = 0$ if $p = 0$

$$B_5 = -\sum_{k=1}^{p-1}\sum_{t=1}^{\infty}[k(t+q)(p-k)t + k^2t^2]\,w_{k,t+q}\,w_{p-k,} \quad \text{if } q \neq 0 \text{ and } p \neq 0$$

and $B_5 = 0$ if $q = 0$ or $p = 0$

$$B_6 = \sum_{k=1}^{\infty}\sum_{t=1}^{\infty}[kt(k+p)(t+q) - k^2(t+q)^2]\,w_{kt}\,w_{k+p,t+q} \quad \text{if } q \neq 0$$

and $B_6 = 0$ if $q = 0$ and $p = 0$

$$B_7 = \sum_{k=1}^{\infty}\sum_{t=1}^{\infty}[k(t+q)(k+p)t - k^2t^2]\,w_{k,t+q}\,w_{k+p,t} \quad \text{if } q \neq 0 \text{ and } p \neq 0$$

and $B_7 = 0$ if $q = 0$ or $p = 0$

$$B_8 = \sum_{k=1}^{\infty}\sum_{t=1}^{\infty}[(k+p)tk(t+q) - (k+p)^2(t+q)^2]\,w_{k+p,t}\,w_{k,t+q} \quad \text{if } q \neq 0 \text{ and } p \neq 0$$

and $B_8 = 0$ if $q = 0$ or $p = 0$

$$B_9 = \sum_{k=1}^{\infty}\sum_{t=1}^{\infty}[(k+p)(t+q)kt - (k+p)^2t^2]\,w_{k+p,t+q}\,w_{kt} \quad \text{if } p \neq 0$$

and $B_9 = 0$ if $p = 0$ and $q = 0$

(These sums are given here since they are probably not elsewhere available for the case in which the origin of co-ordinates is taken at the center of the plate.) The correction coefficients $b_{w(pq)}$ for the initially curved plate are determined from Equation [10] with the w_0-terms replacing the w-terms in each of the B_{0_n} summations.

Each term of Equations [7] and [8] is seen to satisfy the boundary conditions on deflection and moment for a simply supported plate

$$w,\ w_0 = 0 \text{ on } x = \pm a \text{ and on } y = \pm b \quad \ldots\ldots[11]$$

$$\frac{\partial^2(w-w_0)}{\partial x^2} = 0 \text{ on } x = \pm a \text{ and } \frac{\partial^2(w-w_0)}{\partial y^2} = 0 \text{ on } y = \pm b \quad \ldots\ldots[12]$$

The boundary condition of zero shearing stress requires that the resultant load in the plate be constant. This condition is satisfied by Equation [9] since, on substituting into Equation [4] and integrating, it is found that

$$P_x = h\int_{-b}^{b}\sigma_x'\,dy = -2bhp_x, \quad P_y = h\int_{-a}^{a}\sigma_y'\,dx = -2ahp_y \quad \ldots\ldots[13]$$

The last boundary condition may be formed by specifying either the displacement or the normal stress along the plate edge. From Equation [1] the displacement at $x = \pm a$ is seen to be

$$u_a = \int_0^a\left[\epsilon_x' - \frac{1}{2}\left(\frac{\partial w}{\partial x}\right)^2 + \frac{1}{2}\left(\frac{\partial w_0}{\partial x}\right)^2\right]dx \quad \ldots\ldots[1a]$$

On substituting Equations [5], [7], [8], and [9] in this expression, integrating, substituting from Equation [10], and combining, it is seen that uniform displacements are achieved

$$u_a = -\frac{p_x a}{E} + \mu\frac{p_y a}{E} - \frac{\pi^2}{32a}\sum_{m=1,3,}^{\infty}\sum_{n=1,3,}^{\infty}m^2[w_{mn}^2 - w_{0(mn)}^2] \quad \ldots\ldots[14]$$

Similarly

$$v_b = -\frac{p_y b}{E} + \mu\frac{p_x b}{E} - \frac{\pi^2}{32b}\sum_{m=1,3,}^{\infty}\sum_{n=1,3,}^{\infty}n^2[w_{mn}^2 - w_{0(mn)}^2] \quad \ldots\ldots[15]$$

The normal pressure may be expressed by the series

$$p_z = \sum_{r=1,3,}^{\infty}\sum_{s=1,3,}^{\infty}p_{rs}\cos\frac{r\pi x}{2a}\cos\frac{s\pi y}{2b} \quad \ldots\ldots[16]$$

and its coefficients determined from the known pressure distribution by the standard procedure for evaluating Fourier constants. Substituting Equations [7], [8], [9], and [16] into Equation [3], transforming to simple products of odd cosines and matching coefficients of like products as before, the following doubly infinite family of equations is obtained

$$p_{rs} = D\left[\left(\frac{r\pi}{2a}\right)^2 + \left(\frac{s\pi}{2b}\right)^2\right]^2[w_{rs} - w_{0rs}] - p_x h\left(\frac{r\pi}{2a}\right)^2 w_{rs} - p_y h\left(\frac{s\pi}{2b}\right)^2 w_{rs} - \frac{h\pi^4}{64\,a^2b^2}\sum_{n=1}^{9}[A_n - A_{0(n)}] \quad \ldots\ldots[17]$$

where

$$\left.\begin{aligned}
A_1 &= \sum_{k=1,3,}^{r}\sum_{t=1,3,}^{s}[(s-t)k - (r-k)t]^2\,b_{r-k,s-t}\,w_{kt}\\
A_2 &= \sum_{k=0,2,}^{\infty}\sum_{t=0,2,}^{\infty}[t(k+r) - k(t+s)]^2\,b_{kt}\,w_{k+r,t+s}\\
A_3 &= \sum_{k=0,2,}^{\infty}\sum_{t=1,3,}^{\infty}[(k+r)(t+s) - kt]^2\,b_{k,t+s}\,w_{k+r,t}\\
A_4 &= \sum_{k=1,3,}^{\infty}\sum_{t=0,2,}^{\infty}[tk - (k+r)(t+s)]^2\,b_{k+r,t}\,w_{k,t+s}\\
A_5 &= \sum_{k=1,3,}^{\infty}\sum_{t=1,3,}^{\infty}[(t+s)k - (k+r)t]^2\,b_{k+r,t+s}\,w_{kt}\\
A_6 &= \sum_{k=1,3,}^{r}\sum_{t=0,2,}^{\infty}[tk + (r-k)(t+s)]^2\,b_{r-k,t}\,w_{k,t+s}\\
A_7 &= \sum_{k=1,3,}^{r}\sum_{t=1,3,}^{\infty}[(t+s)k + (r-k)t]^2\,b_{r-k,t+s}\,w_{kt}
\end{aligned}\right\} \quad \ldots\ldots[18]$$

$$A_0 = \sum_{k=0,2,}^{\infty} \sum_{t=1,3,}^{s} [(s-t)(k+r)+tk]^2 b_{k,\,s-t}\, w_{k+r,t}$$

$$A_0 = \sum_{k=1,3,}^{\infty} \sum_{t=1,3,}^{s} [(s-t)k + t(k+r)]^2 b_{k+r,\,s-t}\, w_{kt} \quad \left.\begin{array}{l}\\ \\ \\ \end{array}\right\} \ldots [18]\ (cont.)$$

The additional products (A_0) of stress and deflection coefficients are determined from Equations [18] by replacing b_{pq} in each product with $b_{0(pq)}$. It should be noted that the w_{mn}-terms appearing in the products forming A_0 are the total deflection coefficients of Equation [8] and not those of Equation [7].

Effect of Nonuniform Edge Displacements

Equations [14] and [15] verify the uniform edge displacements automatically provided by Equation [9] when its coefficients are determined from the compatibility requirement. However, the addition of mixed products of the type elsewhere employed by Levy (6) results in nonuniform displacements on all four edges.

Deleting the $\bar{p}_y$ term from Equation [9] and adding the following terms

$$\Delta F = \sum_{p=2,4,}^{\infty} \cos\frac{p\pi x}{2a}\left[A_p \cosh\frac{p\pi y}{2a} + C_p\left(\frac{p\pi y}{2a}\right)\sinh\frac{p\pi y}{2a}\right]$$

$$+ \sum_{q=2,4,}^{\infty} \cos\frac{q\pi y}{2b}\left[B_q \cosh\frac{q\pi x}{2b} + D_q\left(\frac{q\pi x}{2b}\right)\sinh\frac{q\pi x}{2b}\right] \ldots [19]$$

one obtains a stress function that is suitable for the study of simply supported, initially nonflat, rectangular plates compressed in one direction (x), and stress-free along the supported edges ($y = \pm b$). Three cases of load application may be distinguished: Case 1, uniform displacement of the loaded edges ($x = \pm a$); Case 2, uniform stress on the loaded edges; and Case 3, uniform strain on the loaded edges. Although Case 2 yields the most general solution, and Case 3 represents the conditions approximated in some tests (1), Case 1 corresponds to conventional test procedure and, therefore, will be developed in detail.

Substitution of Equation [19] in Equation [2] verifies that $\nabla^4 \Delta F \equiv 0$. The b_{pq} coefficients are exactly determined by Equation [10], while the coefficients of ΔF must be determined from applicable boundary conditions. The boundary conditions implicit in Equation [13], zero peripheral shearing stress, are common to all three cases if edge friction is negligibly small. Adding Equations [9] and [19] and substituting into Equation [13], where $\bar{p}_y$ is now zero, it is seen that

$$A_p = -C_p\left[1 + \frac{p\pi b}{2a}\coth\frac{p\pi b}{2a}\right],$$

$$B_q = -D_q\left[1 + \frac{q\pi a}{2b}\coth\frac{q\pi a}{2b}\right] \ldots [20]$$

In the case of uniformly displaced loaded edges only the first summation need be retained. Substituting from Equation [20], the simplified stress function becomes

$$F = -\frac{\bar{p}_x y^2}{2} + \sum_{p=0,2,}^{\infty}\sum_{q=0,2,}^{\infty} [b_{pq} - b_{0(pq)}]\cos\frac{p\pi x}{2a}\cos\frac{q\pi y}{2b}$$

$$- \sum_{p=2,4,}^{\infty} C_p \cos\frac{p\pi x}{2a}\left[\left(1 + \frac{p\pi b}{2a}\coth\frac{p\pi b}{2a}\right)\cosh\frac{p\pi y}{2a}\right.$$

$$\left. - \frac{p\pi y}{2a}\sinh\frac{p\pi y}{2a}\right] \ldots [21]$$

The coefficients of the p-summation are determined from the condition that $\sigma_y' = 0$ at $y = \pm b$. This requirement is satisfied if

$$\left[\cosh\frac{p\pi b}{2a} + \frac{\dfrac{p\pi b}{2a}}{\sinh\dfrac{p\pi b}{2a}}\right] C_p = \sum_{q=0,2,}^{\infty} (-1)^{q/2}[b_{pq} - b_{0(pq)}]$$

$$\text{for } p = 2, 4, \ldots \ldots \ldots [22]$$

The C_p terms are uniquely determined by this infinite set but it is necessary to convert the mixed products in Equation [21] to a double cosine series in order to solve the family of Equation [17]. The hyperbolic term in each product may be replaced by an equivalent cosine series

$$-C_p\left[\left(1 + \frac{p\pi b}{2a}\coth\frac{p\pi b}{2a}\right)\cosh\frac{p\pi y}{2a} - \frac{p\pi y}{2a}\sinh\frac{p\pi y}{2a}\right]$$

$$= \sum_{q=0,2,}^{\infty} c_{pq}\cos\frac{q\pi y}{2b}$$

whose Fourier coefficients are

$$c_{pq} = (-1)^{\frac{q+2}{2}} \frac{\alpha\, p^3 \sinh\dfrac{p\pi b}{2a}}{\pi a^3 b\left[\left(\dfrac{p}{a}\right)^2 + \left(\dfrac{q}{b}\right)^2\right]^2} C_p \ldots [23]$$

where

$$\alpha = \begin{cases} 8 \text{ if } q \neq 0 \\ 4 \text{ if } q = 0 \end{cases}$$

Making this substitution, and the simplification provided by grouping the c-coefficients with those of b

$$e_{pq} = b_{pq} + c_{pq} \ldots [24]$$

Equation [21] may be written

$$F = -\frac{\bar{p}_x y^2}{2} + \sum_{p=0,2,}^{\infty}\sum_{q=0,2,}^{\infty} [e_{pq} - b_{0(pq)}]\cos\frac{p\pi x}{2a}\cos\frac{q\pi y}{2b} \ldots [25]$$

With the total stress coefficients of Equation [24] expressible as quadratic functions of w_{mn}, the family of equations corresponding to Equation [17] becomes

$$p_{rs} = D\left[\left(\frac{r\pi}{2a}\right)^2 + \left(\frac{s\pi}{2b}\right)^2\right]^2 [w_{rs} - w_{0(rs)}] - \bar{p}_x h\left(\frac{r\pi}{2a}\right)^2 w_{rs}$$

$$- \frac{h\pi^4}{64a^2b^2}\sum_{n=1}^{9} [E_n - A_{0(n)}] \ldots [26]$$

where E_n is determined in the same manner as A_n, except that each b_{pq} term of Equations [18] is replaced by the corresponding e_{pq} term from Equation [24]. The deflection coefficients obtained from a solution of Equation [26] permit the evaluation, through Equations [10] and [22], of all the undetermined coefficients of F.

Substituting Equations [5], [19], and [20] into Equation [1a], integrating over the half-length of plate and adding to Equation [14], where $\bar{p}_y$ is now zero, the displacement at $x = \pm a$ is found to be

$$u_a = -\frac{\bar{p}_x a}{E} - \frac{\pi^2}{32a}\sum_{m=1,3,}^{\infty}\sum_{n=1,3,}^{\infty} m^2[w_{mn}^2 - w_{0(mn)}^2] \ldots [27]$$

Similarly

$$v_b = \mu \frac{p_x b}{E} - \frac{\pi^2}{32b} \sum_{m=1,3,}^{\infty} \sum_{n=1,3,}^{\infty} n^2 (w_{mn}^2 - w_{0(mn)}^2) + \frac{\pi}{aE} \sum_{p=2,4,}^{\infty} pC_p \sinh \frac{p\pi b}{2a} \cos \frac{p\pi x}{2a} \quad \ldots\ldots [28]$$

These equations verify the uniform displacement of the loaded edges and the freedom of the supported edges to distort in the plane of the plate.

Numerical Example of Case (1)—Square Plate

Case 1 will be solved for a square plate whose initial shape is described by the first term of Equation [7], the coefficient of which is taken as $w_{0(11)} = 0.1\,h$. This is a plausible eccentricity and it is one that permits comparison with an available solution for undistorted edges (5) in which square plates of the same initial curvature have been examined.

The deflection function of Equation [8] will be limited to the first three terms: w_{11}, w_{13}, and w_{31}. In the case of a flat plate whose edges are constrained to remain straight it can be seen[4] that the fourth deflection coefficient (w_{33}) is smaller than any of the first three, until the load ratio is slightly greater than 4. Furthermore, when p_x is approximately 3.7 p_w (corresponding to an average edge strain ratio of 7.01), three deflection coefficients predict the effective width within 2 per cent of the value determined with six coefficients.[5] Making some allowance for the effect of stress-free supported edges, it is felt that the three coefficients used in the following solution will reasonably describe the deflected shape at load ratios as high as 3. With only three nonzero deflection coefficients, the compatibility equation is

TABLE 1 STRESS COEFFICIENTS FROM EQUATION [10] WHEN $a = b$

$b_{02} = -\frac{E}{32}(W_{11}^2 + 9W_{31}^2 + 2W_{11}W_{13})$	$b_{24} = -\frac{E}{400}(W_{11}W_{13} + 25W_{13}W_{31})$
$b_{04} = -\frac{E}{64}(W_{11}W_{13})$	$b_{40} = -\frac{E}{64}(W_{11}W_{31})$
$b_{06} = -\frac{E}{256}(W_{13}^2)$	$b_{42} = -\frac{E}{400}(W_{11}W_{31} + 25W_{13}W_{31})$
$b_{20} = -\frac{E}{32}(W_{11}^2 + 9W_{13}^2 + 2W_{11}W_{31})$	$b_{44} = -\frac{E}{64}(W_{13}W_{31})$
$b_{21} = -\frac{E}{16}(W_{11}W_{13} + W_{11}W_{31} + 4W_{13}W_{31})$	$b_{60} = -\frac{E}{256}(W_{31}^2)$

identically satisfied by the ten b_{pq}-terms given in Table 1. The two nonvanishing $b_{0(pq)}$-coefficients become

$$b_{0(02)} = b_{0(20)} = -\frac{E}{32} w_{0(11)}^2 = -\frac{Eh^2}{3200}$$

Poisson's ratio is taken as 0.316 to afford comparison with recent literature (4, 5). In general, the solutions are based on $\mu = 0.316$ and $w_{0(11)} = 0.1\,h$, although solutions have been obtained for $\mu = 0$ and $w_{0(11)} = 0$ for comparative purposes.

For a square plate with a three-term deflection function, Equation [22] becomes

$$\left.\begin{aligned} 11.864\,C_2 &= b_{20} - b_{02} + b_{24} - b_{0(20)} \\ 267.77\,C_4 &= b_{40} - b_{42} + b_{44} \\ 6196\,C_6 &= b_{60} \end{aligned}\right\} \quad \ldots\ldots [29]$$

Substituting from Table 1, the additional stress coefficients of Table 3 are obtained. Converting with the aid of Table 2, and adding to the corresponding terms of Table 1, the total stress coefficients of Equation [24] may be obtained. Substituting

[4] Reference (4), Table III.
[5] Ibid., Table V.

TABLE 2 STRESS COEFFICIENTS FROM EQUATION [23] WHEN $a = b$

$C_{20} = -7.3523\,C_2$	$C_{40} = -85.226\,C_4$	$C_{60} = -1314.8\,C_6$
$C_{22} = 3.6762\,C_2$	$C_{42} = 109.089\,C_4$	$C_{62} = 2130.0\,C_6$
$C_{24} = -.5882\,C_2$	$C_{44} = -42.615\,C_4$	$C_{64} = -1260.4\,C_6$
$C_{26} = .1471\,C_2$	$C_{46} = 16.137\,C_4$	$C_{66} = 657.41\,C_6$

TABLE 3 ADDITIONAL STRESS COEFFICIENTS OF EQUATION [21] FOR CASE 1

(Stress-free supported edges, uniformly displaced loaded edges.)

	W_{11}^2	W_{13}^2	W_{31}^2	$W_{11}W_{13}$	$W_{11}W_{31}$	$W_{13}W_{31}$	constants
$10^5 C_2 =$	-2.6340	-23.7062		5.0575		15.8042	$.026340h^3$
$10^6 C_4 =$					-4.9016	17.5056	
$10^7 C_6 =$			-5.6040				

TABLE 4 EQUATIONS OF THE FAMILY OF EQUATION [26] FOR CASE 1

	0 =	0 =	0 =
1	.3704 K_{11}	9.26 K_{13}	9.26 K_{31}
$\frac{p_x(2a)^2}{\pi^2 E h^2}$	$-K_{11}$	$-K_{13}$	$-9K_{31}$
K_{11}^3	.08627	.09968	.06250
$K_{11}^2 K_{13}$	.2990	.6450	.3662
$K_{11}^2 K_{31}$	.1875	.3662	1.0369
$K_{11} K_{13}^2$	.6450	1.0059	1.4019
$K_{11} K_{13} K_{31}$	.7324	2.8058	3.4505
$K_{11} K_{31}^2$	1.0369	1.7253	0
K_{13}^3	.3347	1.9877	1.0458
$K_{13}^2 K_{31}$	1.4019	3.1573	6.3198
$K_{13} K_{31}^2$	1.7253	6.3198	0
K_{31}^3	0	0	5.1117
1	-.03704	0	0
K_{11}	-.000863	-.000997	-.000625
K_{13}	-.000997	-.002139	-.001162
K_{31}	-.000625	-.001162	-.005625

$a = b$, $\mu = 0.316$, and $p_m = 0$, and multiplying by $(2a)^4/(\pi^4 E h^4)$, the first equation of the set of Equation [26] becomes

$$p_{11} = 0 = 0.3704 \left(\frac{w_{11}}{h} - 0.1\right) - \frac{p_x(2a)^3}{\pi^3 E h^3} \left(\frac{w_{11}}{h}\right) - \frac{1}{4Eh^3} \left\{ \sum_{n=1}^{9} E_n - \sum_{n=1}^{9} A_{0(n)} \right\} \quad \ldots\ldots [30]$$

Introducing the dimensionless deflection coefficient $K_{mn} = w_{mn}/h$, and substituting the total stress coefficients, Equation [30] takes the form shown in Table 4. This set of equations, including those corresponding to $p_{13} = 0$ and $p_{31} = 0$, is solved by successive approximation. Solutions in nondimensional form are given in Table 5; the load ratios being based upon the critical stress of a square plate[6] which, for $\mu = 0.316$, is

$$p_w = \frac{\pi^2 D}{h(2b)^2} \left(\frac{b}{a} + \frac{a}{b}\right)^2 = 0.3704 \frac{\pi^2 E h^3}{(2a)^3} \quad \ldots\ldots [31]$$

[6] Reference (2c).

The nondimensional net center deflection given by

$$K_c = \sum_{m=1}^{3}\sum_{n=1}^{3}[K_{mn} - K_{k(mn)}] = K_{11} + K_{13} + K_{31} - 0.1 \ldots [32]$$

is plotted against the corresponding load ratio in Fig. 4. Load-deflection characteristics of the conventional problem[7] have been added for comparison.

From Equations [4] and [21], the median-fiber stress on the loaded edge is

$$\sigma_{x(a)}' = -p_x - \left(\frac{\pi}{2a}\right)^2 \sum_{p=0,2,}^{\infty}\sum_{q=0,2,}^{\infty}(-1)^{p/2}\, q^2[b_{pq} - b_{k(pq)}] \cos\frac{q\pi y}{2a} + \left(\frac{\pi}{2a}\right)^2 \sum_{p=2,4,}^{\infty}(-1)^{p/2}\, p^2 C_p \left[\left(1 - \frac{p\pi}{2}\coth\frac{p\pi}{2}\right)\cosh\frac{p\pi y}{2a} + \frac{p\pi y}{2a}\sinh\frac{p\pi y}{2a}\right] \ldots [33]$$

while that on the transverse center line is found to be

$$\sigma_{x(0)}' = -p_x - \left(\frac{\pi}{2a}\right)^2 \sum_{p=0,2,}^{\infty}\sum_{q=0,2,}^{\infty} q^2\,[b_{pq} - b_{k(pq)}] \cos\frac{q\pi y}{2a} + \left(\frac{\pi}{2a}\right)^2 \sum_{p=2,4,}^{\infty} p^2 C_p \left[\left(1 - \frac{p\pi}{2}\coth\frac{p\pi}{2}\right)\cosh\frac{p\pi y}{2a} + \frac{p\pi y}{2a}\sinh\frac{p\pi y}{2a}\right] \ldots [34]$$

These distributions, drawn to scale in Fig. 2, for a load ratio of 1.737, are seen to differ measurably from those associated with undistorted edges (see Fig. 3, where the corresponding distributions[8] for a load ratio of 1.722 have been indicated).

The median-fiber strain ratios at the center of the plate (D in Fig. 1), and at the mid-point (C) of the loaded edge are computed from Equations [5], [31], [33], and [34]; they are plotted in Figs. 5 and 6. The corresponding strains in a flat plate whose edges are constrained to remain straight have been included for comparison.

[7] Reference (5), fig. 2 which, like the graphs of reference (4), is based on six deflection coefficients.

[8] Reference (4), fig. 3.

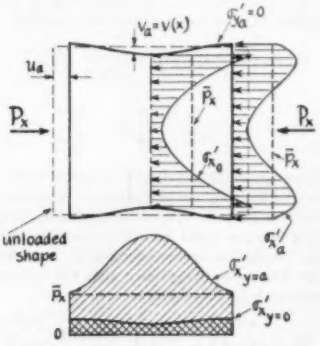

FIG. 2 STRESS DISTRIBUTIONS FOR CASE 1, $\bar{p}_x = 1.737\ p_{cr}$ (Stress-free supported edges, uniformly displaced loaded edges.)

TABLE 5 NUMERICAL VALUES OF DEFLECTION COEFFICIENTS FOR CASE 1

		K_{11}	$\frac{\bar{P}_x(2a)^2}{\pi^2 E h^2}$	$-K_{13}$	$-K_{31}$	K_c	$\frac{\bar{P}_x}{P_{cr}}$
$\mu = 0.316$	$K_{011} = 0.1$	.15	.1245	.000020	.000014	.050	.336
		.25	.2267	.000144	.000112	.150	.612
		.30	.2838	.000264	.000211	.200	.685
		.375	.2828	.000536	.000442	.274	.763
		.50	.3167	.001302	.001109	.398	.855
		.625	.3432	.002555	.002210	.520	.927
		.75	.3672	.00439	.00384	.642	.991
		.875	.3906	.00688	.00606	.762	1.056
		1.00	.4143	.01011	.00890	.881	1.119
		1.25	.4645	.01887	.01679	1.114	1.254
		1.50	.5192	.0313	.02795	1.341	1.402
		1.75	.5788	.0473	.0411	1.562	1.563
		2.00	.6432	.0671	.0574	1.775	1.737
		2.5	.7860	.1179	.0967	2.185	2.122
		3.0	.9455	.1858	.1431	2.575	2.553
		3.5	1.1218	.2640	.1952	2.941	3.029
		4.0	1.3140	.3572	.2516	3.291	3.548
		4.5	1.5228	.462	.296	3.642	4.111
	$K_{011} = 0$	.50	.3916	.001367	.001281	.497	1.057
		.75	.4175	.00448	.00418	.741	1.127
		1.00	.4521	.01023	.00951	.980	1.221
		1.5	.5444	.0315	.0286	1.440	1.470
		2.0	.6622	.0672	.0588	1.874	1.788
		2.5	.8012	.1178	.0984	2.284	2.163
$\mu = 0$	$K_{011} = 0.1$	.50	.2870	.001443	.001227	.397	.861
		.75	.3349	.00485	.00424	.641	1.005
		1.00	.3805	.01113	.00983	.879	1.142
		1.25	.4294	.02082	.01839	1.111	1.288
		1.50	.4829	.03423	.02995	1.336	1.449
		1.75	.5413	.0516	.0445	1.554	1.624
		2.00	.6055	.0729	.0618	1.765	1.817
		2.5	.7437	.1274	.1029	2.170	2.251
		3.0	.9004	.1976	.1515	2.551	2.701
		3.5	1.0729	.2824	.2047	2.913	3.219

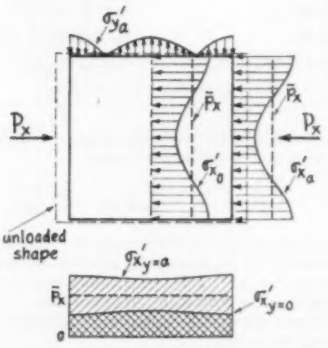

FIG. 3 STRESS DISTRIBUTIONS ASSOCIATED WITH UNDISTORTED EDGES (4), $\bar{p}_x = 1.722\ p_{cr}$

The extreme-fiber bending strain in the direction of loading is

$$\epsilon_x'' = \frac{1}{E}(\sigma_x'' - \mu\sigma_y'')$$

and, on substituting from Equation [6], the value at the center of the plate becomes

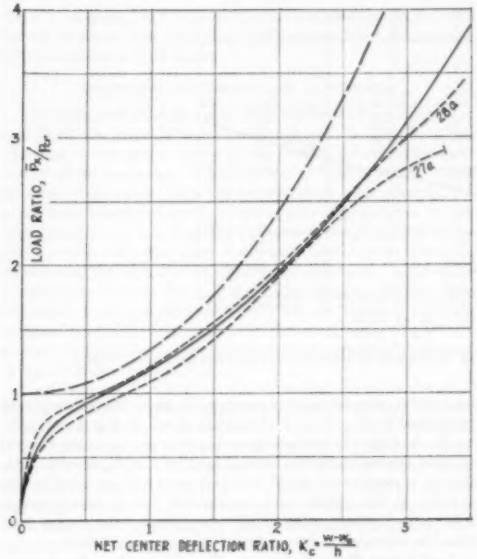

Conventional problem: Straight edges, $w_0 = 0$ $\mu = 0.316$ (Ref. 4)

Case 1: Stress-free supported edges, uniformly displaced loaded edges, $w_0 = 0.1h \cos\frac{2\pi x}{2a} \cos\frac{2\pi y}{2a}$, $\mu = 0.316$ unless otherwise specified

Case 1: Same as above except $w_0 = 0$

Test data from 20-in. × 20-in. × 1/4-in. fiberglas plates, $0.1 < \mu < 0.2$

FIG. 4 DEFLECTION BEHAVIOR OF A SIMPLY SUPPORTED SQUARE PLATE WITH SMALL INITIAL CURVATURE LOADED IN EDGE COMPRESSION

(Symbols used apply to Figs. 4 to 7, inclusive.)

$$\epsilon_x''_{(D)} = \pm \frac{h}{2}\left(\frac{\pi}{2a}\right)^2 \sum_{m=1,3,}^{\infty}\sum_{n=1,3,}^{\infty} m^2[w_{mn} - w_{0(mn)}] \quad . . [35]$$

Denoting the total extreme-fiber strain at the center of the concave side of the plate by ϵ_1 and that on the convex side by ϵ_2, the corresponding ratios of strain and strain difference are

$$\left.\begin{aligned} \frac{\epsilon_2}{\epsilon_{cr}} &= \left(\frac{\epsilon_x''}{\epsilon_{cr}}\right) + \left(\frac{\epsilon_x''}{\epsilon_{cr}}\right)_D \\ \frac{\epsilon_1 - \epsilon_2}{\epsilon_{cr}} &= 2.7 \sum_{m=1,3,}^{\infty}\sum_{n=1,3,}^{\infty} m^2[K_{mn} - K_{0(mn)}] \end{aligned}\right\} \quad . . [36]$$

These extreme-fiber strain ratios are found to vary as shown in Fig. 7.

As a check on the convergence of the deflection function, a more exact solution has been obtained by the inclusion of a fourth term, w_{33}. This additional term requires the formation of four more stress coefficients (b_{39}, b_{93}, b_{57}, and b_{75}) to identically satisfy Equation [2]. Solutions of this expanded set indicate significant changes at load ratios considerably in excess of 1. For example, with $\mu = 0.316$, $K_{0(11)} = 0.1$, and $K_{11} = 3.5$, it was found that $p_s = 2.933\ p_{cr}$, $K_s = 3.009$, and $\epsilon_{0(D)} = -0.051\ \epsilon_{cr}$. The change in the posteritical branch of the center axial-strain curve, Fig. 5, suggests slow convergence in respect to this quantity. The proportionately smaller change in the load-deflection curve, Fig. 4, suggests satisfactory convergence in respect to center deflection.

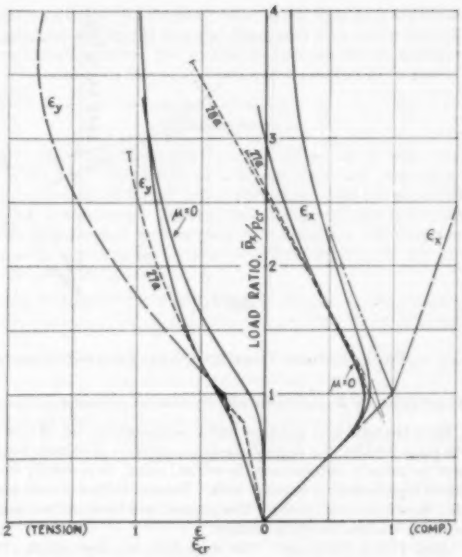

FIG. 5 MEDIAN-FIBER STRAIN RATIOS AT CENTER OF PLATE

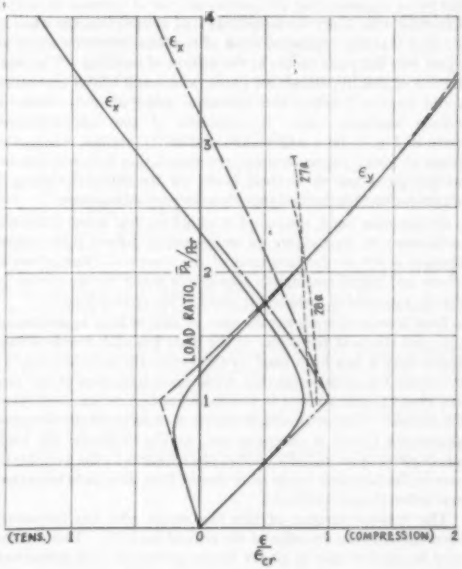

FIG. 6 MEDIAN-FIBER STRAIN RATIOS AT MID-POINT OF LOADED EDGE

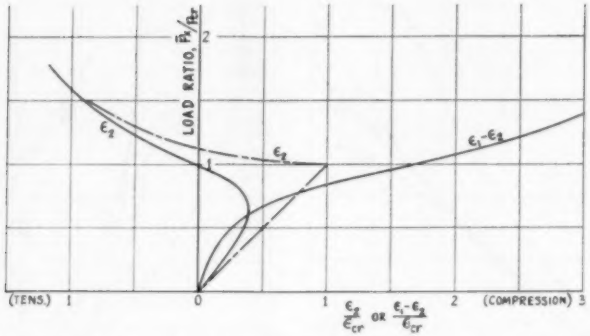

FIG. 7 EXTREME FIBER STRAINS AND STRAIN-DIFFERENCES—IN DIRECTION OF LOADING—AT CENTER OF PLATE, CASE 1

EVALUATION OF TECHNIQUES FOR DETERMINING CRITICAL LOAD

Since the total load in a compressed plate does not fall off when the plate buckles, the drop-of-the-beam criterion of column tests is of no value in determining the critical point; it is usually deduced from deflection or strain data. Some of the many methods that have been employed for this purpose will be examined here in the light of the foregoing solution.

Load Versus Deflection. The suggestion has been made (1) that the critical load be determined by the inflection point of the plot of load against center deflection. The correspondence of this point (representing the maximum rate of increase of lateral deflection with load) to the critical load seems plausible when it is noted that the minimum slope of the load-deflection curve of a perfectly flat plate occurs at the instant of buckling. The verification of this hypothesis for plates with small initial curvature would require locating the minimum slope of each curve—a tedious algebraic task. Examination of the load-deflection curve in Fig. 4 (or a larger-scale plot of it), verifies, within the limits of visual determination, the correlation between the inflection point and the critical load.[9] If the initial deviation is not excessive, this method appears to be very satisfactory.

On the other hand, the top-of-the-knee method is one of limited usefulness; it depends on an inadequately defined point whose location is left to the judgment of the observer. Regardless of where one might reasonably locate this point on the curves in Fig. 4, it would fall measurably short of the critical load.

Load Versus Compressive Strain. A plot of load against average axial strain at the center of the plate has such a well-defined break that it has been used to determine the critical load (1). However, Fig. 5 indicates that while the intersection of the two branches of such a curve is clearly defined, it occurs well below the critical. The surprising linearity of experimentally obtained load-strain plots[10] is deceptive for, as Fig. 5 shows, the load-strain curve of an initially nonflat plate returns to the asymptotic case of the flat plate much more slowly than it departs from that case below the critical load.

The vertical tangent of this load-strain plot has frequently been taken as the criterion of the critical load (7). This method may be applied only to plates whose precritical and postcritical load-strain rates are roughly comparable (as for the isotropic case considered here). In fact, the slopes shown in Fig. 5 are sufficiently dissimilar so that a large-scale plot reveals that the vertical tangent overestimates the critical load by 2 or 3 per cent. Although a number of strain measurements are required in the vicinity of the critical load to establish the transition curve, this method gives a more reliable indication of the critical load than the technique of extrapolating the postcritical slope.

Load Versus Strain Difference. The difference of the extreme-fiber (axial) strains at the center of the plate is shown in Fig. 7. Since the "strain difference" depends only upon the deflection, and not on the mean axial stress, reasoning analogous to that employed in connection with the load-deflection plot suggests that the critical load be determined by the inflection point of the strain-difference curve. Fig. 7 appears to reasonably establish this relationship.

Load Versus Strain Reversal. Fig. 7 shows that the extreme fiber (axial) strain at the mid-point of the convex side reverses its trend well below the critical load. This point of "strain reversal" is probably the least reliable of the methods considered here.

Load Versus Transverse Strain. A plot of load against average transverse strain at the center of the plate (ϵ_y-curves in Fig. 5) is not apt to give a reliable indication of the critical load because of the small magnitudes involved and the absence of pronounced changes in slope.

EXPERIMENTAL EVIDENCE

The theory and solutions of this paper were not available during the test program referred to (1); the critical loads were determined by one or more of the methods described. Of the four different combinations of lamination and load direction tested, only cross-laminated plates loaded parallel to the grain would be suitable for comparison. The load-strain histories of three 20-in. × 20-in. × 1/4-in. specimens of this type have been published (1); the tests of two of these specimens (27*a* and 28*a*) were considered satisfactory. These plates had greater initial deviations than would be expected in metal specimens but no effort could be made in routine testing to determine these eccentricities accurately. Comparison of their load-deflection plots with Fig. 4, and similar published work,[11] suggests that specimen 27*a* had an initial center offset of from 0.1 *h* to 0.15 *h*, while specimen 28*a* had a smaller eccentricity, say, 0.05 *h*.

Although Poisson's ratio was not determined unequivocally for this cross-laminate, it appears to have been between 0.1 and

[9] Space limitations prevent the inclusion of verifying equations, computations, and graphs but it was found that edge loading by either uniform stress or uniform strain gave load-deflection plots almost identical with that for uniform displacement. Essentially the same critical load would be determined by any of the three loading schemes mentioned.

[10] See, for example, reference (1), fig. 8, Group A.

[11] Reference (5), fig. 2.

0.2. Thus since μ fell between the limits considered in the preceding solutions, test data from such material would be acceptable for comparison with theory.

Comparison of Theory and Experiment

The variations of axial strain at the centers of specimens 27*a* and 28*a*[13] are given in nondimensional form in Fig. 5. (The variation of transverse strain at the center, measured on only one of these specimens, is also indicated.) The critical loads of these plates were originally estimated by extrapolating the postcritical branch of the load-strain plot but, in view of the dependence of the break in this curve upon the initial curvature and on Poisson's ratio, these loads have been revised upwardly in reducing the test data to nondimensional form. Guided by the estimated values of $w_{0(1)}$, the critical load of 27*a* has been increased by 12.4 per cent and that of 28*a* by 10 per cent. This compensates for the originally conservative estimates and affords a more reasonable comparison of the trends in strain and deflection in the postcritical regime.

The solution for $\mu = 0$ appears to agree with the measured axial strains. However, as indicated earlier, the inclusion of a fourth term in the deflection function brings the center-strain variation into better agreement with test data. Additional terms probably would further improve the agreement, perhaps to the point where solutions for the limiting cases ($\mu = 0, 0.316$) would bound the test data. In any event, the center axial strain appears to be more adequately described by the present theory than by the solution for undistorted edges.

Additional strains were measured on the axial center line at points 2 in. from the loaded edges. Projecting the indicated strain distribution to the loaded edges and averaging, the mid-point strain varies as shown in Fig. 6. The tendency of this strain to measurably lag the variation predicted by this paper (parts of which were shown to receive satisfactory experimental confirmation in Fig. 5) probably may be explained by unconsidered restraints along the loaded edges. In particular, the friction under the "effective-width" strips may be sufficient to prevent the plate from contracting along the loaded edges as freely as the theory permits. The transverse tensile forces thereby induced may be of such magnitude that the corresponding compresive strains (i.e., Poisson's effect) significantly modify the predicted axial-strain variation. Unfortunately, transverse strains were not measured near the loaded edges; the foregoing explanation will have to rest on its plausibility.

The adjusted load-deflection plots of these two plates are included in Fig. 4. Their agreement with the necessarily restricted solution is satisfactory; the inclusion of additional terms in the deflection function doubtlessly would improve the correlation at high load ratios ($\bar{p}_x > 3\bar{p}_{cr}$).

The axial-strain variation at the mid-point of the supported edge (*B* in Fig. 1) is not recorded here since it is usually of secondary interest; however, the measured strains were found to be in good agreement with this analysis.

If allowance is made for the considerable variations in thickness, elastic modulus, and Poisson's ratio which occur in low-pressure laminates, and for the fact that these tests were conducted on a production schedule, the correlation between the experimental evidence and the theory of this paper appears to be reasonably good.

[13] Reference (1), Fig. 8, group A.

Conclusions

1 The "large deflection" analysis presented in this paper for the edge compression of a simply supported, rectangular, isotropic plate with small initial curvature, stress-free supported edges, and uniformly displaced loaded edges appears sufficiently well substantiated by test data to warrant the following conclusions regarding the experimental determination of the true (flat plate) critical load:

(*a*) It corresponds closely, if not identically, to the inflection points of both the load-deflection curve and the strain-difference curve.

(*b*) It corresponds closely to the vertical tangent of the plot of load against axial strain at the center of the plate.

(*c*) It is underestimated by the junction of the precritical and the postcritical slopes of the load-strain curve in (*b*).

(*d*) It is not reliably indicated by either the top-of-the-knee, the strain-reversal, or the transverse-strain criteria.

2 Within moderate load ratios (say, $\bar{p}_x \lessapprox 3\bar{p}_{cr}$), the behavior of plates whose boundary conditions correspond to those described should be reasonably approximated by the load-deflection graph in Fig. 4 and by stress distributions comparable to those in Fig. 2.

Acknowledgments

The author would like to express his appreciation for the advice and encouragement given him by his thesis adviser, Dr. N. J. Hoff of the Polytechnic Institute of Brooklyn and his gratitude to Samuel Levy of the National Bureau of Standards, for fruitful discusions of the latter's ingenious method.

BIBLIOGRAPHY

1 "The Development of a Technique for Testing Stiff Panels in Edgewise Compression," by N. J. Hoff, B. A. Boley, and J. M. Coan, Proceedings of the Society for Experimental Stress Analysis, vol. 5, no. 2, 1948, pp. 14–24.

2 "Theory of Elastic Stability," by S. Timoshenko, McGraw-Hill Book Company, Inc., New York, N. Y., 1936, (*a*) pp. 390–395, (*b*) p. 323, and (*c*) p. 329.

3 "The Apparent Width of the Plate in Compression," by K. Marguerre, NACA TM No. 833, July, 1937.

4 "Bending of Rectangular Plates With Large Deflections," by Samuel Levy, NACA TN No. 846, May, 1942. (Also available as NACA TR No. 737, 1942.)

5 "Effect of Small Deviations From Flatness on Effective Width and Buckling of Plates in Compression," by Pai C. Hu, E. E. Lundquist, and S. B. Batdorf, NACA TN no. 1124, September, 1946.

6 "Analysis of Square Shear Web Above Buckling Load," by Samuel Levy, K. L. Fienup, and Ruth M. Woolley, NACA TN No. 962, February, 1945.

7 "Methods of Conducting Buckling Tests of Plywood Panels in Compression," by Forest Products Laboratory, Report No. 1554, December, 1946, p. 8.

Some Thin-Plate Problems by the Sine Transform

By L. I. DEVERALL[1] and C. J. THORNE,[2] SALT LAKE CITY, UTAH

General expressions for the deflection of thin rectangular plates are obtained for cases in which two opposite edges have arbitrary but given deflections and moments. The sine transform is used as a part of the method of solution, since solutions can be found for an arbitrary load for each set of edge conditions at the other two edges. Even for the classical cases, the use of the sine transform makes the process of solving the problem much easier. The six general solutions given are those which arise from all possible combinations of physically important edge conditions at the other two edges. Solutions for a specific load function can be found by integration or by the use of a table of sine transforms. Tables useful in application of the method to specific problems are included.

Introduction

THE finite Fourier sine transform is used here to solve problems in bending of thin plates in which two opposite edges of a homogeneous rectangular plate, Fig. 1, have arbitrary but given deflections and moments, and the other two edges have prescribed edge conditions. All of these edge

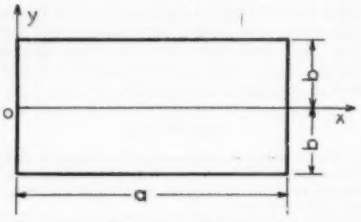

Fig. 1 The Plate

conditions must be consistent with the assumptions of thin-plate theory. The three physically important edge conditions seem to be given deflection and slope perpendicular to the edge, given deflection and moment per unit length about the edge, and given moment per unit length about the edge and reaction per unit length.[3] The possible combinations of these conditions on two opposite edges are the six cases for which solutions are given. Problems with other mathematically possible edge conditions are solvable by the method given here. The edge is called clamped, simply supported, or free, for deflection and slope zero, deflection and moment zero, moment and reaction zero, respectively.

For all edges simply supported, the method of Nadai and Levy[4] requires the determination of a function $w_1(x)$ which represents the deflection of a loaded strip parallel to the x-axis. This function must satisfy the differential equation of bending, and also the edge conditions at $x = 0$, and $x = a$. Also, it is necessary as part of the solution to expand $w_1(x)$ in a Fourier series over $0 < x < a$. For a uniform load, $w_1(x)$ is a polynomial of fourth degree. The sine-transform method does not require the determination of $w_1(x)$.

For a plate with two opposite edges simply supported, and the other two edges clamped, the solution is usually obtained by superposition of solutions. The deflection $w_1(x, y)$ for all edges simply supported is added to the deflection $w_2(x, y)$ for two opposite edges simply supported, and an arbitrary moment distribution at the other edges. The arbitrary moment distribution is determined by requiring the slope of deflection $(w_1 + w_2)$ to be zero at the appropriate edges. The solution of this same problem by the sine-transform method does not require application of the superposition principle, since all solutions by this method are obtained in the same way.

The advantages of the sine-transform method for problems of this type may be summarized as follows: (1) Solutions may be obtained for arbitrary loads in terms of a single trigonometric series; (2) solutions may be found for more general boundary conditions; (3) mathematical technique is simpler; (4) solutions for special cases may be found by substitution in a general formula.

The solution to any specific problem included in the type solved here may be obtained by applying the method presented here, or may be found by substituting in the appropriate case formula. The tables given are useful in carrying out the solution.

The Problem

The deflection $w(x, y)$ of the middle surface of a thin homogeneous isotropic plate must satisfy the following differential equation over the region S bounded by the plate, Fig. 1

$$\frac{\partial^4 w}{\partial x^4} + 2\frac{\partial^4 w}{\partial x^2 \partial y^2} + \frac{\partial^4 w}{\partial y^4} = \frac{q(x, y)}{D} \quad \ldots\ldots [1]$$

where

$q(x, y)$ = load per unit area normal to surface of plate
$D = E h^3/12(1 - \nu^2)$
h = thickness of plate
E = Young's modulus of material
ν = Poisson's ratio of material

In all problems to be considered, the edge conditions, Fig. 1, will be at $x = 0$

$$w(0, y) = w_1(y) \quad \ldots\ldots [2]$$

$$M_x|_{x=0} = -D\left[\frac{\partial^2 w}{\partial x^2} + \nu\frac{\partial^2 w}{\partial y^2}\right]_{x=0} = M_1(y) \quad \ldots\ldots [3]$$

[1] Instructor in Mathematics, University of Utah.

[2] Associate Professor of Mathematics, University of Utah.

[3] "Theory of Plates and Shells," by S. Timoshenko, first edition, McGraw-Hill Book Company, Inc., New York, N. Y., 1940, pp. 89, 91.

Contributed by the Applied Mechanics Division and presented at the Annual Meeting, New York, N. Y., November 26–December 1, 1950, of The American Society of Mechanical Engineers.

Discussion of this paper should be addressed to the Secretary, ASME, 29 West 39th Street, New York, N. Y., and will be accepted until July 10, 1951, for publication at a later date. Discussion received after the closing date will be returned.

Note: Statements and opinions advanced in papers are to be understood as individual expressions of their authors and not those of the Society. Manuscript received by the Applied Mechanics Division, March 13, 1950. Paper No. 50—A-13.

[4] "Theory of Plates and Shells," by S. Timoshenko, pp. 125, 126.

and at $x = a$

$$w(a, y) = w_3(y) \quad [4]$$

$$M_x|_{x=a} = -D\left[\frac{\partial^2 w}{\partial x^2} + \nu\frac{\partial^2 w}{\partial y^2}\right]_{x=a} = M_3(y) \quad [5]$$

The six cases for edge conditions at the other two edges $y = \pm b$ are as follows:

Case 1. Two edges fixed

$$w(x, y) = w_1(x) \text{ at } y = b \quad [6]$$

$$\frac{\partial w}{\partial y} = S_1(x) \text{ at } y = b \quad [7]$$

and

$$w(x, y) = w_2(x) \text{ at } y = -b \quad [8]$$

and

$$\frac{\partial w}{\partial y} = S_2(x) \text{ at } y = -b \quad [9]$$

Case 2. Deflection and moments given, Equations [6] and [8] with

$$M_y = -D\left[\frac{\partial^2 w}{\partial y^2} + \nu\frac{\partial^2 w}{\partial x^2}\right] = M_1(x) \text{ at } y = b \quad [10]$$

and

$$M_y = -D\left[\frac{\partial^2 w}{\partial y^2} + \nu\frac{\partial^2 w}{\partial x^2}\right] = M_2(x) \text{ at } y = -b \quad [11]$$

Case 3. Moments and reactions given, Equations [10] and [11] with

$$R_y = -D\left[\frac{\partial^3 w}{\partial y^3} + (2-\nu)\frac{\partial^3 w}{\partial y\,\partial x^2}\right] = R_1(x) \text{ at } y = b \quad [12]$$

and

$$R_y = -D\left[\frac{\partial^3 w}{\partial y^3} + (2-\nu)\frac{\partial^3 w}{\partial y\,\partial x^2}\right] = R_2(x) \text{ at } y = -b \quad [13]$$

Case 4. One edge fixed ($y = b$), and one with deflection and moment given ($y = -b$), Equations [6], [7], [8], and [11].

Case 5. One edge with moment and reaction given ($y = b$), and one edge fixed ($y = -b$), Equations [8], [9], [10], and [12].

Case 6. One edge with moment and reaction given ($y = b$), and one edge with deflection and moment given ($y = -b$), Equations [8], [10], [11], and [12].

The Sine Transform

Let $y(x)$ be a function which is equal to its Fourier sine series for $0 < x < a$. The finite Fourier sine transform of $y(x)$ is the function $y_s(\alpha)$ obtained by the linear integral operation defined as follows

$$y_s(\alpha) \equiv S[y(x)] = \int_0^a y(x) \sin \alpha x\, dx \quad [14]$$

where $\alpha \equiv n\pi/a$, $(0 < x < a,\ n = 1, 2, \ldots)$.

Since

$$y(x) = \sum_{n=1}^{\infty} b_n \sin \alpha x, \quad (0 < x < a) \quad [15]$$

where

$$b_n = (2/a)\int_0^a y(x) \sin \alpha x\, dx = (2/a)\, y_s(\alpha) \quad [16]$$

we have

$$y(x) = (2/a)\sum_{n=1}^{\infty} y_s(\alpha) \sin \alpha x, \quad (0 < x < a) \quad [17]$$

This expression, Equation [17], for $y(x)$ is the "inverse sine transform" of $y_s(\alpha)$. Repeated integration by parts yields the following formulas for the transforms of second and fourth derivatives

$$S\left[\frac{d^2 y}{dx^2}\right] = -\alpha^2 y_s(\alpha) - \alpha\,[(-1)^n y(a) - y(0)] \quad [18]$$

$$S\left[\frac{d^4 y}{dx^4}\right] = \alpha^4 y_s(\alpha) - \alpha[(-1)^n y'(a) - y'(0)] + \alpha^2\,[(-1)^n\, y(a) - y(0)] \quad [19]$$

When writing the sine transform (or inverse transform) of any function, we shall assume that the function has properties necessary for that transform (or inverse transform) to exist.[4] Also, we assume continuity of all derivatives.

The Solution

By taking the sine transform of Equation [1] with respect to x, we have

$$\frac{d^4 w_s(\alpha, y)}{dy^4} - 2\alpha^2\frac{d^2 w_s(\alpha, y)}{dy^2} + \alpha^4 w_s(\alpha, y) = Q(\alpha, y) \quad [20]$$

where

$$Q(\alpha, y) = \frac{q_s(\alpha, y)}{D} + \alpha\left[(-1)^n\frac{\partial^3 w(a, y)}{\partial x^3} - \frac{\partial^3 w(0, y)}{\partial x^3}\right] + 2\alpha\left[(-1)^n\frac{\partial^3 w(a, y)}{\partial y^2} - \frac{\partial^3 w(0, y)}{\partial y^2}\right] - \alpha^3\,[(-1)^n\, w(a, y) - w(0, y)] \quad [21]$$

This may be written

$$Q(\alpha, y) = \frac{q_s(\alpha, y)}{D} + \alpha\left\{(-1)^{n+1}\left[\frac{M_2(y)}{D} + \nu w_2''(y)\right] + \frac{M_1(y)}{D} + \nu w_1''(y)\right\} + 2\alpha[(-1)^n w_2''(y) - w_1''(y)] - \alpha^3[(-1)^n w_2(y) - w_1(y)] \quad [22]$$

The solution of Equation [20] is

$$w_s(\alpha, y) = (C_1 + C_2 y)\sinh \alpha y + (C_3 + C_4 y)\cosh \alpha y + G(\alpha, y) \quad [23]$$

where $G(\alpha, y)$ is a particular solution of Equation [20] corresponding to the function $Q(\alpha, y)$ (see Table 2).

The transformed edge conditions, Equations [6] to [13], inclusive, are

$$w_s(\alpha, b) = w_{1s}(\alpha) \quad [24]$$

$$w_s'(\alpha, b) = S_{1s}(\alpha) \quad [25]$$

$$w_s(\alpha, -b) = w_{2s}(\alpha) \quad [26]$$

$$w_s'(\alpha, -b) = S_{2s}(\alpha) \quad [27]$$

$$-w_s''(\alpha, b) + \nu\alpha^2 w_s(\alpha, b) + \alpha\nu[(-1)^n w(a, b) - w(0, b)] = M_{1s}(\alpha)/D \quad [28]$$

[4] "Modern Operational Mathematics in Engineering," by R. V. Churchill, first edition, McGraw-Hill Book Company, Inc., New York, N. Y., 1944, pp. 267, 269.

$$-w_s''(\alpha, -b) + \nu\alpha^2 w_s(\alpha, -b) + \alpha\nu\,[(-1)^n w(a, -b) - w(0, -b)] = M_{ss}(\alpha)/D \quad \ldots\ldots [29]$$

$$-w_s'''(\alpha, b) + (2-\nu)\,\alpha^2 w_s'(\alpha, b) + (2-\nu)\,\alpha[(-1)^n w'(a, b) - w'(0, b)] = R_{1s}(\alpha)/D \quad \ldots\ldots [30]$$

$$-w_s'''(\alpha, -b) + (2-\nu)\,\alpha^2 w_s'(\alpha, -b) + (2-\nu)\,\alpha[(-1)^n w'(a, -b) - w'(0, -b)] = R_{2s}(\alpha)/D \quad \ldots [31]$$

where

$$w_s' = \frac{dw_s(\alpha, y)}{dy}, \text{ etc.}$$

From the edge conditions at the edges $y = \pm b$, we can evaluate the constants C_1, C_2, C_3, and C_4 in Equation [23]. We will give first the values of these constants for certain of the edge functions required to be zero (Cases 1(a) to 6(a), inclusive). The values of the constants C_1, C_2, C_3, and C_4 for the edge functions not equal to zero will be written in terms of the corresponding constants for the edge functions equal to zero.

The constants for Cases 1(a) to 6(a), inclusive, are as follows:

Case 1(a). The edges $y = b$, and $y = -b$ clamped; functions w_2, w_4, S_1, and S_2 zero

$$\left.\begin{aligned}
&(\sinh 2ab - 2ab)\,C_1 = b\cosh ab\,[G'(\alpha, b) + G'(\alpha, -b)] - (\cosh ab + ab\sinh ab)\,[G(\alpha, b) - G(\alpha, -b)]\\
&(\sinh 2ab + 2ab)\,C_2 = -\cosh ab\,[G'(\alpha, b) - G'(\alpha, -b)] + \alpha\sinh ab\,[G(\alpha, b) + G(\alpha, -b)]\\
&(\sinh 2ab + 2ab)\,C_3 = b\sinh ab\,[G'(\alpha, b) - G'(\alpha, -b)] - (\sinh ab + ab\cosh ab)\,[G(\alpha, ab) + G(\alpha, -b)]\\
&(\sinh 2ab - 2ab)\,C_4 = -\sinh ab\,[G'(\alpha, b) + G'(\alpha, -b)] + \alpha\cosh ab\,[G(\alpha, b) - G(\alpha, -b)]
\end{aligned}\right\} \quad \ldots\ldots [32]$$

Case 2(a). The edges $y = b$, and $y = -b$ simply supported; functions w_2, w_4, M_3, and M_4 zero

$$\left.\begin{aligned}
&4\alpha\sinh^2 ab\,C_1 = b\cosh ab\,[G''(\alpha, b) - G''(\alpha, -b)] - (2\alpha\sinh ab + \alpha^2 b\cosh ab)\,[G(\alpha, b) - G(\alpha, -b)]\\
&4\alpha\cosh ab\,C_2 = -[G''(\alpha, b) + G''(\alpha, -b)] + \alpha^2\,[G(\alpha, b) + G(\alpha, -b)]\\
&4\alpha\cosh^2 ab\,C_3 = b\sinh ab\,[G''(\alpha, b) + G''(\alpha, -b)] - (2\alpha\cosh ab + \alpha^2 b\sinh ab)\,[G(\alpha, b) + G(\alpha, -b)]\\
&4\alpha\sinh ab\,C_4 = -[G''(\alpha, b) - G''(\alpha, -b)] + \alpha^2[G(\alpha, b) - G(\alpha, -b)]
\end{aligned}\right\} \quad \ldots\ldots [33]$$

Case 3(a). The edges $y = b$ and $y = -b$ free; functions w_1, w_2, M_3, M_4, R_1, and R_2 zero.

$$\left.\begin{aligned}
&\alpha^2[(3-2\nu-\nu^2)\sinh 2ab + 2ab(1-\nu)^2]C_1 = [2\sinh ab + ab(1-\nu)\cosh ab]\,\{G'''(\alpha, b)\\
&+ G'''(\alpha, -b) - \alpha^2(2-\nu)\,[G'(\alpha, b) + G'(\alpha, -b)]\} + [(1+\nu)\cosh ab - ab(1-\nu)\sinh ab]\\
&\{-[G''(\alpha, b) - G''(\alpha, -b)] + \alpha^2\nu[G(\alpha, b) - G(\alpha, -b)]\}\\
&\alpha^2[(3+\nu)\sinh 2ab - 2ab(1-\nu)]C_2 = \cosh ab\,\{\alpha^2(2-\nu)\,[G'(\alpha, b) - G'(\alpha, -b)]\\
&-[G'''(\alpha, b) - G'''(\alpha, -b)]\} + \sinh ab\,\{\alpha^2\nu[G(\alpha, b) + G(\alpha, -b)] - \alpha[G''(\alpha, b) + G''(\alpha, -b)]\}\\
&\alpha^2[(3-2\nu-\nu^2)\sinh 2ab - 2ab(1-\nu)^2]C_3 = [2\cosh ab + ab(1-\nu)\sinh ab]\,\{-\alpha^2(2-\nu)\\
&[G'(\alpha, b) - G'(\alpha, -b)] + [G'''(\alpha, b) - G'''(\alpha, -b)]\} + [\alpha(1+\nu)\sinh ab - (1-\nu)\,\alpha^2 b\cosh ab]\\
&\{\alpha^2\nu[G(\alpha, b) + G(\alpha, -b)] - [G''(\alpha, b) + G''(\alpha, -b)]\}, \quad \alpha^2[(3+\nu)\sinh 2ab + 2ab(1-\nu)]C_4\\
&= \sinh ab\,\{-[G'''(\alpha, b) + G'''(\alpha, -b)] + \alpha^2(2-\nu)[G'(\alpha, b)\\
&+ G'(\alpha, -b)]\} + \cosh ab\,\{-\alpha\,[G''(\alpha, b) - G''(\alpha, -b)] + \alpha^2\nu[G(\alpha, b) - G(\alpha, -b)]\}
\end{aligned}\right\} \quad \ldots\ldots [34]$$

Case 4(a). One edge clamped ($y = b$) and one edge simply supported ($y = -b$); functions w_2, w_4, S_1, and M_4 zero

$$\left.\begin{aligned}
&2\alpha\sinh ab\,(\sinh 4ab - 4ab)\,C_1 = -b\sinh 2ab\,(\sinh 2ab + 2ab)\,G''(\alpha, -b) + 8ab\cosh^2 ab\sinh ab\,G'(\alpha, b)\\
&-\alpha[4ab(\cosh^2 ab\cosh 2ab - 1) + \sinh 4ab]\,G(\alpha, b) + \alpha[4ab(\cosh^4 ab - 1) + 2\alpha^2 b^2\sinh 2ab\\
&\qquad + \sinh 4ab]\,G(\alpha, -b)\\
&2\alpha\cosh ab(\sinh 4ab - 4ab)\,C_2 = 4\,(ab\sinh^2 ab - \sinh ab\cosh^2 ab + ab)G''(\alpha, -b)\\
&-2\alpha\sinh^2 2ab\,G'(\alpha, b) + \alpha^2\sinh 4ab\,G(\alpha, b) + 4\alpha^2\,(\sinh^2 ab\cosh ab - ab\cosh^2 ab)\,G(\alpha, -b)\\
&2\alpha\cosh^2 ab(\sinh 4ab - 4ab)\,C_3 = b\cosh ab\sinh 2ab\,(\sinh 2ab - 2ab)\,G''(\alpha, -b)\\
&+ 8ab\sinh^2 ab\cosh^2 ab\,G'(\alpha, b) + [4\alpha^2 b\cosh ab\,(1 - \sinh^2 ab\cosh 2ab)\\
&- \alpha\cosh ab\sinh 4ab]\,G(\alpha, b) + [4\cosh ab(1 - \sinh^4 ab) + 4\alpha^2 b^2\sinh ab\cosh^2 ab - \alpha\cosh ab\sinh 4ab]\,G(\alpha, -b)\\
&\alpha(\sinh 4ab - 4ab)\,C_4 = \sinh ab(\sinh 2ab + 2ab)\,G''(\alpha, -b) - 4\alpha\cosh^2 ab\sinh ab\,G'(\alpha, b)\\
&\qquad + 2\alpha^2\cosh ab\cosh 2ab\,G(\alpha, b) - 2\alpha^2\,(\cosh^2 ab + ab\sinh ab)\,G(\alpha, -b)
\end{aligned}\right\} \quad \ldots [35]$$

Case 5(a). One edge free ($y = b$), and one edge clamped ($y = -b$); functions w_1, w_2, w_4, S_2, M_4, and R_1 zero

$$a^3F_2C_2 = N_2$$

where

$$\left.\begin{aligned}
&F_2 = (1-\nu)^2 \sinh ab(\sinh 2ab - ab)^2 + 4(1-\nu)(\sinh 2ab - 2ab)(\cosh^2 ab + \nu \sinh^2 ab)\cosh ab \\
&+ 4\cosh 2ab(2ab \cosh ab - \sinh 2ab) + 4\nu \cosh ab(\sinh 2ab - 2ab\cosh 2ab) \\
&N_2 = [2\sinh^2 ab - (1-\nu)\sinh ab \cosh ab(\sinh 2ab - 2ab)]G'''(\alpha, b) \\
&-\alpha[(1-\nu)\sinh^2 ab(\sinh 2ab - 2ab) + \sinh 2ab]G''(\alpha, b) + \alpha^2(2-\nu)[\sinh ab(1-\nu)\cosh ab(\sinh 2ab - 2ab) \\
&- 2\sinh^2 ab]G'(\alpha, b) + \alpha^3(1-\nu)[2(\cosh^2 2ab - \cosh^2 ab) - (1-\nu)\sinh ab \cosh ab(\sinh 2ab - 2ab)](G\alpha', -b) \\
&+ \alpha^3\nu[(1-\nu)\sinh^2 ab(\sinh 2ab - 2ab) + \sinh 2ab]G(\alpha, b) + \alpha^3(1-\nu)[(\sinh 4ab - \sinh 2ab) \\
&- (1-\nu)\sinh^2 ab(\sinh 2ab - 2ab)]G(\alpha, -b) \\
&2F_2\alpha^3 \cosh 2ab\, C_4 = F_2[-\cosh ab\, G'''(\alpha, b) - \alpha \sinh ab\, G''(\alpha, b) + \alpha^2(2-\nu)\cosh ab\, G'(\alpha, b) \\
&- (1-\nu)\alpha^2 \cosh ab\, G'(\alpha, -b) + \alpha^3\nu \sinh ab\, G(\alpha, b) - \alpha^3(1-\nu)\sinh ab \cdot G(\alpha, -b)] \\
&\qquad -N_2[(1+\nu)\sinh 2ab - 2ab(1-\nu)] \\
&\alpha C_2 = C_3 \sinh^2 ab - C_4(\sinh ab \cosh ab - ab) - \sinh ab\, G'(\alpha, -b) - \alpha \cosh ab\, G(\alpha, -b) \\
&\sinh ab\, C_1 = C_2 b \sinh ab + (C_3 - C_4 b)\cosh ab + G(\alpha, -b)
\end{aligned}\right\} \quad \ldots\ldots [36]$$

Case 6(a). One edge free ($y = b$), and one edge simply supported ($y = -b$); functions w_1, w_2, w_4, M_2, M_4, and R_1 zero

$$2\alpha^2(1-\nu)\sinh^2 ab\, C_1 = [-\sinh ab - ab(1-\nu)\cosh ab]G''(\alpha, -b) + [-G''(\alpha, b) + \alpha^2\nu G(\alpha, b)]\sinh ab + \alpha^2[(2-\nu)\sinh ab + ab(1-\nu)\cosh ab]G(\alpha, -b) - 2(M_2/F_2)\cosh ab\,[2\sinh ab + ab(1-\nu)\cosh ab]$$

where

$$\left.\begin{aligned}
&M_2 = -2\sinh^2 ab \cosh ab\, G'''(\alpha, b) - 2\alpha \sinh ab \cosh 2ab\, G''(\alpha, b) + 2\alpha[\sinh ab \\
&- (3+\nu)\sinh ab \cosh^2 ab - ab(1-\nu)\cosh ab]G''(\alpha, -b) + 4\alpha^2(2-\nu)\sinh^2 ab \cosh ab\, G'(\alpha, b) \\
&\qquad + 2\alpha^3\nu \sinh ab \cosh 2ab\, G(\alpha, b) + 2\alpha^3[\sinh ab(3\cosh^2 ab + \nu \sinh^2 ab) \\
&+ ab(1-\nu)\cosh ab]G(\alpha, -b) \\
&F_2 = \alpha[(3+\nu)\sinh 4ab + 4ab(1-\nu)], \quad \alpha C_2 = M_2/F_2 \\
&2\alpha^2(1-\nu)\cosh ab\, C_3 = -G''(\alpha, b) - G''(\alpha, -b) + \alpha^2\nu[G(\alpha, b) + G(\alpha, -b)] - (M_2/F_2)[4\cosh ab \\
&\qquad + 2ab(1-\nu)\sinh ab] \\
&2\alpha \sinh ab\, C_4 = G''(\alpha, -b) - \alpha^2 G(\alpha, -b) + 2(M_2/F_2)\cosh ab
\end{aligned}\right\} \quad \ldots\ldots [37]$$

We shall now find the constants C_1, C_2, C_3, and C_4 for Cases 1 to 6, inclusive:

Case 1. In the constants of Case 1(a), replace

$$G(\alpha, b) \text{ by } G(\alpha, b) - w_{1s}(\alpha) \quad \ldots\ldots [38]$$

$$G(\alpha, -b) \text{ by } G(\alpha, -b) - w_{4s}(\alpha) \quad \ldots\ldots [39]$$

$$G'(\alpha, b) \text{ by } G'(\alpha, b) - S_{1s}(\alpha) \quad \ldots\ldots [40]$$

$$G'(\alpha, -b) \text{ by } G'(\alpha, -b) - S_{2s}(\alpha) \quad \ldots\ldots [41]$$

Case 2. In the constants of Case 2(a), use Equations [38] and [39] and replace

$$G''(\alpha, b) \text{ by } G''(\alpha, b) - \alpha^2\nu w_{1s}(\alpha) - \alpha\nu[(-1)^n w(a, b) - w(0, b)] + M_{2s}(\alpha)/D \quad \ldots\ldots [42]$$

$$G''(\alpha, -b) \text{ by } G''(\alpha, -b) - \alpha^2\nu w_{4s}(\alpha) - \alpha\nu[(-1)^n w(a, -b) - w(0, -b)] + M_{4s}(\alpha)/D \quad \ldots\ldots [43]$$

Case 3. In the constants of Case 3(a), replace

$$G''(\alpha, b) \text{ by } G''(\alpha, b) - \alpha\nu[(-1)^n w(a, b) - w(0, b)] + M_{2s}(\alpha)/D \quad \ldots\ldots [44]$$

$$G''(\alpha, -b) \text{ by } G''(\alpha, -b) - \alpha\nu[(-1)^n w(a, -b) - w(0, -b)] + M_{4s}(\alpha)/D \quad \ldots\ldots [45]$$

$$G'''(\alpha, b) \text{ by } G'''(\alpha, b) - (2-\nu)\alpha[(-1)^n w'(a, b) - w'(0, b)] + R_{1s}(\alpha)/D \quad \ldots\ldots [46]$$

$$G'''(\alpha, -b) \text{ by } G'''(\alpha, -b) - (2-\nu)\alpha[(-1)^n w'(a, -b) - w'(0, -b)] + R_{2s}(\alpha)/D \quad \ldots\ldots [47]$$

Case 4. In the constants of Case 4(a) use Equations [38], [39], [40], and [43].

Case 5. In the constants of Case 5(a) use Equations [44], [46], [39], and [41].

Case 6. In the constants of Case 6(a) use Equations [44], [46], [39], and [43].

The deflection $w(x, y)$ is given by the inverse sine transform of $w_s(\alpha, y)$

$$w(x, y) = (2/a)\sum_{n=1}^{\infty} w_s(n\pi/a, y)\sin(n\pi x/a) \quad \ldots\ldots [48]$$

It should be noted that the foregoing procedure is formal, and for any particular example, the convergence of $w(x, y)$ and its derivatives must be investigated.

In working out particular examples, it is sometimes advantageous to make use of the linear properties of Equation [20] and the sine transform. In addition, if

$$q(x, y) = f(x)\phi(y) \quad \ldots\ldots [49]$$

then

$$q_s(\alpha, y) = f_s(\alpha)\phi(y) \quad \ldots\ldots [50]$$

In many cases, the function $f_s(\alpha)$ can be found from Table 1, and the part of the particular solution $G(\alpha, b)$ corresponding to the term $q_s(\alpha, y)/D$ from Table 2. Table 2 is also useful in getting the parts of the particular solution $G(\alpha, y)$ which correspond to the other terms in the right-hand member of Equation [21]. The second part of Table 1 is useful in case the load function $q(x, y)$ is sectionally continuous, or in case the plate is loaded over only part of its surface.

TABLE 1 SINE TRANSFORMS

	$f(x)$	$f_s(n) = \int_0^a f(x) \sin \alpha x\,dx$, where $\alpha = n\pi/a$	$S\left[f(x)\right]_c^d = \int_c^d f(x) \sin \alpha x\,dx$, $(0 < c < d < a)$
1.	1	$\frac{1 - (-1)^n}{\alpha}$	$(\cos \alpha c - \cos \alpha d)/\alpha$
2.	x	$a(-1)^{n+1}/\alpha$	$(\sin \alpha d - \sin \alpha c)/\alpha^2$ $- (d \cos \alpha d - c \sin \alpha c)/\alpha$
3.	x^2	$a^2(-1)^{n-1}/\alpha$ $-2\left[1 - (-1)^n\right]/\alpha^3$	$2(\cos \alpha d - \cos \alpha c)/\alpha^3$ $+ 2(d \sin \alpha d - c \sin \alpha c)/\alpha^2$ $+ d^2(\cos \alpha d - c^2 \cos \alpha c)/\alpha$
4.	$a - x$	a/α	$a\,S\left[1\right]_c^d - S\left[x\right]_c^d$
5.	$a^2 - x^2$	$a^2 S\left[1\right] - S\left[x^2\right]$	$a^2 S\left[1\right]_c^d - S\left[x\right]_c^d$
6.	$e^{\beta x}$	$\frac{\alpha\left[1-(-1)^n e^{\beta a}\right]}{\alpha^2 + \beta^2}$	$e^{\beta d}(\beta \sin \alpha d - \alpha \cos \alpha d)/(\alpha^2 + \beta^2)$ $- e^{\beta c}(\beta \sin \alpha c - \alpha \cos \alpha c)/(\alpha^2 + \beta^2)$
7.	$\sin(mnx/a)$, $m = 1, 2, \ldots$	$= a/2$, if $n = m$ $= 0$, if $n \neq m$	$\frac{1}{2}\left[d - c + \frac{(\sin 2\alpha c - \sin 2\alpha d)}{2\alpha}\right]$ $\frac{\left[\sin(m/n - 1)\alpha d - \sin(m/n - 1)\alpha c\right]}{2\alpha(m/n - 1)}$ $- \frac{\left[\sin(m/n + 1)\alpha d - \sin(m/n + 1)\alpha c\right]}{2\alpha(m/n + 1)}$
8.	$\sin \beta x$, $\beta \neq m\pi/a$, $n = 1, 2, 3, \ldots$	$\frac{\sin(\beta - \alpha)a}{2(\beta - \alpha)}$ $- \frac{\sin(\beta + \alpha)a}{2(\beta + \alpha}$	Same as second part of No. 7, when $n \neq m$, with $m = a\beta/\pi$.
9.	$\cos(mnx/a)$ $m = 1, 2, \ldots$	$= 0$, $n = n$ $= \frac{\alpha}{\alpha^2 - m^2\pi^2/a^2}\left[1 - (-1)^{n+1}\right]$, $n \neq m$.	$(\cos 2\alpha c - \cos 2\alpha d)/4\alpha$ $\frac{\left[\cos(m\pi/a - \alpha)c - \cos(m\pi/a - \alpha)\,d\right]}{2(\alpha - m\pi/a)}$ $+ \frac{\left[\cos(m\pi/a + \alpha)c - \cos(m\pi/a + \alpha)d\right]}{2(\alpha - m\pi/a)}$
10.	$\cos \beta x$, $b \neq m\pi/a$, $n = 1, 2, 3, \ldots$	$\frac{\alpha\left[1-(-1)^n \cos(\beta\pi/a)\right]}{\alpha^2 - \beta^2}$	Same as second part of No. 9 when $n \neq m$ with $m = a\beta/\pi$.
11.	$f(x) = x$, for $0<x<a/2$ $f(x) = a - x)$, for $a/2<x<a$	$(2/\alpha^2)\sin(\alpha a/2)$	

EXAMPLES

If in Case 2(a) we take w_1, w_2, M_1, and M_2 equal to zero, and $q(x, y) = q_0$, where q_0 is constant, we obtain a solution given by Timoshenko.[6] The values of $q_s(\alpha, y)$ and $G(\alpha, y)$ may be obtained from Table 1 (No. 1) and Table 2 (No. 1).

As a second example, we shall consider a plate with two opposite edges simply supported, and two edges clamped (Case 1(a) with w_1, w_2, M_1, and M_2 zero), and with load function (q_0 constant)

$$\left.\begin{aligned} q(x, y) &= q_0 x,\ 0 < x < a/2 \\ q(x, y) &= q_0(a - x),\ a/2 < x < a \end{aligned}\right\} \ldots\ldots\ldots [51]$$

The function $G(\alpha, y)$ from Table 1 (No. 11), and Table 2 (No. 1) is equal to

$$G(\alpha, y) = q_0(2/\alpha^5 D)\sin(\alpha a/2) \ldots\ldots\ldots [52]$$

The deflection $w(x, y)$ then is

$$w(x, y) = (8q_0/aD)\sum_{n=1}^{\infty}\left[\frac{y \sinh \alpha b \sin(\alpha a/2)\sinh \alpha y}{\alpha^5(\sinh 2\alpha b + 2\alpha b)} - \frac{(\sinh \alpha b + \alpha b \cosh \alpha b)\sin(\alpha a/2)\cosh \alpha y}{\alpha^5(\sinh 2\,\alpha b + 2\,\alpha b)}\right]\sin \alpha x \ldots [53]$$

[6] Reference (3), p. 128.

TABLE 2 PARTICULAR SOLUTIONS

	$g(a, y)$	$G(\alpha, y)$, $\alpha = n\pi/a$
1.	$g(a)$	$g(a)/\alpha^5$
2.	$g(a)\,y$	$g(a)\,y/\alpha^4$
3.	$g(a)(2b - y)$	$g(a)(2b - y)/\alpha^4$
4.	$g(a)(b - y)$	$g(a)(b - y)/\alpha^4$
5.	$g(a)(b + y)$	$g(a)(b + y)/\alpha^4$
6.	$g(a)\sin \beta y$	$g(a)\sin \beta y/(\beta^4 + 2\alpha^2\beta^2 + \alpha^4)$
7.	$g(a)\cos \beta y$	$g(a)\cos \beta y/(\beta^4 + 2\alpha^2\beta^2 + \alpha^4)$
8.	$g(a)\,e^{\beta y}$, $\beta \neq \alpha$	$g(a)\,e^{\beta y}/(\beta^4 - 2\alpha^2\beta^2 + \alpha^4)$
9.	$g(a)\,y^2$	$g(a)(\alpha^2 y^2 + 4)/\alpha^6$
10.	$g(a)(y^2 - b^2)$	$g(a)(\alpha^2 y^2 + 4 - \alpha^2 b^2)/\alpha^6$

$0 < x < a$, $\alpha = (n\pi/a)$

Many more examples could be easily given by using the constants for the different cases, together with various load functions.

The Limit Design of Space Frames[1]

By JACQUES HEYMAN,[2] PROVIDENCE, R. I.

The Greenberg-Prager maximum-minimum method for the limit design of plane frames is extended to space frames. This method furnishes upper and lower bounds for the load factor at collapse, and the bounds may be made as close as is considered necessary by a rational system of successive approximation.

Plane Frames

BEFORE the discussion of space frames, an account will be given of the Greenberg-Prager method[3] of limit design of plane frames. This method furnishes upper and lower bounds for the load factor at collapse of the structure, and by an iterative process, these bounds may be made as close as is considered necessary. For both plane and space frames, the method assumes that the structural deformations are so small that secondary stresses, due to the resulting eccentricity of loading, are negligible.

The fundamental assumption is made that the moment-curvature curve for a member is as shown in Fig. 1. From O to A the behavior is purely elastic. Increase of moment above the value at A is accompanied by a correspondingly greater increase of curvature, such that, at the point B, the moment reaches a value M_o, further bending taking place under the constant moment M_o. This value M_o is referred to as the "full plastic moment" of the member, and any section at which it occurs is called a "yield hinge."

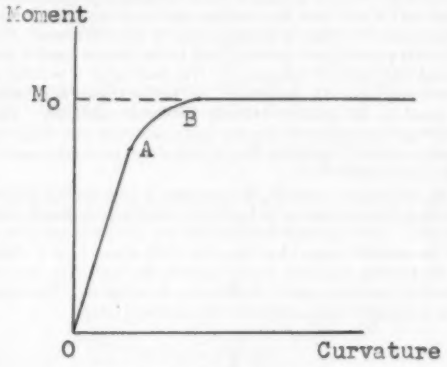

Fig. 1 Moment-Curvature Curve

Consider a plane frame under the action of various loads specified in terms of each other so that they may be defined by the intensity of one of the loads P, say. The problem to be solved is the determination of a factor λ (the load factor at collapse) by which all the loads must be multiplied in order that collapse will just occur.

The Kinematically Sufficient Multiplier. A sufficient number of yield hinges are inserted into the structure at arbitrarily selected points to transform it into a mechanism in the kinematic sense. For example, the mechanism in Fig. 2 derived from a single-bay portal frame has four hinges, and the mechanism derived from the two-bay portal in Fig. 3 has six hinges. As a rule, the number of hinges to be so inserted will exceed by one the number of hinges necessary to render statically determinate that part of the structure which is concerned in the collapse. Initially, at least, the collapse can be considered as a quasi-static process which takes place under constant loads and stresses. In each yield hinge the absolute value of the bending moment equals M_o (if the various members of a frame have different limit moments, then the appropriate value of M_o must be taken for each hinge considered); the sign of the bending moment in any yield hinge follows from the sense in which this hinge deforms as the structure collapses. Of course the bending moments at the assumed yield hinges will not reach these limit values for the given load intensity P, but for some other load intensity νP. The factor ν is readily obtained by the principle of virtual work or ordinary statical analysis. Any load factor ν obtained in this manner by inserting a sufficient number of yield hinges to transform the structure into a mechanism is called a "kinematically sufficient multiplier."

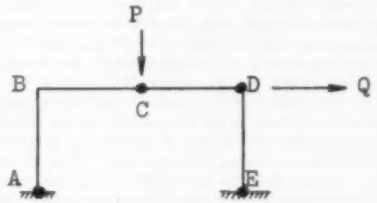

Fig. 2

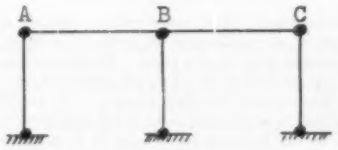

Fig. 3

The Greenberg-Prager principle states that λ, the actual load factor at collapse, is the smallest kinematically sufficient multiplier (ν). The multiplier ν will, in general, be greater than λ be-

---

[1] The results presented in this paper were obtained in the course of research conducted under Contract N7onr-35806 with the Office of Naval Research.

[2] Research Associate, Graduate Division of Applied Mathematics, Brown University; Fellow of Peterhouse, Cambridge, England.

[3] "On Limit Design of Beams and Frames," by H. Greenberg and W. Prager, to be published in the Proceedings of the ASCE.

Contributed by the Applied Mechanics Division and presented at the Annual Meeting, New York, N. Y., November 26–December 1, 1950, of The American Society of Mechanical Engineers.

Discussion of this paper should be addressed to the Secretary, ASME, 29 West 39th Street, New York, N. Y., and will be accepted until July 10, 1951, for publication at a later date. Discussion received after the closing date will be returned.

Note: Statements and opinions advanced in papers are to be understood as individual expressions of their authors and not those of the Society. Manuscript received by the Applied Mechanics Division, February 3, 1950. Paper No. 50—A-4.

cause the yield hinges that were assumed did not correspond to the actual mode of failure of the structure but were chosen only to produce one of several possible mechanisms.

The Statically Admissible Multiplier. A lower bound to the load factor at collapse may be obtained as follows: If a bending-moment distribution is found that is in equilibrium with the given loads and is such that the bending moment at any point is less than or, at most, equal in absolute value to the yield moment M_0, the corresponding load factor (ν') will be less than or equal to the actual load factor at collapse (λ). The load factor ν' is called a "statically admissible multiplier," and the load factor at collapse is equal to the greatest statically admissible multiplier. Any bending-moment distribution that is in equilibrium with the given loads is termed admissible, even though it will not be necessarily the correct distribution.

In working an example, the principle is best applied by examining the mechanism under the kinematically sufficient load factor ν. If the greatest bending moment (obviously not at one of the assumed hinges) has the value KM_0, where $K > 1$, then, if all bending moments are reduced in the ratio K/ν, an admissible bending-moment distribution is obtained. The combined principles then lead to the continued inequality

$$\frac{\nu}{K} \leq \lambda \leq \nu \qquad [1]$$

The load factor λ is now bounded from above and below. Prager and Greenberg were able to show that if one of the hinges in the assumed mode of collapse was shifted to the point of maximum bending moment, then these bounds would be narrowed. There is at present no method of choosing generally the correct hinge to move, but in any specific example the choice is very often limited by kinematic or other considerations. For example, the rectangular portal frame in Fig. 2 must fail with its hinges alternately opening and closing, that is, an opening hinge must lie between two that are closing, and vice versa. Thus the point of maximum moment must lie between one hinge that is opening and one that is closing, and it would be obvious to shift the hinge of the correct sign to that point.

Space Frames

For the purposes of the present paper, a space frame is defined as one whose members lie all in the same plane, all loads acting perpendicularly to this plane. Bending moments whose axes are perpendicular to the plane are assumed to be zero, and hence the shear forces in the plane are zero. Any member of the frame will then be acted on by shear forces parallel to the applied loads and by two moments whose axes lie in the plane, that is, a bending moment (flexural couple) and a torque (twisting couple). This type of frame presents some difficulties when the maximum-minimum principles outlined in the foregoing are applied.

To replace the breakdown criterion of a maximum full plastic moment, the bending moment M and torque T will be connected by some relationship

$$g(M, T) = \text{const} \qquad [2]$$

In this equation it will be noted that shear force is assumed to have no effect on the full plastic moment of the section. This assumption is customary, but, in particular examples, it may be that shear force must be taken into account. For the present purpose of developing a simple method of limit design of space frames, however, this effect will be neglected.

At a hinge defined by Equation [2], von Mises' flow relations will give an expression connecting the rate of twist of the section θ, with the rate of bending, β. The equation may be written as

$$\frac{\theta}{\beta} = \frac{\dfrac{\partial g}{\partial T}}{\dfrac{\partial g}{\partial M}} = G(M, T) \qquad [3]$$

A proof of this relationship suggested by D. C. Drucker is given in the Appendix, where it is also shown that for a box-section beam the breakdown criterion, Equation [2], reduces to

$$g(M, T) = M^2 + \frac{3}{4} T^2 = M_0^2 \qquad [4]$$

if certain simplifying assumptions are made. Here M_0 is the full plastic bending moment when $T = 0$. For the box section, Equation [3] becomes

$$\frac{\theta}{\beta} = \frac{3}{4} \frac{T}{M} \qquad [5]$$

Consider now a space frame which is converted into a mechanism of one degree of freedom by the formation of N plastic hinges. As in the consideration of the plane frame, the bending moments and torques at the hinges may be determined from statical considerations, and, in addition, the value of the load factor necessary to produce this configuration will be determined uniquely.

In working an actual example, the solution of the statical problem, in order to find the values of moments, will be tedious if the frame is at all complicated. The work may be simplified, however, by consideration of the geometry of the distorting frame. The ratio θ_i/β_i for the ith hinge will be known as a pure number if the mechanism has only one degree of freedom. The breakdown condition, Equation [2], and the flow condition, Equation [3], may be combined to give

$$\left.\begin{aligned} g(M_i, T_i) &= \text{const} \\ G(M_i, T_i) &= \text{const} \end{aligned}\right\} \qquad [6]$$

These are two simultaneous (in general, nonlinear) equations for M_i and T_i, which may be solved to give unique values of these moments. (Since the equations may be nonlinear, they may have more than one set of solutions; the physical nature of any particular problem will, however, determine the correct solution to be taken.)

Since the frame is a mechanism at collapse, and since the moments and torques are given uniquely from Equations [6], further distortion from the condition of incipient collapse can occur without any increase in the applied loads, and this distortion will take place under constant moment and torque at any one hinge. The rate at which work is done at each hinge under the constant moment and torque M_i and T_i may thus be written down, and the sum for all the hinges equated to the rate at which work is done by the exterior (constant) loads during this small displacement (principle of virtual work). Thus

$$\sum_{i=1}^{N} M_i \beta_i + \sum_{i=1}^{N} T_i \theta_i = \sum P \cdot \delta \qquad [7]$$

where δ is the displacement of the load P.

In working an example, the conventional assumption is made that the deformations are considered small compared with the over-all dimensions of the structure, so that it is admissible to satisfy the equilibrium conditions in the undeformed rather than in the deformed configuration.

Right-Angle Bent. Consider the simple right-angle bent carry-

ing the load νP as shown in Fig. 4. Suppose that the two members AC and CD are identical and of uniform cross section of box

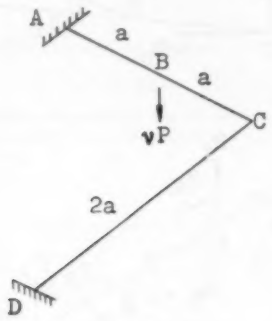

FIG. 4

form, so that the breakdown and flow criteria may be taken as

$$M^2 + \frac{3}{4}T^2 = M_o^2 \quad \ldots\ldots [8]$$

$$\frac{\theta}{\beta} = \frac{3}{4}\frac{T}{M} \quad \ldots\ldots [9]$$

As a first trial, hinges will be inserted at A and D. By consideration of a small displacement of the frame, the rate of twist θ and the rate of bending β are known to be connected by the relations

$$\left.\begin{aligned} \beta_A &= \beta_D \\ \theta_A &= \beta_D \\ \theta_D &= \beta_A \end{aligned}\right\} \quad \ldots\ldots [10]$$

so that at A and D, $\theta = \beta$.

From Equation [9], $M = (3/4)T$, and substitution in Equation [8] leads to

$$M_A = M_D = \frac{3}{\sqrt{21}}M_o \quad \ldots\ldots [11]$$

$$T_A = T_D = \frac{4}{\sqrt{21}}M_o \quad \ldots\ldots [12]$$

By considering a small displacement of the frame and applying the principle of virtual work, or by taking moments for the frame about the line AD in Fig. 5

$$\nu Pa = \frac{14}{\sqrt{21}}M_o$$

or

$$\nu = \frac{14}{\sqrt{21}}\frac{M_o}{Pa} \quad \ldots\ldots [13]$$

The principle of the kinematically sufficient multiplier then states that

$$\lambda \leq \frac{14}{\sqrt{21}}\frac{M_o}{Pa} \quad \ldots\ldots [14]$$

where λ is the actual load factor at collapse. The bending moments and load are sketched in Fig. 5, and taking moments about an axis parallel to AC through D, R_A, the reaction at A is given by

$$R_A = \frac{21}{2\sqrt{21}}\frac{M_o}{a} \quad \ldots\ldots [15]$$

The sagging moment at B is thus equal to

$$\frac{15}{2\sqrt{21}}M_o$$

The torque at B is equal to the torque at A, $(4/\sqrt{21})M_o$. Hence the left-hand side of Equation [8] may be written as

$$M_B^2 + \frac{3}{4}T_B^2 = \frac{(15)^2 + 48}{4(21)} = \left[\frac{1}{2}\sqrt{\frac{273}{21}}\right]^2 M_o^2 \quad \ldots\ldots [16]$$

The yield condition is violated at this point B (and, by analysis, at no other point). Now, if in Fig. 5 all the numerical quanti-

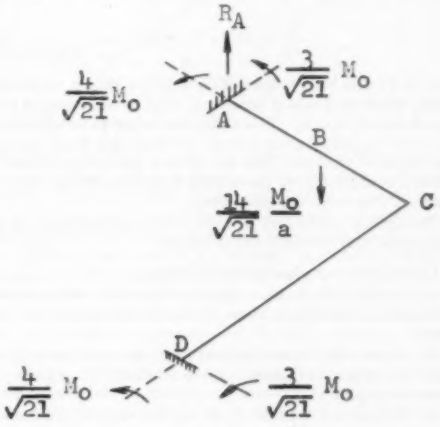

FIG. 5

ties (bending moments, load, shear forces) are multiplied by $2\sqrt{(21/273)}$, a system will be obtained which is statically compatible and in which the bending moments are less than (or equal to, at B) values which satisfy the breakdown criterion. Combination of the principles of the statically admissible and kinematically sufficient multipliers will then give

$$2\sqrt{\frac{21}{273}} \cdot \frac{14}{\sqrt{21}}\frac{M_o}{Pa} \leq \lambda \leq \frac{14}{\sqrt{21}}\frac{M_o}{Pa}$$

or

$$1.75\frac{M_o}{Pa} \leq \lambda \leq 3.05\frac{M_o}{Pa} \quad \ldots\ldots [17]$$

By analogy with the plane-frame problem, the solution should be improved, that is, the bounds narrowed, by the insertion of a hinge at B and the removal of the hinge either at A or at D. However, two obstacles present themselves to this course of action: (1) The bending moment at B is sagging, and those at A and D hogging. (2) Hinges at A and B or at D and B alone will not produce a mechanism. (If hinges are put at D and B, for example, the principle of virtual work will give the moments at these points as zero.)

The actual mode of failure is one in which hinges occur at all three of A, B, and D. Now these three hinges will specify six values of moments, whereas the frame has only three redundancies. One extra relationship is necessary to determine the load in terms of the moments, but there will be two extra values specified that will, in general, not be statically compatible.

General Method for Space Frames. The previous section showed that an apparently anomalous condition was attained in the frame. Two hinges were not sufficient to produce the correct mode of collapse, and the introduction of the third hinge produced two extra values of bending moment that were not necessarily compatible with the applied loads. In actual fact, the introduction of the third hinge gives the resulting mechanism three degrees of freedom.

Suppose that the actual solution of the problem has been attained with the values of bending moment and torque calculated at each of the three hinges to satisfy the breakdown criterion $g(M_i, T_i) = \text{const}$. The flow relationship at each hinge will then be

$$\frac{\theta_i}{\beta_i} = G(M_i, T_i) = \alpha_i \quad \ldots\ldots\ldots\ldots\ldots [18]$$

that is, θ_i/β_i is known, since M_i and T_i are known. For each hinge, therefore, a rate of bending β_i must be accompanied by a rate of twist $\theta_i = \alpha_i\beta_i$. This means that although two directions of motion are permitted at a hinge, the hinge as a whole has only one degree of freedom. This fact gives a clue to the method of solution of the problem; the relation θ_i/β_i at each hinge must be specified in terms of the parameters α_j.

The general method of solution for a structure with R redundancies may be tabulated as follows:

1 Construct a mechanism with N hinges.

2 Calculate $2N - (R + 1)$, where R is the number of redundancies of that part of the structure concerned in the collapse.

3 Specify the mechanism in terms of an arbitrary displacement (one degree of freedom) and in terms of $[2N - (R + 1)]$ parameters α_j.

4 Calculate T_i and M_i from the flow and breakdown criteria in terms of the α_j.

5 If there are N hinges, $(2N - R)$ equilibrium equations may be formulated in terms of M_i, T_i, and ν.

6 Substitute for M_i and T_i in terms of the α_j, and eliminate ν from the equations, giving $[2N - (R + 1)]$ simultaneous (in general, nonlinear) equations for the $[2N - (R + 1)]$ values of the α_j.

7 Solve these equations for the α_j and hence for the values of M_i and T_i at every hinge.

8 The solution that is both kinematically correct and that satisfies the equilibrium conditions has now been obtained. The value of ν will give an upper bound for λ.

9 Check that the yield condition is not violated at any point of the structure. This will give a lower bound for λ.

10 Move or add hinges to the points where the yield criterion is violated and repeat the whole process.

Solution of the Right-Angle Bent. Continuing the solution of the frame in Fig. 4, hinges will be inserted at A, B, and D. The distorted frame will appear as in Fig. 6 (looking along CD). There are three hinges, so that $2N - (R + 1) = 2$, showing that two parameters will be needed to specify the mechanism in terms of one degree of freedom. Take these as

$$\left.\begin{aligned}\theta_A &= x\beta_A\\ \theta_D &= y\beta_D\end{aligned}\right\} \quad \ldots\ldots\ldots\ldots\ldots [19]$$

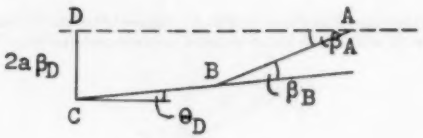

FIG. 6

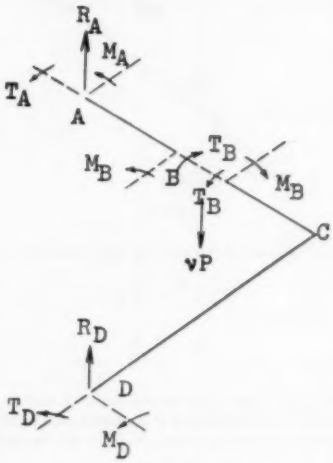

FIG. 7

where x and y are the two unknown parameters. Simple geometrical considerations give

$$\left.\begin{aligned}2\beta_D &= \beta_A + \theta_D\\ \beta_B &= \beta_A - \theta_D\\ \theta_B &= \beta_D - \theta_A\end{aligned}\right\} \quad \ldots\ldots\ldots\ldots\ldots [20]$$

with the signs of the rates of change chosen to give torques of the same signs as those in Fig. 5. (See Fig. 7.)

Combination of Equations [19] and [20] lead to

$$\left.\begin{aligned}\beta_A &= (2 - y)\beta_D\\ \theta_A &= x(2 - y)\beta_D\end{aligned}\right\} \quad \ldots\ldots\ldots\ldots\ldots [21]$$

$$\left.\begin{aligned}\beta_B &= 2(1 - y)\beta_D\\ \theta_B &= [1 - x(2 - y)]\beta_D\end{aligned}\right\} \quad \ldots\ldots\ldots\ldots\ldots [22]$$

$$\left.\begin{aligned}\beta_D &= \beta_D\\ \theta_D &= y\beta_D\end{aligned}\right\} \quad \ldots\ldots\ldots\ldots\ldots [23]$$

expressing the rotations in terms of the one independent degree of freedom, β_D.

Two statical equations are required that do not contain νP. These may be found by consideration of Fig. 7. The torque in AB must be constant, so that

$$T_B = T_A \quad \ldots\ldots\ldots\ldots\ldots [24]$$

(i.e., $M_B = M_A$ from the breakdown criterion). From the equilibrium of the portion BCD of the frame

$$T_B + M_D = 2M_B - 2T_D \quad \ldots\ldots\ldots\ldots\ldots [25]$$

Equation [24] implies that the ratio θ/β is the same at A and at B, so that from Equations [21] and [22]

$$(4 - 3y)x = 1 \quad \ldots\ldots [26]$$

Combination of Equations [24] and [25] gives

$$T_A + M_D = 2M_A - 2T_D \quad \ldots\ldots [27]$$

and using Equations [21] and [23] and the breakdown criterion, Equation [8], in order to calculate torques and moments, Equation [27] becomes

$$\frac{\frac{4}{3}x}{\sqrt{1 + \frac{4x^2}{3}}} + \frac{1}{\sqrt{1 + \frac{4y^2}{3}}} = \frac{2}{\sqrt{1 + \frac{4x^2}{3}}} - \frac{\frac{8}{3}y}{\sqrt{1 + \frac{4y^2}{3}}}$$

or

$$\frac{\left(2 - \frac{4}{3}x\right)}{\sqrt{1 + \frac{4x^2}{3}}} = \frac{\left(1 + \frac{8}{3}y\right)}{\sqrt{1 + \frac{4y^2}{3}}} \quad \ldots\ldots [28]$$

The simultaneous Equations [26] and [28] are best solved by trial and error, and give

$$\left.\begin{aligned} x &= 0.21 \\ y &= 0.28 \end{aligned}\right\} \quad \ldots\ldots [29]$$

The torques and moments may now be calculated and are

$$\left.\begin{aligned} M_A = M_B &= 0.970\, M_o \qquad T_A = T_B = 0.278\, M_o \\ M_D &= 0.950\, M_o \qquad T_D = 0.355\, M_o \end{aligned}\right\} \quad [30]$$

By moments about the line AD in Fig. 7, as before,

$$rPa = M_A + T_A + M_D + T_D$$

that is

$$r = 2.553\, \frac{M_o}{Pa} \quad \ldots\ldots [31]$$

The actual values of moments and loads are given in Fig. 8. The yield condition is nowhere violated, so that

$$\lambda = 2.55\, \frac{M_o}{Pa} \quad \ldots\ldots [32]$$

which, as a check, lies between the previous limits (see Equation [17]) of $1.75\, M_o/Pa$ and $3.05\, M_o/Pa$.

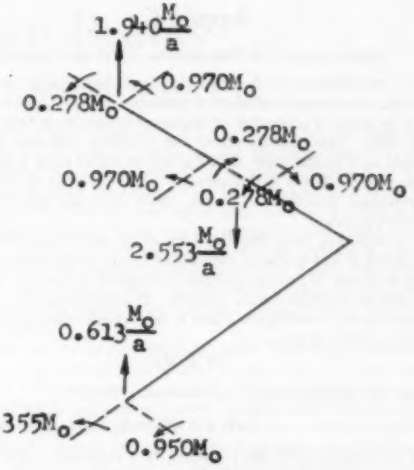

FIG. 8

CONCLUSIONS

The Greenberg-Prager method of bounding the load factor at collapse between arbitrarily close limits gives a very powerful method for the limit design of frames. The application to space frames becomes a little more complicated owing to the introduction into the equations of a certain number of arbitrary parameters, depending on the number of yield hinges assumed and the degree of redundancy of the structure. The simple example worked in this paper does not, however, mask the difficulties to any great extent.

Looking at the problem from the point of view of analysis of any one frame under a given system of loads, it is unlikely that a highly redundant structure will collapse in its entirety. In general, local failure will occur, which reduces in effect the number of redundancies and the number of yield hinges, and hence also the number of equations to be solved in order to obtain the solution. If a specific load system is given, and the structure has to be designed to withstand these loads multiplied by a specific load factor, the solution is more difficult. In general, it would be expected that the best (most economical) design would occur when every part of every member is subjected to moments causing breakdown of the material when the structure is on the point of collapse. This condition is of course impossible to fulfill in practice, but the designer will try to proportion the members so that more hinges than are necessary are formed. However, there are no simple rules at present for the economical design of even plane frames; for example, the rectangular portal frame in Fig. 2 permits of an infinite number of designs all producing collapse by the mode illustrated under the same values of P and Q, and if other modes of collapse are permitted, other infinite sets of solutions are obtained.

In this paper, discussion has been made only of the effect of concentrated loads. In plane frames, and in space frames with straight members (torque in any member is constant), this fact ensures that a hinge will be formed either at a loading point or at a joint where two or more members meet. There is thus a limited number of possible modes of collapse, and the load factor is determined uniquely when the kinematic assumed solution corresponds with the actual solution. For plane frames under distributed loads, or space frames with curved members, it is not possible to say that a hinge will be formed only at a joint. In these cases, when hinges can occur at any place, there is an infinite number of possible modes of collapse; the Greenberg-Prager method is especially valuable here in that the load-factor limits may be made as close as is considered necessary by successive rational trial solutions.

Attention should perhaps be drawn to the fact that the principle of establishing the flow relations at any joint does not introduce any new equations into the analysis but only simplifies the work necessary in order to obtain the solution to any problem. Since the flow relation depends directly on the breakdown criterion, no equations are derived that could not have been established directly from equilibrium considerations of the structure; but the use of such considerations reduces the number of variables in the equations which have to be solved.

Appendix

Orthogonality of Breakdown and Flow Criteria

In establishing the flow criterion for a beam acted on by a torque and moment sufficient to produce complete plasticity, use will be made of a principle of maximum plastic work established by Hill.[4] This principle states that if surface velocities are imposed on a plastic body, then the rate at which work is done by the external forces is a maximum. Hill also showed that this variational principle led to the result that the plastic stress system is unique.

Interpreting these ideas in terms of the beam under bending moment M and torque T, then at any section where these couples are sufficient to produce yielding throughout the section, M and T will be constant during collapse. In addition, if the rates of bending and twisting are β and θ, respectively, then the rate at which work is done is

$$T\theta + M\beta$$

and this expression must be a maximum. Hence

$$\theta\, dT + \beta\, dM = 0 \qquad [33]$$

(This equation gives the condition for a stationary value of the plastic work; that this stationary value is a maximum was shown by Hill[4]). Now the breakdown criterion (Equation [2]) may be differentiated to give

$$\frac{\partial g}{\partial M}\, dM + \frac{\partial g}{\partial T}\, dT = 0 \qquad [34]$$

and comparison with Equation [33] shows that

$$\frac{\theta}{\beta} = \frac{\dfrac{\partial g}{\partial T}}{\dfrac{\partial g}{\partial M}} \qquad [35]$$

This is the expression given as Equation [3].

Combined Bending and Torsion of a Box Beam

Equations will be derived which give expressions for the behavior of a box beam when the material of the cross section is everywhere fully plastic. Suppose the section in Fig. 9 is acted upon by a bending moment M about the axis ox and by a torque T about the axis oz (this axis being the third Cartesian axis not shown in the figure). If the thickness of the webs and flanges is taken to be so small that no appreciable variation in shear stress occurs, then by equilibrium it may be shown that

$$\tau_1 = \frac{T}{2bdt_1} \qquad [36]$$

$$\tau_2 = \frac{T}{2bdt_2} \qquad [37]$$

where τ_1 and τ_2 are the shear stresses in the webs and flanges, respectively, and the other constants of the cross section are defined in Fig. 9. If the corresponding longitudinal stresses produced by the bending moment are σ_1 and σ_2, and the material is

[4] "A Variational Principle of Maximum Plastic Work in Classical Plasticity," by R. Hill, *Quarterly Journal of Mechanics and Applied Mathematics*, Part 1, vol. 1, March, 1948, pp. 18–28.

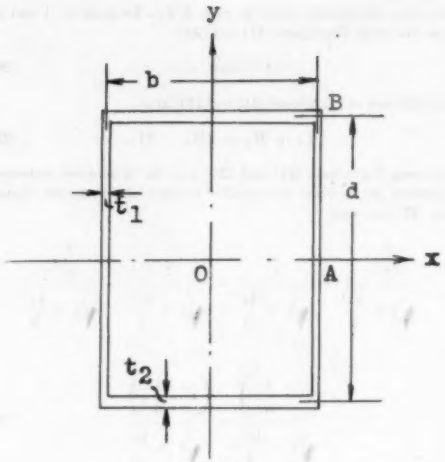

Fig. 9

everywhere fully plastic, then application of the von Mises breakdown criterion leads to

$$\sigma_1^2 + 3\tau_1^2 = 3k^2 \qquad [38]$$

$$\sigma_2^2 + 3\tau_2^2 = 3k^2 \qquad [39]$$

where k is the yield stress in pure shear.

The bending moment M is given by

$$M = bdt_2\sigma_2 \qquad [40]$$

In this equation the contribution to bending moment of the webs has been neglected which is justified if their thickness is small compared with that of the flanges.

Breakdown Criterion for Section. By elimination of the stresses τ_2 and σ_2 between the foregoing equations, the breakdown criterion for the section under the moments M and T becomes

$$M^2 + \frac{3T^2}{4} = 3b^2d^2t_2^2k^2 = M_o^2 \qquad [41]$$

Flow Criterion for Section. Differentiating Equation [41]

$$M \cdot dM + \frac{3}{4}\, T \cdot dT = 0 \qquad [42]$$

and comparison with Equation [35] shows that

$$\frac{\theta}{\beta} = \frac{3}{4}\,\frac{T}{M} \qquad [43]$$

Owing to the approximation made in the expression for M (contribution of flanges neglected), an attempt to establish Equation [43] from first principles will lend to a false result that does not satisfy the orthogonality relationship, Equation [33]. The correct procedure for any section should be to establish the breakdown criterion first, making any approximations that are deemed desirable, and then to derive the flow criterion from Equation [35].

Analysis of Deep Beams

By H. D. CONWAY,[1] L. CHOW,[2] and G. W. MORGAN,[3] ITHACA, N. Y.

This paper presents a method of analyzing the stress distribution in a deep beam of finite length by superimposing two stress functions. The first stress function is chosen in the form of a trigonometric series which satisfies all but one of the boundary conditions—that of zero normal stress on the ends of the beam. The principle of least work is then used to obtain a second stress function giving the distribution of normal stress on the ends which is left by the first stress function. By superimposing the two solutions, all the boundary conditions are satisfied. Two particular cases of a given type of loading are solved in this way to investigate the stresses in a deep beam and their deviation from the ordinary beam theory. In addition, an approximate solution by the numerical method of finite difference is worked out for one of the two cases. Results from the two methods are compared and discussed. A method of obtaining an exact solution to the problem is given in an Appendix.

Nomenclature

The following nomenclature is used in the paper:

σ_x, σ_y = normal components of stress parallel to x and y-axes
τ_{xy} = shearing stress component in a plane perpendicular to x-axis and in a direction parallel with y-axis
ϕ = stress function
$2a$ = length of beam
$2b$ = height of beam
m = any positive integer
α = $m\pi/a$
P = total load at top edge per unit thickness
E = Young's modulus of elasticity
μ = Poisson's ratio
V = strain energy
Δx, Δy = intervals of equal divisions along two axes
λ = $(\Delta y/\Delta x)^2$

Additional symbols are defined where they are introduced.

Introduction

The analyses of deep beams may be classified into three groups; infinite span with periodic loading, infinite span with nonperiodic loading, and span of finite length.

In the first group, the boundary loadings can be represented easily by Fourier series and the problem solved by means of a stress function in the form of an infinite series of hyperbolic functions. Both Craemer (1, 2, 3)[4] and Dischinger (4) used this method to solve a great number of cases, the graphs from Dischinger's paper being reproduced in a pamphlet published by the Portland Cement Association (5). Furthermore, in a different way, Bay (6) analyzed the case of deep beam with supports of equal spans, the span being equal to or less than the height of the beam. He used Filon's solution (7) with the method of superposition, and concluded that beams of infinite length with height greater than span of supports have similar stress distributions to beams with height equal to span. This confirms Dischinger's analysis.

In the second group, difficulty arises from the nonperiodic loading in an infinite span so that Fourier series no longer can be used. The usual method of solution is to represent the boundary loadings in the form of Fourier integrals, and therefore the stress function must also be in the form of an infinite integral. Accordingly, the numerical evaluation of stresses is very laborious. In this way, Bay (8) used the stress function suggested by Seewald (9) and Kármán (10) to solve a shear case of an infinite beam by evaluating the infinite integral graphically.

In the last group, the main difficulty is to satisfy all boundary conditions. Although Fourier series can be used to represent any form of periodic loading, the boundary condition at the two vertical edges cannot be satisfied by this means. The method proposed here is to use a second stress function to eliminate, by means of superposition, the normal stress left at the vertical edges from the first stress function. The second stress function, in the form of a series with adjustable parameters, is determined by applying the principle of least work to the strain-energy integral—a method developed by Timoshenko (11) and used by Goodier (12) in solving other problems. This method involves some approximation due to using a few terms out of an infinite series for the second stress function. However, it yields results which are generally more accurate than those obtained by the finite-difference method. A further method of obtaining the second stress function in the form of a Fourier series is given but was not used to obtain numerical results because of the very considerable labor involved.

Strain-Energy Method

The beam and its loading are shown in Fig. 1. It is assumed that conditions are such as to permit a two-dimensional analysis, i.e., the problem is considered as one of plane stress or plane strain. This assumption is justified if the thickness of the block is either very small or very large.

The first stress function is chosen in the form

$$\phi = -\frac{Px^3}{4a} + \sum_{m=1,2,\cdots}^{\infty} (A_m \cosh \alpha y + B_m y \sinh \alpha y + C_m \sinh \alpha y + D_m y \cosh \alpha y)\cos \alpha x \quad [1]$$

where A_m, B_m, C_m, D_m are constants. This function satisfies the differential equation

$$\nabla^4 \phi = \frac{\partial^4 \phi}{\partial x^4} + 2\frac{\partial^4 \phi}{\partial x^2 \partial y^2} + \frac{\partial^4 \phi}{\partial y^4} = 0$$

The normal and shearing stresses found in the usual manner are

---

[1] Professor of Engineering Mechanics, Cornell University, Ithaca, N. Y. Jun. ASME.

[2] Graduate Student at Cornell University.

[3] Graduate Student at Cornell University.

Contributed by the Applied Mechanics Division and presented at the Annual Meeting, New York, N. Y., November 26–December 1, 1950, of The American Society of Mechanical Engineers.

Discussion of this paper should be addressed to the Secretary, ASME, 29 West 39th Street, New York, N. Y., and will be accepted until July 10, 1951, for publication at a later date. Discussion received after the closing date will be returned.

Note: Statements and opinions advanced in papers are to be understood as individual expressions of their authors and not those of the Society. Manuscript received by the Applied Mechanics Division, October 31, 1949. Paper No. 50—A-7.

[4] Numbers in parentheses refer to the Bibliography at the end of the paper.

$$\sigma_x = \frac{\partial^2\phi}{\partial y^2} = \sum_{m=1,2,\cdots}^{\infty} [(A_m\alpha^2 + 2B_m\alpha)\cosh \alpha y + B_m\alpha^2 y \sinh \alpha y + (C_m\alpha^2 + 2D_m\alpha)\sinh \alpha y + D_m\alpha^2 y \cosh \alpha y]\cos \alpha x$$

$$\sigma_y = \frac{\partial^2\phi}{\partial x^2} = -\frac{P}{2a} - \sum_{m=1,2,\cdots}^{\infty} \alpha^2[A_m \cosh \alpha y + B_m y \sinh \alpha y + C_m \sinh \alpha y + D_m y \cosh \alpha y]\cos \alpha x \quad [2]$$

$$\tau_{xy} = -\frac{\partial^2\phi}{\partial x \partial y} = \sum_{m=1,2,\cdots}^{\infty} [(A_m\alpha^2 + B_m\alpha)\sinh \alpha y + B_m\alpha^2 y \cosh \alpha y + (C_m\alpha^2 + D_m\alpha)\cosh \alpha y + D_m\alpha^2 y \sinh \alpha y]\sin \alpha x$$

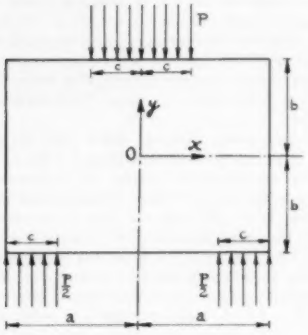

FIG. 1

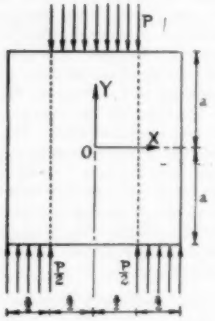

FIG. 2

The solution of the problem is then subject to the following boundary conditions

$$|x| < c,\ y = b, \quad \sigma_y = -\frac{P}{2c}$$

$$c < |x| < a,\ y = b, \quad \sigma_y = 0$$

$$|x| < a - c,\ y = -b,\ \sigma_y = 0$$

$$a - c < |x| < a,\ y = -b,\ \sigma_y = -\frac{P}{2c}$$

$$y = \pm b, \quad \tau_{xy} = 0$$

$$x = \pm a, \quad \tau_{xy} = 0$$

$$x = \pm a, \quad \sigma_x = 0$$

To satisfy the first four conditions, σ_y at the top and bottom edges are taken in the form of Fourier series

At $y = b$

$$\sigma_y = -\frac{P}{2a} - \frac{P}{a}\sum_{m=1,2,\cdots}^{\infty} \frac{\sin \alpha c}{\alpha c}\cos \alpha x$$

At $y = -b$

$$\sigma_y = -\frac{P}{2a} - \frac{P}{a}\sum_{m=1,2,\cdots}^{\infty} (-1)^m \frac{\sin \alpha c}{\alpha c}\cos \alpha x$$

Putting $y = \pm b$ in the second of Equations [2] and equating the corresponding expressions for σ_y, the following relationships are obtained

$$A_m \cosh \alpha b + B_m b \sinh \alpha b + C_m \sinh \alpha b + D_m b \cosh \alpha b = \frac{\sin \alpha c}{\alpha c}\frac{P}{a^2 a}$$

$$A_m \cosh \alpha b + B_m b \sinh \alpha b - C_m \sinh \alpha b - D_m b \cosh \alpha b = (-1)^m \frac{\sin \alpha c}{\alpha c}\frac{P}{a^2 a}$$

The condition of zero shearing stress on the sides $y = \pm b$ gives

$$(A_m\alpha + B_m)\sinh \alpha b + B_m \alpha b \cosh \alpha b = 0$$

$$(C_m\alpha + D_m)\cosh \alpha b + D_m \alpha b \sinh \alpha b = 0$$

The four constants are thus determined by solving these equations. They are given by

$m = 1, 3, 5, \ldots$

$$A_m = B_m = 0$$

$$C_m = \frac{\sin \alpha c}{\alpha c}\frac{P}{a^2 a}\frac{\cosh \alpha b + \alpha b \sinh \alpha b}{\sinh \alpha b \cosh \alpha b - \alpha b}$$

$$D_m = -\frac{\sin \alpha c}{\alpha c}\frac{P}{a a}\frac{\cosh \alpha b}{\sinh \alpha b \cosh \alpha b - \alpha b}$$

$m = 2, 4, 6, \ldots$

$$A_m = \frac{\sin \alpha c}{\alpha c}\frac{P}{a^2 a}\frac{\sinh \alpha b + \alpha b \cosh \alpha b}{\sinh \alpha b \cosh \alpha b + \alpha b}$$

$$B_m = -\frac{\sin \alpha c}{\alpha c}\frac{P}{a a}\frac{\sinh \alpha b}{\sinh \alpha b \cosh \alpha b + \alpha b}$$

$$C_m = D_m = 0$$

It is evident that the condition of zero shearing stress on the sides $x = \pm a$ is automatically satisfied since $\sin m\pi$ is always zero. Therefore only the last one of the boundary conditions remains to be satisfied—that of zero normal stress on the sides $x = \pm a$.

In order to eliminate the normal stress on the sides $x = \pm a$ a second stress function is used. The first step is to calculate the distribution of the normal stress from the first stress function and to approximate to it by means of a polynomial expression to simplify mathematical operations used later. For a block having only this stress distribution on the two ends, it is possible to find a stress function in the form of a polynomial in x and y with undetermined parameters, satisfying all the boundary conditions. The principle of least work is then applied to calculate these

parameters, and thus the second stress function is determined completely. This solution by strain-energy methods would be exact only if an infinite number of parameters were used. However, the results obtained by using only a few parameters are usually quite accurate.

The stresses of the given problem can now be found by subtracting the values given by the second stress function from those given by the first. It is evident that all the boundary conditions are satisfied by the combined stress function. The following two cases are solved in this way.

Case 1. The square block, i.e., $b = a$.

The given loading shown in Fig. 2 with $c = a/2$ reduces the constants A_m, B_m, C_m, D_m to the following expressions

$m = 1, 3, 5, \ldots \quad A_m = B_m = 0$

$$C_m = (-1)^{\frac{m-1}{2}} \frac{2P}{a^3\alpha^2} \frac{\cosh \alpha a + \alpha a \sinh \alpha a}{\sinh \alpha a \cosh \alpha a - \alpha a}$$

$$D_m = (-1)^{\frac{m+1}{2}} \frac{2P}{a^2\alpha^2} \frac{\cosh \alpha a}{\sinh \alpha a \cosh \alpha a - \alpha a}$$

$m = 2, 4, 6, \ldots \quad A_m = B_m = C_m = D_m = 0$

The normal and shearing stresses are thus

$$\left.\begin{aligned}
\sigma_x &= \frac{P}{a} \sum_{m=1,3,5\cdots}^{\infty} (-1)^{\frac{m-1}{2}} \frac{2}{m\pi} \frac{\alpha a \sinh \alpha a \sinh \alpha y - \cosh \alpha a \sinh \alpha y - \alpha y \cosh \alpha a \cosh \alpha y}{\sinh \alpha a \cosh \alpha a - \alpha a} \cos \alpha x \\
\sigma_y &= -\frac{P}{2a} - \frac{P}{a} \sum_{m=1,3,5\cdots}^{\infty} (-1)^{\frac{m-1}{2}} \frac{2}{m\pi} \frac{\alpha a \sinh \alpha a \sinh \alpha y + \cosh \alpha a \sinh \alpha y - \alpha y \cosh \alpha a \cosh \alpha y}{\sinh \alpha a \cosh \alpha a - \alpha a} \cos \alpha x \\
\tau_{xy} &= \frac{P}{a} \sum_{m=1,3,5\cdots}^{\infty} (-1)^{\frac{m-1}{2}} \frac{2}{a} \frac{a \sinh \alpha a \cosh \alpha y - y \cosh \alpha a \sinh \alpha y}{\sinh \alpha a \cosh \alpha a - \alpha a} \sin \alpha x
\end{aligned}\right\} \quad \ldots [3]$$

It will be observed that the direct stress σ_x is zero at the sections $x = \pm a/2$. The distribution of normal stress on the vertical sides is

$$(\sigma_x)_{x=\pm a} = -\frac{P}{a} \sum_{m=1,3,5,\cdots}^{\infty} (-1)^{\frac{m-1}{2}} \frac{2}{m\pi} \times \frac{\alpha a \sinh \alpha a \sinh \alpha y - \cosh \alpha a \sinh \alpha y - \alpha y \cosh \alpha a \cosh \alpha y}{\sinh \alpha a \cosh \alpha a - \alpha a}$$

The polynomial which approximates to this distribution is found to be

$$(\sigma_x)_{x=\pm a} = \frac{P}{a}\left[-0.19430\frac{y}{a} + 0.19685\left(\frac{y}{a}\right)^3 + 0.80474\left(\frac{y}{a}\right)^5 - 0.36677\left(\frac{y}{a}\right)^7\right] \quad \ldots [4]$$

The strain-energy method is now used to eliminate this distribution by means of a second stress function which is taken in the form

$$\phi = \phi_0 + n_1\phi_1 + n_2\phi_2 + n_3\phi_3 + \ldots \quad \ldots [5]$$

in which ϕ_0 satisfies the boundary conditions for ϕ, and ϕ_1, ϕ_2, ϕ_3, do not affect the normal and shearing stresses on the sides if the boundary conditions refer to the stresses. The parameters n_1, n_2, n_3, ... can then be found by the principle of least work. The strain energy for a block of unit thickness is given by

$$V = \frac{1}{2E}\int_{-a}^{a}\int_{-a}^{a} [\sigma_x^2 + \sigma_y^2 - 2\mu\sigma_x\sigma_y + 2(1+\mu)\tau_{xy}^2]\, dx\, dy$$

Since the boundary conditions are prescribed loads and not displacements, the stress distribution is independent of the elastic constants of the material. Hence, taking $\mu = 0$, and putting stresses in terms of the stress function

$$V = \frac{1}{2E}\int_{-a}^{a}\int_{-a}^{a}\left[\left(\frac{\partial^2\phi}{\partial x^2}\right)^2 + \left(\frac{\partial^2\phi}{\partial y^2}\right)^2 + 2\left(\frac{\partial^2\phi}{\partial x \partial y}\right)^2\right] dx\, dy$$

Substituting Equation [5] into this expression for V, one can calculate the parameters from the conditions

$$\frac{\partial V}{\partial n_1} = \frac{\partial V}{\partial n_2} = \frac{\partial V}{\partial n_3} = \ldots\ldots = 0$$

It is sufficiently accurate to take only five terms in the expression for ϕ given by Equation [5]; and, noting that the stress distribution on the vertical sides is antisymmetrical, we assume a function

$$\phi = \phi_0 + (x^2 - a^2)^2 (y^2 - a^2)^2 (n_1 y + n_2 x^2 y + n_3 y^3 + n_4 x^2 y^3)$$

In order for ϕ_0 to satisfy the boundary conditions

$$\phi_0 = \int_c^y \int_c^y (\sigma_x)_{x=\pm a}\, dy\, dy$$

where $(\sigma_x)_{x=\pm a}$ is given by Equation [4].

The conditions for minimum V then lead to the following equations, as given in Goodier's paper (12)

$$\left[\frac{64}{7} + \frac{256}{105} + \frac{64}{55}\right] n_1 a + \left[\frac{64}{77} + \frac{64}{385}\right] n_2 a^3 + \left[\frac{64}{21} + \frac{512}{1155} + \frac{192}{715}\right] n_3 a^5 + \left[\frac{64}{231} + \frac{192}{5005}\right] n_4 a^7 = -\frac{9 \cdot 7 \cdot 5}{128\, a^{15}} \int_0^a \int_0^a \frac{\partial^2\phi_0}{\partial y^2} \cdot \frac{\partial^2\phi_1}{\partial y^2}\, dx\, dy$$

$$\left[\frac{64}{7} + \frac{64}{35}\right] n_1 a + \left[\frac{192}{91} + \frac{256}{105} + \frac{192}{35}\right] n_2 a^3 + \left[\frac{64}{21} + \frac{192}{455}\right] n_3 a^5 + \left[\frac{192}{273} + \frac{512}{1155} + \frac{576}{455}\right] n_4 a^7 = -\frac{11 \cdot 9 \cdot 7 \cdot 5}{128\, a^{17}} \int_0^a \int_0^a \frac{\partial^2\phi_0}{\partial y^2} \cdot \frac{\partial^2\phi_2}{\partial y^2}\, dx\, dy$$

$$\left[\frac{64}{21} + \frac{512}{1155} + \frac{192}{715}\right] n_1 a + \left[\frac{64}{231} + \frac{192}{5005}\right] n_2 a^3 + \left[\frac{832}{231} + \frac{4352}{15015} + \frac{64}{715}\right] n_3 a^5 + \left[\frac{832}{2541} + \frac{192}{15015}\right] n_4 a^7 = -\frac{9 \cdot 7 \cdot 5}{128\, a^{17}} \int_0^a \int_0^a \frac{\partial^2\phi_0}{\partial y^2} \cdot \frac{\partial^2\phi_3}{\partial y^2}\, dx\, dy$$

$$\left[\frac{64}{21} + \frac{192}{455}\right] n_1 a + \left[\frac{192}{273} + \frac{512}{1155} + \frac{576}{455}\right] n_2 a^3$$

$$+\left[\frac{832}{231}+\frac{192}{1365}\right]n_3a^2+\left[\frac{64}{77}+\frac{4352}{15015}+\frac{576}{1365}\right]n_4a^5$$
$$=-\frac{11\cdot9\cdot7\cdot5}{128\,a^{15}}\int_0^a\int_0^a\frac{\partial^2\phi_0}{\partial y^2}\cdot\frac{\partial^2\phi_4}{\partial y^2}\,dx\,dy$$

From these four equations, the parameters have been solved and are given by

$$n_1=-0.031556\,\frac{P}{a^9},\quad n_2=-0.024085\,\frac{P}{a^{10}}$$
$$n_3=-0.009984\,\frac{P}{a^{10}},\quad n_4=-0.055403\,\frac{P}{a^{13}}$$

The normal and shearing stresses from the second stress function are then given by

$$\left.\begin{aligned}
\sigma_x&=\frac{P}{a}\left\{\left[-0.19430\left(\frac{y}{a}\right)+0.19685\left(\frac{y}{a}\right)^3+0.89474\left(\frac{y}{a}\right)^5-0.36677\left(\frac{y}{a}\right)^7\right]\right.\\
&\quad+\left(1-\frac{x^2}{a^2}\right)^2\left(0.12622+0.09634\,\frac{x^2}{a^2}\right)\left[3\left(\frac{y}{a}\right)-5\left(\frac{y}{a}\right)^3\right]\\
&\quad\left.-\left(1-\frac{x^2}{a^2}\right)^3\left(0.01997+0.11081\,\frac{x^2}{a^2}\right)\left[3\left(\frac{y}{a}\right)-20\left(\frac{y}{a}\right)^3+21\left(\frac{y}{a}\right)^5\right]\right\}\\
\sigma_y&=\frac{Py}{a^3}\left(1-\frac{y^2}{a^2}\right)^2\left\{\left(1-3\,\frac{x^2}{a^2}\right)\left(0.12622+0.03994\,\frac{y^2}{a^2}\right)\right.\\
&\quad\left.-\left(1-12\,\frac{x^2}{a^2}+15\,\frac{x^4}{a^4}\right)\left(0.04817+0.11081\,\frac{y^2}{a^2}\right)\right\}\\
\tau_{xy}&=\frac{Px}{a^2}\left(1-\frac{x^2}{a^2}\right)\left(1-\frac{y^2}{a^2}\right)\left\{\left(-0.07805-0.14451\,\frac{x^2}{a^2}\right)\right.\\
&\quad\left.+\left(0.60286-0.27474\,\frac{x^2}{a^2}\right)\left(\frac{y}{a}\right)^2-\left(0.49609-2.32701\,\frac{x^2}{a^2}\right)\left(\frac{y}{a}\right)^4\right\}
\end{aligned}\right\}\quad\ldots[6]$$

The actual stresses can now be calculated by subtracting the values given by Equations [6] from the corresponding values given by Equations [3]. It is evident that the normal stresses left on the vertical sides from the first stress function are neutralised, and therefore a solution satisfying all the boundary conditions is obtained. Stresses on a few sections of the block have been computed from this solution and will later be compared graphically with the results obtained by the finite-difference method and also with those from the simple beam theory.[6]

Case 2. $b/a = 1/2$. The loading in this case is similar to that shown in Fig. 2 except that the length of the plate is twice the height. With $b = a/2$ and $c = a/2$, the constants A_m, B_m, C_m, and D_m become

$m = 1, 3, 5, \ldots.$ $\quad A_m = B_m = 0$

$$C_m=(-1)^{\frac{m-1}{2}}\frac{2P}{\alpha^3a^3}\,\frac{\cosh\frac{\alpha a}{2}+\frac{\alpha a}{2}\sinh\frac{\alpha a}{2}}{\sinh\frac{\alpha a}{2}\cosh\frac{\alpha a}{2}-\frac{\alpha a}{2}}$$

[6] It should be noted that the end points of the loaded regions constitute exceptions to the general boundary conditions required for the upper and lower edges of the beam.

$$D_m=(-1)^{\frac{m+1}{2}}\frac{2P}{\alpha^3a^3}\,\frac{\cosh\frac{\alpha a}{2}}{\sinh\frac{\alpha a}{2}\cosh\frac{\alpha a}{2}-\frac{\alpha a}{2}}$$

$m = 2, 4, 6, \ldots.$ $\quad A_m = B_m = C_m = D_m = 0$

The normal and shearing stresses given by the first stress function are then

$$\left.\begin{aligned}
\sigma_x&=\frac{P}{a}\sum_{m=1,3,5\cdots}^{\infty}(-1)^{\frac{m-1}{2}}\frac{2}{m\pi}\,\frac{\frac{\alpha a}{2}\sinh\frac{\alpha a}{2}\sinh\alpha y-\cosh\frac{\alpha a}{2}\sinh\alpha y-\alpha y\cosh\frac{\alpha a}{2}\cosh\alpha y}{\sinh\frac{\alpha a}{2}\cosh\frac{\alpha a}{2}-\frac{\alpha a}{2}}\cos\alpha x\\
\sigma_y&=-\frac{P}{2a}-\frac{P}{a}\sum_{m=1,3,5\cdots}^{\infty}(-1)^{\frac{m-1}{2}}\frac{2}{m\pi}\,\frac{\frac{\alpha a}{2}\sinh\frac{\alpha a}{2}\sinh\alpha y+\cosh\frac{\alpha a}{2}\sinh\alpha y-\alpha y\cosh\frac{\alpha a}{2}\cosh\alpha y}{\sinh\frac{\alpha a}{2}\cosh\frac{\alpha a}{2}-\frac{\alpha a}{2}}\cos\alpha x\\
\tau_{xy}&=\frac{P}{a}\sum_{m=1,3,5\cdots}^{\infty}(-1)^{\frac{m-1}{2}}\,2\,\frac{\frac{a}{2}\sinh\frac{\alpha a}{2}\cosh\alpha y-y\cosh\frac{\alpha a}{2}\sinh\alpha y}{a\sinh\frac{\alpha a}{2}\cosh\frac{\alpha a}{2}-\frac{\alpha a}{2}}\sin\alpha x
\end{aligned}\right\}\quad\ldots[7]$$

Accordingly, the distribution of normal stress on the vertical sides is

$$(\sigma_x)_{x=\pm a}=-\frac{P}{a}\sum_{m=1,3,5\cdots}^{\infty}(-1)^{\frac{m-1}{2}}\frac{2}{m\pi}\,\frac{\frac{\alpha a}{2}\sinh\frac{\alpha a}{2}\sinh\alpha y-\cosh\frac{\alpha a}{2}\sinh\alpha y-\alpha y\cosh\frac{\alpha a}{2}\cosh\alpha y}{\sinh\frac{\alpha a}{2}\cosh\frac{\alpha a}{2}-\frac{\alpha a}{2}}$$

The polynomial which closely approximates to this distribution has been found to be

$$(\sigma_x)_{x=\pm a} = \frac{P}{a}\left[0.93848\left(\frac{y}{a}\right) + 0.27608\left(\frac{y}{a}\right)^3 + 37.208\left(\frac{y}{a}\right)^5 - 88.481\left(\frac{y}{a}\right)^7\right] \quad \ldots\ldots [8]$$

The second stress function, taken in the same form as that of Case 1, is now determined by applying the conditions for minimum V which give the following values for the parameters

$$n_1 = -0.224136\,\frac{P}{a^3}; \quad n_2 = -0.730517\,\frac{P}{a^{10}};$$

$$n_3 = 0.007944\,\frac{P}{a^{10}}; \quad n_4 = -0.889820\,\frac{P}{a^{12}}$$

Hence the second stress function for this case is

$$\phi = \phi_0 + (x^2 - a^2)^2 (y^2 - b^2)^2 \frac{P}{a^5}\left[-0.224136\,y - 0.730517\,\frac{x^2 y}{a^2} + 0.007944\,\frac{y^3}{a^3} - 0.889820\,\frac{x^2 y^2}{a^4}\right]$$

in which

$$\phi_0 = \int_0^y \int_0^y (\sigma_x)_{x=\pm a}\, dy\, dy$$

where $(\sigma_x)_{x=\pm a}$ is given by Equation [8].

The normal and shearing stresses from this second stress function are thus

$$\left.\begin{aligned}
\sigma_x &= \frac{P}{a}\left\{\left[0.93848\left(\frac{y}{a}\right) + 0.27608\left(\frac{y}{a}\right)^3 + 37.208\left(\frac{y}{a}\right)^5 - 88.481\left(\frac{y}{a}\right)^7\right]\right. \\
&\quad + \left(1 - \frac{x^2}{a^2}\right)^2\left(0.22414 + 0.73052\,\frac{x^2}{a^2}\right)\left[3\left(\frac{y}{a}\right) - 20\left(\frac{y}{a}\right)^3\right] \\
&\quad \left. + \left(1 - \frac{x^2}{a^2}\right)^3\left(0.00794 - 0.88082\,\frac{x^2}{a^2}\right)\left[\frac{3}{8}\left(\frac{y}{a}\right) - 10\left(\frac{y}{a}\right)^3 + 42\left(\frac{y}{a}\right)^5\right]\right\} \\
\tau_{xy} &= \frac{Px}{a^2}\left(1 - \frac{x^2}{a^2}\right)\left(1 - 4\,\frac{y^2}{a^2}\right)\left\{\left(0.03528 - 0.27394\,\frac{x^2}{a^2}\right)\right. \\
&\quad \left. - \left(0.36597 - 4.47783\,\frac{x^2}{a^2}\right)\left(\frac{y}{a}\right)^2 - \left(3.16999 - 6.13977\,\frac{x^2}{a^2}\right)\left(\frac{y}{a}\right)^4\right\}
\end{aligned}\right\} \quad \ldots\ldots [9]$$

The true values of τ_{xy} and σ_x at the sections $x = \pm a/2$ have been calculated by subtracting the values given by Equations [9] from those given by Equations [7] and will later be presented graphically in Figs. 8 and 9 to compare with the results obtained from the simple beam theory.

Finite-Difference Method

This method was given by Bortsch (13) and later used by Bay (14) in his analysis of single-span deep beams. From a mathematical point of view, it is simply a numerical approximate solution to the biharmonic equation $\nabla^4\phi = 0$ with the prescribed boundary conditions. For the sake of visualizing the solution in a physical sense, we may think of ϕ, which is a function of x and y, as analogous to z, the deflection of a plate under bending, which satisfies the equation $\nabla^4 z = -p/D$. With $p = 0$, that is, no load being present, z becomes the ordinate of a curved surface, satisfying the equation $\nabla^4 z = 0$ and the prescribed boundary conditions at the edges. Accordingly, at any point on the curved surface, we may consider $\sigma_x = \partial^2\phi/\partial y^2$ as the curvature of the surface in the y-direction and σ_y as the curvature of the surface in the x-direction. Thus z will be used instead of ϕ hereafter.

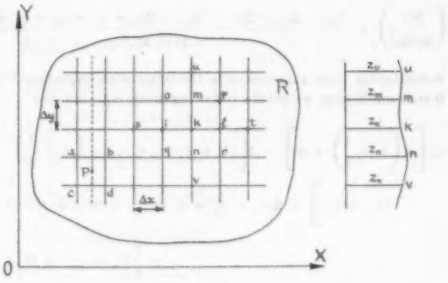

Fig. 3

The fundamental formulas are first derived. Consider a curved surface, with region R as its projection on the x-y plane, as shown in Fig. 3. Divide R into a network of equal divisions, and let z denote the distance from each net-point of the curved surface to the x-y plane, with its subscript indicating the particular point. For sufficiently small divisions, $(\Delta z)/(\Delta x)$ along lines in the x-direction is a good approximation for the value of $\partial z/\partial x$ at the mid-point of the interval under consideration. Thus taking point k for example

$$\left(\frac{\partial z}{\partial x}\right)_k \approx \left(\frac{\Delta z}{\Delta x}\right)_k = \frac{z_l - z_i}{2\,\Delta x}$$

$$\left(\frac{\partial z}{\partial y}\right)_k \approx \left(\frac{\Delta z}{\Delta y}\right)_k = \frac{z_m - z_n}{2\,\Delta y}$$

k being the mid-point of the interval $2\,\Delta x$ and $2\,\Delta y$.

Applying the same reasoning to partial derivatives of higher orders and repeating the operation successively, one obtains for point k

$$\left.\begin{aligned}
\sigma_x &= \frac{\partial^2 z}{\partial y^2} = \frac{z_m - 2z_k + z_n}{(\Delta y)^2} \\
\sigma_y &= \frac{\partial^2 z}{\partial x^2} = \frac{z_l - 2z_k + z_i}{(\Delta x)^2} \\
\tau_{xy} &= -\frac{\partial^2 z}{\partial x \partial y} = \frac{(z_s + z_r) - (z_p + z_q)}{4\,\Delta x\,\Delta y}
\end{aligned}\right\} \quad \ldots\ldots [10]$$

Similarly, the following expressions are derived

$$\left(\frac{\partial^4 z}{\partial x^4}\right)_k = \frac{6z_k - 4z_l - 4z_i + z_t + z_s}{(\Delta x)^4}$$

$$\left(\frac{\partial^4 z}{\partial y^4}\right)_k = \frac{6z_k - 4z_m - 4z_n + z_u + z_v}{(\Delta y)^4}$$

$$\left(\frac{\partial^4 z}{\partial x^2 \partial y^2}\right)_a = \frac{4z_a - 2z_m - 2z_n - 2z_l - 2z_i + z_p + z_q + z_r + z_s}{(\Delta x)^2(\Delta y)^2}$$

Substituting these expressions in the biharmonic equation $\nabla^4 z = 0$ and simplifying, we get the following linear equation in z

$$z_a\left[6\left(\lambda + \frac{1}{\lambda}\right) + 8\right] - 4\left[(1+\lambda)(z_l + z_i) + \left(1 + \frac{1}{\lambda}\right)(z_m + z_n)\right] + 2(z_p + z_q + z_r + z_s) + \lambda(z_l + z_i) + \frac{1}{\lambda}(z_m + z_n) = 0 \quad \ldots [11]$$

where $\lambda = (\Delta y/\Delta x)^2$

A similar equation in z is obtained for each net-point, and therefore a set of simultaneous linear equations is established. The values of z for all points of the network should be such as to satisfy these equations. If the values of z are determined, the values of normal and shearing stresses at any given net-point can be easily calculated by Equations [10]. However, it should be noted that the shearing stresses computed from the last of Equations [10] are not so accurate as the values for the normal stresses because the intervals taken for the difference of z-values are twice as large, being $2(\Delta x)$ and $2(\Delta y)$, respectively. Their accuracy can be improved by taking a section midway between the lines of division (see Fig. 3), and computing the shearing stresses at points such as P, the center of each small rectangle, with the following modified formula

$$(\tau_{xy})_c = \frac{(z_a + z_d) - (z_b + z_c)}{\Delta x\, \Delta y} \quad \ldots [12]$$

The boundary conditions are now to be considered. For rectangular plates with specified values of normal and shearing stresses at the edges, these conditions can be satisfied by fixing the values of z and the cross slopes along the edges. For example, if $\sigma_y = -p$ and $\tau_{xy} = 0$ along a portion of one edge in the x-direction, then $\partial^2 z/\partial x^2 = -p$, and $\partial^2 z/\partial x \partial y = 0$. Since y remains constant along this edge, integration with respect to x gives $z = -px^2/2 + C_1 x + C_2$ and $\partial z/\partial y = K$ where C_1, C_2, and K are constants of integration. Furthermore, if $\sigma_x = 0$ and $\tau_{xy} = 0$ along an edge in the y-direction, then $\partial^2 z/\partial y^2 = 0$ and $\partial^2 z/\partial x \partial y = 0$. Now, x being constant, integration with respect to y gives $z = C_1' y + C_2'$ and $\partial z/\partial x = K'$ along this edge, C_1', C_2' and K' being further constants of integration. These equations are used to determine the values of z along the edges and those for the outside net-points beyond the boundary which are needed for establishing Equation [11] at those interior points adjacent to the boundary. The constants of integration for each portion of the edge can be determined by first choosing a datum point and then computing the values for the other points successively by means of continuity of z and its first partial derivatives. It can be shown that values of $\partial^2 z/\partial x^2$, $\partial^2 z/\partial y^2$, and $\partial^2 z/\partial x \partial y$ are independent of the selected datum, and it is therefore convenient to make z, $\partial z/\partial x$, $\partial z/\partial y$ all equal to zero at a certain datum point on the boundary. The foregoing explanation of the process is illustrated by the following analysis of the square-plate case:

Case of the Square Plate. The boundary conditions here are the same as those for Case 1 of the previous analysis so that results from the two methods may be compared. Since the loading is symmetrical with respect to the y-axis, only one half of the plate is used for calculations. Starting from point A as a datum such that $z_A = 0$, $(\partial z/\partial x)_A = 0$ and $(\partial z/\partial y)_A = 0$, we have for portion AB

$$\sigma_y = 0, \quad \partial^2 z/\partial x^2 = 0, \quad z = C_1 x + C_2$$
$$\tau_{xy} = 0, \quad \partial^2 z/\partial x \partial y = 0, \quad \partial z/\partial y = K$$

With the initial zero values at point A, $C_1 = C_2 = K = 0$ and therefore the equations become $z = 0$ and $\partial z/\partial y = 0$. For portion BC

$$\sigma_y = -p, \quad \partial^2 z/\partial x^2 = -p, \quad z = -px^2/2 + C_1 x + C_2$$
$$\tau_{xy} = 0, \quad \partial^2 z/\partial x \partial y = 0, \quad \partial z/\partial y = K$$

Since at $x = a/2$, $z = 0$, $\partial z/\partial x = 0$, $\partial z/\partial y = 0$ so that $C_1 = pa/2$, $C_2 = -pa^2/8$ and $K = 0$, the equations for portion BC become

$$z = -\frac{px^2}{2} + \frac{pa}{2}x - \frac{pa^2}{8}, \quad \partial z/\partial y = 0$$

The values of z computed for $x = 3a/4$ and $x = a$ are $-\beta$ and -4β, respectively, as shown in Fig. 4. For the edge CD

$$\sigma_x = 0, \quad \partial^2 z/\partial y^2 = 0, \quad z = C_1 y + C_2$$

Since at point C, $z = -pa^2/8$ and $\partial z/\partial y = 0$, therefore

$$C_1 = 0, \quad C_2 = -pa^2/8, \quad z = -pa^2/8$$

Accordingly, all the values of z along the edge CD are -4β. From $\tau_{xy} = 0$ along CD, $\partial z/\partial x = K$. Since at point C, $\partial z/\partial x$ can be computed from the expression for z along BC, $(\partial z/\partial x)_c = -pa/2$. Then $K = -pa/2$, and therefore $\partial z/\partial x = -pa/2$ along CD. Similarly, the equations obtained for portion DE are

$$z = -\frac{pa}{2}x + \frac{3}{8}pa^2, \quad \partial z/\partial y = 0$$

and the equations obtained for portion EF are

$$z = -px^2/2 + pa^2/4, \quad \partial z/\partial y = 0$$

From these equations, the values of z at the various points along the upper edge are obtained, as shown in Fig. 4.

The values of z at those points outside the boundary can be expressed in terms of z-values of the inner points by means of the cross slopes along the boundary. For example, as $\partial z/\partial y = 0$ for the upper edge, therefore $z_a = z_1$, $z_b = z_2$, $z_c = z_3$, and $z_d = z_4$. Similarly for the lower edge, the z-values of the outside points are z_{17}, z_{18}, z_{19}, z_{20}, respectively, as indicated in Fig. 4. Furthermore, for the edge CD, $\partial z/\partial x = -pa/2$. Therefore for computing z_e at point e

$$\frac{z_e - z_4}{2\Delta x} = -\frac{pa}{2}$$

or

$$z_e = z_4 - pa(a/4) = z_4 - 8\beta$$

Likewise, the z-values for the other points outside edge CD are obtained.

Having satisfied the boundary conditions, a set of simultaneous equations for the unknown z-values is obtained. For example, considering point 1, one obtains the following equation by means of Equation [11]

$$z_1\left[6\left(\frac{16}{9} + \frac{9}{16}\right) + 8\right] - 4\left[\left(1 + \frac{16}{9}\right)(2z_2) + \left(1 + \frac{9}{16}\right)(z_4 + 8\beta)\right] + 2(2z_6 + 14\beta) + \frac{16}{9}(2z_4) + \frac{9}{16}(z_9 + z_1) = 0$$

Thus each inner point gives one equation so that there are twenty

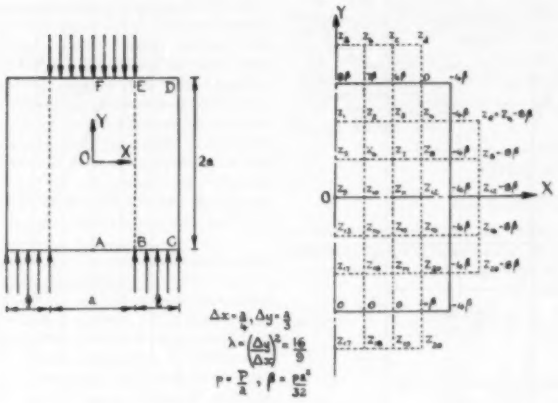

FIG. 4

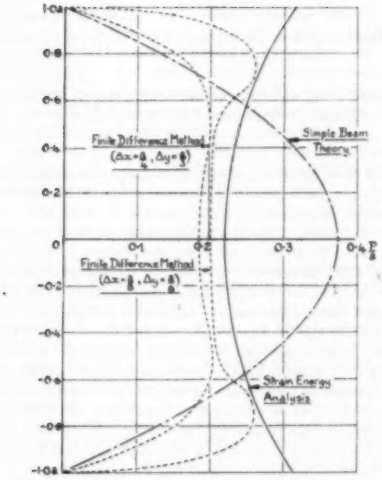
Finite Difference Method
$(\Delta x = \frac{a}{4}, \Delta y = \frac{a}{3})$
Simple Beam Theory
Finite Difference Method
$(\Delta x = \frac{a}{8}, \Delta y = \frac{a}{6})$
Strain Energy Analysis
$\frac{P}{a}$

FIG. 5 VARIATION OF τ_{xy} ON SECTIONS $x = \pm a/2$ FOR SQUARE PLATE

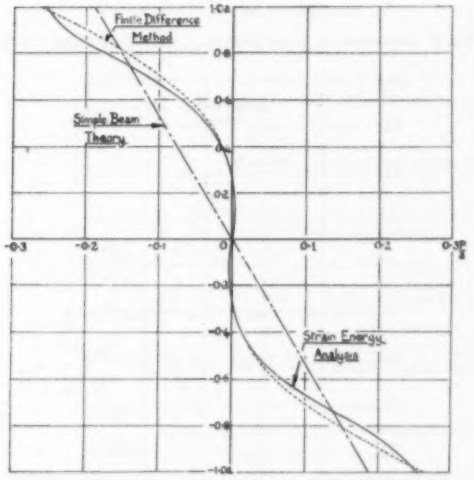

FIG. 6 VARIATION OF σ_x ON SECTIONS $x = \pm a/2$ FOR SQUARE PLATE

equations for the twenty unknown z-values. Solving these equations

$z_1 = 6.917$;	$z_2 = 6.038$;	$z_3 = 3.535$;	$z_4 = -0.018$
$z_5 = 5.440$;	$z_6 = 4.754$;	$z_7 = 2.778$;	$z_8 = -0.239$
$z_9 = 4.000$;	$z_{10} = 3.500$;	$z_{11} = 2.000$;	$z_{12} = -0.500$
$z_{13} = 2.560$;	$z_{14} = 2.246$;	$z_{15} = 1.222$;	$z_{16} = -0.761$
$z_{17} = 1.083$;	$z_{18} = 0.962$;	$z_{19} = 0.465$;	$z_{20} = -0.982$

all numerical values being in units of β.

Having determined the z-values, the normal and shearing stresses at any point of the network may be found by means of Equations [10]. For example, the bending stress at $x = a/2$, $y = a$ is

$$\sigma_x = \frac{2(3.535 - 4)\beta}{(\Delta y)^2} = \frac{2(3.535 - 4) \times \frac{pa^2}{32}}{(a/3)^2} = -0.262\ p$$

and the shearing stress at $x = a/2$, $y = 0$ is

$$\tau_{xy} = \frac{(4.754 - 0.761) - (2.246 - 0.239)}{4\left(\frac{a}{4}\right)\left(\frac{a}{3}\right)} \times \frac{pa^2}{32} = 0.186\ p$$

The values of τ_{xy} and σ_x thus computed for the section $x = a/2$ are plotted and compared in Figs. 5 and 6 with the results of the strain-energy method and also with those obtained from the simple beam theory. As mentioned before, the values of the shearing stresses would be more accurate if Equation [12] with respect to

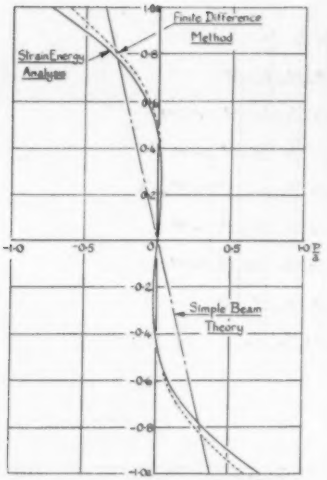

FIG. 7 VARIATION OF σ_x ON SECTION $x = 0$ FOR SQUARE PLATE

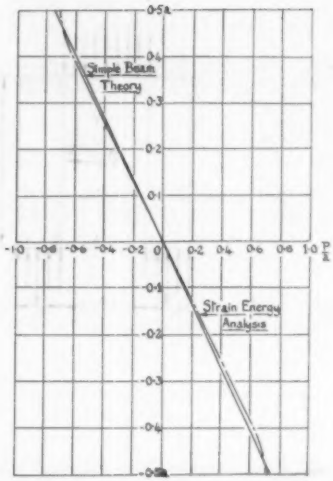

FIG. 9 VARIATION OF σ_x ON SECTIONS $x = \pm a/2$ FOR PLATE WITH $b/a = 1/2$

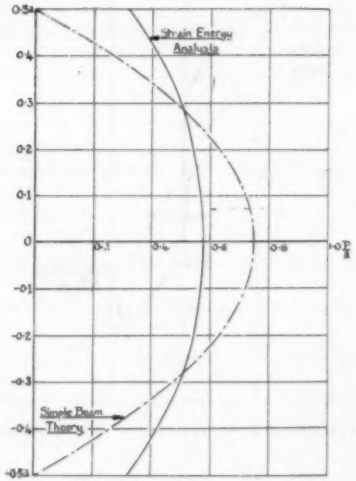

FIG. 8 VARIATION OF τ_{xy} ON SECTIONS $x = \pm a/2$ FOR PLATE WITH $b/a = 1/2$

the center points of the small rectangles was used. However, as the shearing stresses at the section $x = a/2$ are required, this is not immediately applicable. Therefore values of z, found by interpolation with curve plotting, have been used to give more accurate values of τ_{xy} at $x = a/2$ by decreasing the intervals by one half. These values of τ_{xy} are also shown in Fig. 5. It is seen that this curve of τ_{xy} approaches the one obtained from the strain-energy method more closely than the previous one. Values of σ_x for the section $x = 0$ have also been calculated and are compared graphically in Fig. 7 with the results of the strain-energy method and with those given by the simple beam theory.

The variation of τ_{xy} and σ_x for the sections $x = \pm a/2$ in the plate with $b/a = 1/2$ are given in Figs. 8 and 9, respectively.

CONCLUSIONS

It is seen that, for the square plate, the actual maximum bending stresses are much greater than those predicted by the simple beam theory. However, for a plate having the ratio $b/a = 1/2$, the bending stresses from the strain-energy method are almost identical with those obtained from the simple beam theory. The actual shearing-stress distribution for the square plate differs considerably from the conventional parabolic form given by the simple beam theory, whereas the agreement between the results is better for the case of $b/a = 1/2$. In order to be able to draw precise conclusions regarding the relation between the results obtained by the simple beam theory and by the more exact analysis, it would be necessary to investigate other cases with various ratios of b/a and different types of loading. However, judging from the present results, it seems very likely that it is not necessary to decrease the ratio b/a much below $1/2$ for the simple beam theory to yield quite accurate results.

It is of interest to note that discontinuity of normal stress on the boundary, such as at $x = a/2$, produces discontinuity of shearing stress at the same point. There is no shearing stress on the boundary, but the value of the localized shearing stress at points very near the edge in this particular section is $(1/\pi)(P/a)$, as given by the two cases of the analysis by the strain-energy method. In general, it can be shown that the value of this localized shearing stress is always equal to the difference of the normal stresses on the edge at that particular point divided by π, regardless of the ratio b/a. This shows that the value depends upon the local conditions only. Thus the maximum shearing stress for beams with uniform load p at the top cannot be less than p/π. For deep beams with ratio $b/a = 1$ or greater, the maximum shearing stress occurs extremely close to the edge and its value is p/π; but for beams with ratio $b/a = 1/2$ or less, the maximum shearing stress occurs near the center of the depth and its value becomes greater than p/π so that the localized stress is then insignificant. This phenomenon indicates a transition from a

case where shear is dominant to a case where bending is dominant. Furthermore, for plates with large ratios of b/a, the distribution of shearing stress is more or less uniform throughout the depth except near the edges where the localized stress becomes considerably greater than the average value. Hence the ratio b/a bears a close relation to the effect of the pressure p at the loaded edge on the shearing-stress distribution in a transverse section. The effect of the pressure p, as seen from the results of analysis, is to tend to shift the maximum peak of shearing stress out of the central portion of the depth toward the loaded edge. As the ratio b/a decreases, the effect becomes negligible and the simple theory for long beams becomes valid which disregards the effect of the pressure p.

Results from the two methods of obtaining the stresses agree fairly well with each other. The finite-difference method is reasonably accurate for determining the normal stresses at various points, but less accurate for shearing stresses. This is probably because the x-value at the particular point is used in computing the normal stresses whereas, for the shearing stress, it is necessary to use the x-values at the four corners of a rectangle circumscribing the point so that the result is more or less an average stress for the two adjacent sections. Moreover, the finite-difference method has the characteristic of rounding off peaks of maximum stresses; this may be seen from Figs. 5 and 7. This is evidently due to the use of finite intervals instead of infinitesimal ones. However, the finite-difference method has the advantage that boundary conditions, no matter how complex, can be satisfied. The method usually indicates the true variation of stress with fairly accurate values for the stresses. However, the method does not give the values of localized stresses or the exact position of the maximum shearing stress.

It may also be mentioned here that data from photoelastic tests confirm, in a general manner, the results given by the mathematical analyses presented in this paper.

BIBLIOGRAPHY

1 "Spannungen in wandartigen Balken bei feldweise wechselnder Belastung," by H. Craemer, *Zeitschrift für angewandte Mathematik und Mechanik*, vol. 10, 1930, pp. 209–218.

2 "Spannungen in durchlaufenden Scheiben bei Vollbelastung aller Felder," by H. Craemer, *Beton und Eisen*, vol. 22, 1933, pp. 233–237.

3 "Die Beanspruchungen durchlaufender Tragwände durch Massenkräfte, besonders Reibung," by H. Craemer, *Abhandlungen der Internationale Vereinigung für Brücken- und Hochbau*, Zürich, Switzerland, vol. 3, 1935, pp. 47–55.

4 "Beitrag zur Theorie der Halbscheibe und des wandartigen Trägers," by F. Dischinger, *Abhandlungen der Internationale Vereinigung für Brücken- und Hochbau*, Zürich, Switzerland, vol. 1, 1932, pp. 69–93.

5 "Design of Deep Girders," by Structural Bureau, Portland Cement Association, Concrete Information No. ST 66.

6 "Der wandartige Träger auf unendlich vielen Stützen," by H. Bay, *Ingenieur-Archiv*, vol. 3, 1932, pp. 435–446.

7 "On an Approximate Solution of the Bending of a Beam of Rectangular Cross Section Under Any System of Loads," by L. N. G. Filon, *Philosophical Transactions of the Royal Society*, London, series A, vol. 201, 1903, p. 63.

8 "Die schiefen Hauptzugspannungen beim Eisenbetonbalken," by H. Bay, *Ingenieur-Archiv*, vol. 4, 1933, p. 244.

9 "Die Spannungen und Formanderungen von Balken mit rechteckigem Querschnitt," by F. R. Seewald, Abhandlungen aus dem Aerodyn. Inst. der Tech. Hochschule, Aachen, vol. 7, 1927.

10 "Über die Grundlagen der Balken-Theorie," by Th. von Kármán, Abhandlungen aus dem Aerodyn. Inst. der Tech. Hochschule, Aachen, vol. 7, 1927.

11 "The Approximate Solution of Two-Dimensional Problems in Elasticity," by S. Timoshenko, *Philosophical Magazine*, vol. 47, 1924, p. 1095.

12 "Compression of Rectangular Blocks, and the Bending of Beams by Non-Linear Distributions of Bending Forces," by J. N. Goodier, Trans. ASME, vol. 54, 1932. Paper No. APM—54-17.

13 "Die Ermittlung der Spannungen in beliebig begrenzten Scheiben," by R. Bortsch, Aus den Sitzungsberichten der Akademie der Wissenschaften in Wien, math.-naturwiss. Klasse, Abtlg. IIa, vol. 138, 1929.

14 "Über den Spannungszustand in hohen Trägern und die Bewehrung von Eisenbetontragwänden," by H. Bay, Stuttgart, Germany, 1931, 64 pp.

15 "Flächentragwerke," by K. Girkmann, Springer-Verlag, Vienna, Austria, 1946.

Appendix

The Exact Solution

The normal stress on the vertical sides of the plate may be eliminated by the introduction of a second stress function in a manner similar to that suggested by Girkmann (15)

$$\phi' = \sum_{m=1,3,5,\cdots}^{\infty} \frac{1}{\gamma^2}(E_m \sinh \gamma y + F_m \gamma y \cosh \gamma y) \cos \gamma x + \sum_{n=1,2,3,\cdots}^{\infty} \frac{1}{\epsilon^2}(G_n \cosh \epsilon x + H_n \epsilon x \sinh \epsilon x) \sin \epsilon y$$

where

$$\gamma = \frac{m\pi}{2a} \text{ and } \epsilon = \frac{n\pi}{b}$$

The stresses given by this stress function are

$$\sigma_x = \sum_{m=1,3,5,\cdots}^{\infty} [(E_m + 2F_m) \sinh \gamma y + F_m \gamma y \cosh \gamma y] \cos \gamma x - \sum_{n=1,2,3,\cdots}^{\infty} (G_n \cosh \epsilon x + H_n \epsilon x \sinh \epsilon x) \sin \epsilon y$$

$$\sigma_y = -\sum_{m=1,3,5,\cdots}^{\infty} (E_m \sinh \gamma y + F_m \gamma y \cosh \gamma y) \cos \gamma x + \sum_{n=1,2,3,\cdots}^{\infty} [(G_n + 2H_n) \cosh \epsilon x + H_n \epsilon x \sinh \epsilon x] \sin \epsilon y$$

$$\tau_{xy} = \sum_{m=1,3,5,\cdots}^{\infty} [(E_m + F_m) \cosh \gamma y + F_m \gamma y \sinh \gamma y] \sin \gamma x - \sum_{n=1,2,3,\cdots}^{\infty} [(G_n + H_n) \sinh \epsilon x + H_n \epsilon x \cosh \epsilon x] \cos \epsilon y$$

The next step is to expand the normal stress on the vertical sides in a Fourier series of the form

$$(\sigma_x)_{x=\pm a} = \sum_{n}^{\infty} a_n \sin \epsilon y$$

The boundary conditions to be satisfied are then

$$x = \pm a, \quad \sigma_x = \sum_{n}^{\infty} a_n \sin \epsilon y$$
$$y = \pm b, \quad \sigma_y = 0$$
$$x = \pm a, \quad \tau_{xy} = 0$$
$$y = \pm b, \quad \tau_{xy} = 0$$

The first two boundary conditions give the equations

$$G_n = -a_n \operatorname{sech} \epsilon a - H_n \epsilon a \tanh \epsilon a$$
$$E_m = -F_m \gamma b \coth \gamma b$$

Hence, by using these equations, the last two boundary conditions will give two equations in two unknowns. In the first of these equations, it is necessary to expand $\cosh \gamma y$ and $\gamma y \sinh \gamma y$ in a Fourier series of $\cos \epsilon y$ whereas, in the second, it is necessary to expand $\sinh \epsilon x$ and $\epsilon x \cosh \epsilon x$ in a Fourier series of $\sin \gamma x$. A system of equations then results which may be solved by considering only a finite number of terms. In view of the very considerable labor which is involved, and the approximation of considering only a finite number of terms, it was decided that the strain-energy method be used.

A Fourier Integral Solution for the Plane-Stress Problem of a Circular Ring With Concentrated Radial Loads

By CARL W. NELSON,[1] BERKELEY, CALIF.

A Fourier integral solution for the stresses in a straight bar of uniform cross section loaded by various combinations of loads applied normally to the edges of the bar was published by L. N. G. Filon in 1903 (3).[2] Solutions for the stresses in circular rings, loaded on one or both boundaries by radial loads, have been limited to Fourier-series solutions for closed circular rings (1, 12, 13, 14, 15), except that solutions in closed form have been obtained for the limiting cases which occur either when the inner radius becomes very small or when the outer radius becomes very large. This paper presents a Fourier integral solution for the plane-stress problem of a curved bar bounded by two concentric circles and loaded by radial loads on the circular boundaries. It treats only the particular case of a curved bar in equilibrium under the action of two equal and opposite radial forces, one on each boundary. However, the method can be extended so as to deal with other combinations of loads. Sufficient numerical results are given to show that the Fourier integral method permits the calculation of numerical values of the stresses in the particular case considered. It is the purpose of this paper to show that the Fourier integral method can be used successfully in what is probably the simplest problem of concentrated loads acting on a curved bar and to furnish a background of material for use in less simple problems such as bending of curved bars due to concentrated loads.

Introduction

In this paper, a Fourier integral solution is developed for a portion of a circular ring loaded as shown in Fig. 1(*b*). This is of course a special case of the general problem of a portion of a circular ring loaded by any balanced system of forces acting on the inner and outer curved boundaries. The particular case selected for treatment in this paper was chosen, because of its simplicity, as a suitable problem to use in developing a method and procedures. However, it seems certain that the method used in this paper can be used to advantage for the solution of many problems which arise in machine design.

It can be shown that the solution which will be presented for the problem in Fig. 1(*b*) reduces to the known Fourier integral solution for the straight beam in Fig. 1(*a*) when the ratio of radii a/b, approaches unity. It can also be shown that the solution which will be obtained for Fig. 1(*b*) agrees with the known Fourier-series solution for the hollow cylinder in Fig. 1(*c*), (15), except for a very small discrepancy due to the fact that the circular ring in Fig. 1(*c*) is a closed ring. The Fourier integral solution for Fig. 1(*b*) will be found to be convenient for values

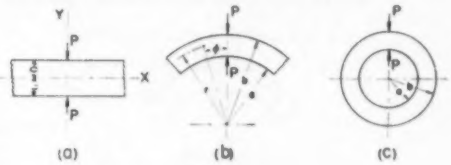

Fig. 1

of a/b close to unity and down to $a/b = 0.5$ or even less. The Fourier-series solution for Fig. 1(*c*) is convenient to use for values of a/b close to zero and up to $a/b = 0.5$ or even more. Thus there is a range of values of a/b throughout which the two solutions can be compared. The Fourier integral solution of this paper furnishes a link between the known solutions for Figs. 1(*a*) and (*c*).

The procedure used in finding the stress function for Fig. 1(*b*) parallels the procedure used by Coker and Filon (2), for various straight-beam problems such as that of Fig. 1(*a*).

Review of General Theory

Two-dimensional plane-stress or plane-strain problems in elasticity are often solved in terms of Airy's stress function which will be denoted by ψ. This stress function must satisfy the differential equation

$$\nabla^2\nabla^2\psi = 0 \qquad [1]$$

where ∇^2 stands for the Laplace operator which, in polar coordinates (r, ϕ) is

$$\nabla^2 = \frac{\partial^2}{\partial r^2} + \frac{1}{r}\frac{\partial}{\partial r} + \frac{1}{r^2}\frac{\partial^2}{\partial \phi^2}$$

The stresses are to be determined from the stress function by the equations

$$\sigma_r = \frac{1}{r}\frac{\partial \psi}{\partial r} + \frac{1}{r^2}\frac{\partial^2 \psi}{\partial \phi^2} \qquad [2]$$

$$\sigma_\phi = \frac{\partial^2 \psi}{\partial r^2} \qquad [3]$$

$$\tau_{r\phi} = -\frac{\partial}{\partial r}\left(\frac{1}{r}\frac{\partial \psi}{\partial \phi}\right) \qquad [4]$$

Stresses determined by the foregoing procedure will satisfy equilibrium and compatibility requirements. In any particular prob-

[1] Assistant Professor, Engineering Design Division, University of California. Jun. ASME.

[2] Numbers in parentheses refer to the Bibliography at the end of the paper.

Contributed by the Applied Mechanics Division and presented at the Annual Meeting, New York, N. Y., November 26–December 1, 1950, of The American Society of Mechanical Engineers.

Discussion of this paper should be addressed to the Secretary, ASME, 29 West 39th Street, New York, N. Y., and will be accepted until July 10, 1951, for publication at a later date. Discussion received after the closing date will be returned.

Note: Statements and opinions advanced in papers are to be understood as individual expressions of their authors and not those of the Society. Manuscript received by the Applied Mechanics Division, February 21, 1950. Paper No. 50—A-16.

lem, a proper combination of solutions of Equation [1] must be formed so that boundary conditions will be satisfied.

Of the various possible solutions of Equation [1], the solutions of the form

$$\psi_n = (a_n r^n + b_n r^{n+2} + a_n' r^{-n} + b_n' r^{-n+2}) \cos n\phi \ldots [5]$$

and

$$\psi_n = (c_n r^n + d_n r^{n+2} + c_n' r^{-n} + d_n' r^{-n+2}) \sin n\phi \ldots [6]$$

are sufficient for problems of the type considered in this paper.

Statement of Problem and Method of Solution

Fig. 1(*b*) illustrates the problem which will be solved in this paper. Although the loads in Fig. 1(*b*) are concentrated, it will be convenient to consider a slightly more general problem temporarily. Fig. 2 shows a portion of a circular ring loaded, not

Fig. 2

by concentrated forces, but by normal forces which are uniformly distributed from $\phi = -\beta$ to $\phi = \beta$ on both boundaries $r = a$ and $r = b$. For equilibrium it must be assumed that

$$(\sigma_r)_{r=a} = \frac{b}{a}(\sigma_r)_{r=b} = -\frac{b}{a}p \ldots [7]$$

After the stress function for Fig. 2 has been obtained, the corresponding stress function for Fig. 1(*b*) will be the limit obtained by letting β approach zero in the stress function for Fig. 2.

Derivation of a Stress Function to Satisfy Boundary Conditions

Because of the symmetry of Fig. 2, solutions of Equation [1] in the form given by Equation [6] need not be considered. We have to consider only the solutions given by Equation [5] and, in these solutions, n is not necessarily an integer. Any number of such solutions may be combined to form the complete stress function for Fig. 2. The solutions must be combined in such a way that the boundary-stress conditions for Fig. 2 will be satisfied.

The boundary-stress conditions for Fig. 2 are

$$(\sigma_r)_{r=a} = \frac{b}{a}(\sigma_r)_{r=b} \ldots [8]$$

$$(\sigma_r)_{r=b} = F(\phi) \ldots [9]$$

$$(\tau_{r\phi})_{r=a} = 0 \ldots [10]$$

$$(\tau_{r\phi})_{r=b} = 0 \ldots [11]$$

where $F(\phi)$ is an even function of ϕ. The explicit expression for $F(\phi)$ does not need to be given immediately. It is sufficient to note, for the present, that the formula for expressing a function as a Fourier cosine integral gives us

$$F(\phi) = \frac{2}{\pi}\int_0^\infty d\lambda \int_0^\infty F(\lambda)\cos n\phi \cdot \cos n\lambda \cdot d\lambda \ldots [12]$$

and this integral expression is generally valid for $0 < \phi < \infty$ but, in the present case, it is valid for $-\infty < \phi < \infty$, because $F(\phi)$ is an even function.

The contribution of ψ_n to the stresses σ_r and $\tau_{r\phi}$ is found by applying Equations [2] and [4], respectively. When the indicated operations are performed on ψ_n, we get

$$(\sigma_r)_n = -[n(n-1)a_n r^{n-2} + (n+1)(n-2)b_n r^n + n(n+1)a_n' r^{-n-2} + (n-1)(n+2)b_n' r^{-n}]\cos n\phi \ldots [13]$$

$$(\tau_{r\phi})_n = [n(n-1)a_n r^{n-2} + n(n+1)b_n r^n - n(n+1)a_n' r^{-n-2} - n(n-1)b_n' r^{-n}]\sin n\phi \ldots [14]$$

It is convenient in the present problem to apply boundary conditions of Equations [8], [10], and [11] first. These three conditions can be satisfied separately for the stresses contributed by each ψ_n. From Equations [13] and [14], we find that the equations expressing conditions [8], [10], and [11] are, respectively

$$n(n-1)a_n a^{n-2} + (n+1)(n-2)b_n a^n + n(n+1)a_n' a^{-n-2} + (n-1)(n+2)b_n' a^{-n} = \frac{b}{a}[n(n-1)a_n b^{n-2} + (n+1)(n-2)b_n b^n + n(n+1)a_n' b^{-n-2} + (n-1)(n+2)b_n' b^{-n}] \ldots [15]$$

$$n(n-1)a_n a^{n-2} + n(n+1)b_n a^n - n(n+1)a_n' a^{-n-2} - n(n-1)b_n' a^{-n} = 0 \ldots [16]$$

$$n(n-1)a_n b^{n-2} + n(n+1)b_n b^n - n(n+1)a_n' b^{-n-2} - n(n-1)b_n' b^{-n} = 0 \ldots [17]$$

By simultaneous solution of Equations [15], [16], and [17], any three of the four constants a_n, b_n, a_n', b_n' can be expressed in terms of the remaining one. Expressing the others in terms of a_n' and substituting the results into Equation [5], we obtain

$$\psi_n = \frac{-a_n'}{(n-1)ab(b^{n-1} - a^{n-1})}\left[\frac{n(b^2-r^2)}{b}\left(\frac{r^n}{a^n} + \frac{a^n}{r^n}\right) + \frac{n(r^2-a^2)}{a}\left(\frac{b^n}{r^n} + \frac{r^n}{b^n}\right) + \frac{(b^2+r^2)}{b}\left(\frac{r^n}{a^n} - \frac{a^n}{r^n}\right) + \frac{(r^2+a^2)}{a}\left(\frac{b^n}{r^n} - \frac{r^n}{b^n}\right)\right]\cos n\phi \ldots [18]$$

ψ_n will still satisfy all of the conditions imposed so far if we replace the fraction preceding the brackets in Equation [18] by a different constant. Let f denote this new constant. However, although f is constant in each ψ_n, we propose to use, in general, a different f in each ψ_n, and this may be indicated by writing

$f(n)$ rather than f to show that f is a function of n. It is a constant only if we are considering a particular f for a particular ψ_n, and the fact that f does not vary with the co-ordinates (r, ϕ). Next we can multiply each ψ_n by Δn and take the sum of many stress functions so obtained, getting

$$\sum_{n=0,\Delta n,2\Delta n,\cdots}^{\infty} \psi_n \cdot \Delta n = \sum_{n=0,\Delta n,2\Delta n,\cdots}^{\infty} f(n) g(r, n) \cos n\phi \cdot \Delta n \quad [19]$$

where $g(r, n)$ is used to denote the quantity in the brackets of Equation [18]. The limit of the stress function given by Equation [19] as Δn approaches zero is

$$\psi = \int_0^\infty f(n) \cdot g(r, n) \cdot \cos n\phi \cdot dn \quad [20]$$

This stress function satisfies Equation [1] and boundary conditions [8], [10], [11]. We still have to satisfy boundary condition [9].

Equation [12] gives us one expression for $(\sigma_r)_{r=b} = F(\phi)$.

Another expression for $(\sigma_r)_{r=b}$ can be obtained from Equation [20] by performing the differentiations indicated in Equation [2] and then substituting $r = b$ into the resulting expression for σ_r. First we get

$$\sigma_r = \int_0^\infty \frac{(1 - n^2)}{r^2} f(n) \cdot h(r, n) \cdot \cos n\phi \cdot dn \quad [21]$$

where

$$h(r, n) = \left[\begin{array}{l} \dfrac{n(b^2 - r^2)}{b} \left(\dfrac{r^n}{a^n} + \dfrac{a^n}{r^n} \right) \\ + \dfrac{n(r^2 - a^2)}{a} \left(\dfrac{b^n}{r^n} + \dfrac{r^n}{b^n} \right) \\ + \dfrac{2r^2}{b} \left(\dfrac{r^n}{a^n} - \dfrac{a^n}{r^n} \right) \\ + \dfrac{2r^2}{a} \left(\dfrac{b^n}{r^n} - \dfrac{r^n}{b^n} \right) \end{array} \right]$$

and substitution of $r = b$ into Equation [21] gives

$$(\sigma_r)_{r=b} = -\frac{2}{b} \int_0^\infty (n^2 - 1) \cdot f(n) \cdot \left[\left(\frac{b^n}{a^n} - \frac{a^n}{b^n} \right) + n \left(\frac{b}{a} - \frac{a}{b} \right) \right] \cos n\phi \cdot dn \quad [22]$$

Equating the two expressions for $(\sigma_r)_{r=b}$ given by Equations [12] and [22], we get

$$\frac{2}{\pi} \int_0^\infty d\alpha \int_0^\infty F(\lambda) \cos n\phi \cdot \cos n\lambda \cdot d\lambda = -\frac{2}{b} \int_0^\infty (n^2 - 1) f(n) \left[\left(\frac{b^n}{a^n} - \frac{a^n}{b^n} \right) + n \left(\frac{b}{a} - \frac{a}{b} \right) \right] \cos n\phi \cdot dn \quad [23]$$

from which

$$\frac{1}{\pi} \int_0^\infty F(\lambda) \cos n\lambda \cdot d\lambda = -\frac{1}{b} (n^2 - 1) f(n) \left[\left(\frac{b^n}{a^n} - \frac{a^n}{b^n} \right) + n \left(\frac{b}{a} - \frac{a}{b} \right) \right] \quad [24]$$

Solving the latter equation for $f(n)$ gives

$$f(n) = \frac{-\dfrac{b}{\pi} \displaystyle\int_0^\infty F(\lambda) \cdot \cos n\lambda \cdot d\lambda}{(n^2 - 1) \left[\left(\dfrac{b^n}{a^n} - \dfrac{a^n}{b^n} \right) + n \left(\dfrac{b}{a} - \dfrac{a}{b} \right) \right]} \quad [25]$$

Therefore

$$\psi = -\frac{b}{\pi} \int_0^\infty \frac{\left\{ g(r, n) \cos n\phi \cdot dn \displaystyle\int_0^\infty F(\lambda) \cdot \cos n\lambda \cdot d\lambda \right\}}{(n^2 - 1) \left[\left(\dfrac{b^n}{a^n} - \dfrac{a^n}{b^n} \right) + n \left(\dfrac{b}{a} - \dfrac{a}{b} \right) \right]} \quad [26]$$

Equation [26] gives the stress function for a large class of problems in which Conditions [8], [9], [10], [11] are fulfilled with $F(\phi)$ an even function of ϕ.

Returning to the specific problem of Fig. 2, we have

$$F(\phi) = (\sigma_r)_{r=b} = 0 \text{ for } -\infty < \phi < -\beta$$

$$F(\phi) = -p \text{ for } -\beta < \phi < \beta$$

$$F(\phi) = 0 \text{ for } \beta < \phi < \infty$$

Therefore

$$\int_0^\infty F(\lambda) \cdot \cos n\lambda \cdot d\lambda = \int_0^\beta (-p) \cdot \cos n\lambda \cdot d\lambda = -\frac{p}{n} \sin n\lambda \Big|_0^\beta = -\frac{p}{n} \sin n\beta \quad [27]$$

For the limiting case when β becomes very small, but the total load on each boundary remains finite and equal to P, we get

$$\lim_{\beta \to 0} \int_0^\infty F(\lambda) \cos n\lambda \cdot d\lambda = \lim_{\beta \to 0} \left(-\frac{p}{n} \sin n\beta \right) = -\frac{P}{2b} \quad [28]$$

Therefore the stress function for Fig. 1(*b*) is

$$\psi = \frac{P}{2\pi} \int_0^\infty \frac{g(r, n) \cdot \cos n\phi \cdot dn}{(n^2 - 1) \left[\left(\dfrac{b^n}{a^n} - \dfrac{a^n}{b^n} \right) + n \left(\dfrac{b}{a} - \dfrac{a}{b} \right) \right]} \quad [29]$$

By substituting

$$z = n \log \frac{1}{\alpha}, \quad \text{where } \alpha = \frac{a}{b} \quad [30]$$

Equation [29] can be put in the form

$$\psi = \frac{P}{2\pi} \int_0^\infty \left\{ \begin{array}{l} \left[\begin{array}{l} \dfrac{(b^2 - r^2)}{b \log \dfrac{1}{\alpha}} \cdot z \cosh Az \\ + \dfrac{(r^2 - a^2)}{a \log \dfrac{1}{\alpha}} z \cosh Bz \\ + \dfrac{(b^2 + r^2)}{b} \cdot \sinh Az \\ + \dfrac{(r^2 + a^2)}{a} \cdot \sinh Bz \end{array} \right] \\ \hline \left[\left(\dfrac{z}{\log \dfrac{1}{\alpha}} \right)^2 - 1 \right] \left[\sinh z + Xz \right] \end{array} \right\} \frac{\cos \Phi z \cdot dz}{\log \frac{1}{\alpha}} \quad [31]$$

where the following new symbols have been introduced:

$$\left.\begin{aligned} \Phi &= \frac{\phi}{\log\frac{1}{\alpha}}, \quad A = \frac{\log\frac{r}{a}}{\log\frac{1}{\alpha}}, \quad B = \frac{\log\frac{b}{r}}{\log\frac{1}{\alpha}} \\ X &= \frac{\sinh\log\frac{1}{\alpha}}{\log\frac{1}{\alpha}} = \frac{1-\alpha^2}{2\alpha\log\frac{1}{\alpha}} \end{aligned}\right\} \quad \ldots\ldots [32]$$

It should be noted that A and B are positive numbers between zero and unity and that

$$A + B = 1 \quad \ldots\ldots [33]$$

Determination of Stresses From Stress Function

The stresses for the problem in Fig. 1(b) may be obtained from the stress function of Equation [31] by applying Equations [2], [3], [4]. The results are given in the following form because the expressions for $(\sigma_r + \sigma_\phi)$ and $(\sigma_r - \sigma_\phi)$ are shorter than those for σ_r and σ_ϕ.

$$\sigma_r + \sigma_\phi = -\frac{2P}{\pi\log\frac{1}{\alpha}}\left[\frac{1}{b}\int_0^\infty \frac{\sinh Az\cdot\cos\Phi z\cdot dz}{\sinh z + zX} + \frac{1}{a}\int_0^\infty \frac{\sinh Bz\cdot\cos\Phi z\cdot dz}{\sinh z + zX}\right] \quad \ldots\ldots [34]$$

$$\sigma_r - \sigma_\phi = -\frac{2P}{\pi\left(\log\frac{1}{\alpha}\right)^2}\left[\frac{\left(\frac{b^2}{r^2}-1\right)}{2b}\int_0^\infty \frac{z\cdot\cosh Az\cdot\cos\Phi z\cdot dz}{\sinh z + zX} + \frac{\left(1-\frac{a^2}{r^2}\right)}{2a}\int_0^\infty \frac{z\cdot\cosh Bz\cdot\cos\Phi z\cdot dz}{\sinh z + zX}\right] \quad \ldots\ldots [35]$$

$$\tau_{r\phi} = \frac{2P}{\pi\left(\log\frac{1}{\alpha}\right)^2}\left[\frac{\left(\frac{b^2}{r^2}-1\right)}{4b}\int_0^\infty \frac{z\cdot\sinh Az\cdot\sin\Phi z\cdot dz}{\sinh z + zX} - \frac{\left(1-\frac{a^2}{r^2}\right)}{4a}\int_0^\infty \frac{z\cdot\sinh Bz\cdot\sin\Phi z\cdot dz}{\sinh z + zX}\right] \quad \ldots\ldots [36]$$

The first integral in Equation [35] can be obtained by taking $\partial/\partial A$ of the first integral in Equation [34]. Similarly, the first integral in Equation [36] is obtained by taking $-\partial/\partial\Phi$ of the first integral in Equation [34]. The remaining three integrals in Equations [34], [35], [36] differ from the three just considered only by having B in place of A. It will be recalled that A and B are both positive numbers between zero and unity.

From the foregoing it is apparent that all of the stresses can be obtained after the integral

$$\int_0^\infty \frac{\sinh Az\cdot\cos\Phi z\cdot dz}{\sinh z + zX}$$

has been evaluated. G. Mesmer (6) evaluated this integral with $X = 1$, for specific values of A and Φ, by use of a planimeter. The integral can be expressed finally in a series of products of powers of A and Φ. As a first step, using the Maclaurin series for $\sinh Az$ and $\cos\Phi z$, the product $\sinh Az\cdot\cos\Phi z$ can be replaced by its Maclaurin series. Then

$$\begin{aligned} &\int_0^\infty \frac{\sinh Az\cdot\cos\Phi z\cdot dz}{\sinh z + zX} \\ &= 2AI_1 \\ &+ 2(A^3 - 3\Phi^2A)I_3 \\ &+ 2\left(A^5 - \frac{4\cdot5}{1\cdot2}\Phi^2A^3 + 5\Phi^4A\right)I_5 \\ &+ 2\left(A^7 - \frac{6\cdot7}{1\cdot2}\Phi^2A^5 + \frac{4\cdot5\cdot6\cdot7}{1\cdot2\cdot3\cdot4}\Phi^4A^3 - 7\Phi^6A\right)I_7 \\ &+ 2\left(A^9 - \frac{8\cdot9}{1\cdot2}\Phi^2A^7 + \frac{6\cdot7\cdot8\cdot9}{1\cdot2\cdot3\cdot4}\Phi^4A^5 - \frac{4\cdot5\cdot6\cdot7\cdot8\cdot9}{1\cdot2\cdot3\cdot4\cdot5\cdot6}\Phi^6A^3 + 9\Phi^8A\right)I_9 \\ &+ - - - - - - \end{aligned} \quad \ldots [37]$$

where

$$I_k = \frac{1}{2(k!)}\int_0^\infty \frac{z^k dz}{\sinh z + zX} \quad \ldots\ldots [38]$$

The coefficients I_k do not depend on the co-ordinates A, Φ. They depend only on X which is a constant for any given value of the ratio $\alpha = a/b$. For $X = 1$, corresponding to the case of a straight beam, values of I_k were published by R. C. J. Howland (4, 5). Howland's table is reprinted in reference (7). In the present problem, X varies from $X = 1$ when $\alpha = 1$ to $X = 1.0820$ when $\alpha = 0.5$. Assuming that we are interested in values of α between 0.5 and 1.0, we have to consider only those values of X between 1.0 and 1.1.

The evaluation of the integrals $I_k(X)$ will be accomplished by reducing them to a Taylor series in powers of $(X - 1)$. The procedure for obtaining $I_k(X)$ in Taylor series form is lengthy and is given in the Appendix. This will permit a casual reader to

TABLE 1 VALUES OF COEFFICIENTS IN TAYLOR SERIES FOR $I_k(X)$

k	a_k	b_k	c_k	d_k	e_k	f_k	g_k
1	0.768574538	0.268574538	0.109586886	0.047491792	0.021259309	0.009711913	0.004499095
3	0.827710296	0.132993684	0.035635378	0.011549405	0.004137479	0.001577163	0.000627217
5	0.925475998	0.061798066	0.010565827	0.002532346	0.000722281	0.000229149	0.000078128
7	0.972698993	0.024313008	0.002558337	0.000446434	0.000100587	0.000026445	0.000007710
9	0.990949179	0.008490577	0.000526646	0.000065686	0.000011578	0.000002508	0.000000623
11	0.997188575	0.002707718	0.000095821	0.000008371	0.000001141	0.000000202	0.000000043
13	0.999163823	0.000819434	0.000015884	0.000000952	0.000000099	0.000000014	0.000000003
15	0.999758559	0.000238902	0.000002455	0.000000099	0.000000008	0.000000001	0.000000000
17	0.999931719	0.000067914	0.000000360	0.000000010	0.000000001	0.000000000	
19	0.999980979	0.000018969	0.000000051	0.000000001	0.000000000		
21	0.999994762	0.000005231	0.000000007	0.000000000			
23	0.999998570	0.000001429	0.000000001				
25	0.999999613	0.000000387	0.000000000				
27	0.999999896	0.000000104					
29	0.999999972	0.000000028					
31	0.999999993	0.000000007					
33	0.999999998	0.000000002					
35	0.999999999	0.000000001					
37	1.000000000	0.000000000					

follow the main steps of a basically simple procedure for obtaining the stresses in the problem here considered without having to concern himself with all of the mathematical details.

The results of the Taylor series development of $I_k(X)$ are summarized in Table 1. The coefficients a_k, b_k, etc., in Table 1, are the constants in the expansion

$$I_k(X) = \frac{1}{2(k!)}\int_0^\infty \frac{z^k dz}{\sinh z + z\,X} = a_k - b_k(X-1) + c_k(X-1)^2 - d_k(X-1)^3 + \ldots \quad [39]$$

Having obtained Table 1, it would now be possible to evaluate the integral given by Equation [37] for particular values of X, Φ, and A. However, Equation [37] would be very inconvenient to use because of the fact that the I_k are nearly equal to unity so that many terms would be required in order to obtain a numerical value for the summation expressed by the right side of Equation [37]. To overcome this difficulty, let Equation [37] be rewritten as follows

$$\int_0^\infty \frac{\sinh Az \cdot \cos \Phi z \cdot dz}{\sinh z + zX} = 2\begin{bmatrix} A \\ +(A^3 - 3\Phi^2 A) \\ +\left(A^5 - \frac{4\cdot 5}{1\cdot 2}\Phi^2 A^3 + 5\Phi^4 A\right) \\ +\ - - - - - \end{bmatrix} - 2\begin{bmatrix} A(1-I_1) \\ +(A^3 - 3\Phi^2 A)(1-I_3) \\ +\left(A^5 - \frac{4\cdot 5}{1\cdot 2}\Phi^2 A^3 + 5\Phi^4 A\right)(1-I_5) \\ +\ - - - - - \end{bmatrix} \quad [40]$$

It can be shown that

$$\int_0^\infty \frac{\sinh Az \cdot \cos \Phi z \cdot dz}{\frac{1}{2}e^z} = 2\begin{bmatrix} A \\ +(A^3 - 3\Phi^2 A) \\ +(A^5 - \frac{4\cdot 5}{1\cdot 2}\Phi^2 A^3 + 5\Phi^4 A) \\ +\ - - - - - \end{bmatrix} \quad [41]$$

but the integral on the left side of Equation [41] is an elementary type which can be evaluated by means of Equation [415] of reference (10) so as to obtain

$$\int_0^\infty \frac{\sinh Az \cdot \cos \Phi z \cdot dz}{\frac{1}{2}e^z} = \int_0^\infty e^{-(1-A)z}\cos \Phi z \cdot dz - \int_0^\infty e^{-(1+A)z}\cos \Phi z \cdot dz = \frac{(1-A)}{(1-A)^2+\Phi^2} - \frac{(1+A)}{(1+A)^2+\Phi^2} \quad [42]$$

Combining Equations [40], [41], and [42], we get

$$\int_0^\infty \frac{\sinh Az \cdot \cos \Phi z \cdot dz}{\sinh z + zX} = \frac{(1-A)}{(1-A)^2+\Phi^2} - \frac{(1+A)}{(1+A)^2+\Phi^2} - 2\begin{bmatrix} A(1-I_1) \\ +(A^3 - 3\Phi^2 A)(1-I_3) \\ +(A^5 - \frac{4\cdot 5}{1\cdot 2}\Phi^2 A^3 + 5\Phi^4 A)(1-I_5) \\ +\ - - - - - - - - - \end{bmatrix} \quad [43]$$

In most cases only a few terms of the series inside the brackets on the right side of Equation [43] will be required because the quantities $(1 - I_k)$ are small and diminish rapidly toward zero as k increases.

By taking the partial derivative of both sides of Equation [43] with respect to A we get

$$\int_0^\infty \frac{z\cosh Az \cdot \cos \Phi z \cdot dz}{\sinh z + zX} = \frac{(1-A)^2 - \Phi^2}{[(1-A)^2+\Phi^2]^2} + \frac{(1+A)^2 - \Phi^2}{[(1+A)^2+\Phi^2]^2} - 2\begin{bmatrix} (1-I_1) \\ +3(A^2 - \Phi^2)(1-I_3) \\ +5(A^4 - \frac{3\cdot 4}{1\cdot 2}\Phi^2 A^2 + \Phi^4)(1-I_5) \\ +7(A^6 - \frac{5\cdot 6}{1\cdot 2}\Phi^2 A^4 + \frac{3\cdot 4\cdot 5\cdot 6}{1\cdot 2\cdot 3\cdot 4}\Phi^4 A^2 - \Phi^6)(1-I_7) \\ +\ - - - - - \end{bmatrix} \quad [44]$$

and, by taking $-(\partial/\partial\Phi)$ of both sides of Equation [43], we get

$$\int_0^\infty \frac{z\sinh Az \cdot \sin \Phi z \cdot dz}{\sinh z + zX} = \frac{2(1-A)\Phi}{[(1-A)^2+\Phi^2]^2} - \frac{2(1+A)\Phi}{[(1+A)^2+\Phi^2]^2} - 2\begin{bmatrix} (2\cdot 3\Phi A)(1-I_3) \\ +(4\cdot 5\Phi A^3 - 4\cdot 5\Phi^3 A)(1-I_5) \\ +(6\cdot 7\Phi A^5 - \frac{4\cdot 5\cdot 6\cdot 7}{1\cdot 2\cdot 3}\Phi^3 A^3 + 6\cdot 7\Phi^5 A)(1-I_7) \\ +(8\cdot 9\Phi A^7 - \frac{6\cdot 7\cdot 8\cdot 9}{1\cdot 2\cdot 3}\Phi^3 A^5 + \frac{4\cdot 5\cdot 6\cdot 7\cdot 8\cdot 9}{1\cdot 2\cdot 3\cdot 4\cdot 5}\Phi^5 A^3 \\ -8\cdot 9\Phi^3 A)(1-I_9) \\ +\ - - - - - - - - - \end{bmatrix} \quad [45]$$

Now the stresses at any point in the curved bar in Fig. 1(*b*) can be calculated by using Equations [34], [35], [36] and [43], [44], [45].

Applications

The main purpose of including the calculations which follow is to indicate that the expressions for the stresses are now in a usable form from which numerical values of the stresses can be calculated. Since the stresses in this particular problem cannot be expected to differ greatly from the stresses due to similarly applied loads acting on a straight bar, it is not necessary to show a large number of curves for the stresses at various sections of a curved bar.

It can be shown from Equations [34] and [35] that the tangential stress at the inner edge of the curved bar, for the example shown in Fig. 1(*b*), is

$$(\sigma_\theta)_{A=a} = (\sigma_r)_{A=a} + \frac{4P}{\pi(b-a)}\cdot\frac{2X^2}{(1+\alpha)}\left[\frac{(1-\Phi^2)}{(1+\Phi^2)^2}\right] - \frac{4P}{\pi(b-a)}\cdot\frac{2X^2}{(1+\alpha)}[(1-I_3) - 3\Phi^2(1-I_5) + 5\Phi^4(1-I_7) - - -] \quad [46]$$

The term $(\sigma_r)_{A=0}$ is zero at every point except the point $\Phi = 0$, which is the point at which one of the loads P is applied. Using Equation [39] and the coefficients in Table 1, the values of the coefficients $(1 - I_k)$ for the case $\alpha = a/b = 0.9$ were calculated and are given in Table 2.

TABLE 2 VALUES OF $(1 - I_k)$ FOR $\alpha = 0.9$

(Corresponds to $X - 1 = 0.001851167$)

k	$(1 - I_k)$	k	$(1 - I_k)$	k	$(1 - I_k)$	k	$(1 - I_k)$
1	0.231922263	11	0.002816437	21	0.000005248	31	0.000000007
3	0.172535776	13	0.000837694	23	0.000001432	33	0.000000002
5	0.074638365	15	0.000241884	25	0.000000388	35	0.000000001
7	0.027346006	17	0.000068407	27	0.000000105	37	0.000000000
9	0.009066481	19	0.000019056	29	0.000000028		...

Fig. 3 shows the curve of $(\sigma_\phi)_{A=0}$ for $\alpha = 0.9$ plotted against

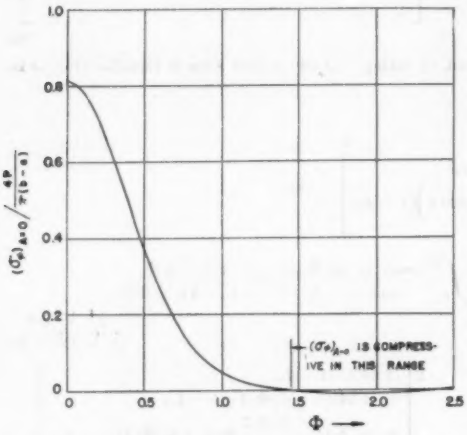

FIG. 3 TANGENTIAL STRESS ALONG INNER EDGE OF CURVED BAR OF FIG. 1(b), FOR $\alpha = a/b = 0.9$

the co-ordinate $\Phi = \phi/\log 1/\alpha$. It will be noted that points are plotted for values of Φ up to $\Phi = 2.5$. The series of Equation [46] can be used at best only up to values of Φ approaching $\Phi = 2$. For values of Φ greater than $\Phi \approx 1.5$, it was necessary to use Euler's transformation (9) in order to put Equation [46] into the following form

$$(\sigma_\phi)_{A=0} = (\sigma_r)_{A=0} + \frac{4P}{\pi(b-a)} \cdot \frac{2X^2}{(1+\alpha)} \left[\frac{1-\Phi^2}{(1+\Phi^2)^2}\right]$$

$$- \frac{4P}{\pi(b-a)} \cdot \frac{2X^2}{(1+\alpha)} \cdot \frac{4}{\Phi^2} \begin{bmatrix} 0.231922263\, g & - 1.83850705\, g^2 \\ + 2.06213284\, g^3 & - 0.3171688\, g^4 \\ - 0.338250\, g^5 & - 0.198124\, g^6 \\ - 0.04779\, g^7 & + 0.04905\, g^8 \\ + 0.0851\, g^9 & + 0.073\, g^{10} \\ + 0.025\, g^{11} & - 0.03\, g^{12} \\ - \cdots\cdots & \end{bmatrix} \quad \cdots\cdots [47]$$

where

$$g = \left[\frac{\frac{\Phi^2}{4}}{1 + \frac{\Phi^2}{4}}\right]$$

Inspection of Equation [47] will disclose why all possible significant figures were retained in the coefficients tabulated in Table 2. The figures retained in the coefficients of the powers of g in Equation [47] are all the significant figures that remain after Euler's transformation has been applied. Equation [47] permits the calculation of $(\sigma_\phi)_{A=0}$ for values of Φ up to and slightly beyond $\Phi = 2.5$. This would not have been possible if fewer significant figures had been retained in Table 2.

TABLE 3 TANGENTIAL STRESS AT INNER EDGE OF CURVED BAR WITH $\alpha = 0.9$, FIG. 1(b)

(Calculated points for curve in Fig. 3)

Φ	$(\sigma_\phi)_{A=0} \div \left[\frac{4P}{\pi(b-a)} \cdot \frac{2X^2}{(1+\alpha)}\right]$	$(\sigma_\phi)_{A=0} \div \frac{4P}{\pi(b-a)}$
0	0.7681*	0.8115
0.1	0.7437	0.7858
0.2	0.6758*	0.7140
0.3	0.5777	0.6104
0.4	0.4663*	0.4927
0.5	0.3568	0.3770
0.6	0.2598*	0.2745
0.7	0.1804	0.1906
0.8	0.1195*	0.1263
0.9	0.0755	0.0797
1.0	0.0452*	0.04770
1.2	0.01290	0.01363
1.4	0.00164	0.00173
1.6	−0.00112	−0.00118
1.8	−0.00117	−0.00123
2.0	−0.00068	−0.00072
2.2	−0.00031	−0.00033
2.5	−0.000	−0.000

* Values to be compared with those in Table 4.

The values of $(\sigma_\phi)_{A=0}$ which were used in plotting the curve in Fig. 3 are summarized in Table 3. The intermediate column in Table 3 is included partly to facilitate showing how $(\sigma_\phi)_{A=0}$ for the curved bar (with $\alpha = 0.9$) compares with $(\sigma_\phi)_{A=0}$ for a straight bar. Table 4 gives a few values of $(\sigma_\phi)_{A=0}$ for either edge of a straight bar loaded as in Fig. 1(a). The stresses in Table 4 will be observed to differ only slightly from the corresponding values in the intermediate column of Table 3.

TABLE 4 TANGENTIAL STRESS AT EITHER EDGE OF STRAIGHT BAR, FIG. 1(a)

$\Phi = \frac{x}{2c}$	$(\sigma_\phi)_{A=0} \div \frac{2P}{\pi c}$
0	0.7686
0.2	0.6762
0.4	0.4667
0.6	0.2601
0.8	0.1197
1.0	0.0453

The curve in Fig. 3, with a different vertical scale, serves also to show how $(\sigma_\phi)_{A=1}$ (i.e., the tangential stress at the outer edge) varies with Φ because in the particular example considered

$$(\sigma_\phi)_{A=1} = \frac{a}{b}(\sigma_\phi)_{A=0}$$

Since Φ is a dimensionless quantity defined in Equations [32] as

$$\Phi = \frac{\phi}{\log \frac{1}{\alpha}}$$

it will help, in the interpretation of Figure 3, to note that $\Phi = 1$ corresponds to $\phi = 0.1054$ radians $= 6.03$ deg. A better way to visualize the meaning of $\Phi = 1$ is to note that for a straight beam, $\Phi = 1$ corresponds exactly to the cross section $x = 2c$ in Fig. 1(a), while, for a curved beam, $\Phi = 1$ corresponds nearly to the cross section obtained by beginning at $\Phi = 0$ and measuring a distance $x = b - a$ along the arc of the circle $r = \sqrt{ab}$ in Fig. 1(b). This circle $r = \sqrt{ab}$ or $A = 1/2$ has another signifi-

cance in the example in Fig. 1(*b*). This is the only circle, besides $r = a$ and $r = b$, along which σ_r and σ_ϕ are the principal stresses.

A comparison of Equation [46] with the corresponding equation as obtained by a Fourier-series solution (15) will substantiate some of the statements made in the first part of this paper. The Fourier-series solution for the tangential stress at the inner edge of the curved bar in Fig. 1(*c*), except at the point of load application, is

$$(\sigma_\phi)_{A=0} = \frac{2P}{\pi b}\left[\frac{1}{2\alpha(1+\alpha)} + \cos\phi\,\frac{(3-\nu+\alpha^2+\nu\alpha^2)}{4\alpha(1+\alpha^2)}\right] + \frac{2P}{\pi b}\sum_{n=2,3,4,5\cdots}^{\infty}\frac{n\alpha^{n-2}(1-\alpha^2)\cos n\phi}{(1-\alpha^{2n})+n\alpha^{n-1}(1-\alpha^2)} \quad \ldots [48]$$

where ν is Poisson's ratio.

This is the result obtained by putting $r = a$ (using the notations of this paper) into Valnberg's (15) equation for $\sigma_r + \sigma_\phi$ for the case of plane stress. For values of α from zero to about $\alpha = 0.5$, Equation [48] is convenient to use. However, for $\alpha = 0.9$, the coefficients in the Fourier series decrease very slowly, so that the Fourier-series solution is almost unusable for thin rings. For example, with $\alpha = 0.9$, the Fourier-series coefficients in Equation [48] are 0.5540 for $n = 2$ and 0.1233 for $n = 40$.

The reader is referred to Valnberg's paper for diagrams showing how σ_r and σ_ϕ vary with the co-ordinates r and ϕ for the case shown in Fig. 1(*c*), with $\alpha = 0.5$. The diagrams indicate that, in the bottom half of the ring shown in Fig. 1(*c*), the stresses are practically negligible. Therefore the stresses in the top half of the ring would not be changed much if the bottom half of the ring were cut off. This indicates that the Fourier integral solution for Fig. 1(*b*) agrees with the Fourier-series solution for Fig. 1(*c*), except for a small discrepancy.

The present paper is the result of an attempt by the author to overcome the difficulties which arise in Fourier-series solutions for thin curved bars due to slow convergence of the series.

Conclusions

The Fourier integral method can be applied to plane-stress problems of curved bars and numerical results can be obtained without excessively lengthy calculations by using the integrals tabulated in Table 1 of this paper. Table 1 can also be used to advantage in plane-stress problems for straight bars. The Fourier integral method is sufficiently tedious so that approximate methods should be looked for and utilized instead whenever possible.

Acknowledgments

The advice and encouragement of Prof. S. Timoshenko of Stanford University during the investigation which led to this paper are hereby acknowledged. Mr. Chin-Tse Yang, a graduate student at the University of California, and Mr. Charles R. Sackett, former graduate student at the University of California, took part in the calculations in the early stages of the investigation.

Bibliography

1 "Theory of Elasticity," by S. Timoshenko, McGraw-Hill Book Company, Inc., New York, N. Y., 1934, chapt. 2, p. 44, and chapt. 3, p. 52.

2 "A Treatise on Photo-Elasticity," by E. G. Coker and L. N. G. Filon, Cambridge University Press, London, England, 1931, chapt. 5, pp. 415–443.

3 "On an Approximate Solution for the Bending of a Beam of Rectangular Cross Section Under any System of Load, With Special Reference to Points of Concentrated or Discontinuous Loading," by L. N. G. Filon, Philosophical Transactions of the Royal Society of London, England, vol. 201, series A, 1903, p. 63.

4 "On the Stresses in the Neighborhood of a Circular Hole in a Strip Under Tension," by R. C. J. Howland, Philosophical Transactions of the Royal Society of London, England, vol. 229, series A, 1929–1930, p. 49.

5 "Bi-Harmonic Analysis in a Perforated Strip," by R. C. J. Howland and A. C. Stevenson, Philosophical Transactions of the Royal Society of London, England, vol. 232, series A, 1933–1934, p. 155.

6 "Vergleichende spannungsoptische Untersuchungen und Fliessversuche unter konzentriertem Druck," by G. Mesmer, *Technische Mechanik und Thermodynamik*, vol. 1, 1930, part 2, pp. 85–100; vol. 1, 1930, part 3, pp. 106–112.

7 "Stresses in a Notched Strip Under Tension," by Chih-Bing Ling Journal of Applied Mechanics, Trans. ASME, vol. 69, 1947, pp. A275–A280.

8 "Nouvelles Tables d'Intégrales Définies," by D. Bierens de Haan, edition of 1867, corrected, reprinted by G. E. Stechert & Company, New York, N. Y., 1939, Table 84, p. 125, and Table 86, p. 127.

9 "Advanced Calculus," by E. B. Wilson, Ginn & Company, Boston, Mass., 1911, pp. 448–449, p. 446.

10 "A Short Table of Integrals," by B. O. Peirce, third revised edition, Ginn & Company, Boston, Mass., 1929, Formula 354, p. 48.

11 "Numerical Values of the First Twelve Powers of π, of Their Reciprocals, and of Certain Other Related Quantities," by J. W. L. Glaisher, Proceedings of the London Mathematical Society, vol. 8, from November, 1876, to November, 1877, p. 140.

12 "The Stresses in a Circular Ring," by L. N. G. Filon, Selected Engineering Papers No. 12, Institution of Civil Engineers, London, England, 1924.

13 "Stresses and Displacements in a Hollow Circular Cylinder," by Carl W. Nelson, doctoral thesis, University of Michigan, 1939 (unpublished).

14 "Critical Stresses in a Circular Ring," by E. A. Ripperger and N. Davids, Proceedings of the American Society of Civil Engineers, vol. 72, 1946, pp. 159–168.

15 "The Local Stresses in a Plane Ring-Shaped Disk Under Two Concentrated Forces" (in Russian), by D. V. Valnberg, *Prikladnaya Matematika i Mekhanika*, Moscow, Russia, vol. 13, 1949, pp. 151–158. See Review 228, Applied Mechanics Reviews, February, 1950.

Appendix

Integration of $\int_0^\infty \frac{z^n\,dz}{\sinh^n z}$

In the main part of this paper the need for obtaining values of

$$I_k = \frac{1}{2(k!)}\int_0^\infty \frac{z^k\,dz}{\sinh z + zX} \quad (k = 1, 3, 5, \text{ etc.}) \quad \ldots [49]$$

was indicated. Further, it was pointed out that we are interested in odd integral values of k and values of X between 1.0 and about 1.1. The Maclaurin series for I_k can be obtained by division and is

$$I_k = \frac{1}{2(k!)}\left[\int_0^\infty \frac{z^k\,dz}{\sinh z} - X\int_0^\infty \frac{z^{k+1}\,dz}{\sinh^2 z} + X^2\int_0^\infty \frac{z^{k+2}\,dz}{\sinh^3 z} - - -\right] \quad \ldots [50]$$

It will be found that this series is nonconvergent for $X > 1$, the range of values of X in which we are interested. However, this difficulty will be removed by transforming the Maclaurin series of Equation [50] into a Taylor's series of the form indicated in Equation [39]. In obtaining the Taylor's series for $I_k(X)$, the numerical values of the coefficients in Equation [50], for the case of $k = 1$, will be needed. This means that we need a table of values of

$$\int_0^\infty \frac{z^n\,dz}{\sinh^n z}, \text{ for } n = 1, 2, 3, \text{ etc.}$$

The latter integral can be evaluated for any positive integral value of n by means of the definite integrals (8)

$$\int_0^\infty \frac{x^{2n-1}\,dx}{\sinh x} = \frac{(2^{2n}-1)B_{2n-1}\,\pi^{2n}}{2n} \quad \ldots\ldots [51]$$

$$\int_0^\infty \frac{x^{2n}\,dx}{\sinh^2 x} = B_{2n-1}\,\pi^{2n} \quad \ldots\ldots [52]$$

and the following formula

$$\int_0^\infty \frac{x^m\,dx}{\sinh^n x} = \frac{m(m-1)}{(n-1)(n-2)} \int_0^\infty \frac{x^{m-2}\,dx}{\sinh^{n-2} x} - \frac{(n-2)}{(n-1)} \int_0^\infty \frac{x^m\,dx}{\sinh^{n-2} x} \quad \ldots\ldots [53]$$

In Equations [51] and [52], the constants B_{2n-1} are Bernoulli numbers, i.e.

$$B_1 = \frac{1}{6},\ B_3 = \frac{1}{30},\ B_5 = \frac{1}{42},\ B_7 = \frac{1}{30},\ \text{etc.}$$

and n is a positive integer. In Equation [53], m and n are positive integers never less than 3 (n = 3, 4, 5, etc.) and, furthermore, m must be equal to or greater than n.

Equation [53] was obtained by taking the limits of integration from zero to infinity in the following formula

$$\int \frac{x^m\,dx}{\sinh^n x} = -\frac{x^{m-1}}{(n-1)(n-2)} \frac{[m \sinh x + (n-2)\,x \cosh x]}{\sinh^{n-1} x} + \frac{m(m-1)}{(n-1)(n-2)} \int \frac{x^{m-2}\,dx}{\sinh^{n-2} x} - \frac{(n-2)}{(n-1)} \int \frac{x^m\,dx}{\sinh^{n-2} x} \quad \ldots\ldots [54]$$

Equation [54] is the result obtained by substituting xi for x in reference (8),[3] and then using the relations

$$\sin xi = i \sinh x,\ \cos xi = \cosh x$$

where

$$i = \sqrt{-1}$$

The manner in which

$$\int_0^\infty \frac{z^n\,dz}{\sinh^n z}$$

can be evaluated by means of Equations [51] to [53] is as follows: Equation [53] is applied repeatedly, first to the integral itself and then to each of the two integrals obtained by the first application of Equation [53], etc., until the original integral has been reduced to a sum of several integrals all of which can be evaluated by use of Equation [51] or Equation [52]. Table 5 gives values of

$$\int_0^\infty \frac{z^n\,dz}{\sinh^n z}$$

for values of n from 1 to 40.

Table 5 is more extensive than is needed in this particular problem, but it was prepared with the thought that the same integrals will be needed in many other problems.

While any of the values in Table 5 can be calculated[4] by use of Equations [51] to [53] if sufficient time is available, it is much faster, for $n \geq 16$, to use the following formula derived by the author

$$\int_0^\infty \frac{z^n\,dz}{\sinh^n z} = \sqrt{3\pi}\left(1 + \frac{3}{20}\frac{1}{n} - \frac{13}{1120}\frac{1}{n^2} - \frac{27}{3200}\frac{1}{n^3} + \frac{52791}{3,942,400}\frac{1}{n^4} - \frac{482,427}{66,560,000}\frac{1}{n^5} - .012456\frac{1}{n^6} + .0386\frac{1}{n^7} - 0.0274\frac{1}{n^8} + \ldots\right) \quad \ldots [55]$$

The line under the last one or two figures of some of the coefficients in Equation [55] indicates a slight uncertainty in these figures.

Equation [55] may be obtained by changing the variable in

$$\int_0^\infty \frac{z^n\,dz}{\sinh^n z}$$

by the substitution

$$\frac{\sinh z}{z} = 1 + q^2 = 1 + \frac{z^2}{3!} + \frac{z^4}{5!} + \text{— — — — —} \quad \ldots [56]$$

Solving for z explicitly in terms of q by reversion of series [9] gives

$$z = \sqrt{6}\left(q - \frac{3}{20}q^3 + \frac{321}{5600}q^5 - \frac{3197}{112,000}q^7 + \frac{445,617}{27,596,800}q^9 - \frac{1,766,784,699}{179,379,200,000}q^{11} + \text{— — — — —} \right) \quad \ldots [57]$$

From Equation [57], dz may be obtained. Next, it is advantageous to substitute

$$q^2 = \frac{\cos^2\theta}{\sin^2\theta}$$

When the latter substitution is made, we get

$$\int_0^\infty \frac{z^n\,dz}{\sinh^n z} = \sqrt{6}\int_0^{\frac{\pi}{2}} \sin^{2n-2}\theta \cdot d\theta \left[1 - \frac{9}{20}\frac{\cos^2\theta}{\sin^2\theta} + \frac{321}{1120}\frac{\cos^4\theta}{\sin^4\theta} - \text{— — — —}\right] \quad \ldots [58]$$

Using a table of definite integrals (10), we get

TABLE 5 VALUES OF $\int_0^\infty \frac{z^n\,dz}{\sinh^n z}$

n	$\int_0^\infty \frac{z^n\,dz}{\sinh^n z}$	n	$\int_0^\infty \frac{z^n\,dz}{\sinh^n z}$
1	2.467 401 100 272	21	0.477 078 979 656
2	1.644 934 066 848	22	0.465 961 047 262
3	1.314 135 111 192	23	0.455 585 675 544
4	1.125 221 066 274	24	0.445 873 739 561
5	0.999 439 238 627	25	0.436 757 434 360
6	0.908 070 438 691	26	0.428 178 274 745
7	0.837 858 186 226	27	0.420 085 510 670
8	0.781 736 036 017	28	0.412 434 859 914
9	0.735 550 586 070	29	0.405 187 485 598
10	0.696 680 842 888	30	0.398 309 164 549
11	0.663 380 891 473	31	0.391 769 605 788
12	0.634 437 094 804	32	0.385 541 858 144
13	0.608 976 234 735	33	0.379 601 993 140
14	0.586 351 587 139	34	0.373 928 414 646
15	0.566 073 939 382	35	0.368 501 830 828
16	0.547 763 144 838	36	0.363 304 826 969
17	0.531 120 843 132	37	0.358 321 660 102
18	0.515 906 208 059	38	0.353 538 058 193
19	0.501 931 672 421	39	0.348 941 048 041
20	0.489 082 408 761	40	0.344 518 807 159

[3] Equation 354, p. 48.

[4] Using values of powers of π tabulated by Glaisher (11).

$$\int_0^\infty \frac{z^n\,dz}{\sinh^n z} = \sqrt{6}\,\frac{1\cdot3\cdot5\cdots(2n-3)}{2\cdot4\cdot6\cdots(2n-2)}\,\frac{\pi}{2}\left\{1+\frac{9}{20}\left[1-\frac{2n-2}{2n-3}\right]+\frac{321}{1120}\left[1-2\,\frac{2n-2}{2n-3}+\frac{(2n-2)(2n-4)}{(2n-3)(2n-5)}\right]+\cdots\right\} \quad [59]$$

The series inside the braces in Equation [59] may be expressed in powers of $1/n$, giving

$$\int_0^\infty \frac{z^n\,dz}{\sinh^n z} = \sqrt{6}\,\frac{1\cdot3\cdot5\cdots(2n-3)}{2\cdot4\cdot6\cdots(2n-2)}\,\frac{\pi}{2}\left\{1-\frac{9}{40n}-\frac{549}{4480\,n^2}-\cdots\right\} \quad [60]$$

It can be shown that, for large values of n

$$\frac{1\cdot3\cdot5\cdots(2n-3)}{2\cdot4\cdot6\cdots(2n-2)} = \frac{1}{\sqrt{n\pi}}\left(1+\frac{3}{8n}+\frac{25}{128}\,\frac{1}{n^2}+\frac{105}{1024}\,\frac{1}{n^3}+\frac{1659}{32768}\,\frac{1}{n^4}+\frac{6237}{262{,}144}\,\frac{1}{n^5}+\cdots\right) \quad [61]$$

When the latter result is substituted into Equation [60], we obtain Equation [55].

It has been checked that Equation [55] gives the correct value of

$$\int_0^\infty \frac{z^n\,dz}{\sinh^n z}$$

to ten significant figures for $n = 10$ and to twelve significant figures for $n = 16$. The formula is asymptotic, rather than convergent.

Integration of $I_k(X)$

If the various I_k are expressed in a form obtained by applying Equation [50] to each of the integrals in Equation [52], a comparison of I_1 with I_3, I_2 with I_4, etc., shows that the I_k are related to each other by the differential relation

$$\frac{d}{dX}\left[X\,\frac{d}{dX}\,(XI_{k+2})\right] = \frac{1}{(k+1)(k+2)}\left[\frac{1}{X^2}\,\frac{d^2}{dX^2}\,(X^{k+2}I_k)\right] - \frac{1}{(k+1)(k+2)}\,\frac{d^2}{dX^2}\,I_k \quad [62]$$

If we replace I_{k+2} and I_k in Equation [62] by their Taylor's series expressions as given by Equation [39], and replace X by $[(X-1)+1]$ and then equate coefficients of like powers of $(X-1)$ in the left and right members of the resulting equation, the following algebraic equations are obtained

$$c_{k+2} = \frac{3}{2}\,b_{k+2} - \frac{1}{2}\,a_{k+2} + \frac{1}{1\cdot2}\left[\frac{(k+1)(k+2)}{(k+1)(k+2)}\,a_k - \frac{2(k+2)}{(k+1)(k+2)}\,b_k\right] \quad [63]$$

$$d_{k+2} = \frac{5}{3}\,c_{k+2} - \frac{2}{3}\,b_{k+2} + \frac{1}{2\cdot3}\left[\frac{(k+2)(k+3)}{(k+1)(k+2)}\,b_k - \frac{4(k+3)}{(k+1)(k+2)}\,c_k\right] \quad [64]$$

By means of Equation [63], the third column of Table 1, excepting c_1, can be obtained, provided all the coefficients in the first two columns of the table (i.e., all the a_k and b_k) are known. By means of the proper one of the recurrence formulas, the nth column of Table 1 can be obtained, except for the coefficient with subscript 1, provided the two preceding columns have been completed first. To get c_1, it is convenient to use

$$c_1 + c_3 + c_5 + \cdots = (b_1 - c_1) \quad [65]$$

or

$$c_1 = \frac{1}{2}\,b_1 - \frac{1}{2}\,(c_3 + c_5 + c_7 + \cdots)$$

Equation [65] may be proved as follows

$$\begin{aligned} c_1 + c_3 + c_5 + \cdots &= \frac{1}{2}\int_0^\infty \frac{\left(z^2 + \frac{z^4}{3!} + \frac{z^6}{5!} + \cdots\right)dz}{(\sinh z + z)^2} \\ &= \frac{1}{2}\int_0^\infty \frac{z^2 \sinh z\,dz}{(\sinh z + z)^2} = \frac{1}{2}\int_0^\infty \frac{z^2 dz}{(\sinh z + z)^2} \\ &\quad - \frac{1}{2}\int_0^\infty \frac{z^2 dz}{(\sinh z + z)^2} \\ &= (b_1 - c_1) \end{aligned}$$

Similarly, it can be shown that

$$d_1 = \frac{1}{2}\,c_1 - \frac{1}{2}\,(d_3 + d_5 + d_7 + \cdots) \quad [66]$$

Equations such as [63] and [64] are not available for obtaining the a_k and b_k in Table 1. For the purpose of finding the a_n, let the Maclaurin developments of the first several I_k be represented as follows

$$I_1 = A_1 - A_2X + A_3X^2 - A_4X^3 + \cdots \quad [67]$$

$$I_3 = C_1 - C_2X + C_3X^2 - C_4X^3 + \cdots \quad [68]$$

$$I_5 = E_1 - E_2X + E_3X^2 - E_4X^3 + \cdots \quad [69]$$

Then

$$a_1 = I_1(1) = A_1 - A_2 + A_3 - A_4 + \cdots \quad [70]$$

$$a_3 = I_3(1) = C_1 - C_2 + C_3 - C_4 + \cdots \quad [71]$$

and so forth, where, according to Equation [50]

$$A_n = \frac{1}{2}\int_0^\infty \frac{z^n\,dz}{\sinh^n z}$$

so that each A_n is available by taking one half of the proper value in Table 5.

To obtain a_5 by means of Equation [71], it is necessary first to express the C_n in terms of the A_n. This can be done by substituting the expressions for I_1 and I_3, as given by Equations [67] and [68] into Equation [62]. This substitution gives

$$\begin{aligned} C_1 - 4C_2X + 9C_3X^2 - \cdots &= \left(\frac{2\cdot3}{2\cdot3}\,A_1 - \frac{1\cdot2}{2\cdot3}\,A_2\right) - \left(\frac{3\cdot4}{2\cdot3}\,A_2 - \frac{2\cdot3}{2\cdot3}\,A_3\right)X \\ &\quad + \left(\frac{4\cdot5}{2\cdot3}\,A_3 - \frac{3\cdot4}{2\cdot3}\,A_4\right)X^2 - \left(\frac{5\cdot6}{2\cdot3}\,A_4 - \frac{4\cdot5}{2\cdot3}\,A_5\right)X^3 \\ &\quad + \cdots \end{aligned} \quad [72]$$

Similarly, the E_n can be obtained from the C_n by substituting

the expressions for I_3 and I_{b_3} as given by Equations [68] and [69] into Equation [62].

Assuming that the a_n have been determined as just explained, there are several ways in which the b_n can be found. One way is to use the formulas

$$b_3 = a_3 + \frac{A_3}{2\cdot 3} - \frac{2}{3}a_1 - \frac{1}{3}\left(A_1 - \frac{1}{2}A_2 + \frac{1}{3}A_3 - - - - - -\right) \quad \ldots\ldots [73]$$

$$b_5 = a_5 + \frac{C_3}{4\cdot 5} - \frac{2}{5}a_3 - \frac{3}{5}\left(C_1 - \frac{1}{2}C_2 + \frac{1}{3}C_3 - - - - - -\right) \quad \ldots\ldots [74]$$

$$b_7 = a_7 + \frac{E_3}{6\cdot 7} - \frac{2}{7}a_5 - \frac{5}{7}\left(E_1 - \frac{1}{2}E_2 + \frac{1}{3}E_3 - - - - - -\right) \quad \ldots\ldots [75]$$

and, finally

$$b_1 = \frac{1}{2}a_1 - \frac{1}{2}(b_3 + b_5 + b_7 + - - - - - - - - - -) \ldots [76]$$

Equations [73] to [75] were obtained by multiplying both sides of Equation [62] by dX and then integrating both sides of the resulting equation between the limits 0 and 1. Equation [76] will be recognized as another equation of the same family as Equations [65] and [66].

The reader is referred to Table 1 for the results of the calculations which have been outlined in this section of the Appendix.

The Torsion of Elastic Spheres in Contact[1]

By J. L. LUBKIN,[2] KANSAS CITY, MO.

A small torsional couple is applied about the axis of symmetry of a system of two elastic spheres (or solids of revolution) which have been pressed together by a force perpendicular to their common tangent plane. This problem may be reduced to a "problem of the plane," and it has been found that in the absence of slip on the interface, the tangential traction is singular on the bounding circle. Hence the assumption of no slip is physically untenable. In the present solution allowance is made for slip by assuming that the tangential component of traction, for the area over which slip has progressed, is equal to the product of a constant friction coefficient and the normal or Hertzian distribution. A continuous expression for the traction is developed. A formula relating the radial depth of penetration of slip to the magnitude of the applied moment is given, and another relating this moment to the rotation of the contact surface of one of the bodies with respect to remote points in that body.

Notation

The following notation is used in the paper:

G = modulus of elasticity in shear

$u_r, u_\theta, u_z = r, \theta, z$ components of displacement (cylindrical co-ordinates)

$\sigma_z, \tau_{rz}, \tau_{z\theta}$ = cylindrical co-ordinate components of traction on planes z = const

Additional symbols are defined as introduced.

Introduction

The principal results of the Hertz theory of the contact of two elastic solids pressed together by a force normal to their common tangent plane have been outlined in Reference (1).[3] Several solutions involving the superposition of additional force systems on Hertzian contact are also discussed in this reference and further contributions made. The present paper re-examines the boundary-value problem of the section of reference (1) entitled "Twisting Couple: Boundary Conditions," a procedure necessitated by results physically (although not mathematically) inconsistent with the hypothesis. In this problem the boundary conditions for the case of a torsional couple superposed on the Hertz normal force are formulated on the assumption that no slip occurs on the small surface of contact between the two solids involved. The surface traction that satisfies these conditions, however, is singular on the boundary of the contact area. Some form of irreversible readjustment (slip) must therefore be expected to take place, and these effects will now be studied for the case of the circular contact surface.

The Boundary-Value Problem

Suppose two homogeneous, isotropic, elastic solids of revolution are placed in contact at a point O, their axes of symmetry colinear, remaining unstressed, Fig. 1(*a*). Take the common tangent plane as that of r and θ, and the normal through O as the

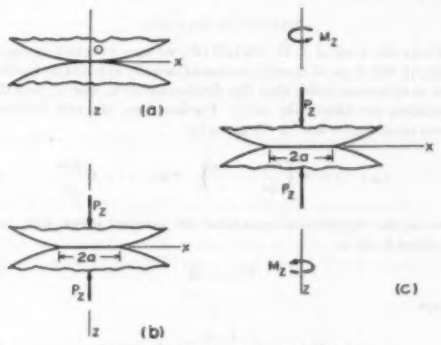

Fig. 1 Geometric Configuration

(*a*, Spheres in contact only at O. *b*, Hertzian contact with force P_z. *c*, Torsional couple M_z added after Hertzian contact is established.)

axis of z. Let the two bodies be pressed together by a force P_z, directed along Oz. The Hertz theory gives the radius a, of the circular area of contact, Fig. 1(*b*), and the formula

$$p = \frac{3P_z}{2\pi a^3}\sqrt{a^2 - r^2} \qquad [1]$$

for the distribution of normal pressure p over the contact area.

Now let an additional system of couples be superposed so that one body exerts on the other a positive torque M_z, about the axis Oz. The sign is reckoned by the right-hand rule, Fig. 1(*c*). If there is no slip on the interface, it may be shown that, expressed as a problem of the semi-infinite solid $z \geq 0$, the boundary conditions are (1)

$$u_\theta = -\beta r, \quad u_r = \sigma_z = 0 \qquad r \leq a, \quad z = 0 \qquad [2]$$

$$\tau_{rz} = \tau_{z\theta} = \sigma_z = 0 \qquad r > a, \quad z = 0 \qquad [3]$$

$$\lim\,(u_r, u_\theta, u_z) = 0 \qquad \text{as } \sqrt{r^2 + z^2} \to \infty \qquad [4]$$

where β is the angle of rigid rotation of the entire contact surface relative to distant lines in the solid. Because the shearing stress on the contact surface becomes infinite as $r \to a$ (reference 1), slip must be expected to occur, starting at the boundary $r = a$ and presumably progressing inward to a radius $r = a' < a$. We retain Equations [3] and [4] and need modify only Equation [2]. In the circular annulus $a' < r < a$ the tangential component of traction is assumed to fall to the maximum available. Following Cattaneo (2), this value is taken as the product of a constant

---

[1] This paper is from a doctoral thesis by the author, presented at Columbia University, June, 1950.

[2] Research Engineer, Midwest Research Institute. Jun. ASME.

[3] Numbers in parentheses refer to the Bibliography at the end of the paper.

Contributed by the Applied Mechanics Division and presented at the Annual Meeting, New York, N. Y., November 26–December 1, 1950, of The American Society of Mechanical Engineers.

Discussion of this paper should be addressed to the Secretary, ASME, 29 West 39th Street, New York, N. Y., and will be accepted until July 10, 1951, for publication at a later date. Discussion received after the closing date will be returned.

Note: Statements and opinions advanced in papers are to be understood as individual expressions of their authors and not those of the Society. Manuscript received by the Applied Mechanics December 7, 1949. Paper No. 50—A-1.

friction coefficient f and the normal pressure p of Equation [1]. We shall also require the surface traction to remain finite for $r \leqslant a'$. The rigid rotation β remains unaffected for the region $r \leqslant a'$, $z = 0$, across which the two bodies behave as if rigidly joined. Expressed analytically

$$u_\theta = -\beta r, \quad u_r = \sigma_z = 0 \quad r \leq a', \quad z = 0 \ldots\ldots [5]$$

$$\tau_{z\theta} = \frac{3fP_z}{2\pi a^3}\sqrt{a^2 - r^2}, \quad \tau_{rz} = \sigma_z = 0 \quad a' \leqslant r \leqslant a, \quad z = 0 \ldots [6]$$

The complete solution of the boundary-value problem thus involves finding solutions of the three equilibrium equations, subject to boundary conditions, Equations [3] to [6]. This amounts to finding the tractions on the "circular disk" $r \leqslant a'$, $z = 0$, which, together with the given tractions for $r \geqslant a'$ (Equations [6], [3]), give rise to a rigid rotation of the disk, of amount β (Equation [5]).

Method of Solution

From the work of J. H. Michell (3), we may conclude immediately, in this type of (purely torsional) axially symmetric loading of a semi-infinite solid, that the displacements u_r and u_z, and the dilatation are identically zero. Furthermore, the only nonzero stress components are $\tau_{r\theta}$, $\tau_{z\theta}$, given by

$$\tau_{r\theta}(r, z) = G\left(\frac{\partial u_\theta}{\partial r} - \frac{u_\theta}{r}\right), \quad \tau_{z\theta}(r, z) = G\frac{\partial u_\theta}{\partial z} \ldots\ldots [7]$$

Two of the equilibrium equations are satisfied identically, and the third leads to

$$\nabla^2\omega = 0 \ldots\ldots [8]$$

where

$$2\omega(r, z) = \frac{1}{r}\frac{\partial}{\partial r}[ru_\theta(r, z)] \ldots\ldots [9]$$

is the z-component of rotation. From Hooke's law we have

$$2G\frac{\partial\omega}{\partial z} = \frac{1}{r}\frac{\partial}{\partial r}(r\tau_{r\theta}) \ldots\ldots [10]$$

Substituting Equations [3] to [6] appropriately in Equations [9] and [10], we formulate the following conditions for the harmonic function ω_1 on $z = 0$

$$\omega = -\beta \quad r \leqslant a' \ldots\ldots [11]$$

$$2G\frac{\partial\omega}{\partial z} = \begin{cases} \dfrac{3fP_z}{2\pi a^3}\dfrac{1}{r}\dfrac{d}{dr}\left(r\sqrt{a^2 - r^2}\right) & a' < r < a \\ 0 & r > a \end{cases} \ldots [12]$$

Introducing the notation $(\tau_{z\theta})_{r<a',\, z=0} = \tau_\beta(r)$, from Equation [10] with $z = 0$, we have for τ_β

$$2G\left[\frac{\partial\omega}{\partial z}\right]_{\substack{r<a' \\ z=0}} = \frac{1}{r}\frac{d}{dr}[r\tau_\beta] \ldots\ldots [13]$$

Solution for $\partial\omega/\partial z$

In the potential-theory problem for ω, let $\omega = \omega_1 + \omega_2' + \omega_2''$, all harmonic, such that on $z = 0$

$$\omega_1 = -\beta \qquad r \leqslant a' \ldots [14]$$

$$\frac{\partial\omega_1}{\partial z} = 0 \qquad r > a' \ldots [15]$$

$$\frac{\partial\omega_2'}{\partial z} = \frac{3fP_z}{4G\pi a^3}\frac{1}{r}\frac{d}{dr}\left(r\sqrt{a^2 - r^2}\right) \qquad r < a \ldots [16]$$

$$\frac{\partial\omega_2'}{\partial z} = 0 \qquad r > a \ldots [17]$$

$$\omega_2' + \omega_2'' = 0 \qquad r \leqslant a' \ldots [18]$$

$$\frac{\partial\omega_2''}{\partial z} = 0 \qquad r > a' \ldots [19]$$

Now if $V(r, z)$ is harmonic and satisfies the boundary condition $-\partial V/\partial z = h(r)$ on the plane $z = 0$, the solution that vanishes at infinity may be written (4)

$$V(r, z) = \int_0^\infty e^{-\rho z} J_0(\rho r)d\rho \int_0^\infty h(\rho)J_0(\rho\rho)\rho d\rho \ldots [20]$$

according as $z \geqslant 0$. (J_n is the nth order Bessel function of the first kind). $V(r, z)$ has been taken as even in z, so that (using the language of the theory of electrostatic potential) if $\delta(r)$ be the density of an axially symmetric distribution of "charge" on $z = 0$

$$\delta(r) = -\frac{1}{2\pi}\left[\frac{\partial V}{\partial z}\right]_{0^+} \ldots\ldots [21]$$

Since we are here concerned only with the solid $z \geqslant 0$, $\partial V/\partial z$ will be interpreted as identical with $[\partial V/\partial z]_{0^+}$.

The harmonic function satisfying Equations [14] and [15] is known to be (4)

$$\omega_1(r, z) = \frac{-2\beta}{\pi}\int_0^\infty e^{-kz} J_0(kr)\frac{\sin ka'}{k}dk \ldots [22]$$

and on $z = 0$

$$\frac{\partial\omega_1}{\partial z} = \frac{-2\beta}{\pi r}\frac{d}{dr}\left(\sqrt{a'^2 - r^2}\right) \qquad r < a' \ldots [23]$$

$$\omega_1 = \frac{-2\beta}{\pi}\sin^{-1}\frac{a'}{r} \qquad r > a' \ldots [24]$$

Adapting Equation [20] to Equations [16] and [17], an expression for ω_2' is obtained, which, upon integration by parts, in virtue of the formula[4] $dJ_0(x)/dx = -J_1(x)$, becomes

$$\omega_2' = \frac{-3fP_z}{4G\pi a^3}\int_0^\infty e^{-kz} J_0(kr)dk \int_0^a k\rho\, J_1(k\rho) \times \sqrt{a^2 - \rho^2}\, d\rho \ldots [25]$$

Using the power series[5] for $J_1(k\rho)$ and integrating termwise, we obtain a series recognizable[6] as that for $J_1^2\left(\frac{ka}{2}\right)$, so that

$$\omega_2'(r, z) = -\frac{3fP_z}{8Ga}\int_0^\infty e^{-kz} J_0(kr)J_1^2\left(\frac{ka}{2}\right)dk \ldots [26]$$

Then by Equations [26] and [18], we find

$$\omega_2''(r, 0) = \frac{3fP_z}{8Ga}\int_0^\infty J_0(kr)J_1^2\left(\frac{ka}{2}\right)dk \quad r \leqslant a' \ldots [27]$$

Reviewing Equations [18] and [19] in the light of Equation [21] it is seen that the function $\omega_2''(r, z)$ may be regarded as arising from a distribution of charge, say, of density $\delta_2''(r)$, on the circular disk $r \leqslant a'$, $z = 0$, whose potential is specified by Equation [27]. The distribution of density on the disk and the potential

[4] Reference (5), p. 45.
[5] Ibid., p. 40.
[6] Ibid., p. 147.

on the rest of the plane are given in terms of the potential on the disk by Beltrami's formulas (6)

$$\delta_z''(r) = \frac{-1}{\pi^2 r}\frac{d}{dr}\int_r^{a'}\frac{s\,ds}{\sqrt{s^2-r^2}}\frac{d}{ds}\int_0^s\frac{\omega_z''(t,0)\,dt}{\sqrt{s^2-t^2}} \qquad r < a' \ldots [28]$$

$$\omega_z''(r,0) = \frac{2}{\pi}\int_0^{a'}\frac{ds}{\sqrt{r^2-s^2}}\frac{d}{ds}\int_0^s\frac{\omega_z''(t,0)\,dt}{\sqrt{s^2-t^2}} \qquad r > a' \ldots [29]$$

Using Equations [21] and [27] in Equation [28], for $r < a'$, $z = 0$,

$$\frac{4Gr\alpha}{3fP_z}\frac{\partial\omega_z''}{\partial z} = \frac{1}{r}\frac{d}{dr}\int_r^{a'}\frac{s\,ds}{\sqrt{s^2-r^2}}\frac{d}{ds}\int_0^s\int_0^\infty\frac{tJ_0(kt)J_1\left(\frac{ka}{2}\right)}{\sqrt{s^2-t^2}}\,dt\,dk \ldots [30]$$

Now (4)

$$\int_0^s\frac{tJ_0(kt)}{\sqrt{s^2-t^2}}\,dt = \frac{\sin ks}{k}$$

so that noting Neumann's definite integral[7] for J_1^2, we have for all the terms to the right of d/ds

$$\frac{2}{\pi}\int_0^\infty\frac{\sin\frac{ka}{2}}{k}\,dk\int_0^{\frac{\pi}{2}}J_0(ka\sin\theta)\cos 2\theta\,d\theta$$

But[8]

$$\int_0^\infty J_0(ka\sin\theta)\frac{\sin ks}{k}\,dk = \begin{cases}\sin^{-1}\left(\dfrac{s}{a\sin\theta}\right) & s \leqslant a\sin\theta \\ \dfrac{\pi}{2} & s \geqslant a\sin\theta\end{cases}$$

Substituting this result, and operating with d/ds, we obtain

$$\frac{2}{\pi}\int_{\sin^{-1}(s/a)}^{\frac{\pi}{2}}\frac{\cos 2\theta\,d\theta}{\sqrt{a^2\sin^2\theta - s^2}}$$

Inserting this expression in the formula for $\partial\omega_z''/\partial z$, we may now integrate with respect to s. Further integration (including one by parts to remove an inverse trigonometric function) gives, on $z = 0, r < a'$

$$\frac{\partial\omega_z''}{\partial z} = \frac{-3fP_z}{4G\pi a^2}\frac{1}{r}\frac{d}{dr}\left(r\sqrt{a^2-r^2}\right) + \frac{3fP_z a}{2G\pi^2 r}\frac{d}{dr}\Phi(r) \ldots [31]$$

$$\Phi(r) = \sqrt{a'^2-r^2}\int_{\sin^{-1}(a'/a)}^{\frac{\pi}{2}}\frac{\sin^2\theta\cos^2\theta\,d\theta}{(a^2\sin^2\theta - r^2)\sqrt{a^2\sin^2\theta - a'^2}} \ldots [32]$$

Finally, adding Equations [16], [23], and [31], for $z = 0, r < a'$

$$\frac{\partial\omega}{\partial z} = \frac{1}{r}\frac{d}{dr}\left\{\frac{-2\beta}{\pi}\sqrt{a'^2-r^2} + \frac{3fP_z a}{2G\pi^2}\Phi(r)\right\} \ldots [33]$$

Solution for τ_β

Comparison of Equations [33] and [13] shows that

$$r\tau_\beta = L - \frac{4\beta G}{\pi}\sqrt{a'^2-r^2} + \frac{3fP_z a}{\pi^2}\Phi(r) \ldots [34]$$

where L is a constant of integration, evaluated by using the requirement that τ_β is finite. Then $\lim r\tau_\beta = 0$ as $r \to 0$, and inserting the value for L thus obtained, it is easy to show that $\lim \tau_\beta = 0$ as $r \to 0$. If now we define

$$k' = a'/a, \quad k = \sqrt{1-k'^2} \ldots [35]$$

the sequence of substitutions $\theta = \pi/2 - \psi$ and $\sin\psi = k\sin\alpha$ converts Equation [34] (with the appropriate expression for L) to

$$\tau_\beta = \left[\frac{4\beta G}{\pi} - \frac{3fP_z}{\pi^2 a^2}k^2\mathbf{D}\right]\left(\frac{a' - \sqrt{a'^2-r^2}}{r}\right) + \frac{3fP_z}{\pi^2 a^2}\frac{r\sqrt{a'^2-r^2}}{a^2}\times \int_0^{\pi/2}\frac{\frac{a^2k^2}{a^2-r^2}\sin^2\alpha}{\left(1-\frac{a^2k^2}{a^2-r^2}\sin^2\alpha\right)\sqrt{1-k^2\sin^2\alpha}}\,d\alpha \ldots [36]$$

where $\mathbf{D}$ is a tabulated (7) complete elliptic integral, of modulus k

$$\mathbf{D} = (\mathbf{K} - \mathbf{E})/k^2 \ldots [37]$$

Here $\mathbf{K}$ and $\mathbf{E}$ are, respectively, the complete elliptic integrals of the first and second kinds, modulus k. The integral of Equation [36] is $\pi(n, k, \pi/2) - \mathbf{K}$, where $\pi(n, k, \pi/2)$ is the complete elliptic integral of the third kind, of modulus k and parameter n

$$n = -\frac{a^2k^2}{a^2-r^2} = -\frac{a^2-a'^2}{a^2-r^2} \ldots [38]$$

For r from 0 to a', n ranges from $-k^2$ to -1 and consequently may be written ($0 \leq \theta \leq \pi/2$)

$$n = -1 + k'^2\sin^2\theta \ldots [39]$$

The function π may be expressed (8) in terms of elliptic integrals of the first and second kinds, F and E, respectively (modulus k' and angle θ)

$$\frac{k'^2\sin\theta\cos\theta}{\sqrt{1-k'^2\sin^2\theta}}(\pi - \mathbf{K}) = \frac{\pi}{2} + \mathbf{K}F(k',\theta) - \mathbf{E}F(k',\theta) - \mathbf{K}E(k',\theta) \ldots [40]$$

All terms for Equation [40] may be calculated by eliminating n in Equations [38] and [39], yielding

$$\pi - \mathbf{K} = \frac{a}{r}\sqrt{\frac{a^2-r^2}{a'^2-r^2}}\left[\frac{\pi}{2} + k^2\mathbf{D}F(k',\theta) - \mathbf{K}E(k',\theta)\right] \ldots [41]$$

By Equation [41], Equation [36] becomes

$$\tau_\beta = \left[\frac{4\beta G}{\pi} - \frac{3fP_z k^3}{\pi^2 a^2}\mathbf{D}\right]\left(\frac{a' - \sqrt{a'^2-r^2}}{r}\right) + \frac{3fP_z}{\pi^2 a^2}\sqrt{1-\frac{r^2}{a^2}}\left\{\frac{\pi}{2} + k^2\mathbf{D}F(k',\theta) - \mathbf{K}E(k',\theta)\right\} \ldots [42]$$

Setting $r = a'$ in Equation [42] proves that τ_β is finite for the entire contact area; its continuity at a' will be investigated later.

[7] Reference (5), p. 32.
[8] Ibid., p. 405.

But τ_β is expressed in terms of the two parameters β and a'/a. The relation between them is found in the next section.

Relation Between Angle of Twist and Penetration of Slip

The equation relating β and a'/a may be derived from a study of the displacement $u_\theta(r, 0)$, $r \geq a'$. Setting $z = 0$ in Equation [9], and integrating

$$ru_\theta(r, 0) = 2\int_{a'}^{r} R\omega(R, 0)dR + H \quad \ldots\ldots [43]$$

where H is a constant. Now $\omega = \omega_1 + \omega_2' + \omega_2''$, and we already have the first two parts. We thus need only $\omega_2''(R, 0)$, $R \geq a'$. Using Equations [27] and [29] and noting the similarity of the latter to Equation [28], it is possible to arrive at the following $(R \geq a')$

$$\omega_2''(R, 0) = \frac{3fP_z}{2G\pi^2 a}\int_0^{a'} \frac{ds}{\sqrt{R^2 - s^2}} \times \int_{\sin^{-1}(s/a)}^{\pi/2} \frac{\cos 2\theta\, d\theta}{\sqrt{a^2 \sin^2\theta - s^2}} \quad \ldots\ldots [44]$$

Equation [26] (with $z = 0$) provides $\omega_2'(R, 0)$, and Equation [24] yields $\omega_1(R, 0)$. The integration proceeds without difficulty, using the formula[9] $\int xJ_0(x)dx = xJ_1(x)$.

The final expression for $u_\theta(r, 0), r \geq a'$ is

$$u_\theta(r, 0) = \frac{-2\beta}{\pi}\left[r \sin^{-1}\frac{a'}{r} + a'\sqrt{1 - \frac{a'^2}{r^2}}\right] - \frac{3fP_z}{4Ga}\int_0^\infty J_1(kr)J_1^2\left(\frac{ka}{2}\right)\frac{dk}{k} - \frac{H'}{r} + \frac{3fP_z}{G\pi^2 a}\int_0^{a'}\int_{\sin^{-1}(s/a)}^{\pi/2} \frac{\cos 2\theta\sqrt{1 - \frac{s^2}{r^2}}}{\sqrt{a^2 \sin^2\theta - s^2}}\, ds d\theta \quad \ldots\ldots [45]$$

where H' is a new constant including H. In Equation [45] let $r \to \infty$. Then, by Equation [4], $u_\theta \to 0$ and we find

$$\frac{Ga^2}{fP_z}\beta = \frac{3a}{4\pi a'}\int_0^{a'}\int_{\sin^{-1}(s/a)}^{\pi/2} \frac{\cos 2\theta\, d\theta\, ds}{\sqrt{a^2 \sin^2\theta - s^2}} \quad \ldots\ldots [46]$$

Reversing the order of integration plus the transformations to ψ and α in the foregoing gives

$$\frac{Ga^2}{fP_z}\beta = \frac{3k^2}{4\pi}\mathbf{D} \quad \ldots\ldots [47]$$

which is the desired relation between the angle of twist and the penetration of slip. Substituting Equation [47] in Equation [42], we have

$$\tau_\beta = \frac{3fP_z}{\pi^2 a^2}\sqrt{1 - \frac{r^2}{a^2}}\left[\frac{\pi}{2} + k^2\mathbf{D}F(k', \theta) - \mathbf{K}E(k', \theta)\right] \quad [48]$$

But the value of Equation [48] at $r = a'$ is precisely that attained there by the "Hertzian" distribution given in boundary condition Equation [6]. Hence τ_β is continuous at $r = a'$. Fig. 2 illustrates a typical profile for $\tau_{z\theta}(r, 0)$.

Torque-Twist Relation

The twisting moment is given by

$$M_z = 2\pi\int_0^a \tau_{z\theta}(r, 0)\, r^2\, dr$$

[9] Reference (5), p. 132.

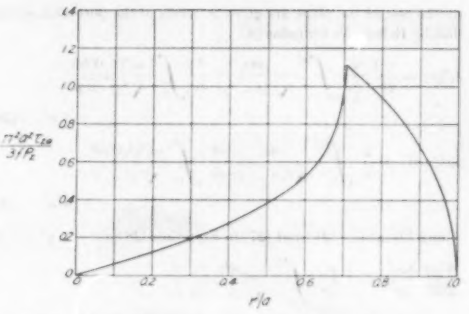

Fig. 2 Profile of Distribution of $\tau_{z\theta}$ on Contact Surface for $a'/a = 1/\sqrt{2}$

where $\tau_{z\theta}$ is obtained from Equations [6] $(a' \leq r \leq a)$ and [48] $(r \leqslant a')$. With the aid of integration by parts and the substitution $r/a' = \sin\alpha$, we find

$$\frac{M_z}{fP_z a} = \frac{1}{4\pi}\left\{\frac{3\pi^2}{4} + k'k^2\left[6\mathbf{K} + (4k'^2 - 3)\mathbf{D}\right] - 3k\mathbf{K}\sin^{-1}k' + 3k^2\left[\mathbf{K}\int_0^{\pi/2}\frac{\sin^{-1}(k'\sin\alpha)d\alpha}{(1 - k'^2\sin^2\alpha)^{3/2}} - \mathbf{D}\int_0^{\pi/2}\frac{\sin^{-1}(k'\sin\alpha)}{\sqrt{1 - k'^2\sin^2\alpha}}\, d\alpha\right]\right\} \quad \ldots\ldots [49]$$

The definite integrals were computed numerically, and Table 1 gives the relations between $M_z/fP_z a$ and $k' = a'/a$, and between $M_z/fP_z a$ and $Ga^2\beta/fP_z$. A straight line of slope 16/3, representing the initial rigidity obtained in the no-slip solution quoted in reference (1), is drawn on the moment-twist

TABLE 1 M_z AND β RELATED TO a'/a

$k = a'/a$	$Ga^2\beta/fP_z$	$M_z/fP_z a$
1	0	0
0.95	0.0190	0.0938
0.9	0.0385	0.1764
0.85	0.0586	0.2482
0.8	0.0794	0.3105
0.7	0.1234	0.4082
0.6	0.1716	0.4805
0.5	0.2257	0.5286
0.4	0.2885	0.5592
0.3	0.3656	0.5769
0.2	0.4692	0.5855
0	∞	0.5890

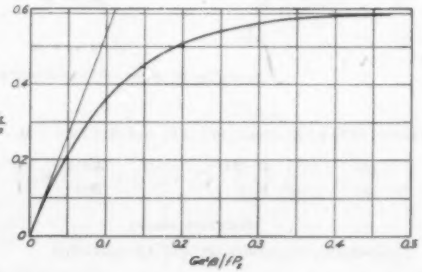

Fig. 3 Curve Relating Twisting Moment M_z and Angle of Twist β

curve in Fig. 3, showing the expected tangency at the origin. (Our β is $\beta/2$ in reference 1.)

Inspection of Fig. 3 shows that slip results in a nonlinear torque-twist relation in the torsion of elastic solids of revolution in Hertzian contact.

ACKNOWLEDGMENT

The author is greatly indebted to Prof. R. D. Mindlin, both for suggesting this problem, and for his advice on its solution. The author also wishes to thank Prof. F. J. Murray for counsel on proofs of existence and convergence of improper integrals.

BIBLIOGRAPHY

1 "Compliance of Elastic Bodies in Contact," by R. D. Mindlin, JOURNAL OF APPLIED MECHANICS, Trans. ASME, vol. 71, 1949, p. A-259.

2 "Sul contatto di due corpi elastici: distribuzione locale degli sforzi," by C. Cattaneo, Accademia dei Lincei, Rendiconti, Series 6, vol. 27, 1938, pp. 342–348, 434–436, 474–478.

3 "The Transmission of Stress Across a Plane of Discontinuity in an Isotropic Elastic Body, and the Potential Solution for a Plane Boundary," by J. H. Michell, Proceedings of the London Mathematical Society, London, England, Series 1, vol. 31, 1899, pp. 183–192.

4 "Hydrodynamics," by H. Lamb, sixth edition, Dover Publications, New York, N. Y., 1945, pp. 137–138.

5 "A Treatise on the Theory of Bessel Functions," by G. N. Watson, second edition, Cambridge University Press, London, England, 1944.

6 "History of the Theory of Elasticity," by Isaac Todhunter and Karl Pearson, Cambridge University Press, London, England, vol. 2, part II, 1893, p. 258.

7 "Tables of Functions," by E. Jahnke and F. Emde, fourth edition, Dover Publications, New York, N. Y., 1945, pp. 73 and 83.

8 "An Elementary Treatise on Elliptic Functions," by A. Cayley, Bell and Sons, London, England, 1876, p. 140, art. 183.

Influence of Flame Front on the Flow Field

By H. S. TSIEN,[1] PASADENA, CALIF.

Flame front is a region in the flow field where rapid change in the chemical composition of the fluid occurs with consequent release of chemical energy in the form of heat. In the majority of cases the phenomenon is a very complicated one involving the heat transfer by conduction and radiation, the changes in concentration of the different components by diffusion and chemical reaction. Owing to this and the difficult problem of chemical kinetics, only recently the complete theory of flame front has been formulated, particularly by the group under J. O. Hirschfelder.[2] Fortunately, as a result of the rapid rate of chemical reaction, the thickness of the flame front under ordinary conditions is generally very small, being less than 1 mm. Therefore, if one is interested in the influence of flame front on the flow field but not on the detailed structure of the flame, the flame can be assumed as infinitesimally thin, and only the final changes of the state of fluid due to combustion need be considered. This procedure is entirely analogous to that of treating the shock wave as having zero thickness in studying dynamics of compressible fluids. This simplification will be adopted for the present investigation.

NEGLECTING the change in specific heats of the gas by combustion and assuming perfect gas, very simple relations for quantities before the combustion and after the combustion can be obtained. This will be determined first. With these relations, the production of vorticity due to nonuniform condition before the flame front will be studied. After these preliminary results, the problem of flame width in a two-dimensional combustion chamber of constant width with a flame holder at the center will be solved approximately. This problem was first solved by A. C. Scurlock.[3] The present calculation is, however, very much simpler and is extended to take into account the compressibility of the gas. The effect of compressibility gives an anomalous spreading of the flame in the channel, and its significance in the efficiency of combustion and combustion-chamber design will be discussed.

Flame Front

Consider the flame front to be stationary, and the unburned gas flows into it with a normal velocity S and leaves it with a velocity w_2; S is then the normal flame velocity. Let p, ρ, and γ be the pressure, density, and the ratio of specific heats, respectively. The subscript 1 will denote quantities before the combustion and the subscript 2 after the combustion. Then the equation of continuity is

$$\rho_1 S = \rho_2 w_2 \qquad [1]$$

The momentum equation is

$$\rho_1 S^2 + p_1 = \rho_2 w_2^2 + p_2 \qquad [2]$$

If λ is the ratio of the stagnation temperature after combustion to the stagnation temperature before the combustion, the energy equation is

$$\lambda\left[\frac{1}{2}S^2 + \frac{\gamma}{\gamma-1}\frac{p_1}{\rho_1}\right] = \frac{1}{2}w_2^2 + \frac{\gamma}{\gamma-1}\frac{p_2}{\rho_2} \qquad [3]$$

Consider the quantities ρ_1, S, and λ as given by the detailed theory of flame or by experiment. Then Equations [1], [2], and [3] are three equations for the three unknowns w_2, p_2, and ρ_2. The solution corresponding to normal burning can be written as follows

$$\frac{w_2}{S} = \frac{\rho_1}{\rho_2} = \lambda + \frac{\gamma+1}{2}\lambda(\lambda-1)\mathbf{M}_1^2 + \frac{\gamma+1}{2}\lambda(\lambda-1)\left\{1+(\gamma+1)(\lambda-1)\right\}\mathbf{M}_1^4 + \cdots \qquad [4]$$

$$\frac{p_2}{p_1} = 1 - \gamma(\lambda-1)\mathbf{M}_1^2 - \frac{\gamma+1}{2}\gamma\lambda(\lambda-1)\mathbf{M}_1^4 - \frac{\gamma+1}{2}\gamma\lambda(\lambda-1)\left\{1+(\gamma+1)(\lambda-1)\right\}\mathbf{M}_1^6 + \cdots \qquad [5]$$

The temperature ratio T_2/T_1 is

$$\frac{T_2}{T_1} = \lambda - \frac{\gamma-1}{2}\lambda(\lambda-1)\mathbf{M}_1^2 - \frac{\gamma^2-1}{2}\lambda^2(\lambda-1)\mathbf{M}_1^4 + \cdots \qquad [6]$$

In these equations, the quantity $\mathbf{M}_1$ is the ratio of the flame velocity S to the sound velocity a_1 in gas before the combustion, or the Mach number of the flame. Since, under ordinary conditions, S is of the order of 1 fps while a_1 is of the order of 1000 fps, $\mathbf{M}_1$ is very small and generally only the first terms in Equations [4], [5], and [6] are necessary.

Production of Vorticity by Flame

It is known that in a nonviscous and non-heat-conducting fluid, if the pressure is only a function of density, then the vorticity of any fluid element is a constant. These conditions of flow are satisfied approximately by real fluid without heat addition or combustion. Most fluid motions of practical interest originate from a uniform state, where vorticity is zero or the motion is irrotational. Then the motion will remain irrotational. This irrotationality of flow simplifies greatly the analysis of the field. Hence it is of interest to investigate the extent to which this condition is destroyed by flame front. In other words, the production of vorticity by flame should be calculated.

For simplicity, consider the two-dimensional flow. Let the gas be of uniform composition and having a constant sum of en-

---

[1] Robert H. Goddard Professor of Jet Propulsion, Daniel and Florence Guggenheim Jet Propulsion Center, California Institute of Technology. Mem. ASME

[2] "Theory of Propagation of Flames. Part I. General Equations," by J. O. Hirschfelder and C. E. Curtiss, Third Symposium on Combustion, Flames and Explosion Phenomena, Williams and Wilkins, Baltimore, Md., 1949, pp. 121–127.

"Theory of Flame Propagation," *Journal of Chemical Physics*, vol. 17, 1949, p. 1076.

[3] "Flame Stabilization and Propagation in High-Velocity Gas Streams," by A. C. Scurlock, Meteor Report no. 19, Massachusetts Institute of Technology, 1948.

Presented at the 1950 Heat Transfer and Fluid Mechanics Institute, Los Angeles, Calif., June 28–30, 1950.

Discussion of this paper should be addressed to the Secretary, ASME, 29 West 39th Street, New York, N. Y., and will be accepted until July 10, 1951, for publication at a later date. Difcussion received after the closing date will be returned.

Note: Statements and opinions advanced in papers are to be understood as individual expressions of their authors and not those of the Society. Manuscript received by the Applied Mechanics Division, October 23, 1950.

thalpy and the kinetic energy, or isoenergetic, before combustion. In view of the generally irrotational flow without combustion, the flow before the flame front will be assumed to be irrotational and thus isentropic. The problem specifically is then to calculate the vorticity ω after the flame. Let σ be the specific entropy and ψ the stream function. Then it is known[4] that for steady flows

$$\omega = \rho_2 T_2 \frac{d\sigma_2}{d\psi_2} \quad \ldots\ldots [7]$$

where again the subscript 2 denotes quantities after the flame front. For perfect gas, Equation [7] can be written as

$$\omega = \frac{1}{\gamma - 1} p_2 \frac{d}{d\psi_2} \left\{ \log \left(\frac{p_2}{p_1} \right) - \gamma \log \left(\frac{\rho_2}{\rho_1} \right) + \log \frac{p_1}{\rho_1^\gamma} \right\} \quad \ldots [8]$$

Before the flame, σ_1 is constant, so p_1/ρ_1^γ is constant. Since $d\psi_2 = d\psi_1$, Equation [8] simplifies to

$$\omega = \frac{1}{\gamma - 1} p_1 \left(\frac{p_2}{p_1} \right) \frac{d}{d\psi_1} \left\{ \log \left(\frac{p_2}{p_1} \right) + \gamma \log \left(\frac{\rho_1}{\rho_2} \right) \right\} \quad \ldots [9]$$

The pressure ratio p_2/p_1 and the density ratio ρ_2/ρ_1 are given by Equations [4] and [5]. Therefore the production of vorticity is controlled by the variation of the flame Mach number $\mathbf{M}_1$ or S/a_1 and the parameter λ along the flame front.

Perhaps due to very intense transport phenomena generated by the large temperature rise in the flame, the normal flame velocity S is observed to be only weakly dependent upon the local conditions before combustion. According to H. Sachsse,[5] the normal flame velocity of methane-oxygen mixture is increased to 3 times the value at room temperature by preheating the mixture to 1000 C. Later experiments by Sachsse and E. Bartholomé[6] indicated an increase of approximately 30 per cent in flame velocity by preheating various gas mixtures from 20 to 100 C. From this evidence, it seems that the normal flame velocity increases roughly as the absolute temperature of the "unburned" gas mixture. The experiments on the influence of pressure on the flame velocity do not seem to give conclusive results, but in any event, the influence is not large. Therefore, for the computation of the production of vorticity by flame front, two separate cases can be considered. For the first case, the flame speed S is taken to be a constant. For the second case, the flame speed S is to be proportional to the absolute temperature T_1.

Write

$$\left.\begin{aligned} \frac{p_2}{p_1} &= F \\ \frac{\rho_1}{\rho_2} &= G \end{aligned}\right\} \quad \ldots\ldots [10]$$

Then Equation [9] can be written as

$$\omega = \frac{1}{\gamma - 1} F \left[\left\{ \frac{1}{F} \frac{\partial F}{\partial \mathbf{M}_1^2} + \frac{\gamma}{G} \frac{\partial G}{\partial \mathbf{M}_1^2} \right\} \left(p_1 \frac{d\mathbf{M}_1^2}{dp_1} \right) + \left\{ \frac{1}{F} \frac{\partial F}{\partial \lambda} + \frac{\gamma}{G} \frac{\partial G}{\partial \lambda} \right\} \left(p_1 \frac{d\lambda}{dp_1} \right) \right] \frac{dp_1}{d\psi_1} \quad \ldots\ldots [11]$$

[4] "On Rotational Gas Flows," by A. Vazsonyi, *Quarterly of Applied Mathematics*, vol. 3, 1945, pp. 29–37.

[5] "Über die Temperaturabhängigkeit der Flammengeschwindigkeit und das Temperaturgefälle in der Flammenfront," by H. Sachsse, *Zeitschrift für physikalische Chemie* (A), vol. 180, 1937, pp. 305–313.

[6] "Beiträge zur Frage der Flammengeschwindigkeit," by H. Sachsse and E. Bartholomé, *Zeitschrift für Elektrochemie und angewandte physikalische Chemie*, vol. 53, 1949, pp. 183–190.

If ΔH is the heat addition per unit mass of the gas due to chemical reaction, then from the definition of λ

$$\lambda = \frac{\Delta H}{\frac{1}{2} S^2 + \frac{\gamma}{\gamma - 1} \frac{p_1}{\rho_1}} + 1 \quad \ldots\ldots [12]$$

Therefore λ is not a constant, in spite of the fact that the heat released ΔH can be considered as a constant with good approximation.

For the first case, S is a constant, and

$$\mathbf{M}_1^2 = \frac{S^2}{a_0^2} \left(\frac{a_0}{a_1} \right)^2 = \frac{S^2}{a_0^2} \left(\frac{p_0}{p_1} \right)^{\frac{\gamma - 1}{\gamma}}$$

where the subscript 0 refers to the stagnation condition before the flame. Then

$$p_1 \frac{d\mathbf{M}_1^2}{dp_1} = -\frac{\gamma - 1}{\gamma} \frac{S^2}{a_1^2} = -\frac{\gamma - 1}{\gamma} \mathbf{M}_1^2 \quad \ldots\ldots [13]$$

Similarly

$$p_1 \frac{d\lambda}{dp_1} = -\frac{\gamma - 1}{\gamma} (\lambda - 1) \frac{1}{1 + \frac{\gamma - 1}{2} \mathbf{M}_1^2} \quad \ldots\ldots [14]$$

For the second case, S is proportional to the temperature T_1 or to a_1^2. Then

$$\mathbf{M}_1^2 = \frac{S_0^2}{a_0^2} \left(\frac{a_1}{a_0} \right)^2 = \frac{S_0^2}{a_0^2} \left(\frac{p_1}{p_0} \right)^{\frac{\gamma - 1}{\gamma}}$$

Therefore

$$p_1 \frac{d\mathbf{M}_1^2}{dp_1} = \frac{\gamma - 1}{\gamma} \frac{S_0^2}{a_0^2} \left(\frac{a_1}{a_0} \right)^2 = \frac{\gamma - 1}{\gamma} \mathbf{M}_1^2 \quad \ldots\ldots [15]$$

The corresponding derivative of λ is

$$p_1 \frac{d\lambda}{dp_1} = -\frac{\gamma - 1}{\gamma} (\lambda - 1) \frac{1 + (\gamma - 1)\mathbf{M}_1^2}{1 + \frac{\gamma - 1}{2} \mathbf{M}_1^2} \quad \ldots\ldots [16]$$

The derivative of pressure p_1 with respect to ψ_1 can be expressed in a more convenient form: If q_1 is the magnitude of velocity immediately ahead of the shock, n the normal distance from streamline to streamline, then

$$d\psi_1 = \rho_1 q_1 \, dn$$

Furthermore, the balance of centripetal forces by pressure requires

$$\frac{dp_1}{dn} = -\frac{\rho_1 q_1^2}{R_1}$$

where R_1 is the radius of curvature of the streamline immediately ahead of the shock, positive when the streamline is concave with respect to positive direction of q_1. From these two relations

$$\frac{dp_1}{d\psi_1} = -\frac{q_1}{R_1} \quad \ldots\ldots [17]$$

By substituting Equations [13], [14], and [17] into Equation [11], and by using Equations [4] and [5], the vorticity ω generated by the flame front for the case of constant flame speed S can be determined. By substituting Equations [15], [16], and [17] into Equation [11], the vorticity ω for the case of variable flame speed can be computed.

However, it is important to note that the value of the flame

speed is generally so small as to make M_1 negligible compared with unity. Then $p_1(dM_1^2/dp_1)$ is negligibly small in comparison with $p_1(d\lambda/dp_1)$ and the latter is approximately the same for both cases, i.e.

$$p_1 \frac{d\lambda}{dp_1} \cong -\frac{\gamma - 1}{\gamma}(\lambda - 1) \quad \text{for} \quad M_1^2 \ll 1 \ldots\ldots [18]$$

By making the same approximation for the functions of F and G and their derivatives, the vorticity generated ω is simply

$$\omega \cong \frac{q_1}{R_1}\left(\frac{\lambda - 1}{\lambda}\right) \quad \text{for} \quad M_1^2 \ll 1 \ldots\ldots [19]$$

It is seen from Equation [19] that when $R_1 \to \infty$, $\omega \to 0$ as expected. Furthermore, when no combustion occurs, no heat is added, and $\lambda = 1$, then $\omega = 0$. But when there is combustion, the combustion will generate appreciable vorticity of the order of q_1/R_1.

Flame Width in a Uniform Channel

The problem of spreading of the flame in a homogeneous premixed combustible from an idealized point flame holder located at the axis of a two-dimensional uniform channel, Fig. 1, was

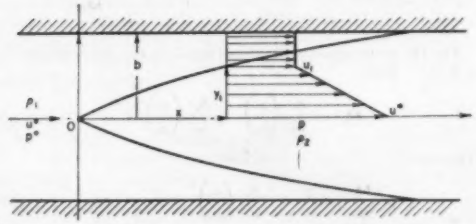

Fig. 1 Flame Propagation in a Two-Dimensional Combustion Chamber of Constant Width From the Point Flame Holder 0

first solved by A. C. Scurlock.[3] For interpreting the experimental data, he needs the relation between the flame width y_1 and the fraction of gas burned. He assumes for simplicity of calculation, that the fluid is a perfect incompressible fluid. The assumption of incompressible flow is justified on the ground that the velocity of flow is small compared with the speed of sound. This means then the flame Mach number M_1 is negligibly small. From Equations [4], [5], and [6], it is seen that

$$\frac{\rho_1}{\rho_2} = \lambda, \quad \frac{p_2}{p_1} \cong 1 \ldots\ldots [20]$$

Therefore under the assumption of incompressible flow, the effect of combustion is to change the density by a factor of λ (the ratio of stagnation temperatures) while the pressure remains constant. Scurlock then observed that since he is interested in cases where the flow velocities are very much larger than the normal flame velocity S, the flame fronts will be inclined at small angles from the channel axis. The result is that all streamlines are nearly parallel to the channel axis. Then as an approximation, the magnitude of velocity at any point is taken to be the magnitude of x-component u (parallel to the channel axis) of velocity, and neglect the effects of the curvature of the streamlines. If curvature of the streamlines is neglected, the pressure variation in the y-direction (normal to the channel axis) due to centrifugal forces must be also neglected. Equation [20] further shows that there is no pressure change by crossing the flame front: then it is evident that the pressure p in any cross section of the channel must be constant, whether in the unburned gas or the burned gas. This means the pressure is continuous in the whole field. Therefore the velocity u must also be continuous by crossing the flame front.

The entire problem is then reduced to a quasi-one-dimensional calculation: The fluid density is constant in respective regions of unburned and burned regions. The ratio of densities is λ. The unburned gas flows with constant uniform velocity u^0 and density ρ_1 until it reaches the section containing the flame holder 0, Fig. 1. The gas immediately after the flame holder has still the same velocity u^0 but a density $\rho_2 = \rho_1/\lambda$. At a section x downstream of the flame holder, the velocity at the channel axis is increased to u^* and the velocity in the unburned gas, uniform in the unburned region of the section, is increased from u^0 to u_1. The pressure p at x is, however, smaller than the pressure p^0 of the approaching unburned gas. By using Bernoulli's theorem

$$\left.\begin{aligned} \frac{1}{2}\rho_1(u_1^2 - u^{0^2}) &= p^0 - p \\ \frac{1}{2}\rho_2(u^{*2} - u^{0^2}) &= p^0 - p \end{aligned}\right\} \ldots\ldots [21]$$

Therefore by eliminating p

$$\frac{u^*}{u^0} = \sqrt{1 + \lambda\left(\frac{u_1^2}{u^{0^2}} - 1\right)} \ldots\ldots [22]$$

This equation shows that u^* is always larger than u_1.

At the section x, the velocity u in the burned region decreases from the value u^* at the axis to u_1 at the flame front $y = y_1$. Scurlock,[4] using a laborious numerical method, has computed the velocity profile for various values of λ. Fig. 2 is taken from his paper. The accuracy of the result is, of course, predicated by the assumptions. That it cannot be exact is seen by using the result of the previous section. Along the axis, the curvature of streamline is zero. From Equation [19], the vorticity $(\partial v/\partial x - \partial u/\partial y)$ along the axis is then always zero. Furthermore the y-component of velocity v is by symmetry zero along the axis. Therefore $\partial v/\partial x$ is zero along the axis. The $\partial u/\partial y$ must be also zero along the axis. This is not so in Scurlock's result. This discrepancy must be, nevertheless, localized. In gross features then, Scurlock's results are accurate for the purpose of flame-width determinations.

On the other hand, if gross features are the only results that can be expected from the simplified quasi-one-dimensional calculation, the calculation could be made very much simpler: Take the velocity profile from $y = 0$ to $y = y_1$ to be linear. Then with Equation [22]

$$\frac{u}{u^0} = \sqrt{1 + \lambda\left(\frac{u_1^2}{u^{0^2}} - 1\right)} - \left\{\sqrt{1 + \lambda\left(\frac{u_1^2}{u^{0^2}} - 1\right)} - \frac{u_1}{u^0}\right\}\frac{y}{y_1} \ldots\ldots [23]$$

The condition that the same mass must flow through each section then specifies

$$\rho_2 \int_0^{y_1} u\, dy + \rho_1 (b - y_1) u_1 = \rho_1 b u^0 \ldots\ldots [24]$$

where b is the half width of the channel. By substituting Equation [23] into [24] and by observing $\rho_1/\rho_2 = \lambda$

$$\frac{1}{2\lambda}\left(\frac{y_1}{b}\right)\left[\sqrt{\left(1 + \lambda\frac{u_1^2}{u^{0^2}} - 1\right)} + \frac{u_1}{u^0}\right] + \frac{u_1}{u^0}\left(1 - \frac{y_1}{b}\right) = 1$$

By solving for (y_1/b), denoted by η, one has the simple relation

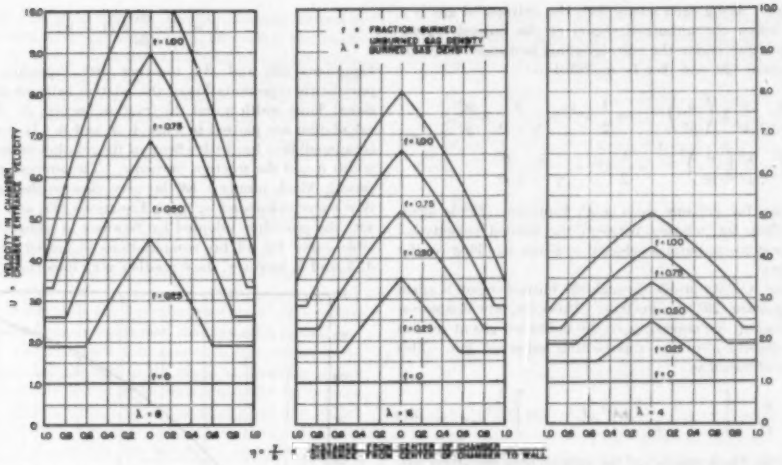

FIG. 2 VELOCITY PROFILE IN COMBUSTION CHAMBER WITH DIFFERENT FLAME WIDTH AND AT VARIOUS DENSITY RATIOS
(Computed by A. C. Scurlock, reference 3.)

$$\eta = \frac{y_1}{b} = \frac{U - 1}{\left(1 - \frac{1}{2\lambda}\right) U - \frac{1}{2\lambda}\sqrt{1 + \lambda\,(U^2 - 1)}} \quad \ldots [25]$$

where

$$U = u_1/u^0 \quad \ldots [26]$$

The fraction of the gas burned f is

$$f = 1 - \frac{\rho_1 (b - y_1) u_1}{\rho_1\, b\, u^0} = 1 - U(1 - \eta) \quad \ldots [27]$$

By combining Equation [25] with [26]

$$f = \frac{(U - 1)\left[\sqrt{1 + \lambda(U^2 - 1)} + U\right]}{(2\lambda - 1)U - \sqrt{1 + \lambda(U^2 - 1)}} \quad \ldots [28]$$

Equations [25] and [27] can be considered as the parametric representation of the relation between the nondimensional flame width η and the fraction burned f. Computations[7] using these equations have been carried out for $\lambda = 4$, 6, and 8. The results are compared with Scurlock's results in Fig. 3. The agreement is satisfactory. It seems then there is no need for the complicated numerical procedure of Scurlock.[8]

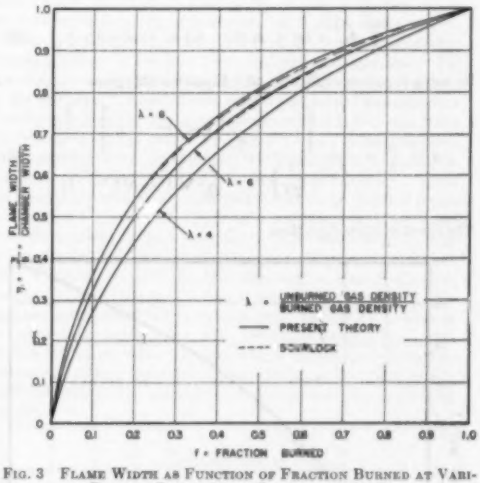
λ = 8
λ = 6
λ = 4
λ = UNBURNED GAS DENSITY / BURNED GAS DENSITY
PRESENT THEORY
SCURLOCK
η = FLAME WIDTH / CHANNEL WIDTH
f = FRACTION BURNED

FIG. 3 FLAME WIDTH AS FUNCTION OF FRACTION BURNED AT VARIOUS DENSITY RATIOS λ, FOR INCOMPRESSIBLE FLUID

EFFECT OF COMPRESSIBILITY ON FLAME WIDTH

Since the cases of interest are cases where the normal flame speed is small compared with the gas velocity, it is reasonable to speak of compressible flow of gas in general while still considering the flame Mach number M_1 in Equations [4], [5], and [6] to be negligibly small. Then the conclusions drawn in the previous section about changes of density and pressure in crossing the flame front still hold. In particular, the temperature of the gas is increased by a factor λ in crossing the flame holder. The λ at different points of the flame front is not the same as shown by Equation [12]. However, λ will be taken to be a constant as an approximation. Only here Bernoulli's equation must be modified for the compressibility effects. Therefore, in place of Equation [21]

$$\left.\begin{aligned} \frac{1}{2}\,u^{02} + c_p\,T^0 &= \frac{1}{2}\,u^{02} + c_p\,\lambda T^0 \\ \frac{1}{2}\,u_1^2 + c_p T_1 &= \frac{1}{2}\,u^{02} + c_p T^0 \end{aligned}\right\} \quad \ldots [29]$$

where T^0, T_1, and T^0 are the temperatures of the approaching unburned gas, the unburned gas at section x, and the burned gas at section x and the channel axis; c_p is the specific heat at con-

[7] The author is indebted to Mr. D. Shonerd for carrying out the numerical computations in this paper.

[8] In the Appendix, a complete mathematical formulation of Scurlock's problem is given.

stant pressure. Along each streamline, the entropy of gas is a constant in either the unburned region or the burned region. Therefore, in either region the corresponding isentropic relations hold. Equations [29] can then be modified to

$$\left.\begin{aligned} \frac{1}{2}u^{0^2} + \frac{\gamma}{\gamma-1}\frac{p^0}{\rho^0}\lambda\left(\frac{p}{p^0}\right)^{\frac{\gamma-1}{\gamma}} &= \frac{1}{2}u^{0^2} + \frac{\gamma}{\gamma-1}\lambda\frac{p^0}{\rho^0} \\ \frac{1}{2}u_1^2 + \frac{\gamma}{\gamma-1}\frac{p^0}{\rho^0}\left(\frac{p}{p^0}\right)^{\frac{\gamma-1}{\gamma}} &= \frac{1}{2}u^{0^2} + \frac{\gamma}{\gamma-1}\frac{p^0}{\rho^0} \end{aligned}\right\} \quad [30]$$

By eliminating the pressure ratio p/p^0, Equation [22] is again obtained. Thus the relation between the burned velocity u^0 at the axis and the unburned velocity u_1 is not modified by the compressibility.

If the linear velocity profile through the burned region is again assumed, Equation [23] remains true. However, now it is necessary to distinguish the density ρ_1 of the unburned gas at section x from the density ρ^0 of the approaching unburned gas. This ratio is easily obtained as

$$\frac{\rho_1}{\rho^0} = \left[1 - \frac{\gamma-1}{2}\mathbf{M}^{0^2}(U^2-1)\right]^{\frac{1}{\gamma-1}} \quad [31]$$

where $\mathbf{M}^0$ is the Mach number of the approaching unburned gas, u^0/a^0, and U is again u_1/u^0. By using the approximation that the density of fluid decreases by the constant factor $1/\lambda$ after crossing the flame, the continuity condition is now

$$\frac{\rho_1}{\lambda}\int_0^{y_1} u\,dy + \rho_1(b-y_1)u_1 = \rho^0 b u^0 \quad [32]$$

By using Equations [23] and [31], Equation [32] gives

$$\eta = \frac{y_1}{b} = \frac{U - \left[1 - \frac{\gamma-1}{2}\mathbf{M}^{0^2}(U^2-1)\right]^{-\frac{1}{\gamma-1}}}{\left(1-\frac{1}{2\lambda}\right)U - \frac{1}{2\lambda}\sqrt{1+\lambda(U^2-1)}} \quad [33]$$

The fraction burned f is then

$$f = 1 - \frac{\rho_1}{\rho_0}U(1-\eta) \quad [34]$$

Equations [33] and [34] together with Equation [31] are the parametric representation of the relation between the nondimensional flame width η and the fraction burned, f. The results of calculation are plotted in Figs. 4, 5, and 6. It is seen that the compressibility has little effect on the relation between the flame width η and the fraction burned f. The curves at different approach Mach numbers $\mathbf{M}^0$ lie very close to the incompressible-flow curve calculated by using Equations [25] and [28]. Therefore the procedure adopted by Scurlock in using the incompressible curve for all his computations is indeed justified. Figs. 4, 5, and 6, however, show another very important feature of the

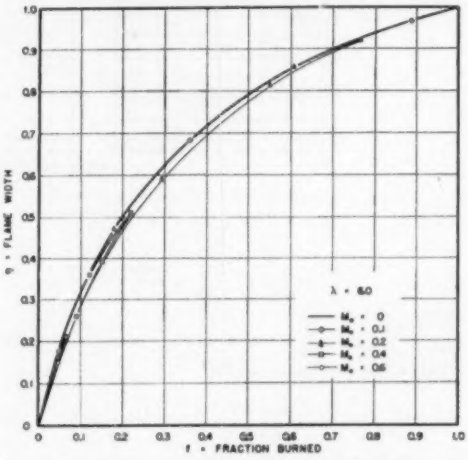

FIG. 5 FLAME WIDTH AS FUNCTION OF FRACTION BURNED AT DENSITY RATIO $\lambda = 6$ FOR VARIOUS INITIAL MACH NUMBERS $\mathbf{M}^0$

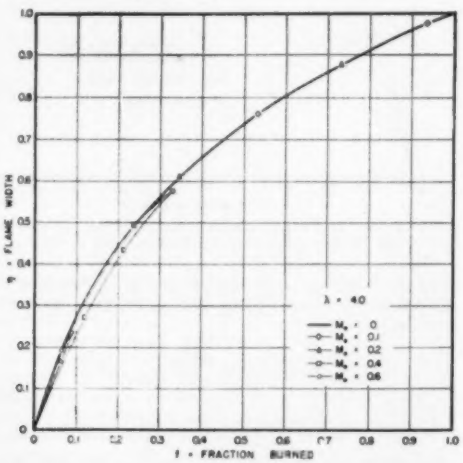

FIG. 4 FLAME WIDTH AS FUNCTION OF FRACTION BURNED AT DENSITY RATIO $\lambda = 4$ FOR VARIOUS INITIAL MACH NUMBERS $\mathbf{M}^0$

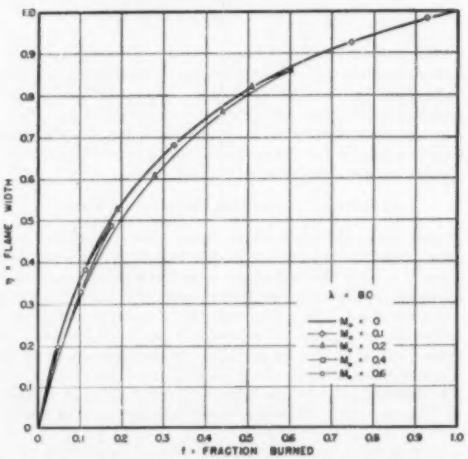

FIG. 6 FLAME WIDTH AS FUNCTION OF FRACTION BURNED AT DENSITY RATIO $\lambda = 8$ FOR VARIOUS INITIAL MACH NUMBERS $\mathbf{M}^0$

problem: Both the flame width η and the fraction burned f, have maximum values at higher M^0. For $M^0 = 0.4$, the maximum flame width is only $^1/_2$ of the channel width and the maximum amount of gas burned is only $^1/_4$ of the input. At higher values of M^0, these fractions are even smaller. This definitely shows that for a combustion chamber of constant width, as assumed in the present analysis, it will be difficult if not impossible to have complete combustion at high flow velocities, even with a good flame holder to initiate the flame.

What is the physical situation which causes this anomaly? By crossing the flame front the flow velocity is maintained, but the temperature of the gas is increased by λ times. Therefore the Mach number of the gas is reduced by combustion. In other words, the Mach number of the unburned gas is always higher than the Mach number of the burned gas. With equal reduction in pressure, the stream tube will contract less if the Mach number is higher. In fact, for supersonic flow, the stream tube will expand instead of contract when the pressure is reduced. Therefore the effect of compressibility of the gas is to make the width of the unburned gas relatively larger than the width for incompressible fluid. The effect is more prominent when the initial Mach number is higher. Therefore there will be one initial Mach number M_c^0, called the critical Mach number, for a given value of λ, at which

$$\frac{d\eta}{dU} = 0 \quad \text{at} \quad \eta = 1, \quad U = U_c \qquad [35]$$

If the initial Mach number M^0 is greater than M_c^0, then $\frac{d\eta}{dU} = 0$ at $\eta < 1$. Then the flame width will not be able to increase beyond the value of η corresponding to that at $d\eta/dU = 0$. It seems that for complete combustion M^0 should be less than M_c^0.

Equations [33] and [35] give the following conditions for the critical state

$$\left(1 - \frac{1}{2\lambda}\right) - \frac{1}{2}\frac{U_c}{\sqrt{1 + \lambda(U_c^2 - 1)}} = 1 - M_c^{0^2} U_c \left\{1 - \frac{\gamma - 1}{2} M_c^{0^2} (U_c^2 - 1)\right\}^{-\frac{\gamma}{\gamma - 1}} \qquad [36]$$

$$\left(1 - \frac{1}{2\lambda}\right) U_c - \frac{1}{2\lambda}\sqrt{1 + \lambda(U_c^2 - 1)} = U_c - \left\{1 - \frac{\gamma - 1}{2} M_c^{0^2} (U_c^2 - 1)\right\}^{-\frac{1}{\gamma - 1}} \qquad [37]$$

From Equations [36] and [37]

$$\frac{\gamma - 1}{2} M_c^{0^2} = \frac{\lambda U_c + \sqrt{1 + \lambda(U_c^2 - 1)}}{\left(\frac{\gamma + 1}{\gamma - 1} U_c^2 - 1\right)\left\{\lambda U_c + \sqrt{1 + \lambda(U_c^2 - 1)}\right\} - 2\frac{\lambda - 1}{\gamma - 1} U_c} \qquad [38]$$

This equation and Equation [36] can be used to determine the relation between M_c^0, λ, and U_c by numerical method. The Mach number M_c corresponding to U_c at the critical state is

$$M_c^2 = \frac{M_c^{0^2} U_c^2}{1 - \frac{\gamma - 1}{2} M_c^{0^2} (U_c^2 - 1)} \qquad [39]$$

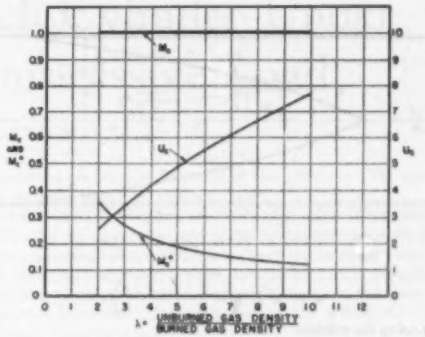

FIG. 7 CRITICAL CONDITIONS FOR COMPLETE COMBUSTION AT VARIOUS DENSITY RATIOS λ

The results of calculation are given in Fig. 7 where M_c^0, M_c, U_c are plotted against λ. From the previous discussion it is seen that in order to have complete combustion, the approach Mach number M^0 must be kept below the critical value M_c^0. For a heating ratio $\lambda = 8$, M_c^0 is only 0.15. Then the velocity for complete combustion is below 200 fps. It is interesting to observe that the local Mach number M_c, for the unburned gas at the critical state, is very close to unity but slightly supersonic.

It is unfortunate that the results of the present theoretical analysis cannot be checked with Scurlock's experiments. The few critical cases recorded by Scurlock with high inlet velocity to the combustion chamber and small flame holder are made in a combustion chamber too short to ascertain whether the flame reached the chamber wall. This is, of course, natural as Scurlock concentrated his attention on the flame-holder performance, but not in the flame-spreading and combustion efficiency. From the present investigation it would seem that the problem of flame-spreading and combustion efficiency is a problem by itself, apart from the problem of flame holding, or flame initiation. In fact, one should not limit oneself only to combustion chambers of constant width, as it is evident that the way to achieve complete combustion at high approach Mach number is to use an expanding combustion chamber for reducing the flow Mach number as the combustion progresses. The present analysis is only a beginning in this problem. It serves to point out the general importance of mutual influence of flame front and the flow, and to show specifically the limitations of constant-width combustion chambers.

Appendix

FORMULATION OF SCURLOCK'S PROBLEM AS AN INTEGRAL EQUATION

Let the flame width increase from ξ to $\xi + d\xi$ when distance downstream of the flame holder increases from t to dt, Fig. 8. The mass of unburned gas at t is $\rho_1(b - \xi)v$ where v is the velocity of the unburned gas at t (i.e., at $x = t$, $u_1 = v$). The decrease in the mass flow of unburned gas, or the mass of gas burned dm between t and $t + dt$ is thus

$$dm = -\rho_1 d[(b - \xi)v] \qquad [40]$$

At section x, this fraction of burned mass occupies the width dy with a velocity u and density (ρ_1/λ). From Bernoulli's equation applied between section t to x, one has, similar to Equation [22]

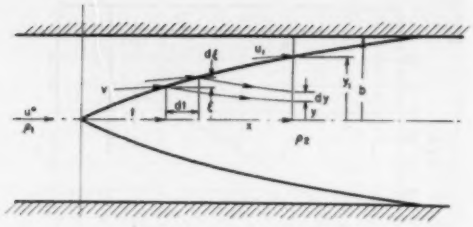

FIG. 8 SCUBLOCK'S PROBLEM

$$u = \sqrt{\lambda}\sqrt{u_1^2 - \left(1 - \frac{1}{\lambda}\right)v^2} \quad \ldots\ldots [41]$$

By using the relation

$$\frac{\rho_1}{\lambda} u\, dy = dm$$

and Equation [40]

$$dy = -\sqrt{\lambda}\,\frac{d\,[(b-\xi)v]}{\sqrt{u_1^2 - \left(1 - \frac{1}{\lambda}\right)v^2}} \quad \ldots\ldots [42]$$

The streamline passing through $y = 0$ corresponds to $v = u^0$ and the streamline passing through $y = y_1$ corresponds to $v = u_1$. Therefore, by integrating Equation [42]

$$y_1 = -\sqrt{\lambda}\int_{v=u^0}^{v=u_1} \frac{d\,[(b-\xi)v]}{\sqrt{u_1^2 - \left(1 - \frac{1}{\lambda}\right)v^2}} \quad \ldots\ldots [43]$$

Result of a partial integration of Equation [43] can be written in nondimensional variables as

$$\eta(U) = \frac{\lambda}{(\lambda-1)^{1/2}}\left\{\sin^{-1}\sqrt{\frac{\lambda-1}{\lambda}} - \sin^{-1}\frac{1}{U}\sqrt{\frac{\lambda-1}{\lambda}}\right\} + \frac{1}{\sqrt{\lambda}}\int_1^U \frac{V^2}{\left[U^2 - \left(1 - \frac{1}{\lambda}\right)V^2\right]^{1/2}}\eta(V)\,dV \quad \ldots\ldots [44]$$

where $V = v/u^0$ and $\eta(V) = \xi/b$.

Equation [44] is an integral equation of the second kind for the unknown function $\eta(U)$. When λ is large, a very accurate value of η can be obtained by replacing the η (V) in the integral of Equation [44] by the approximate value given by Equation [25].

Buckling of a Sandwich Cylinder Under Uniform Axial Compressive Load

By A. CEMAL ERINGEN,[1] CHICAGO, ILL.

A boundary-value problem of elasticity for a thick hollow circular cylinder is solved under the following boundary conditions, namely, (*a*) on the lateral surfaces, displacements are specified as arbitrary functions of the longitudinal co-ordinates only, and (*b*) at both ends, the radial displacements and the longitudinal surface forces are taken to be equal to zero. The displacements, strains, and stresses are obtained in terms of these arbitrary displacement functions. The stresses determined are used to obtain the buckling load of a sandwich cylinder, which employs the thick hollow cylinder as the core. Two simultaneous differential equations are obtained from the equilibrium conditions between the contacting lateral surfaces of the sandwich material (faces) and the core. Numerical calculations and curves are made of the buckling stress for a given core material and for two types of face materials employed in aircraft design. In a special case, when the radius approaches infinity, the result is found to be in good agreement with previously published experimental results. No test data for the general case were available to the author during the preparation of this paper.

Introduction

In recent years the attainment of higher speeds in aircraft has increased the importance of surface smoothness in aerodynamic studies and has added this factor to the fundamental principles of aircraft design, namely, more strength and less weight. These three principles are all reflected in the properties of sandwich structures made of thin faces of high-strength materials glued to the lateral surfaces of lightweight cores.

This paper establishes a formula for determining the buckling load of a circular sandwich cylinder subjected to a compressive load uniformly distributed on the ends of the faces. Consequently, this solution may be regarded as the first instability problem of a sandwich-type airplane fuselage.

The analysis involves two distinct problems, namely, (*a*) a boundary-value problem in elasticity of a thick hollow circular cylinder, and (*b*) the instability of a sandwich cylinder. Within the limitations of small-deflection theory, the solution of the boundary-value problem is given in terms of four arbitrary deflection functions which are specified on the lateral surfaces of the cylinder. The solution is required to satisfy the additional condition that the longitudinal component of stress and the radial displacements are zero on the ends of the cylinder. The system is assumed to have rotational symmetry.

In the buckling problem the radial deflection of the faces is assumed to be identical to that of the lateral surfaces of the core. This approximation is within reason since the faces are very thin and have high strength. Thus two simultaneous differential equations of equilibrium are obtained in terms of the foregoing deflection functions. The eigenvalues of the differential equations give the critical load.

Problem 1 A Boundary-Value Problem of Elasticity for Thick Hollow Circular Cylinder

Differential Equations. The equations of equilibrium, referred to cylindrical co-ordinates (1)[2] in which rotational symmetry exists, are given by

$$\left.\begin{aligned} \frac{\partial \sigma_r}{\partial r} + \frac{\partial \tau_{rz}}{\partial z} + \frac{\sigma_r - \sigma_\theta}{r} &= 0 \\ \frac{\partial \tau_{rz}}{\partial r} + \frac{\partial \sigma_z}{\partial z} + \frac{\tau_{rz}}{r} &= 0 \end{aligned}\right\} \quad [1]$$

where the body forces are zero.

Hooke's law may be expressed as

$$\left.\begin{aligned} \sigma_r &= \lambda\Delta + 2\mu\epsilon_r \\ \sigma_\theta &= \lambda\Delta + 2\mu\epsilon_\theta \\ \sigma_z &= \lambda\Delta + 2\mu\epsilon_z \\ \tau_{rz} &= \mu\gamma_{rz} \\ \tau_{r\theta} &= \tau_{\theta z} = 0 \end{aligned}\right\} \quad [2]$$

where

$$\Delta = \frac{1}{r}\frac{\partial (ru)}{\partial r} + \frac{\partial w}{\partial z} \quad [3]$$

and the strains are

$$\left.\begin{aligned} \epsilon_r &= \frac{\partial u}{\partial r} \\ \epsilon_\theta &= \frac{u}{r} \\ \epsilon_z &= \frac{\partial w}{\partial z} \\ \gamma_{rz} &= \frac{\partial u}{\partial z} + \frac{\partial w}{\partial r} \\ \gamma_{r\theta} &= \gamma_{\theta z} = 0 \end{aligned}\right\} \quad [4]$$

Substitution of Equations [2], [3], and [4] into Equations [1] leads to

$$\left.\begin{aligned} \frac{\partial}{\partial r}\left[\frac{1}{r}\frac{\partial}{\partial r}(ru)\right] + A\frac{\partial^2 u}{\partial z^2} + (1-A)\frac{\partial^2 w}{\partial r \partial z} &= 0 \\ \frac{A}{r}\frac{\partial}{\partial r}\left(r\frac{\partial w}{\partial r}\right) + \frac{\partial^2 w}{\partial z^2} + (1-A)\frac{1}{r}\frac{\partial^2 (ru)}{\partial r \partial z} &= 0 \end{aligned}\right\} \quad [5]$$

[1] Research Assistant Professor of Mechanics, Illinois Institute of Technology; Consultant, Applied Mechanics Research Department, Armour Research Foundation, Chicago, Ill.

Contributed by the Applied Mechanics Division and presented at the Annual Meeting, New York, N. Y., November 26–December 1, 1950, of The American Society of Mechanical Engineers.

Discussion of this paper should be addressed to the Secretary, ASME, 29 West 39th Street, New York, N. Y., and will be accepted until July 10, 1951, for publication at a later date. Discussion received after the closing date will be returned.

Note: Statements and opinions advanced in papers are to be understood as individual expressions of their authors and not those of the Society. Manuscript received by the Applied Mechanics Division, April 19, 1950. Paper No. 50—A-3.

[2] Numbers in parentheses refer to the Bibliography at the end of the paper.

where

$$\left.\begin{aligned} A &= \frac{\mu}{\lambda + 2\mu} \\ \mu &\equiv G \\ \lambda &= \frac{\nu E}{(1+\nu)(1-2\nu)} \\ G &= \frac{E}{2(1+\nu)} \end{aligned}\right\} \quad \ldots\ldots [6]$$

are constant. λ and μ are Lamé constants and are related to E, G, and ν (modulus of elasticity, shear modulus, and Poisson's ratio, respectively) by Equations [6].

Boundary Conditions: (See Fig. 1)

At $r = a_1$ $u(a_1, z) = u_0(a_1, z)$ ..... [7]

$w(a_1, z) = w_0(a_1, z)$ ..... [8]

$r = a_2$ $u(a_2, z) = u_0(a_2, z)$ ..... [9]

$w(a_2, z) = w_0(a_2, z)$ ..... [10]

$z = 0$ $u(r, 0) = 0$ ..... [11]

$\dfrac{\partial w(r, 0)}{\partial z} = 0$ ..... [12]

$z = L$ $u(r, L) = 0$ ..... [13]

$\dfrac{\partial w(r, L)}{\partial z} = 0$ ..... [14]

The arbitrary functions, $u_0(a_1, z)$, $w_0(a_1, z)$ and $u_0(a_2, z)$, $w_0(a_2, z)$, are specified on the boundaries, $r = a_1$ and $r = a_2$, respectively. The physical significance of Equations [12] and [14] is that $\sigma_z = 0$ and $\epsilon_z = 0$ at $z = 0$ and $z = L$. This is evident by first substituting Equations [11], [12], [13], [14], [3] into σ_z of Equations [2] and also by inspection of ϵ_z of Equations [4].

Solution of Boundary-Value Problem. Let the displacements, $u(r, z)$ and $w(r, z)$, be represented by[5]

$$\left.\begin{aligned} u(r, z) &= \sum_{m=1}^{\infty} U_m(r) \sin \frac{m\pi z}{L} \\ w(r, z) &= \sum_{m=1}^{\infty} W_m(r) \cos \frac{m\pi z}{L} \\ (m &= 1, 2, \ldots.) \end{aligned}\right\} \quad \ldots\ldots [15]$$

It can be shown readily that Equations [15] satisfy all four of the boundary conditions, that is, Equations [11], [12], [13], and [14].

Substitution of Equations [15] into Equations [5] yields

$$\left.\begin{aligned} &\frac{d^2U_m}{dr^2} + \frac{1}{r}\frac{dU_m}{dr} - \left[A\left(\frac{m\pi}{L}\right)^2 + \frac{1}{r^2}\right] U_m \\ &\qquad - (1 - A)\frac{m\pi}{L}\frac{dW_m}{dr} = 0 \\ &\frac{d^2W_m}{dr^2} + \frac{1}{r}\frac{dW_m}{dr} - \frac{1}{A}\left(\frac{m\pi}{L}\right)^2 W_m \\ &\qquad + \frac{1 - A}{A}\frac{m\pi}{L}\frac{1}{r}\frac{d(rU_m)}{dr} = 0 \end{aligned}\right\} \quad [16]$$

The solution to the foregoing equations is

$$\left.\begin{aligned} U_m(r) &= C_{1m}I_1(\rho) + C_{2m}\rho I_0(\rho) + C_{3m}K_1(\rho) + C_{4m}\rho K_0(\rho) \\ W_m(r) &= C_{1m}I_0(\rho) + C_{2m}[\rho I_1(\rho) + \gamma I_0(\rho)] - C_{3m}K_0(\rho) \\ &\quad - C_{4m}[\rho K_1(\rho) - \gamma K_0(\rho)] \end{aligned}\right\} \quad [17]$$

where C_{1m}, C_{2m}, C_{3m}, and C_{4m} are constants of integration and

$$\left.\begin{aligned} \rho &= \frac{m\pi r}{L} \\ \gamma &= \frac{2}{1 - A} \end{aligned}\right\} \quad [18]$$

$I_0(\rho)$, $I_1(\rho)$ and $K_0(\rho)$, $K_1(\rho)$ are Bessel functions of the first and second kind, respectively, and both of zero and first order with imaginary arguments

$I_n(\rho)$ and $K_n(\rho)$ are given by (6)

$$\left.\begin{aligned} I_n(\rho) &= \sum_{s=0}^{\infty} \frac{(\rho/2)^{n+2s}}{s!\Gamma(n + s + 1)} \\ K_n(\rho) &= \frac{1}{2}\pi \frac{I_{-n}(\rho) - I_n(\rho)}{\sin n\pi} \text{ (see note[6])} \end{aligned}\right\} \quad [19]$$

C_{1m} to C_{4m} may be evaluated by using the boundary conditions, Equations [7] to [10]. It is more convenient to use $U_m(r)$ and $W_m(r)$ instead of $u(r, z)$ and $w(r, z)$ at this point. Using Fourier's theorem, $U_m(r)$ and $W_m(r)$ may be obtained as

$$\left.\begin{aligned} U_m(r) &= \frac{2}{L}\int_0^L u(r, z) \sin \frac{m\pi z}{L}\, dz \\ W_m(r) &= \frac{2}{L}\int_0^L w(r, z) \cos \frac{m\pi z}{L}\, dz \\ (m &= 1, 2, \ldots.) \end{aligned}\right\} \quad [20]$$

from which

$$\left.\begin{aligned} U_m(a_i) &= \frac{2}{L}\int_0^L u_0(a_i, z) \sin \frac{m\pi z}{L}\, dz \\ W_m(a_i) &= \frac{2}{L}\int_0^L w_0(a_i, z) \cos \frac{m\pi z}{L}\, dz \\ (m &= 1, 2, 3, \ldots.),\ (i = 1, 2) \end{aligned}\right\} \quad [21]$$

The use of the boundary conditions, Equations [7] to [10], in Equations [17] by means of Equations [21] leads to

$$\left.\begin{aligned} &C_{1m}I_1(\alpha_1) + C_{2m}\alpha_1 I_0(\alpha_1) + C_{3m}K_1(\alpha_1) + C_{4m}\alpha_1 K_0(\alpha_1) = U_m(a_1) \\ &C_{1m}I_1(\alpha_2) + C_{2m}\alpha_2 I_0(\alpha_2) + C_{3m}K_1(\alpha_2) + C_{4m}\alpha_2 K_0(\alpha_2) = U_m(a_2) \\ &C_{1m}I_0(\alpha_1) + C_{2m}[\alpha_1 I_1(\alpha_1) + \gamma I_0(\alpha_1)] - C_{3m}K_0(\alpha_1) - C_{4m}[\alpha_1 K_1(\alpha_1) - \gamma K_0(\alpha_1)] = W_m(a_1) \\ &C_{1m}I_0(\alpha_2) + C_{2m}[\alpha_2 I_1(\alpha_2) + \gamma I_0(\alpha_2)] - C_{3m}K_0(\alpha_2) - C_{4m}[\alpha_2 K_1(\alpha_2) - \gamma K_0(\alpha_2)] = W_m(a_2) \end{aligned}\right\} \quad [22]$$

where

$$\alpha_1 = \frac{m\pi a_1}{L}, \quad \text{and} \quad \alpha_2 = \frac{m\pi a_2}{L}$$

[5] This method of attack has been used previously by various authors for solving boundary-value problems related to the circular cylinder (see, for instance, References 1, 2, 3, 10).

[6] The limit should be taken when n is an integer.

From Equations [22] C_{1m} to C_{4m} are obtained as

$$C_{1m} = \frac{\Delta_1}{\Delta}, \quad C_{2m} = \frac{\Delta_2}{\Delta}, \quad C_{3m} = \frac{\Delta_3}{\Delta}, \quad C_{4m} = \frac{\Delta_4}{\Delta} \qquad [23]$$

where

$$\Delta_1 = \begin{vmatrix} U_m(a_1) & a_1 I_0(a_1) & & K_1(a_1) & a_1 K_0(a_1) \\ U_m(a_2) & a_2 I_0(a_2) & & K_1(a_2) & a_2 K_0(a_2) \\ W_m(a_1) & a_1 I_1(a_1) + \gamma I_0(a_1) & & -K_0(a_1) & -a_1 K_1(a_1) + \gamma K_0(a_1) \\ W_m(a_2) & a_2 I_1(a_2) + \gamma I_0(a_2) & & -K_0(a_2) & -a_2 K_1(a_2) + \gamma K_0(a_2) \end{vmatrix}$$

$$\Delta_2 = \begin{vmatrix} I_1(a_1) & U_m(a_1) & K_1(a_1) & a_1 K_0(a_1) \\ I_1(a_2) & U_m(a_2) & K_1(a_2) & a_2 K_0(a_2) \\ I_0(a_1) & W_m(a_1) & -K_0(a_1) & -a_1 K_1(a_1) + \gamma K_0(a_1) \\ I_0(a_2) & W_m(a_2) & -K_0(a_2) & -a_2 K_1(a_2) + \gamma K_0(a_2) \end{vmatrix}$$

$$\Delta_3 = \begin{vmatrix} I_1(a_1) & a_1 I_0(a_1) & & U_m(a_1) & a_1 K_0(a_1) \\ I_1(a_2) & a_2 I_0(a_2) & & U_m(a_1) & a_2 K_0(a_2) \\ I_0(a_1) & a_1 I_1(a_1) + \gamma I_0(a_1) & & W_m(a_1) & -a_1 K_1(a_1) + \gamma K_0(a_1) \\ I_0(a_2) & a_2 I_1(a_2) + \gamma I_0(a_2) & & W_m(a_2) & -a_2 K_1(a_2) + \gamma K_0(a_2) \end{vmatrix} \qquad [24]$$

$$\Delta_4 = \begin{vmatrix} I_1(a_1) & a_1 I_0(a_1) & & K_1(a_1) & U_m(a_1) \\ I_1(a_2) & a_2 I_0(a_2) & & K_1(a_2) & U_m(a_2) \\ I_0(a_1) & a_1 I_1(a_1) + \gamma I_0(a_1) & & -K_0(a_1) & W_m(a_1) \\ I_0(a_2) & a_2 I_1(a_2) + \gamma I_0(a_2) & & -K_0(a_2) & W_m(a_2) \end{vmatrix}$$

$$\Delta = \begin{vmatrix} I_1(a_1) & a_1 I_0(a_1) & & K_1(a_1) & a_1 K_0(a_1) \\ I_1(a_2) & a_2 I_0(a_2) & & K_1(a_2) & a_2 K_0(a_2) \\ I_0(a_1) & a_1 I_1(a_1) + \gamma I_0(a_1) & & -K_0(a_1) & -a_1 K_1(a_1) + \gamma K_0(a_1) \\ I_0(a_2) & a_2 I_1(a_2) + \gamma I_0(a_2) & & -K_0(a_2) & -a_2 K_1(a_2) + \gamma K_0(a_2) \end{vmatrix}$$

The foregoing determinants, together with Equations [23] and [17], substituted into Equations [15], give the solution of the boundary-value problem. The strains and stresses then can be obtained by subsequent substitution of Equations [15] into Equations [4] and [2].

A Special Case. The following special case is important because of its simplicity and usability in the buckling phenomena treated in the second problem.

Let us assume that

$$W_m(a_1) = W_m(a_2) = 0 \qquad [25]$$

Then the stresses may be formulated by using Equations [2] and [3], as

$$\begin{aligned} \sigma_r &= \sum_{m=1}^{\infty} \sum_{i=1}^{2} \mu R_{im}(\rho) U_m(a_i) \frac{m\pi}{L} \sin \frac{m\pi z}{L} \\ \sigma_\theta &= \sum_{m=1}^{\infty} \sum_{i=1}^{2} \mu \Theta_{im}(\rho) U_m(a_i) \frac{m\pi}{L} \sin \frac{m\pi z}{L} \\ \sigma_z &= \sum_{m=1}^{\infty} \sum_{i=1}^{2} \mu Z_{im}(\rho) U_m(a_i) \frac{m\pi}{L} \sin \frac{m\pi z}{L} \\ \tau_{rz} &= \sum_{m=1}^{\infty} \sum_{i=1}^{2} \mu T_{im}(\rho) U_m(a_i) \frac{m\pi}{L} \cos \frac{m\pi z}{L} \\ \tau_{r\theta} &= \tau_{\theta z} = 0 \end{aligned} \qquad [26]$$

$$\begin{aligned} R_{im}(\rho) &= \sum_{j=1}^{4} D_i^j(a_1, a_2) R_j(\rho) \\ \Theta_{im}(\rho) &= \sum_{j=1}^{4} D_i^j(a_1, a_2) \Theta_j(\rho) \\ Z_{im}(\rho) &= \sum_{j=1}^{4} D_i^j(a_1, a_2) Z_j(\rho) \\ T_{im}(\rho) &= \sum_{j=1}^{4} D_i^j(a_1, a_2) T_j(\rho) \\ (i &= 1, 2), \ (j = 1, 2, 3, 4) \end{aligned} \qquad [27]$$

Here Δ is given by the last of Equations [24], and

$$\begin{aligned} D_1^1(a_1, a_2) = D_2^1(a_2, a_1) &= -\frac{1}{\Delta} \begin{vmatrix} a_1 I_0(a_1) & & K_1(a_1) & a_1 K_0(a_1) \\ a_1 I_1(a_1) + \gamma I_0(a_1) & & -K_0(a_1) & -a_1 K_1(a_1) + \gamma K_0(a_1) \\ a_2 I_1(a_2) + \gamma I_0(a_2) & & -K_0(a_2) & -a_2 K_1(a_2) + \gamma K_0(a_2) \end{vmatrix} \\ D_1^2(a_1, a_2) = D_2^2(a_2, a_1) &= \frac{1}{\Delta} \begin{vmatrix} I_1(a_1) & K_1(a_1) & a_1 K_0(a_1) \\ I_0(a_1) & -K_0(a_1) & -a_1 K_1(a_1) + \gamma K_0(a_1) \\ I_0(a_2) & -K_0(a_2) & -a_2 K_1(a_2) + \gamma K_0(a_2) \end{vmatrix} \\ D_1^3(a_1, a_2) = D_2^3(a_2, a_1) &= -\frac{1}{\Delta} \begin{vmatrix} I_1(a_1) & a_1 I_0(a_1) & & a_1 K_0(a_1) \\ I_0(a_1) & a_1 I_1(a_1) + \gamma I_0(a_1) & & -a_1 K_1(a_1) + \gamma K_0(a_1) \\ I_0(a_2) & a_2 I_1(a_2) + \gamma I_0(a_2) & & -a_2 K_1(a_2) + \gamma K_0(a_2) \end{vmatrix} \\ D_1^4(a_1, a_2) = D_2^4(a_2, a_1) &= \frac{1}{\Delta} \begin{vmatrix} I_1(a_1) & a_1 I_0(a_1) & K_1(a_1) \\ I_0(a_1) & a_1 I_1(a_1) + \gamma I_0(a_1) & -K_0(a_1) \\ I_0(a_2) & a_2 I_1(a_2) + \gamma I_0(a_2) & -K_0(a_2) \end{vmatrix} \end{aligned} \qquad [28]$$

and

$$
\left.
\begin{aligned}
R_1(\rho) &= \frac{2}{\rho}\,[\rho I_0(\rho) - I_1(\rho)] \\
R_2(\rho) &= 2[(1-2\nu)I_0(\rho) + \rho I_1(\rho)] \\
R_3(\rho) &= -\frac{2}{\rho}\,[\rho K_0(\rho) + K_1(\rho)] \\
R_4(\rho) &= 2[(1-2\nu)\,K_0(\rho) - \rho K_1(\rho)] \\
\Theta_1(\rho) &= \frac{2}{\rho}\,I_1(\rho) \\
\Theta_2(\rho) &= 2(1-2\nu)\,I_0(\rho) \\
\Theta_3(\rho) &= \frac{2}{\rho}\,K_1(\rho) \\
\Theta_4(\rho) &= 2(1-2\nu)\,K_0(\rho) \\
Z_1(\rho) &= -2I_0(\rho) \\
Z_2(\rho) &= -2[2(2-\nu)\,I_0(\rho) + \rho I_1(\rho)] \\
Z_3(\rho) &= 2K_0(\rho) \\
Z_4(\rho) &= -2[2(2-\nu)\,K_0(\rho) - \rho K_1(\rho)] \\
T_1(\rho) &= 2I_1(\rho) \\
T_2(\rho) &= 2[\rho I_0(\rho) + 2(1-\nu)I_1(\rho)] \\
T_3(\rho) &= 2K_1(\rho) \\
T_4(\rho) &= 2[\rho K_0(\rho) - 2(1-\nu)\,K_1(\rho)]
\end{aligned}
\right\} \quad \ldots\ldots [29]
$$

Problem 2 Buckling of Circular Sandwich Cylinder Under Uniform Axial Compressive Load

Differential Equations. Let us consider a sandwich cylinder composed of a thick hollow circular cylinder (core), for which a boundary-value problem was previously solved, and the faces, as shown in Fig. 2. Assume that the face thickness t_f is small compared to the inside radius, a_1. Then the deflections, $u[a_1 + (t_f/2), z]$ and $u[a_2 + (t_f/2), z]$, of the faces may be replaced by the boundary-displacement functions, $u_0(a_1, z)$ and $u_0(a_2, z)$, of the core. A uniform axial compressive load N is applied to the ends of each face. The problem is to obtain the critical value of the compressive load N, for which the cylinder buckles.[5]

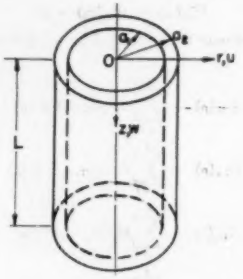

Fig. 1

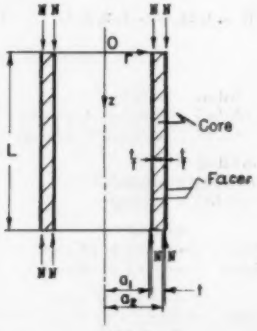

Fig. 2

The following differential equations are obtained from the equilibrium conditions of an infinitesimal element of each face[6]

$$
D_f \frac{d^4 u_0(a_k, z)}{dz^4} + N \frac{d^2 u_0(a_k, z)}{dz^2} + \frac{E_f t_f}{a_k^2}\, u_0(a_k, z) + \sigma_r(a_k, z) - \frac{t_f}{2}\,\frac{d\tau(a_k, z)}{dz} = 0 \;(k = 1, 2) \quad \ldots [30]
$$

where

$$
D_f = \frac{E_f t_f^3}{12(1-\nu_f^2)} \quad \ldots [31]
$$

is the bending rigidity. Substitution of the values of σ_r and τ given by Equations [26] leads to

$$
D_f \frac{d^4 u_0(a_k, z)}{dz^4} + N \frac{d^2 u_0(a_k, z)}{dz^2} + \frac{E_f t_f}{a_k^2}\, u_0(a_k, z) + \sum_{m=1}^{\infty} \sum_{i=1}^{2} \mu S_{im}(a_k)\, U_m(a_i)\, \frac{m\pi}{L} \sin \frac{m\pi z}{L} = 0 \quad \ldots [32]
$$

$$
(i, k = 1, 2), \; (m = 1, 2, \ldots)
$$

where

$$
\left.
\begin{aligned}
S_{im}(a_k) &= R_{im}(a_k) + \frac{1}{2}\,\tau_f T_{im}(a_k) \\
&\qquad (i, k = 1, 2), \; (m = 1, 2, \ldots) \\
\tau_f &= \frac{m\pi t_f}{L}
\end{aligned}
\right\} \quad \ldots [33]
$$

Boundary Conditions. At

$$
z = 0 \quad u_0(a_k, 0) = 0 \quad \ldots [34]
$$

$$
\frac{d^2 u_0(a_k, 0)}{dz^2} = 0 \quad \ldots [35]
$$

$$
z = L \quad u_0(a_k, L) = 0 \quad \ldots [36]
$$

$$
\frac{d^2 u_0(a_k, L)}{dz^2} = 0 \quad \ldots [37]
$$

for

$$
(k = 1, 2)
$$

The boundary conditions represent zero deflections and moments at the ends of each face which correspond to the condition of simple support. The instability problem is then reduced to finding an eigenvalue solution of the two simultaneous differential equations, Equations [32], satisfying eight boundary conditions, Equations [34] to [37].

Solution of Buckling Problem. Let

---

[5] In practice the core material is much softer than the face material, i.e., $E_f t_f \gg Et$; thus the uniform compression load N applied to the ends of the cylinder will be carried by the faces. This explains why $\sigma_z(r, 0)$ and $\sigma_z(r, L)$ in the core are taken to be zero (see problem 1, Equations [12] and [14]. It is also worth while to note that there will be shear forces τ_{rz} acting at the ends of the core as indicated by problem 1, Equations [26], because of the friction between the load-applying device and the core.

[6] Buckling of a sandwich cylinder under the distributed bending moment $N \cdot t$ can be obtained from Equation [30] by placing $-N$ instead of N in one of these equations (3).

$$w_0(a_k, z) = \sum_{m=1}^{\infty} U_m(a_k) \sin \frac{m\pi z}{L} \quad \ldots\ldots [38]$$

$$(k = 1, 2), \ (m = 1, 2, \ldots .)$$

Equation [38] is chosen such that all of the eight boundary conditions are satisfied. Furthermore, the form of this equation is the same as Equations [15] of problem 1. Substitution of Equation [38] into Equations [32] yields two simultaneous linear equations for $U_m(a_1)$ and $U_m(a_2)$. Hence

$$\left.\begin{aligned} &\left[D_f\left(\frac{m\pi}{L}\right)^4 - N\left(\frac{m\pi}{L}\right)^2 + \frac{E_f t_f}{a_1^2} + \mu\frac{m\pi}{L}S_{1m}(a_1)\right] U_m(a_1) + \mu\frac{m\pi}{L}S_{2m}(a_1)U_m(a_2) = 0 \\ &\mu\frac{m\pi}{L}S_{1m}(a_2)U_m(a_1) + \left[D_f\left(\frac{m\pi}{L}\right)^4 - N\left(\frac{m\pi}{L}\right)^2 + \frac{E_f t_f}{a_2^2} + \mu\frac{m\pi}{L}S_{2m}(a_2)\right] U_m(a_2) = 0 \end{aligned}\right\} \quad \ldots\ldots [39]$$

A nontrivial solution exists when

$$\begin{aligned} &\left[D_f\left(\frac{m\pi}{L}\right)^4 - N\left(\frac{m\pi}{L}\right)^2 + \frac{E_f t_f}{a_1^2} + \mu\frac{m\pi}{L}S_{1m}(a_1)\right]\left[D_f\left(\frac{m\pi}{L}\right)^4 - N\left(\frac{m\pi}{L}\right)^2 + \frac{E_f t_f}{a_2^2} + \mu\frac{m\pi}{L}S_{2m}(a_2)\right] \\ &\quad - \mu^2\left(\frac{m\pi}{L}\right)^2 S_{1m}(a_2)S_{2m}(a_1) = 0 \quad \ldots [40] \end{aligned}$$

$$(m = 1, 2, \ldots .)$$

The critical value of N is obtained from this equation and expressed in the following form after dividing by t_f and calling $\sigma_{cr} = N_{cr}/t_f$

$$\sigma_{cr} = \sigma_f + \sigma_s \quad \ldots\ldots [41]$$

where

$$\left.\begin{aligned} \sigma_f &= \frac{E_f}{12(1-\nu_f^2)}\tau_f^2 + \frac{E_f}{2}\left(\frac{1}{\alpha_1^2} + \frac{1}{\alpha_2^2}\right) \\ \sigma_s &= G_c\frac{S_{1m}(a_1) + S_{2m}(a_2)}{2\tau_f} + \left\{\left[\frac{E_f}{2}\left(\frac{1}{\alpha_1^2} - \frac{1}{\alpha_2^2}\right) + \frac{S_{1m}(a_1) - S_{2m}(a_2)}{2\tau_f}\right]^2 + \frac{S_{1m}(a_2)\cdot S_{2m}(a_1)}{\tau_f^2}\right\}^{1/2} \end{aligned}\right\} \quad \ldots [42]$$

and G_c is substituted for μ.

It is of interest to note that σ_f, given by the first of Equations [42], is nothing but the buckling stress of a uniformly compressed circular cylinder without the core. Therefore it may be concluded that σ_s, given by the second of Equations [42], represents the contribution of shear deformation and the normal stresses of the core. When no core exists, $\sigma_s = 0$ and σ_{cr} reduce to the well-known solution for a thin cylinder (2). It is further of interest to see that, when $a_1, a_2 \to \infty$ as $(a_2 - a_1) \to$ const in the limit, Equation [41] must check the buckling stress of a beam. Similarity exists between the results of reference (3) and Equation [41] in this case. Furthermore, numerical examples for large a_1 and a_2 are in agreement with the experimental results published in references (4) and (5).

Simplification for Large Values of $\alpha_1 = (m\pi a_1)/L$ *and* $\alpha_2 = m\pi a_2/L$. In most practical problems α_1 and α_2 are very large; consequently it is of special interest to consider this case. For large values of x Bessel functions (7), $I_n(x)$ and $K_n(x)$, may be expressed as

$$\left.\begin{aligned} I_n(x) &= (2\pi z\cosh\beta)^{-1/2}\cdot e^{x(\cosh\beta - \beta\sinh\beta)} \\ K_n(x) &= \pi(2\pi z\cosh\beta)^{-1/2}\cdot e^{-x(\cosh\beta - \beta\sinh\beta)} \end{aligned}\right\} \quad \ldots [43]$$

where

$$s = x\sinh\beta \quad \ldots\ldots [44]$$

From Equations [43], $I_0(x)$ and $K_0(x)$ are obtained

$$\left.\begin{aligned} I_0(x) &= (2\pi x)^{-1/2}\, e^x \\ K_0(x) &= \pi(2\pi x)^{-1/2}\cdot e^{-x} \end{aligned}\right\} \quad \ldots\ldots [45]$$

For $I_1(x)$ and $K_1(x)$, β is obtained from Equation [44]. For $x > 10$, $\sinh\beta < 0.1$ and $\cosh < 1.003$. Hence if β is taken as zero, the error in $(\cosh\beta - \beta\sinh\beta)$ and $\cosh\beta$ is less than 1 per cent and 0.3 per cent, respectively, which may be accepted as a good approximation. Thus

$$\left.\begin{aligned} I_1(x) &= (2\pi x)^{-1/2}\cdot e^x \\ K_1(x) &= \pi(2\pi x)^{-1/2}\cdot e^{-x} \end{aligned}\right\} \quad \ldots\ldots [46]$$

for

$$x > 10$$

Substitution of Equations [45] and Equations [46] into the Equations [27] for $\rho = \alpha_1, \alpha_2$ yields

$$\left.\begin{aligned} R_{1m}(\alpha_1) &= \frac{4}{\Delta_1}\sqrt{\frac{\alpha_2}{\alpha_1}}\left(\sinh\tau + \frac{\tau}{\gamma}\cosh\tau\right) \\ R_{1m}(\alpha_2) &= \frac{4}{\Delta_1\alpha_2}\left(\frac{\alpha_2}{2}\sinh 2\tau - \cosh 2\tau + 1 + \alpha_2\frac{\tau}{\gamma} + 2\frac{\tau^2}{\gamma^2}\right) \\ R_{2m}(\alpha_1) &= -\frac{4}{\Delta_1\alpha_1}\left(\frac{\alpha_1}{2}\sinh 2\tau + \cosh 2\tau - 1 + \alpha_1\frac{\tau}{\gamma} - 2\frac{\tau^2}{\gamma^2}\right) \\ R_{2m}(\alpha_2) &= -\frac{4}{\Delta_1}\sqrt{\frac{\alpha_1}{\alpha_2}}\left(\sinh\tau + \frac{\tau}{\gamma}\cosh\tau\right) \\ T_{1m}(\alpha_1) &= \frac{4}{\Delta_1\gamma}\sqrt{\frac{\alpha_2}{\alpha_1}}\,\tau\sinh\tau \\ T_{1m}(\alpha_2) &= 2\mu \\ T_{2m}(\alpha_1) &= 2\mu \\ T_{2m}(\alpha_2) &= \frac{4}{\Delta_1\gamma}\sqrt{\frac{\alpha_1}{\alpha_2}}\,\tau\sinh\tau \end{aligned}\right\} \quad \ldots [47]$$

where

$$\Delta_1 = \cosh 2\tau - 1 - 4\frac{\tau^2}{\gamma^2} \qquad (m = 1, 2, \ldots .)$$

Equations [47] and [33] are more suitable in the calculation of σ_{cr} expressed in Equation [41] as long as $\alpha_1 = m\pi a_1/L$ and $\alpha_2 = m\pi a_2/L$ are greater than 10, which is usually the case. For an airplane fuselage, α_1 and α_2 are even greater than 40. In the numerical examples, Equations [47] are used.

Results and Conclusions

For a given core and face materials, the critical stress, σ_{cr}, is

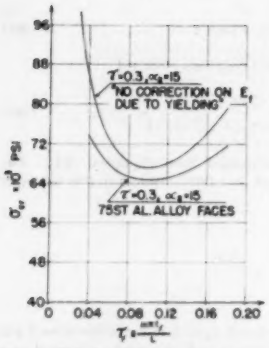

FIG. 3 BUCKLING STRESS OF SANDWICH CYLINDER WITH AND WITHOUT CORRECTION ON E_f FOR 75S-T ALUMINUM-ALLOY FACES
(Core is made of CCA with E_c = 2000 psi.)

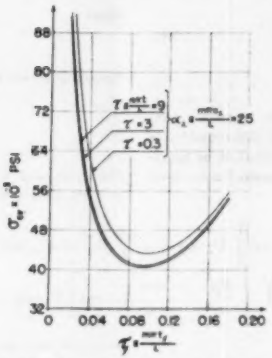

FIG. 4 BUCKLING STRESS OF SANDWICH CYLINDER; ALUMINUM-ALLOY 75S-T FACES WITH E_f = 10.5 × 10⁶ PSI, AND CCA CORE WITH E_c = 2000 PSI
(Use below σ_{cr} = 50,000 psi.)

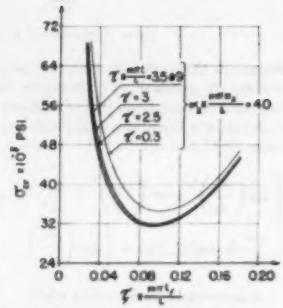

FIG. 5 BUCKLING STRESS OF SANDWICH CYLINDER; ALUMINUM-ALLOY 75S-T FACES WITH E_f = 10.5 × 10⁶ PSI, AND CCA CORE WITH E_c = 2000 PSI
(Use below σ_{cr} = 50,000 psi.)

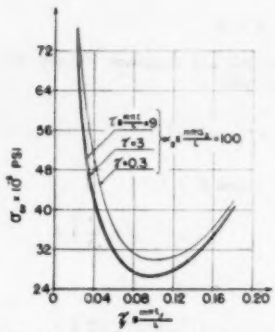

FIG. 6 BUCKLING STRESS OF SANDWICH CYLINDER; ALUMINUM-ALLOY 75S-T FACES WITH E_f = 10.5 × 10⁶ PSI, AND CCA CORE WITH E_c = 2000 PSI
(Use below σ_{cr} = 50,000 psi.)

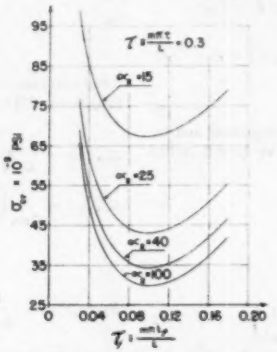

FIG. 7 BUCKLING STRESS OF SANDWICH CYLINDER; ALUMINUM-ALLOY 75S-T FACES AND CCA CORE WITH E_c = 2000 PSI
(Use for $\sigma_{cr} \leq$ 50,000 psi.)

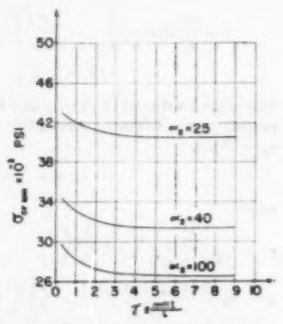

FIG. 8 MINIMUM BUCKLING STRESS OF SANDWICH CYLINDER; ALUMINUM-ALLOY 75S-T FACES AND CCA CORE WITH E_c = 2000 PSI

plotted as a function of the three parameters, α_3, τ, and τ_f, where

$$\alpha_3 = \frac{m\pi a_3}{L}, \quad \tau = \frac{mrl}{L} \quad \text{and} \quad \tau_f = \frac{mrl_f}{L}$$

The sandwich cylinder considered is composed of a core, where E_c = 2000 psi, and G_c = 800 psi, and a face material of either aluminum alloy 75S-T or of aluminum alloy 24S-T Alclad. This core is similar to cellulose-cellulose-acetate. The critical stress differs for the two aluminum alloys only beyond the proportional limit. The von Kármán-Engesser reduced modulus curves, where $E_{red} = 2EE_t/(E + E_t)$, as given in Fig. 16, are used to modify the stresses beyond the proportional limit. All theoretical curves for 24S-T Alclad are modified along with one curve for 75S-T (that is, $\alpha_3 = 15$).

The following four types of curves are plotted:

σ_{cr} versus τ_f, for τ variable, α_3 fixed (Figs. 3 to 6)
σ_{cr} versus τ_f, for τ fixed, α_3 variable (Fig. 7)
$(\sigma_{cr})_{min}$ versus τ, for α_3 variable (Fig. 8)
$(\sigma_{cr})_{min}$ versus α_3, for τ variable (Fig. 9)

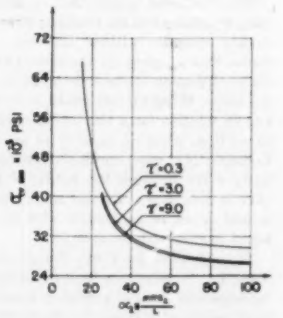

FIG. 9 (*right*) MINIMUM BUCKLING STRESS OF SANDWICH CYLINDER; ALUMINUM-ALLOY 75S-T FACES AND CCA CORE WITH E_c = 2000 PSI

All the values of the critical stress, σ_{cr}, are collected in Table 1. The same type of modified curves are plotted for 24S-T Alclad in Figs. 10 to 15. A trial-and-error procedure is used to modify the curves for critical stresses beyond the proportional limit, Table 2.

TABLE 1 $\sigma_{cr} = F(\alpha_2, \tau, \tau_1)$ PSI FOR ALUMINUM-ALLOY 75S-T FACES (E_f = 10.5 × 10⁶ PSI), AND A CORE WITH E_c = 2000 PSI, AND G_c = 800 PSI

α_2 =	15	Corrected For	25			40					100		
τ_1 τ =	0.3	75-ST	0.3	3	9	0.3	2.5	3	3.5	9	0.3	3	9
0.01	210,968		194,595	166,370	161,092	190,695	163,702	161,528	160,320	159,142	190,943	161,130	158,692
0.02	126,633		105,647	91,882	90,766	99,104	85,686	84,605	84,003	83,416	96,701	81,801	80,566
0.03	98,851		76,363	67,418	66,691	68,940	60,048	59,330	58,930	58,540	65,649	55,725	54,891
0.04	85,343	73,800	62,132	55,220	55,065	54,270	47,640	47,104	46,866	46,514	50,535	43,098	42,465
0.05	77,654		54,032	48,945	48,529	45,907	40,635	40,208	39,971	39,739	41,906	35,962	35,449
0.06	72,962		49,089	44,967	44,630	40,791	36,424	36,069	35,872	35,680	36,612	31,663	31,230
0.07	70,061	66,200	46,089	42,597	42,315	37,607	33,871	33,583	33,412	33,251	33,301	29,663	28,687
0.08	68,344		44,214	41,300	41,061	35,697	32,463	32,200	32,053	31,911	31,299	27,593	27,261
0.09	67,479		43,291	40,779	40,573	34,704	31,845	31,612	31,483	31,353	30,230	26,939	26,639
0.12	68,292	65,197	44,097	42,392	42,253	35,293	33,265	33,098	32,997	32,803	30,748	28,286	28,053
0.18	79,257	71,800	55,611	54,715	54,648	46,752	45,399	45,287	45,225	45,165	41,982	40,347	40,181

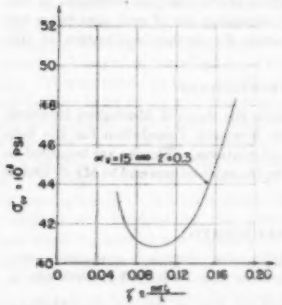

FIG. 10 BUCKLING STRESS OF SANDWICH CYLINDER; ALUMINUM-ALLOY 24S-T ALCLAD FACES WITH E_{red} TAKEN FROM FIG. 16, AND CCA CORE WITH E_c = 2000 PSI

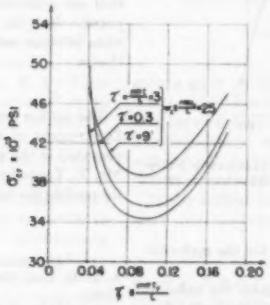

FIG. 11 BUCKLING STRESS OF SANDWICH CYLINDER; ALUMINUM-ALLOY 24S-T ALCLAD FACES WITH E_{red} TAKEN FROM FIG. 16, AND CCA CORE WITH E_c = 2000 PSI

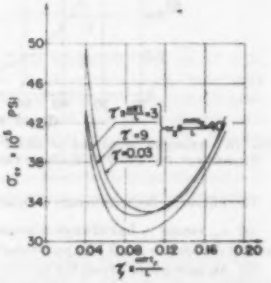

FIG. 12 BUCKLING STRESS OF SANDWICH CYLINDER; ALUMINUM-ALLOY 24S-T ALCLAD FACES WITH E_{red} TAKEN FROM FIG. 16, AND CCA CORE WITH E_c = 2000 PSI

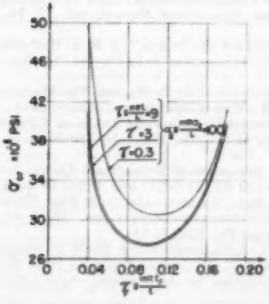

FIG. 13 BUCKLING STRESS OF SANDWICH CYLINDER; ALUMINUM-ALLOY 24S-T ALCLAD FACES WITH E_{red} TAKEN FROM FIG. 16, AND CCA CORE WITH E_c = 2000 PSI

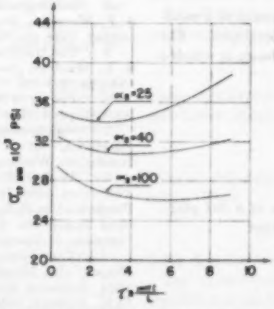

FIG. 14 MINIMUM BUCKLING STRESS OF SANDWICH CYLINDER; ALUMINUM-ALLOY 24S-T ALCLAD FACES AND CCA CORE WITH E_c = 2000 PSI

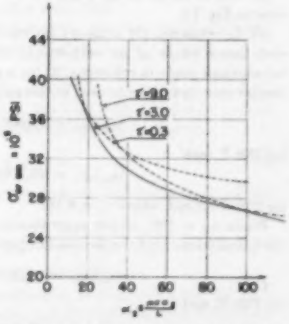

FIG. 15 MINIMUM BUCKLING STRESS OF SANDWICH CYLINDER; ALUMINUM-ALLOY 24S-T ALCLAD FACES AND CCA CORE WITH E_c = 2000 PSI

TABLE 2 $\sigma_{cr} = F(\alpha_2, \tau, \gamma)$ PSI FOR ALUMINUM-ALLOY 24S-T ALCLAD FACES (E_f = 10.5 × 10^6 PSI), AND A CORE WITH E_c = 2000 PSI, AND G_c = 800 PSI
(E_{red} used for correction beyond proportional limit, taken from Fig. 16)

α_2 =	15	25			40			100		
γ = / τ_f	0.3	0.3	3	9	0.3	3	9	0.3	3	9
0.04		49,685	43,720	47,503	49,352	42,706	43,251	49,722	41,858	41,832
0.06	43,661									
0.07		37,174	35,387	39,969	34,851	31,900	33,651	32,985	28,852	28,694
0.08	41,169									
0.12	41,183	36,181	35,156	39,847	33,291	31,941	33,500	30,532	28,097	28,071
0.18	48,360	44,492	43,212	47,281	42,473	41,087	42,078	41,294	39,676	39,617

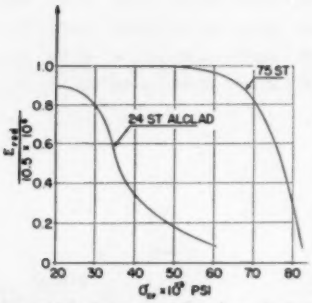

FIG. 16 REDUCED MODULUS OF 24S-T ALCLAD CALCULATED FROM REFERENCE (8) AND 75S-T CALCULATED FROM REFERENCE (9)

The following deductions are of interest:

(*a*) σ_{cr} versus τ_f has always a minimum, and for the materials used it occurs at $\tau_f = 0.10$, approximately.

(*b*) An increase of τ from 0.3 to 3 decreases slightly the value of the minimum critical stress. Further increase of τ does not affect appreciably $(\sigma_{cr})_{min}$ as can be observed in Figs. 8 and 14.

(*c*) $(\sigma_{cr})_{min}$ decreases as α_2 increases; however, after a limit of about $\alpha_2 = 80$, this decrement is slight, as observed in Figs. 7 and 9.

(*d*) For efficient design purposes to choose α_2 and τ, one can refer to Fig. 15.

(*e*) In reference (3) a theory for the buckling stress of a sandwich beam made of an orthotropic core was developed. The calculations made in reference (3) for a sandwich beam in which a similar core material was used in this paper gives

$$(\sigma_{cr})_{min} = 24{,}600 \text{ psi}$$

for 75S-T, and

$$(\sigma_{cr})_{min} = 23{,}700 \text{ psi}$$

for 24S-T Alclad, where $\tau_f = 0.10$.

When $\alpha_2 = 100$, which approximates the case of a flat plate, the calculations made in the present paper reveal that

$$(\sigma_{cr})_{min} = 26{,}200 \text{ psi}$$

for 75S-T, and

$$(\sigma_{cr})_{min} = 26{,}000 \text{ psi}$$

for 24S-T Alclad.

Any further increase in the parameter α_2 affects the minimum critical stress negligibly. The minimum critical stress occurs surprisingly enough at $\tau_f = 0.10$.

The test results published in reference (4) for the buckling of a sandwich beam made of cellulose-cellulose-acetate core and aluminum alloy 24S-T Alclad gives a value of $(\sigma_{cr})_{min}$ = 24,500 psi, when the size of the specimens are converted to τ and τ_f. These results by no means validate all other cases, but at least they are a favorable indication of the analysis presented in this paper. It is our wish that increasing use of such structures will soon produce sufficient interest for further verification of this theory.

ACKNOWLEDGMENT

The author wishes to thank the Applied Mechanics Research Department of the Armour Research Foundation for the help provided in the numerical calculations. Thanks are tendered to Mr. T. Taner for his help in the calculations and to Mr. S. Dokos for reading the manuscript.

BIBLIOGRAPHY

1 "A Treatise on the Mathematical Theory of Elasticity," by A. E. H. Love, Dover Publication, New York, N. Y., fourth edition, 1944.

2 "Theory of Elastic Stability," by S. Timoshenko, McGraw-Hill Book Company, Inc., New York, N. Y., and London, England, 1936.

3 "Solution of the Two-Dimensional Mixed-Mixed Boundary Value Problem of Elasticity for Rectangular, Orthotropic Media and Application to the Buckling of Sandwich Beams," by A. Cemal Eringen (thesis for PhD in Applied Mechanics, Polytechnic Institute of Brooklyn, N. Y., 1948).

4 "Bending and Buckling of Sandwich Beams," by N. J. Hoff and S. E. Mautner, *Journal of the Aeronautical Sciences*, vol. 15, December, 1948, pp. 707–720.

5 "The Buckling of Sandwich Type Panels," by N. J. Hoff and S. E. Mautner, *Journal of the Aeronautical Sciences*, vol. 12, July, 1945, pp. 285–297.

6 "Theory of Bessel Functions," by G. N. Watson, The Macmillan Company, New York, N. Y. (Cambridge), second edition, 1944.

7 "Smithsonian Mathematical Formulae and Tables of Elliptic Functions," by E. P. Adams and R. L. Hippesley, Smithsonian Institution, Washington, D. C., 1947.

8 "Typical Tensile and Compressive Stress-Strain Curves for Aluminum Alloy 24-ST, Alclad 24-ST, 24 S-RT, and Alclad 24 S-RT Products," by R. L. Templin, E. C. Hartman, and D. A. Paul, Technical Paper No. 6, Aluminum Research Laboratories, Aluminum Company of America, Pittsburgh, Pa., 1942, p. 15.

9 "The Column Strength of Aluminum Alloy 75-ST Extruded Shapes," by Marshal Holt and T. R. Leary, Technical Note No. 1004, National Advisory Committee for Aeronautics, Washington, D. C., January, 1946.

10 "On the Elastic Equilibrium of Circular Cylinders Under Certain Practical Systems of Load," by L. N. G. Filon, Philosophical Transactions of the Royal Society of London, series A, vol. 198, 1902, pp. 147–233.

The Propagation of Longitudinal Waves of Plastic Deformation in a Bar of Material Exhibiting a Strain-Rate Effect[1]

By L. E. MALVERN,[2] PITTSBURGH, PA.

The theory of propagation of longitudinal waves of plastic deformation is extended to apply to materials in which the stress is a function of the instantaneous plastic strain and strain rate. Solutions are given for an idealized flow law and compared with solutions based upon earlier theories which neglect strain-rate effect.

Introduction

THE theory of the propagation of a transient wave of plastic deformation, such as occurs in impact loading beyond the elastic range is of comparatively recent origin. In 1930 L. H. Donnell (1)[3] introduced a nonlinear superposition method for treating the loading wave resulting from longitudinal impact on a bar of material having a nonlinear stress-strain relation. This method has been developed further by M. P. White and LeVan Griffis (2–4), who also considered reflection of waves and the additional deformation which occurs after the impact load is removed. The partial differential equations governing the wave propagation were derived independently by G. I. Taylor (5, 6) in England and Th. von Kármán (7, 8) in America, under the assumption of an invariant stress-strain relation independent of strain rate. Applications and extensions of this theory have been made by several investigators (9–14), and a substantially similar theory was developed independently in Russia (15–17).

A series of longitudinal impact tests performed at the California Institute of Technology (18–22) gave fairly good agreement with the theory, but there were some discrepancies. In particular, it was found that the observed force-time variation at the fixed end of the bar showed a higher stress than the theory predicted, which indicated that stress increments were propagated at a higher wave speed than predicted. It was suggested (19) that these discrepancies might be due to strain-rate effect which was neglected in the theory, since considerable deviation from the static stress-strain relation is to be expected at the high strain rates occurring in deformation under impact. The present report extends the theory to materials in which the stress is a function of the instantaneous strain and strain rate.

Proposed Flow Laws for Tension and Compression

A relation between the nominal tensile stress σ (force per unit initial cross-sectional area), plastic strain ϵ^p (permanent change in length per unit initial length), and plastic strain rate $\dot{\epsilon}^p$ has been proposed (23–26) of the form

$$\sigma = \phi(\epsilon^p, \dot{\epsilon}^p) \qquad [1]$$

H. Deutler (25) found that the logarithmic law

$$\sigma = \sigma_1 + A \ln \frac{\dot{\epsilon}^p}{B}$$

gave a good representation of his tensile-test data for $\dot{\epsilon}^p \geq B$, where σ_1 is the stress for $\dot{\epsilon}^p = B$. The law appeared to be valid whether or not the test was carried out at a constant strain rate. The logarithmic dependence on strain rate had been proposed earlier by P. Ludwik (23) on empirical grounds and L. Prandtl (24) as a result of a physical theory of plastic flow.

If it is desired to compare the stresses with those obtained in a static test, the logarithmic dependence may be put in the form

$$\sigma = f(\epsilon) + a \ln (1 + b\dot{\epsilon}^p)$$

where $\sigma = f(\epsilon)$ is the static stress-strain relation, and the total strain ϵ is the sum of the elastic strain ϵ' and the plastic strain ϵ^p. This equation yields

$$\dot{\epsilon}^p = \{e^{[\sigma - f(\epsilon)]/a} - 1\}/b$$

which suggests the generalization that the plastic strain rate is a function of $\sigma - f(\epsilon)$, the excess of the instantaneous stress over the stress at the same strain in a static test.

The theory to be developed applies, however, to the more general law obtained by solving Equation [1] for $\dot{\epsilon}^p$, namely

$$E_0\dot{\epsilon}^p = g(\sigma, \epsilon)$$

where the Young's modulus E_0 has been introduced for convenience in combining with the elastic strain rate $\dot{\epsilon}'$ given by

$$E_0\dot{\epsilon}' = \dot{\sigma} \qquad [2]$$

(Elastic deformation is assumed to be independent of strain rate.) Then

$$E_0\dot{\epsilon} = \dot{\sigma} + g(\sigma, \epsilon) \qquad [3]$$

is the flow law when plastic deformation occurs.

The static stress-strain relation $\sigma = f(\epsilon)$ is interpreted as a succession of equilibrium states such that plastic flow occurs only when the flow condition

$$\sigma > f(\epsilon) \qquad [4]$$

is satisfied; otherwise the elastic law, Equation [2], applies. The use of this flow condition implies that if the strain rate during

---

[1] The results presented in this paper were obtained in the course of research conducted at Brown University under contract N7onr-385 sponsored jointly by the Office of Naval Research and the Bureau of Ships, and are part of a thesis submitted in partial fulfillment of the requirements for the degree of Doctor of Philosophy at Brown University, October, 1949.

[2] Assistant Professor of Mathematics, Carnegie Institute of Technology.

[3] Numbers in parentheses refer to the Bibliography at the end of the paper.

Contributed by the Applied Mechanics Division and presented at the Annual Meeting, New York, N. Y., November 26–December 1, 1950, of The American Society of Mechanical Engineers.

Discussion of this paper should be addressed to the Secretary, ASME, 29 West 39th Street, New York, N. Y., and will be accepted until July 10, 1951, for publication at a later date. Discussion received after the closing date will be returned.

Note: Statements and opinions advanced in papers are to be understood as individual expressions of their authors and not those of the Society. Manuscript received by the Applied Mechanics Division, May 31, 1950. Paper No. 50—A-18.

the test is finally reduced to zero so that a state of equilibrium under load is reached, the equilibrium point will lie on the static stress-strain curve. Thus the amount of strengthening obtained is independent of the strain-rate history up to the equilibrium point. This is probably not strictly true, although the experimental results of Deutler (25) appeared to agree with this hypothesis.

The elastic law also applies until the initial yield is reached. The initial yield strain ϵ_y and yield stress $\sigma_y = E_0\epsilon_y$ have been considered as constant for all finite strain rates in the applications that have been made of the present theory. Several experimental investigators have reported cases in which yield stress is increased for tests at high rates of strain, the percentage increase in yield stress being generally greater than that of the stresses at larger strains.[4]

By a suitable choice of function $g(\sigma, \dot{\epsilon})$, however, the stress-strain curves for various strain rates can be made to approximate the elastic line for any desired range of strain above ϵ_y so that an apparent increase in yield stress is produced. This formulation implies that the material is brought to a state of incipient plastic flow after a given amount of elastic strain, independent of the elastic strain rate, but that the plastic flow requires time in which to become appreciable so that the additional strain beyond ϵ_y is at first mainly elastic. If an instantaneous load application is assumed in an impact problem, an elastic shock wave travels along the bar, and it is consistent with the foregoing remarks to assume that in such a shock wave the elastic law applies even above the ordinary yield strain, since time is required for plastic flow to occur. It is recognized that the elastic shock wave is an idealization since the load application is not in fact instantaneous, although it is extremely rapid.

This proposed flow law in its general form applies either to tensile or compressive impact provided that compressive stress and strain are reckoned positive in the case of compressive impact. The static nominal stress-strain relation will differ for the two cases.

The law, Equation [3], applies at each section of the bar, but it cannot be applied to the bar as a whole since the stress, strain, and strain rate are not uniform along the bar under conditions of impact loading. It is necessary to consider the propagation of the wave of plastic deformation in order to interpret the impact behavior. V. V. Sokolovsky (28) has previously treated wave propagation for a special case of the law, Equation [3], an elastic-viscous-plastic material without work-hardening in which $g(\sigma - \sigma_y)$ is a function only of $\sigma - \sigma_y$, the excess of the instantaneous stress over the initial yield stress.

Equations Governing Wave Propagation

The propagation of a longitudinal wave of plastic deformation in a bar of material obeying the law, Equation [3], is governed by the following system of three first-order partial differential equations

$$\left.\begin{aligned} \frac{\partial \sigma}{\partial x} &= \rho \frac{\partial v}{\partial t} \\ \frac{\partial \epsilon}{\partial t} &= \frac{\partial v}{\partial x} \\ E_0 \frac{\partial \epsilon}{\partial t} &= \frac{\partial \sigma}{\partial t} + g(\sigma, \epsilon) \end{aligned}\right\} \quad \ldots\ldots\ldots\ldots [5]$$

in which x is the initial distance from the impact end of the bar to the cross section, v is particle velocity (assumed constant over each cross section), and ρ is the initial density. The first equation is the longitudinal equation of motion of an element of the bar; the second is a consequence of the fact that $\epsilon = \partial u/\partial x$ and $v = \partial u/\partial t$, where $u(x, t)$ is the displacement at time t of the cross section which was initially at distance x from the impact end of the bar. The third equation is the law, Equation [3].

Illustrative Solutions

The results of numerical integration of the system of Equations [5] will be compared with solutions based on the earlier theory which neglected strain-rate effect (11). For this purpose an idealized form of the law, Equation [3], was used in which $g(\sigma, \dot{\epsilon}) = k[\sigma - f(\epsilon)]$, where k is a multiplicative constant. In this case the plastic strain rate is proportional to $\sigma - f(\epsilon)$, the excess of stress over the stress at the same strain in a static test. The law, Equation [3], then becomes

$$E_0\dot{\epsilon} = \dot{\sigma} + k[\sigma - f(\epsilon)] \quad \ldots\ldots\ldots\ldots [6]$$

This idealization considerably simplified the computation, as also did the use of an analytic expression for the static plastic stress-strain relation which approximates curves obtained for some hardened-aluminum specimens for strains up to about 0.01 in. per in. The relation used was

$$f(\epsilon) = 20{,}000 - \frac{10}{\epsilon} \quad \ldots\ldots\ldots\ldots [7]$$

with the constants

$$E_0 = 10^7 \text{ psi}$$
$$\sigma_y = 10^4 \text{ psi}$$
$$\rho = 2.5 \times 10^{-4} \text{ lb sec}^2/\text{in.}^4$$

The static stress-strain curve given by Equation [7] is the lower curve in Fig. 1. The other curves in Fig. 1 were computed for various constant strain rates according to Equations [6, 7] to show the effect of strain rate according to this law when propaga-

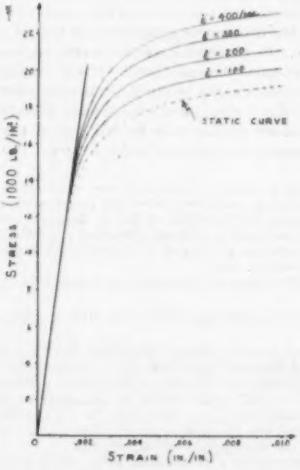

Fig. 1 Stress-Strain Curves at Different Constant Strain Rates According to Equations [6, 7]

[4] See, for example, the paper by Brown and Vincent (27).

tion effects are not considered. The value assumed for the constant k was

$$k = 10^6 \text{ per sec}$$

This value of k gives an increase in stress over the static value of approximately 10 per cent for a strain rate of 200 per sec, which is of the order of magnitude of stress increase at an average strain rate of 200 per sec found by Habib (29) in compression tests on small copper cylinders.

Two cases of impact on a semi-infinite bar were treated with the laws, Equations [6, 7]. In the first case the impact velocity v_0 is supposed applied instantaneously at $x = 0$, while in the second case the applied velocity rises exponentially toward v_0.

Case I. Instantaneous Application of Impact-End Velocity. At time $t = 0$ the end $x = 0$ of a semi-infinite bar lying along the positive x-axis is supposed instantaneously set in motion by a tensile impact with velocity

$$v_0 = -600 \text{ ips}$$

Fig. 2 compares the solution obtained with the solution for the same problem neglecting strain-rate effect. Level curves of strain are plotted in the x, t-plane. The solid curves are for the speed law, Equation [6], while the broken lines are for the solution neglecting strain-rate effect. The broken lines are straight lines emanating from the origin, the wave fronts of constant strain for the simple wave solution.

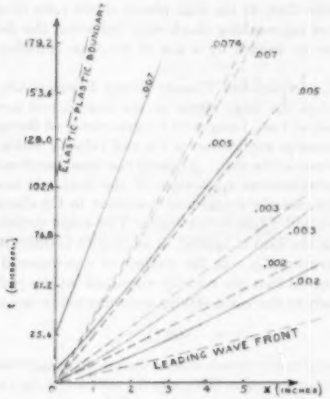

FIG. 2 COMPARISON OF LEVEL LINES OF STRAIN IN THE x, t-PLANE WITH THE SOLUTION NEGLECTING STRAIN-RATE EFFECT (BROKEN LINES)

It is seen from Fig. 2 that the strain-rate effect causes the small strains to be propagated more rapidly at first. As the strain rates become smaller away from the origin, the level lines for the two solutions become approximately parallel, at least for the smaller strains. With the larger strains, however, the situation is reversed; the strain-rate effect retards the propagation. The solution neglecting strain-rate effect gives a constant-state region above the wave front of maximum strain $\epsilon = 0.0074$, while in the solution with strain-rate effect there is no constant-state region. The dot-dash curve marks the boundary of continuous transition from plastic to elastic behavior which occurred near the impact end even when the end velocity was constant according to the solution with strain-rate effect. Along this boundary the static stress-strain relation $\sigma = f(\epsilon)$ holds, while σ and ϵ are not constant, but decrease slowly with increasing x and t. This continuous unloading boundary had to be determined by a trial-and-error procedure. Because of the great amount of time required by this procedure, the solution was not carried out very far into the field.

According to the simple-wave solution, the stress and strain are constant along the leading wave front $x = c_0 t$ ($c_0 = \sqrt{E_0/\rho}$ is the speed of propagation of longitudinal elastic waves in the bar). The solution with strain-rate effect, however, gives a higher stress near the impact end, since the elastic law is assumed to apply even above σ_y for the shock wave. It was possible to integrate the equations along the leading wave front to get a transcendental equation for the stress, namely

$$t = \frac{2}{k}\left[\frac{10{,}000}{\sigma - 10{,}000} - \frac{1}{2} + \ln\frac{20{,}000}{\sigma - 10{,}000}\right] \quad \ldots\ldots [8]$$

The stress just after the passage of the leading wave front as given by this equation is plotted versus x in Fig. 3. It is seen that the stress jumps instantaneously to 30,000 psi, the value for a completely elastic impact, but rapidly falls to very nearly the yield stress of 10,000 psi as the wave propagates and plastic strain develops. According to the solution neglecting strain-rate effect, the stress would be 10,000 psi all along the leading wave front.

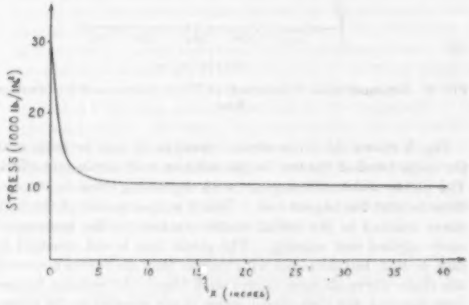

FIG. 3 LEADING WAVE-FRONT STRESS

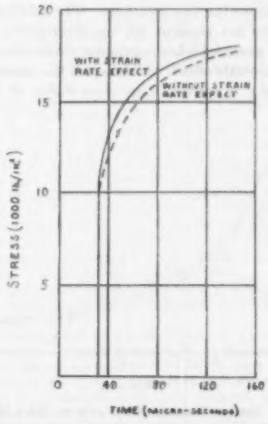

FIG. 4 STRESS-TIME VARIATION AT $x = 6.4$ IN.

Fig. 4 compares the stress-time variation at $x = 6.4$ in. for the two solutions. The stress at each instant is higher for the solution with strain-rate effect. This shows that even with the idealized speed law, the strain-rate effect can account for the discrepancy observed in the stress-time variation at the fixed end of impact specimens.

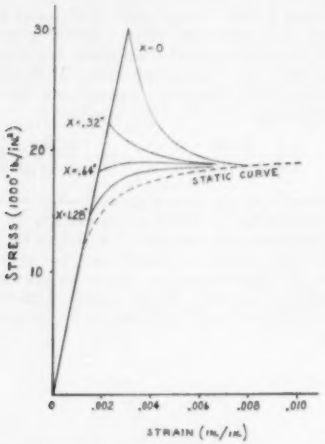

FIG. 5 STRESS-STRAIN VARIATION AT FOUR SECTIONS NEAR IMPACT END

Fig. 5 shows the stress-strain variation at four sections near the impact end of the bar for the solution with strain-rate effect. The plastic deformation occurs with decreasing stress in the sections nearest the impact end. This is a consequence of the high stress reached in the initial elastic reaction to the instantaneously applied end velocity. The strain rate is not constant at each section, but decreases with time so that the curves approach the static curve (broken curve) with time. At sections farther from the end, the high elastic stress is not reached so the stress-strain curves more nearly resemble the static curve.

The strain distribution along the bar at $t = 102.4$ microsec is shown in Fig. 6 for the two solutions. The solution with strain-rate effect does not account for the discrepancy in maximum strain since it gives a higher maximum strain than the solution, neglecting strain-rate effect, which is just the opposite of the correction needed. Moreover, there is no region of uniform strain

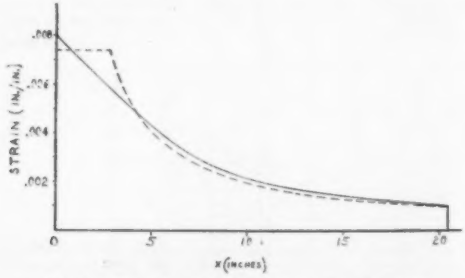

FIG. 6 STRAIN DISTRIBUTION AT $t = 102.4$ MICROSEC
(Broken line is solution neglecting strain-rate effect.)

near the impact end such as was found in constant-velocity tensile-impact tests on aluminum and copper (18, 19).

A more realistic speed law than the linear law, Equation [6], for example, an exponential dependence on $\sigma - f(\epsilon)$, might give more satisfactory results; but it is not likely that any law of the type considered would give a constant-strain region. These laws express a nonlinear viscous behavior so that strain continues to increase until $\sigma = f(\epsilon)$. It may be remarked that a change in the constant k in the present solution merely has the effect of changing the time scale and does not affect the shape of the strain distributions obtained.

Some observed residual-strain distributions after compressive impact on lead specimens (20, 30) did not show a constant-strain region at the higher impact velocities. D. S. Clark (30) characterized the deformation in these cases as a flowing deformation. According to White and Griffis' theory of compressive impact (3), a flowing deformation intermediate between that of a plastic solid and that of a viscous fluid was predicted (30) for lead at much higher impact velocities than those used in the experiments while plastic shock-wave deformation would be expected at the highest velocities used. The shock-wave theory would, however, give a constant-strain region which was not observed. It is thus possible that, at the high plastic strain rates involved in a deformation approaching shock-wave behavior, the deformation of lead can be treated by a law of the type considered in this report.

Case II. Impact-End Velocity Rising Exponentially. It was believed that the large strain at the impact end according to the solution of Case I might be a consequence of the assumption of instantaneous application of the end velocity which produced the high stress at the end. A second case was therefore computed for noninstantaneous application of the load. It was thought that in this case the continuous transition to the elastic state at the impact end might be avoided. The exact variation of end velocity as the load is applied in an impact is difficult to determine experimentally. In the absence of experimental evidence, it was assumed that the velocity magnitude at the end increased continuously to the value 600 ips according to the exponential law

$$v = -600\,(1 - e^{-\alpha t}) \qquad [9]$$

The constant α was chosen so that the velocity magnitude reached 90 per cent of the value 600 ips in 0.1 millisec as shown in Fig. 7.

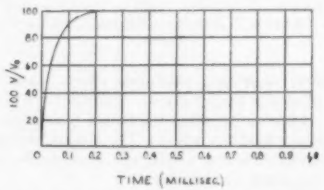

FIG. 7 EXPONENTIAL RISE OF VELOCITY AT IMPACT END

This variation of end velocity was suggested in a report of the California Institute of Technology experimental work (18).

When the velocity rises in this manner, there is no initial elastic shock wave. The boundary values $\sigma = \epsilon = v = 0$ apply along the leading elastic wave front $x = c_0 t$. Plastic yielding occurs when the end velocity reaches the value $-c_0\epsilon_y = -200$ ips which occurs at $t = 17.61 \times 10^{-4}$ sec. Fig. 8 compares the level curves of strain in this case for an impact lasting 0.3 millisec with those obtained for the same type of loading neglecting strain-rate effect. It is seen that the two solutions give more nearly the same level curves of strain in this case. The region between

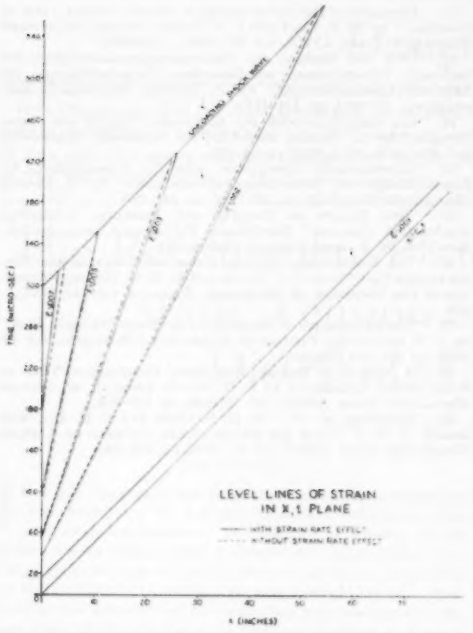

FIG. 8 COMPARISON OF SOLUTION FOR EXPONENTIAL RISE OF END VELOCITY WITH SOLUTION NEGLECTING STRAIN-RATE EFFECT

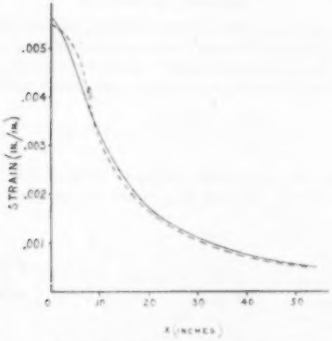

FIG. 9 RESIDUAL-STRAIN DISTRIBUTION AFTER UNLOADING, FOLLOWING IMPACT WITH EXPONENTIAL RISE OF END VELOCITY (Broken curve neglects strain-rate effect.)

the line $x = c_0 t$ and the line marked $\epsilon = 0.001$ is an elastic loading region. That above the line marked unloading shock wave is the elastic unloading region, assuming instantaneous release of the applied load at $t = 0.3$ millisec. In the case reported, the unloading shock wave was not absorbed, so the residual strain for the bar could be computed in so far as desired by using the shock conditions.

Fig. 9 shows the residual-strain distribution after unloading, following the 0.3-millisec impact. The broken curve is for the solution neglecting strain-rate effect. Thus the two solutions give close agreement for this assumed loading, which gave a maximum strain rate of about 65 per sec at the impact end. A greater difference would be obtained for more rapid application of end velocity giving higher strain rates, or if a smaller value of k were used implying a more pronounced strain-rate dependence. Changing the value of k in this case does not merely change the time scale because the applied end velocity is not independent of time. The strain at the impact end is again higher than for the solution neglecting strain-rate effect although by a smaller amount than in Case I. Neither solution shows a constant-strain region because the end velocity was not constant. For an impact of longer duration, the solution neglecting strain-rate effect would show an approximately constant strain region because the velocity rise is substantially completed in 0.3 millisec, as seen in Fig. 7. The solution was not carried out for a longer impact duration because a continuous transition from plastic to elastic state began at the impact end at about $t = 0.32$ millisec even for this type of loading, and it was already evident that the type of strain-rate effect considered would not account for the discrepancy in the maximum strain between experiment and the theory neglecting strain-rate effect.

CONCLUSIONS

It is concluded that an assumed flow law, according to which the stress is a function of the instantaneous strain and strain rate, can account for discrepancies observed in the stress-time variation at the fixed end of impact specimens. The strain-rate effect causes the stress increments to be propagated at a higher wave speed than was predicted by the theory based on the static stress-strain relation. This type of flow law does not, however, account for the discrepancy observed in the magnitude of the maximum strain. Moreover, this type of law fails to predict a uniform strain region near the impact end of constant-velocity impact specimens, such as has been observed in tests with copper and aluminum, although it may be possible to use such a law to account for the impact behavior of lead at the higher velocities where no uniform strain region was observed.

BIBLIOGRAPHY

1 "Longitudinal Wave Transmission and Impact," by L. H. Donnell, Trans. ASME, vol. 52, 1930, pp. 153–167.

2 "The Permanent Strain in a Uniform Bar Due to Longitudinal Impact," by M. P. White and LeVan Griffis, JOURNAL OF APPLIED MECHANICS, Trans. ASME, vol. 69, 1947, pp. 337–343.

3 "The Propagation of Plasticity in Uniaxial Compression," by M. P. White and LeVan Griffis, JOURNAL OF APPLIED MECHANICS, Trans. ASME, vol. 70, 1948, pp. 256–260.

4 "On the Impact Behaviour of a Material With a Yield Point," by M. P. White, JOURNAL OF APPLIED MECHANICS, Trans. ASME, vol. 71, 1949, pp. 39–52.

5 "Propagation of Earth Waves From an Explosion," by G. I Taylor, British Official Report RC 70, 1940.

6 "The Plastic Wave in a Wire Extended by an Impact Load," by G. I. Taylor, British Official Report RC 329, 1942.

7 "On the Propagation of Plastic Deformation in Solids," by Th. von Kármán, NDRC Report No. A-29 (OSRD No. 365), 1942.

8 "The Propagation of Plastic Deformation in Solids," by Th. von Kármán and P. Duwez, presented at the Sixth International Congress for Applied Mechanics, Paris, France, 1946.

9 "Addendum to von Kármán's Theory of the Propagation of Plastic Deformation in Solids," by C. Zener and J. H. Hollomon, NDRC Memo. A-37M (OSRD No. 659), 1942.

10 "A Note on von Kármán's Theory of the Propagation of Plastic Deformation in Solids," by H. F. Bohnenblust, NDRC Memo. A-41M (OSRD No. 664), 1942.

11 "The Propagation of Plastic Waves in Tension Specimens of Finite Length," by Th. von Kármán, H. F. Bohnenblust, and D. H. Hyers, NDRC Report No. A-103 (OSRD No. 946), 1942.

12 "Graphical Solutions for Problems of Strain Propagation in Tension," by H. F. Bohnenblust, J. V. Charyk, and D. H. Hyers, NDRC Report No. A-131 (OSRD No. 1204), 1943.

13 "Plastic Waves in Compression, Including the Stopping

Process for a Cylindrical Slug Striking a Rigid Plate," by E. H. Lee, British Official Report, A.P.P. Coordinating Subcommittee Paper No. 57, 1943.

14 "The Behavior of Longitudinal Stress Waves Near Discontinuities in Bars of Plastic Material," by Le Van Griffis, NDRC Report No. A-212 (OSRD No. 1799), 1943.

15 "Propagation of a Wave of Unloading," by K. A. Rakhmatulin, *Prikladnaia Matematika i Mekhanika*, vol. 9, 1945, pp. 91–100 (Russian).

16 "Longitudinal Oscillations of Bars," by G. S. Shapiro, *Prikladnaia Matematika i Mekhanika*, vol. 10, 1946, pp. 597–616 (Russian).

17 "On the Propagation of Plane Elastic-Plastic Waves," by K. A. Rakhmatulin and G. S. Shapiro, *Prikladnaia Matematika i Mekhanika*, vol. 12, 1948, pp. 369–374 (Russian).

18 "The Propagation of Plastic Strain in Tension," by P. E. Duwez, D. S. Wood, and D. S. Clark, NDRC Report No. A-99, (OSRD No. 931), 1942.

19 "The Effect of Stopped Impact and Reflection on the Propagation of Plastic Strain in Tension," by P. E. Duwez, D. S. Wood, D. S. Clark, and J. V. Charyk, NDRC Report no. A-108 (OSRD No. 988), 1942.

20 "The Propagation of Plastic Strain in Compression," by P. E. Duwez, D. S. Clark, and H. E. Martens, NDRC Report No. M302 (OSRD No. 3886), 1944.

21 "An Experimental Study of the Propagation of Plastic Deformation Under Conditions of Longitudinal Impact," by P. E. Duwez and D. S. Clark, Proceedings of the American Society for Testing Materials, vol. 47, 1947, pp. 502–532.

22 "Discussion of the Forces Acting in Tension Impact Tests of Materials," by D. S. Clark and P. E. Duwez, JOURNAL OF APPLIED MECHANICS, Trans. ASME, vol. 70, 1948, pp. 243–247.

23 "Über den Einfluss der Deformationsgeschwindigkeit bei bleibenden Deformationen mit besonderer Berucksichtigung der Nachwirkungserscheinungen," by P. Ludwik, *Physikalische Zeitschrift*, vol. 10, 1909, pp. 411–417.

24 "Ein Gedankenmodell zur kinetischen Theorie der festen Koerper," by L. Prandtl, *Zeitschrift für angewandte Mathematik und Mechanik*, vol. 8, 1928, pp. 85–106.

25 "Experimentelle Untersuchen ueber die Abhaengigkeit, der Zugspannungen von Verformungsgeschwindigkeit," by H. Deutler *Physikalische Zeitschrift*, vol. 33, 1932, pp. 247–296.

26 "First Report on Viscosity and Plasticity, Amsterdam Academy of Sciences," Nordemann Publishing Company, Inc., New York, N. Y., second edition, 1939, p. 181.

27 "The Relationship Between Stress and Strain in the Tensile Impact Test," by A. F. C. Brown and N. D. G. Vincent, Proceedings of The Institution of Mechanical Engineers, vol. 145, 1941, p. 126.

28 "The Propagation of Elastic-Viscous-Plastic Waves in Bars," by V. V. Sokolovsky, *Prikladnaia Matematika i Mekhanika*, vol. 12, 1948, pp. 261–280 (Russian).

29 "A Method of Making High-Speed Compression Tests on Small Copper Cylinders," by E. T. Habib, JOURNAL OF APPLIED MECHANICS, Trans. ASME, vol. 70,1948, pp. 248–255.

30 "Discussion of (3)," by D. S. Clark and E. H. Lee, with closure by M. P. White and LeVan Griffis, JOURNAL OF APPLIED MECHANICS, Trans. ASME, vol. 71, 1949, pp. 219–221.

Design Data

It is important that the data contained in technical papers be made readily available to designing engineers. In order to satisfy these needs of industry, this section of the Journal includes a concise presentation of data and information drawn chiefly from papers previously published by the Applied Mechanics Division of The American Society of Mechanical Engineers.

The Rectangular Plate Subjected to Hydrostatic Tension and to Uniformly Distributed Lateral Load

By R. F. MORSE[1] and H. D. CONWAY[2]

Introduction

In a previous paper,[3] the distribution of deflection and stress was determined for a simply supported rectangular plate subjected simultaneously to uniformly distributed lateral loading and to either tensile or compressive forces acting on a pair of opposite edges and in the plane of the plate. Graphs for the central deflection and moments were presented in this paper. Precisely the same method of solution has now been used for the case where all four edges of the plate are subjected to uniform tension. Details of the calculations are omitted and only equations and graphs for the deflections and moments are given.

Analysis of Problem

Fig. 1 indicates the problem which has been analyzed, all edges of the plate being subjected to tensile forces P per unit length acting in the plane of the plate. Using the method and notation of the previous paper[3] and solving the small-deflection equation

$$D\nabla^4\omega = q + P\left(\frac{\partial^2\omega}{\partial x^2} + \frac{\partial^2\omega}{\partial y^2}\right)$$

subject to the specified boundary conditions, the maximum deflection occurs at the center and is given by the equation

$$\omega_{max} = \frac{4q}{\pi D}\sum_{m=1,3,5}^{\infty}\frac{(-1)^{\frac{m-1}{2}}}{m\alpha_m^2\beta_m^2}\left[1 + \frac{\alpha_m^2}{\frac{P}{D}\cosh\frac{\beta_m b}{2}} - \frac{\beta_m^2}{\frac{P}{D}\cosh\frac{\alpha_m b}{2}}\right]$$

where $\alpha_m = m\pi/a$ and $\beta_m^2 = \alpha_m^2 + P/D$. The bending moments per unit length of plate are, with the usual notation

$$M_x = \frac{4q}{\pi}\sum_{m=1,3,5}^{\infty}\frac{1}{m\beta_m^2}\left[1 + \frac{(\alpha_m^2 - \nu\beta_m^2)\cosh\beta_m y}{\frac{P}{D}\cosh\frac{\beta_m b}{2}} - \frac{(1-\nu)\beta_m^2\cosh\alpha_m y}{\frac{P}{D}\cosh\frac{\alpha_m b}{2}}\right]\sin\frac{m\pi x}{a}$$

$$M_y = \frac{4q}{\pi}\sum_{m=1,3,5}^{\infty}\frac{1}{m\beta_m^2}\left[\nu + \frac{(\nu\alpha_m^2 - \beta_m^2)\cosh\beta_m y}{\frac{P}{D}\cosh\frac{\beta_m b}{2}} + \frac{(1-\nu)\beta_m^2\cosh\alpha_m y}{\frac{P}{D}\cosh\frac{\alpha_m b}{2}}\right]\sin\frac{m\pi x}{a}$$

Using the dimensionless factor P/P_E, where $P_E = \pi^2 D/b^2$, the foregoing equations for the deflection and bending moments may be written in the form

$$\omega_{max} = \alpha\frac{qb^4}{Eh^3};\quad M_x = \beta qb^2;\quad M_y = \gamma qb^2$$

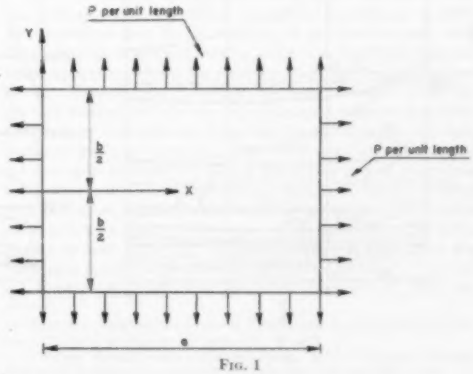

Fig. 1

[1] Delco Appliance Division, General Motors Corporation, Rochester, N. Y. Jun, ASME.

[2] Professor of Mechanics, Cornell University, Ithaca, N. Y. Jun. ASME.

[3] "Bending of Rectangular Plates Subjected to a Uniformly Distributed Lateral Load and to Tensile or Compressive Forces in the Plane of the Plate," by H. D. Conway, Journal of Applied Mechanics, Trans. ASME, vol. 71, 1949, p. A-301.

Note: Statements and opinions advanced in papers are to be understood as individual expressions of their authors and not those of the Society. Manuscript received by the Applied Mechanics Division, Oct. 12, 1950.

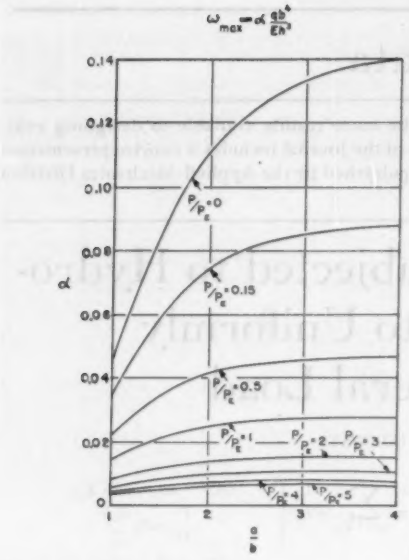

FIG. 2

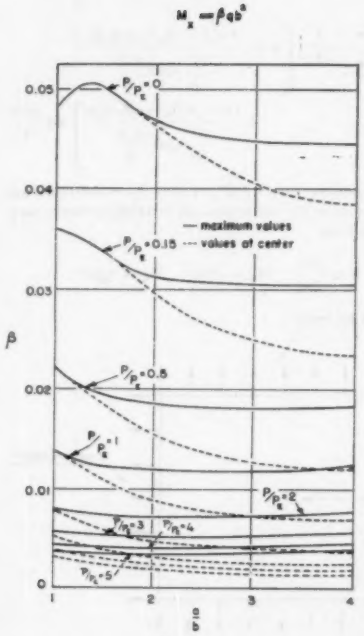

FIG. 3

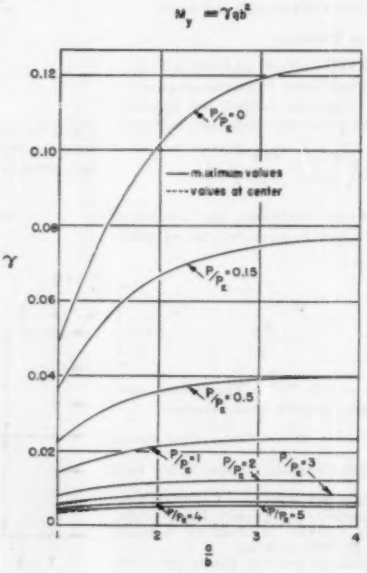

FIG. 4

where the constants α, β, and γ are functions of P/P_E and a/b. The maximum values of α, β, and γ, as well as those occurring at the plate center, are plotted against a/b for various values of P/P_E in Figs. 2, 3, and 4, respectively; the value of Poisson's ratio assumed was 0.3. To obtain the best possible convergence in the summation of the series for the bending moments, use may be made of the summation suggested by Contini[4]

$$\frac{4}{\pi}\sum_{m=1,3,5}^{\infty}\frac{1}{m\beta_m^2}\sin\frac{m\pi x}{a} = \frac{1}{\frac{P}{D}}\left[1 - \frac{\cosh\frac{a}{2}\left(\sqrt{\frac{P}{D}}\left[1-\frac{2x}{a}\right]\right)}{\cosh\frac{a}{2}\sqrt{\frac{P}{D}}}\right]$$

As in the case of loading which is confined to a pair of opposite edges, the maximum deflection always occurs at the center of the plate, but the maximum values of the bending moments M_x and M_y do not. In order to find the maximum values of the factors β and γ, a series of points were chosen along the X-axis in Fig. 1 and the values of the factors computed for these points. Similar traverses were then made in the Y-direction from each of the maximum points on the X-axis.

It was found that the maximum values of β occur along the X-axis and generally move further from the center with increasing a/b ratios. Also, there is a tendency for increasing values of P/P_E to move the location of the maximum value of M_x away from the center. Maximum values of M_y occurred at the center of the plate for all values of P/P_E and a/b investigated with the exception of $a/b = 1$–2 with $P/P_E = 1$–5. The deviations of the maximum values of M_y from the center occur on the line $x = a/2$ in Fig. 1. Decreasing the value of P/P_E and increasing a/b generally decreases the distance that the maximum value of M_y occurs from the center. For the range of P/P_E and a/b investigated, the maximum deviation of $M_{x(\max)}$ from the center of the plate was about 0.45 a, while that of $M_{y(\max)}$ was about 0.30 b.

If the values of $M_{x(\max)}$ and $M_{y(\max)}$ are determined for any specific values of P/P_E and a/b from Figs. 3 and 4, the maximum normal stresses in the X and Y-directions are, respectively

$$\frac{P}{h} + \frac{6M_{x(\max)}}{h^2}$$

and

$$\frac{P}{h} + \frac{6M_{y(\max)}}{h^2}$$

[4] See discussion by Roberto Contini of the paper given in reference (3); this discussion appears in the JOURNAL OF APPLIED MECHANICS, Trans. ASME, vol. 72, 1950, pp. 99–100.

Discussion

Engineering Steels Under Combined Cyclic and Static Stresses[1]

H. Majors, Jr.[2] A careful reading and analysis of this paper reveals a large number of conditions that have been investigated for which the author is to be praised; but it is disturbing, indeed, to find that the results seem to plot better in terms of stresses due to a particular loading system than from a consideration of the state of stress upon a small element. In the final application, one would like to know the effect of the state of cyclic variation of stress and static stresses upon the endurance limit in order to solve any state-of-stress problem.

With this consideration the test data for solid specimens of this fine paper has been replotted and compared with a modified Gerber relation using exponent $n = 2.5$ rather than $n = 2.0$, as indicated in Fig. 1, herewith. Any comments on this method of analysis would be appreciated. If there were one concise method of

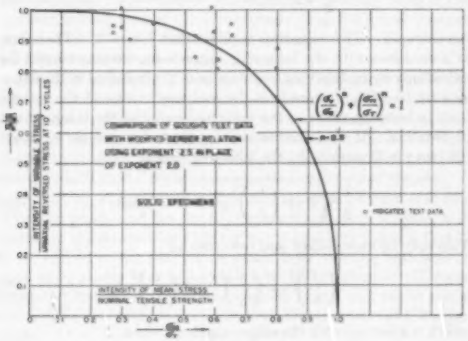

Fig. 1

plotting to summarize the results, it would be of inestimable value for engineering purposes.

The following nomenclature is used in Fig. 1

$$\frac{\sqrt{\sigma_{1a}^2 - \sigma_{1a}\sigma_{2a} + \sigma_{2a}^2}}{\sqrt{2}} = \sigma_a$$

where

σ_a = intensity of amplitude of stress
σ_{1a} = amplitude of maximum principal stress
σ_{2a} = amplitude of minimum principal stress

$$\frac{\sqrt{\sigma_{1m}^2 - \sigma_{1m}\sigma_{2m} + \sigma_{2m}^2}}{\sqrt{2}} = \sigma_m$$

where

σ_m = intensity of mean stress or static stress
σ_{1m} = component of mean stress of the maximum principal stress
σ_{2m} = component of mean stress of the minimum principal stress
σ_e = endurance limit under uniaxial state of stress with zero mean stress. Sometimes called complete reversal of stress in bending
σ_t = nominal tensile strength

Does the author feel that this is bad correlation?

The nominal tensile strength appears low for this steel BS specification S 65A when the other physical properties are considered. Did the author take tensile coupons in different directions?

It would be of interest to discuss the method of calibrating the combined stress-fatigue testing machine especially the dynamic part of the loading system. Were electric resistance wire strain gages used in any manner for calibration purposes?

The shape of the fracture line above the endurance limit is of great interest for the design of machine parts subjected to combined stresses for a limited life. It would be of great interest to see the various plots of nominal stress versus cycles of stressing. Also, it is of great interest to determine the effect of stress concentrations for limited life as compared to 10,000,000 cycles of stressing.

It is realized that one is dealing with nominal stresses, but it is quite disturbing to find in some of the tests where the maximum stress of the cycle was higher than the nominal tensile strength.

Some comments were made about the fractures, but it was not clear if the fractures were typical fatigue fractures or if they were a combination of fatigue fracture and plastic flow.

W. N. Findley.[3] The author is to be congratulated on the quality of his extensive investigation of the effect of combined stress on the fatigue strength of ferrous metals.

In his present and previous writings on combined stress, the author has shown that the ratio of the fatigue strength in banding to that in torsion is not the same for different materials as is required by the rational theories of failure of elastic action. Consequently, he has proposed two empirical expressions, the ellipse quadrant for ductile metals and the ellipse arc for cast irons which avoid this difficulty by including as constants the values of the fatigue strengths in pure bending (b) and in pure torsion (t).

Prof. J. J. Guest[4] objected that the ellipse arc was not new but was derivable from a rational expression he proposed in 1900. The objections seem to the writer to be not well founded since the derivation required collecting terms in a particular way and squaring the two sides of the resulting equation without reference to any physical significance for this manipulation. However, the fact remains that the two equations are related as described, but Professor Guest did not show that the author's test data substantiate the Guest equation. The Guest equation is only one of the two roots obtained by taking the square root of the ellipse arc in the required manner. Actual behavior of the test material may fit the root represented by the Guest equation, it may fit the other root, or it may fit both roots. If the actual behavior is described by both roots then the Guest equation may not be the most basic relation since it is not sufficiently general. If the actual behavior is described by the Guest equation only, then the

[1] By H. J. Gough, published in the June, 1950, issue of the Journal of Applied Mechanics, Trans. ASME, vol. 72, pp. 113–125.

[2] Director, Engineering Experiment Station, University of Alabama. Mem. ASME.

[3] Research Associate Professor of Theoretical and Applied Mechanics, University of Illinois, Urbana, Ill.

[4] "Recent Research on Combined Stress," by J. J. Guest, Proceedings of the Institute of Automobile Engineers, vol. 35, 1940, p. 33.

ellipse arc may be too general, and it would seem best to replace it by the Guest equation.

The ellipse arc is given by

$$\left(\frac{q}{t}\right)^2 + \left(\frac{b}{t} - 1\right)\left(\frac{f}{b}\right)^2 + \left(2 - \frac{b}{t}\right)\frac{f}{b} = 1 \quad [1]$$

using the author's nomenclature. The two roots in question are

$$\text{Guest: } \sqrt{f^2 + 4q^2} + \left(\frac{2t}{b} - 1\right)f = 2t \quad [2]$$

$$\text{The other: } -\sqrt{f^2 + 4q^2} + \left(\frac{2t}{b} - 1\right)f = 2t \quad [3]$$

It is easily shown by substituting into the foregoing equations the data obtained by the author[5] for tests of cast irons that the data satisfy Equations [1] and [2] herewith, equally well but do not satisfy Equation [3]. Hence it would seem that the ellipse arc is too general and the Guest equation should be used instead. Actually, the Guest equation is the easiest to use, especially when expressed in terms of principal stresses, since the equation is linear. In terms of principal stresses $\sigma_1 < \sigma_3 < \sigma_2$ the Guest equation is

$$(\sigma_1 - \sigma_3) + \left(\frac{2t}{b} - 1\right)(\sigma_1 + \sigma_3) = 2t \quad [4]$$

Equation [4] also has the advantage of being applicable to all states of combined stress—not just bending and torsion. Its validity, of course, has yet to be established for many combinations of stress.

From our present knowledge of the structure of metals, it is difficult to account for variations in the ratio b/t between different isotropic metals composed of polycrystalline aggregates. Hence it seems appropriate to consider whether lack of isotropy may be the cause of the observed variations. A striking example of the effect of anisotropy on this ratio is to be found in the author's data on the splined shaft. In this case the anisotropy is caused by external shape and not by structure of the material. However, it seems possible that rolled bars may have internal "shape" characteristics caused by slag or other inclusions, etc., which may produce an effect similar to the anisotropic stress concentration of the splined shaft.

The concept of anisotropic stress concentration may be illustrated by considering the effect of machining a set of parallel grooves on the surface of a flat plate of isotropic material. The grooves would have almost no effect on the stress resulting from bending couples in the planes containing the grooves, but the peak stresses produced by the same bending couples in planes normal to the grooves would be increased. Thus the grooves produce an anisotropic stress concentration, that is, a stress concentration whose properties depend on the direction of stressing.

The writer has been unable to determine the status of the materials tested by the author with respect to isotropy. Since this is an important question in studies of combined stress, it would be most helpful if some data on the isotropy of the subject materials under fatigue conditions could be provided.

If we assume, pending further evidence on isotropy, that variations in b/t are the result of anisotropy, then we cannot discard any of the rational theories of failure because of variations in b/t. Instead, we may attempt to correct for anisotropy. The Guest Equation [4] may be considered to be such an equation since it includes, in addition to the principal stresses at failure of elastic action, the values of b and t. These are introduced in the equation in such a way that the resulting expression is satisfied by the test data for pure bending or pure torsion regardless of the ratio b/t, as is also true of the ellipse arc and quadrant.

It seems reasonable to assume, as a first approximation, that anisotropy in the strength of a material may be similar to the effect of a straight groove in that it may raise the local stress above that predicted by the formulas used for isotropic materials for stresses normal to the direction of the groove but not parallel to it. Then in specimens prepared and tested as described by the author[6] we may expect that anisotropy of the material will raise (or lower) the nominal stress computed from the twisting moment more than (or less than) the stress computed from the bending moment; and that the per cent change in the bending or twisting stresses caused by anisotropy will be independent of the ratio of the bending to twisting moment applied.

With this hypothesis we may then re-examine any of the rational theories of inelastic action (which require specific values of the ratio b/t) by multiplying the nominal twisting stress by a correction constant for each material such that the resulting equation satisfies the conditions for pure bending and pure torsion.

For example, the maximum shear-stress theory may be written in the author's notation as follows

$$\frac{1}{2}\sqrt{f^2 + 4q^2} = \text{const} = t \quad [5]$$

for example. This equation requires that $b/t = 2$. Therefore, in accordance with the foregoing suggestions, we may correct for anisotropy by multiplying every value of q introduced in the equation by $(b_1)/(2t_1)$, where b_1 is the measured value of the fatigue limit in bending, and t_1 is the measured value of the fatigue limit in twisting. If we substitute the adjusted value $q_1 = (b_1 q)/(2t_1)$ for q in Equation [5], the following results

$$\frac{1}{2}\sqrt{f^2 + \left(\frac{b_1}{t_1}\right)^2 q^2} = t = \text{const} \quad [6]$$

This may be rationalized and rewritten as

$$\left(\frac{f}{b_1}\right)^2 + \left(\frac{q}{t_1}\right)^2 = 4\left(\frac{t}{b_1}\right)^2 \quad [7]$$

which is identical with the ellipse quadrant since

$$4\left(\frac{t}{b_1}\right)^2 = 1; \left(t = \frac{b_1}{2t_1}\, t_1\right).$$

Thus the ellipse quadrant may be considered to be a rationalized equation for the maximum shearing stress with a correction for anisotropy. Of course, proof of the effect of anisotropy must be sought before the validity of the foregoing explanation may be demonstrated.

The author's data offer additional evidence on the subject of anisotropy, if we may consider stress raisers as producing stress concentrations of varying degrees of isotropy. As noted previously, the splined shaft is a markedly anisotropic stress raiser. The test data for the splined shaft shown in Fig. 12 of the paper indicate that the test points to the left of C follow closely the ellipse quadrant (or arc) based on the bending b and torsion t fatigue strengths of the splined shaft, which is an anisotropic stress raiser, and do not follow the ellipse quadrant (or arc) based on b and t for the oilhole, which is more nearly an isotropic stress raiser having about the same stress concentration in torsion as the splined shaft. Thus the known anisotropy in stress concentration produces an effect on the fatigue strength under combined

[5] "Properties of Some Materials for Cast Crankshafts, With Special Reference to Combined Stresses," by H. J. Gough and H. V. Pollard, Proceedings of the Institute of Automobile Engineers, vol. 31, 1937, p. 821.

[6] In these tests the direction of rolling had a constant relation to the planes of applied bending and twisting moments.

bending and torsion which is similar to the effect of the assumed anisotropy in the material for which the foregoing correction procedure was suggested.

The fact that the data from most steels tested by the author fitted the ellipse arc when the specimens contained circumferential grooves may be the effect of the pronounced anisotropy of this stress raiser superimposed on the anisotropy of the material. Possibly anisotropy caused by grooves, etc., is of a different nature than that existing in the metal of rolled bars so that a correction equation of the Guest type, Equation [2], (or ellipse arc) is more accurate than the corrected shear Equation [6] herewith.

If this were true, data from tests in which the stress raisers employed were more nearly isotropic should fit the corrected shear equation (or ellipse quadrant) more closely than the data from the grooved specimens. The data of Figs. 10, 11, and 12 of the paper, for the oilhole, small fillet, and splines, respectively, would seem to admit of this interpretation. The anisotropy of each of these stress raisers is substantially less than that of the groove, and the data in each case scatter about or between the curves for the ellipse arc and quadrant instead of the ellipse arc alone.

In many of the tests which the author reported, in which large static stresses were employed in addition to the alternating stresses, the resulting maximum stress must surely have caused considerable yielding with a resulting redistribution of stress in the specimen. For example, the maximum bending stress at the endurance limit for test (3), as reported in Fig. 5(*a*), is 69 tons per square inch whereas the ultimate strength of the material was only 64.8 tons per square inch.

It would be helpful if the author would indicate whether the stresses reported in these instances were corrected for the yielding or are nominal stresses. The actual maximum stress produced in bending or twisting beyond the yield point is less than the nominal stress, so that the actual mean stress may be much less than indicated if the stresses reported are nominal stresses.

If yielding was involved in the tests reported in Figs. 6(*b*) and (*c*) of the paper, and the stresses shown are nominal stresses, correction of the stresses for yielding would probably move points 7, 8, 13, and 14 to the left. This would tend to bring both sets of data more nearly into agreement with an equation of the form suggested by Davis, Nimhanminie and Huitt, and would make the agreement with the equation of Hohenemser and Prager worse.

It may be of interest to mention that tests such as reported in Figs. 5, 6, and 7 of the paper, in which the system of alternating stresses is unlike the system of static stresses superimposed upon it (alternating bending with static torsion, for example) produce a situation in which the state of combined stress changes during the stress cycle.

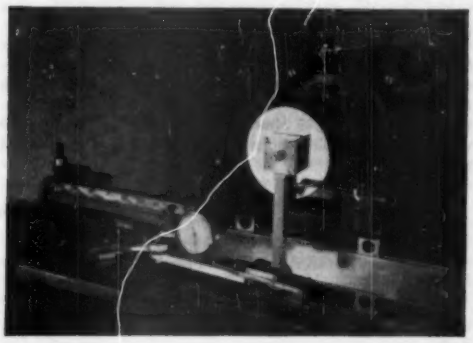

FIG. 2 COMBINED BENDING AND TORSION FATIGUE MACHINE

It may be appropriate at this time to mention that the writer started a somewhat similar investigation in 1942, which is still in progress. A portion of the data is now being prepared for publication.

The writer's investigation included a study of the simultaneous effects of combined bending and torsion (alternating in phase), together with superimposed mean static stresses having the same proportion of bending and torsion as the alternating stresses. (In the author's tests the proportion of bending and torsion in the mean stresses was independent of the proportions in the alternating stresses.) Tests were conducted on a fatigue machine of the constant amplitude-of-deflection type by adding a simple fixture as shown in Fig. 2 of this discussion. The test program included tests of round and grooved specimens at several different combinations of bending and torsion and several values of mean stress on the following materials: Aluminum alloys M68 (now called 76S-T61) and 25S-T; SAE 4340 steel,[7] heat-treated to two hardness values; SAE 1020 steel; and a slightly alloyed inoculated cast iron.

The values of mean stress selected were such as to cause plastic yielding in the specimen tested at the highest mean stress in each combination of bending and torsion. Some of the data from these tests have been analyzed and stresses corrected for the yielding which occurred. While the study is not yet complete, preliminary examination shows that the effect of the mean stress is different for different materials. Present indications are that the fatigue strength (based on the alternating stress) changed very little with increase in mean stress for the 4340 steel and 25S-T aluminum alloy. However, the fatigue strength of M68 aluminum alloy decreased with increase in mean stress.

T. J. DOLAN.[8] The author has presented an exceedingly interesting summary and analysis of important data that are applicable in predicting the behavior of machine components in which biaxial states of repeated stress are encountered. His lucid presentation of this complex subject and correlation of the various states of stress with simple mathematical expressions in the form of ellipse quadrants or ellipse arcs should prove very useful for purposes of machine design.

The unavoidable statistical nature of fatigue-test data makes it impossible to obtain perfect correlations with any simple mathematical relationships, such as the commonly employed "theories of failure" expressing criteria for yielding in members subjected to static loads. In view of the inherent variations in the material which produce scatter in experimental results, the correlations of the combined torsion and bending data with the ellipse segments appear to be well within the limits of experimental error.

Of particular importance are the data indicating that the superposition of a static stress causes only a small amount of reduction in the allowable alternating stress (even though the static stress is high in relation to the ultimate strength of the material). For members containing initial or residual stresses, the effect on the stress history is the same as that of adding a static or mean stress to the alternating stresses imposed by external loads. Some investigators have suggested that any initial stress is directly additive to the stresses produced by external loads and hence produces a marked reduction in fatigue strength as judged by the maximum stress reached in the cycle. However, the data

[7] "The Effect of State of Stress and Range of Stress on Fatigue Strength," by W. N. Findley and B. C. Hanley, First Progress Report to the Office of Naval Research on an Investigation of the Behavior of Materials Under Repeated Stress, University of Illinois, December, 1946, p. B2.

[8] Research Professor of Theoretical and Applied Mechanics, University of Illinois, Urbana, Ill. Mem. ASME.

presented in the paper give further evidence that only a small decrease in fatigue strength should be attributed to a large residual tensile or shear stress (unless the material properties of the steel were altered by the method of inducing the residual stress).

In a paper covering as wide a scope of variables as that under discussion, one hesitates to ask questions regarding the effect of other variables. However, in all engineering materials a certain degree of anisotropy exists due to the methods of forging or rolling and to the presence of segregation, nonmetallic inclusions, etc. Therefore the superposition of different combinations of bending and torsion subject the metal to different orientations of the principal stresses with respect to the direction of minimum strength properties within the bar. Did observations during the test program give any indication of the extent to which anisotropy the material may have affected the relative numerical values of endurance limit as the orientation of the principal stress was altered (by the superposed torsion) from a longitudinal direction to the 45-deg plane?

It would be interesting to have the author comment upon the types of failure observed for these different states of stress. Did the inception and initial propagation of cracks follow any regular pattern with respect to the directions of the principal stresses? More specifically, it would be helpful to know whether the types of fracture give any clue as to the mode of failure, that is, whether they resulted from microscopic displacements of material in shear, in tension, or in some complex combination of these two actions. Was there any evidence that nonmetallic inclusions served as nuclei from which the fatigue fractures initiated? Any comments on these points that the author would care to make in his closure would be greatly appreciated.

JOHN M. LESSELLS.[9] This paper adds considerably to the very scant experimental knowledge previously available on the behavior of steels under combined stress. A considerable part of the known data had already been provided by the same author in a previous paper. The chief and extremely important additions covered by the present paper refer to the effects of discontinuities such as fillets, oilholes, or splines on the fatigue strength under combined stress.

The data given on the effects of superimposing static bending and torsional stress on cyclic stress of either or the same kind should prove of extreme use to designers. The results substantiate, and of course considerably broaden, the conclusions arrived at by Lea[10] regarding the minor effect of superimposing a static torsional stress on a reversed bending stress. Reference to this work was omitted from the author's bibliography.

R. E. PETERSON.[11] This paper must be considered one of the outstanding contributions to the field of fatigue of metals. It is certain that future machine-design textbooks will draw heavily from the results of this paper. The paper consists mainly of a presentation of extensive data and is, therefore, not a particularly controversial one. The writer has made use of some of the data, and it may be of interest to summarize the results briefly.

If we consider geometrically similar notches, the theoretical "stress-concentration factor" is, of course, the same, regardless of absolute size. However, if we make fatigue tests, of geometrically similar notched members, we find that the notch effect decreases as the notch radius is made smaller. This "size-effect" problem has not yet been solved in a fundamental manner. In the meantime, we have been using a method for design purposes which may be of interest and which can be compared with data contained in the present paper.

We define the "fatigue notch factor" K_f as the endurance limit of the unnotched specimen divided by the endurance limit of the notched specimen. We also define the notch sensitivity q, as $(K_f - 1)/(K_t' - 1)$ where K_t' = theoretical factor.[12] This gives us a notch-sensitivity scale from zero (when $K_f = 1$, no notch effect) to 1.0 (when $K_f = K_t'$, full theoretical effect). Plots of q versus notch radius r, tend to give, for any specific material, a band of values which can be represented by an average curve.[13]

If we plot data from the present paper we obtain the results shown in Fig. 3 of this discussion. It is too much to expect that

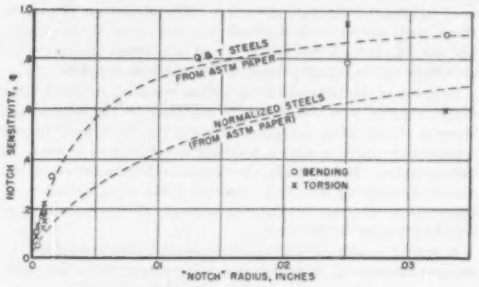

FIG. 3 q-VALUES FOR TEST BARS WITH GROOVES, HOLES, SHOULDER FILLETS
(Based on Gough data—heat-treated alloy steels.)

anything but rough agreement could be obtained with the previously published curves.[13] The main point of interest is that the small notches show a small effect, which is a result which would be predicted from the afore-mentioned q-curves.

A word of caution is in order. Note that we have been discussing geometrically similar notches. It should not be concluded that a smaller r by itself results in an increased fatigue strength. If, for example, we consider a shaft with constant minimum and maximum diameters and connect these with a shoulder step having a fillet radius r, then decreasing this radius results in a continually decreasing fatigue strength. In this case we are departing from geometrical similarity. The present discussion applies to such cases as a small transverse hole and semicircular or other grooves of fixed ratio of notch depth to notch radius.

The author's excellent data will be useful in many ways, apart from their obvious application to design. To those of us interested in the mechanics of materials, it is a source of satisfaction that the author chose this subject for his Presidential Address before The Institution of Mechanical Engineers, and that he was willing to present and have published a summary of this work in this country.

CORRECTIONS

The following additions and corrections should be made in the text of the paper:

[9] Associate Professor of Mechanical Engineering, Massachusetts Institute of Technology, Cambridge, Mass. Mem. ASME.

[10] "Combined Torsional and Repeated Bending Stresses," by F. C. Lea and H. P. Budgen, *Engineering*, vol. 122, 1926, p. 242.

[11] Manager, Mechanics Department, Westinghouse Research Laboratories, East Pittsburgh, Pa.

[12] Discussion of paper by R. E. Peterson and A. M. Wahl, JOURNAL OF APPLIED MECHANICS, Trans. ASME, vol. 58, 1936, p. A-146.

[13] "Relation Between Life Testing and Conventional Test of Materials," by R. E. Peterson, ASTM Bulletin No. 133, March, 1945, pp. 9–16.

1 Footnote to first column of page 115 with asterisk after word "determinations."

* These classifications are as follows:

D = fatigue limit definitely indicated
LD = fatigue limit less definitely indicated
I = fatigue limit indefinitely indicated

2 Footnote to first column of page 119 with asterisk after word "arc" line 3, paragraph 5.

* The general form of ellipse arc is expressed by

$$\frac{\sigma^2}{b^2} + \frac{\tau^2}{b^2}\left(\frac{b}{f} - 1\right) + \frac{\tau}{b}\left(2 - \frac{b}{f}\right) = 1$$

$\doteq b$ = fatigue limit under reversed plane bending stresses only
$\doteq f$ = fatigue limit under reversed shearing stresses only

3 Page 122, paragraph 3, line 4, should read as follows: "under reversed torsional stresses, a marked reduction in strength should occur. Somewhere between $\theta = 0$ deg and $\theta = 90$ deg, therefore, a marked change, of a discontinuous nature, ...

4 Page 125, Reference 11.

"Photoelasticity," by M. M. Frocht, John Wiley & Sons, Inc., New York, N. Y., 1948.

Author's Closure

It is most gratifying that this paper should have prompted such helpful and thought-provoking contributions as discussion; some of these are in themselves original contributions to our knowledge; all will be studied closely by those interested in the fatigue failure of metals under combined stresses.

The complete paper consisted of two parts of which the second part only is reproduced in the Journal of Applied Mechanics; as the present discussion necessarily involves some knowledge of the contents of the first part, a very brief reference to these may be useful, especially as the majority of the results had not previously been published. The materials investigated included steels of ten chemical compositions, two of which were tested in each of two forms of heat-treatment, providing twelve ductile steels, covering a range of tensile strength of from 28 to 108 tons per in.^{2}; for contrast, two cast irons were also included, giving a total of fourteen test materials. Two of the steels were tested in the forms of both solid and hollow specimens. To determine the effect of one form of discontinuity, tests were made on seven of the steels, using solid specimens containing a "sharp" circumferential V-notch. The complete series of fatigue limits under combined fatigue stresses were determined for each material and form of specimen under all combinations of *reversed* bending and *reversed* torsional couples between the "end-points" of the fatigue limits under reversed bending stresses and reversed torsional stresses: in all cases reported in part 1 of the paper, the mean stress of each kind of stress cycle was *zero*. Thus two variables only were explored. The results when analyzed led to the primary conclusion that, within the limits of the investigation: "The resistance to these combined stresses of ductile steels, when tested in the form of solid or hollow cylinders, free from stress-concentration effects, is represented by an 'ellipse quadrant,' as previously defined. On the other hand, the resistance of cast irons, also of ductile steels, when a stress-concentration effect is present, is represented by an 'ellipse arc,' as previously defined." Table 1 lists the test materials, with the experimental end-point values: the tests on grooved specimens are not included.

In the second stage of the research, the results of which form the subject of the present paper, the fatigue resistance of one material only, the S 65A steel, was explored under *four* stress variables, the additional two being static bending and static torsional stresses.

Reverting to the discussion, I will first give the further information asked for.

In reply to Mr. Majors, Jr.: (1) The tensile strength of the material, 65 tons per in.^{2}, is the specification figure; no tensile tests were made in directions other than the longitudinal bar axis. (2) The methods adopted for the calibration of the testing machine enable the two operations involved to be carried out with a high degree of accuracy, much greater than could be expected using strain gages. (*a*) To calibrate the *springs*, the vertical side arms *L*, connecting the cross arm *H*, and the two pairs of springs *E*, are removed. Two 4:1 horizontal levers are placed in position resting on hard steel balls which fit into the lower spherical seatings in which the side arms normally rest: the fulcra of these levers are hard-steel knife-edges which rest against hard-steel flat seatings mounted on the casting *G*; the loading ends of the levers are fitted with knife-edge seatings on which rests a crossbar carrying a scale pan at its midlength. Weights are applied to the scale pan and the deflections of the springs accurately measured using slip gages; a load-deflection calibration diagram is thus obtained. (*b*) For the estimation of the *vertical inertia forces* due to the out-of-balance weights *W*, attached to the revolving disks, all that is really necessary—provided that the machine is correctly tuned—is the accurate measurement of the masses of these weights and the observed speed of the disks. An independent check method is also employed. Using a very stiff calibration specimen, a static load-deflection diagram of the specimen is obtained, again using a horizontal loading-lever arrangement; the recorded deflections are those of a fine crossline engraved on the end of the loading arm *A* observed through a measuring microscope. With the machine again assembled for operation and using each pair of out-of-balance weights, singly and in combination, a load-deflection curve is determined under running conditions, the loads being calculated from the masses of the weights and the disk speeds; as before, the deflections of the engraved crossline are employed. Excellent agreement of the two calibrations was always obtained, to within less than $\doteq 1/2$ of one per cent: this agreement also checks that the machine is indeed correctly tuned and that, as assumed, the damping characteristics of the vibrating system are negligible. Check calibrations on both springs and dynamic loading were regularly made during the test program and showed that the accuracy of the machines was excellently maintained throughout. (3) In regard to the shapes of the *S/N* curves, all the curves are being published in the full report[3] of the research: the total number of such curves is 266, in about 85 per cent of which the data plot fairly regularly, on an $S/\log N$ basis, to give the usual form of diagram and a clearly defined value of the fatigue limit. (4) In regard to the fractures, all were typical fatigue failures. I should add that the machine was closely adjusted so as to shut down automatically when the range of strain of the specimen sensibly increased and, usually, the end of the test thus coincided with the first appearance of fatigue cracks. (5) With the highest value of static bending stress ($34\,1/2$ tons per in.^{2}), the bending fatigue limit was clearly defined at $\doteq 34\,1/2$ tons per in.^{2}, giving the nominal safe range, under repeated bending

TABLE 1

Material (S and H denote solid and hollow specimens, respectively)	Tensile strength, tons per sq in.	Izod value ft lb	Fatigue Limits, Tons per in.^{2} Reversed bending Stresses (A)	Reversed torsional Stresses (B)	Ratio, (A/B)
0.1 per cent C steel (S)	27.9	89	$\doteq 17.4$	$\doteq 9.85$	1.77
0.1 per cent C steel (H)	27.9	89	$\doteq 17.5$	$\doteq 9.15$	1.91
0.4 per cent C steel (S)	42.0	50	$\doteq 21.5$	$\doteq 13.4$	1.60
0.4 per cent C steel (S)	30.9	33	$\doteq 17.8$	$\doteq 10.1$	1.76
0.9 per cent C steel (S)	54.9	$3\,1/2$	$\doteq 22.8$	$\doteq 15.6$	1.46
3 per cent Ni steel (S)	34.1	100	$\doteq 22.2$	$\doteq 13.3$	1.67
$3/3\,1/2$ per cent Ni steel (S)	46.8	86	$\doteq 28.8$	$\doteq 17.3$	1.66
Cr-Va steel (S)	48.7	96	$\doteq 27.8$	$\doteq 16.7$	1.66
$3\,1/2$ per cent Ni Cr steel (S)	58.0	76	$\doteq 35.0$	$\doteq 22.8$	1.54
$3\,1/2$ per cent Ni Cr steel (H)	58.0	76	$\doteq 33.6$	$\doteq 20.5$	1.64
$3\,1/2$ per cent Ni Cr steel (S)	58.1	$5\,1/2$	$\doteq 33.0$	$\doteq 21.0$	1.57
S.65A steel (S)	64.8	90	$\doteq 37.8$	$\doteq 24.0$	1.58
Ni Cr Mo steel (S)	80.5	55	$\doteq 42.8$	$\doteq 22.2$	1.93
Ni Cr steel (S)	108	24	$\doteq 52.5$	$\doteq 29.3$	1.79
"Silal" cast iron	14.9	1/2	$\doteq 15.6$	$\doteq 14.2$	1.10
"Nicrosilal" cast iron	14.2	$1\,1/2$	$\doteq 16.4$	$\doteq 13.7$	1.20

stresses, of 69 tons per in.^{2} although the tensile strength of the steel was 65 tons per in.^{2} only. This value is, of course, a nominal stress, calculated using the simple bending formula; similar results have been reported in the literature for other ductile materials. This point is also referred to by Prof. W. N. Findley, who inquires if the bending and torsional-stress values reported in the paper are nominal stresses or have been corrected for yielding. Nominal stresses only are reported throughout. In fact, it is not clear on what basis of stress redistribution these nominal stress values should be corrected and the publication of Professor Findley's method will be awaited with considerable interest.

In reply to Professor Dolan, no tests were made to determine the degree of anisotropy of the materials tested. With the exception of the cast irons, all the materials were initially in the form of rolled bar and, although these were carefully heat-treated, one would entirely agree with Professor Dolan that some effects due to original forming operations would persist, including possible effects due to segregation, nonmetallic inclusions, etc. But the regularity of the variation in fatigue resistance as the principal stress changes from the direction of the specimen axis to one making 45 deg with that axis does not suggest that this variation can be due, to any appreciable extent, to anisotropy of the material, but is primarily a real stress effect. For this regularity of variation is a feature observed with all the materials tested, whereas the degree of anisotropy present in the various materials would be expected to differ considerably. There was certainly no evidence whatever that nonmetallic inclusions served as nuclei for fatigue cracking. In regard to the plane of initial fracture, the slope of the trace of the earliest cracks on the surface of the specimen was carefully measured and recorded in every case and compared with the stress system. The cast irons *always* fractured on or near the planes of maximum principal stress (or strain): the agreement was remarkable. But with the steels, the directions were, in general, so haphazard that no general correlation with the stress system was possible. These remarks apply to the specimens free from surface discontinuities: where stress concentrations were present, these naturally determined the location and initial paths of the fatigue cracks.

I trust that the foregoing reply supplies the additional information requested in regard to the actual data and observations obtained. The discussion also contributes much helpful thought and speculation on the meaning, interpretation, and general applications of the results, and I welcome this opportunity of joining in the discussion of these broader aspects.

Mr. Major's regret is fully shared that the results of this research do not lead to the conclusion that the fatigue resistance of a metal, under combined static and cyclic bending and torsion, conform to a single criterion which can be stated in terms of the applied stress system only; such a result would have been admirable both from the theoretical and design aspects. But, although I feel that a review of the mass of fatigue data now generally available in the literature suggests that metals and alloys exhibit individual or group characteristics and that general conformity to any single stress criterion is most unlikely, I hasten to add that this research would have been conducted differently had not its primary purpose been to afford guidance to practical design. Solid or thick-walled specimens only have been used, chosen because such are used in engineering practice; as a result, the data afforded relate only to *nominal* stress values, a point repeatedly referred to in the discussion. A closer investigation of the basic problem would certainly have been made if direct stresses (tension or compression) had been used instead of bending stresses and all tests carried out using very thin-walled specimens. Table 1 includes results of tests made on two steels using both hollow and solid specimens; the effect of the specimen form, on the torsional fatigue limits in particular, is evident. But an even greater difficulty arises due to "scale effect" on which subject Mr. Peterson writes with such authority. Much more work must, of course, be carried out in this subject: nevertheless, evidence appears to be accumulating that this effect is real and, moreover, that its extent varies from material to material. If it becomes established that, using identical material and strict conditions of geometrical similarity, the fatigue strength is a function of "size," something more than a knowledge of the applied loading system must clearly be required to evaluate fatigue strength. Having this unsatisfactory situation in mind, I deliberately refrained from putting forward any approximate expression which would correlate the results obtained from the tests on the S 65A steel reported in the paper. For such an expression must be empirical and cannot be of general application: in regard to the latter point, the well-known variations between the M/R relation for different metals and alloys is sufficient evidence. For these reasons, I do not favor the method of plotting adopted by Mr. Majors and illustrated in his Fig. 1; the experimentally determined portions of the M/R curve, under both static bending and torsion, are given in my Figs. 5(a) and 5(b) and these do not conform with a Gerber parabola with any exponent; the same lack of resemblance is evident in my Fig. 6(a), relating to a mild steel under direct stresses. The other major factor which prevents the derivation of any general expression, however approximate, is the variation, from material to material, of the ratio A/B of the values of the simple "end points," shown in the last column of Table 1 of results.

But, however little new information may have been provided in relation to the basic problem, I hope and believe that the results of the investigation will be really helpful to a designer of a metal component subjected to combinations of static and cyclic bending and torsional loadings. From the extensive available literature, he should select or make an approximate estimate of the values of the simple end points and of the M/R relations under simple bending and torsion. With these data and the information provided in the paper and using the appropriate ellipse quadrant or arc (in cases of doubt, conservatively using the arc relation) he should be able to build up the three-dimensional field for his particular material and thus obtain a rational basis of design; he will, naturally, bring in a suitable factor of safety based on his knowledge and experience of the actual working conditions. But, of course, much more work on these lines must be carried out on a variety of engineering materials.

I am indebted to Professor Findley for his most interesting discussion of the ellipse arc and its identity with the Guest equation, when suitably rewritten. I fully agree with this identity, which is acknowledged in part 1 of the paper. The ellipse arc was first put forward, during the present researches, merely as a simple geometrical form which fitted the test results obtained with cast irons and was used as a purely empirical relation; until more is known about the real criterion of failure, it appears wise to continue to regard it as such. Equally interesting are Professor Findley's thoughts and speculations on the possible effect of anisotropy on the f/q relation: I cannot, however, comment usefully on this in the absence of any data on the anisotropy of the materials used. The publication of his own tests on combined bending and torsional stresses will be awaited with great interest. He presents additional evidence of the variation of the shape of the M/R relation for different materials: this supports the view previously expressed that it is unwise to attempt any general expression for fatigue resistance as this must, necessarily, assume some particular form of M/R relation.

Natural Frequencies of Continuous Beams of Uniform Span Length[1]

E. D'APPOLONIA.[2] The authors have developed an interesting graphical representation for the natural frequencies of continuous beams of uniform span length. They have stated that the network may be used as a guide in estimating the frequencies of beams of unequal span length. For certain problems such an estimate is often sufficient; for others a more "exact" solution is required. A method of analysis presented by E. Saibel[3] can be used to obtain this more exact solution. The method is quite general and can be applied to the solution of natural frequencies of beams of varying cross section, span length, and conditions of end restraint. The method is readily applied, and the solution can be carried through to any desired degree of accuracy.

In the method developed by Saibel, the intermediate restraints or supports are removed, leaving what has been called a simple beam; that is, a beam with end supports which are free, pinned, or fixed. The nodes of vibration or eigenfunctions with the corresponding frequencies or eigenvalues of this simple beam are known or can be determined readily. The deflection of the continuous beam is then represented as a generalized Fourier series in terms of the eigenfunctions of the simple beam. The restraints at the intermediate supports are introduced through undetermined multipliers. Then either by means of Lagrange's equations of motion or by minimizing the total potential energy, the frequency equation for the restrained system is obtained. The solution of the frequency equation yields the desired values of natural frequencies.

L. E. GOODMAN[4] AND J. G. SUTHERLAND.[4] The authors have presented a useful compilation of data on the natural frequencies of continuous beams of uniform span length. They list the first twenty-five natural frequencies of such beams, using the classical, Bernoulli-Euler, theory of flexure. In the appendix to the paper it is correctly stated that the effect of rotatory inertia and shear deflection, neglected in the classical analysis, is to reduce the tabulated natural frequencies. To estimate the magnitude of this reduction, when it is small, reference is made in the paper to an adaptation of the well-known formula of Timoshenko[5]

$$f_i/f_{ei} = [1 - n_i^2(r/l)^2(\pi^2/2)(1 + \alpha E/G)]. \quad [1]$$

where, following the notation of the authors

f_i = frequency of ith mode (in cycles per sec) including the corrections for rotatory inertia and shear

f_{ei} = frequency of ith mode as determined by the Bernoulli-Euler flexure theory. This is the f_i of the authors' Equation [1]. It is the frequency which would be obtained by use of Tables 1 to 3 of the paper

n_i = mode number $(1, 2, 3, \ldots)$ of sinusoidal modes

r/l = radius of gyration of beam cross section divided by distance between simple supports

α = shear-deflection coefficient (identical with Timoshenko's $1/k'$)

E/G = ratio of moduli of elasticity in tension and shear $(= 2(1 + \mu))$, where μ represents Poisson's ratio.

It is natural to ask the question: "What is the magnitude of this correction when it is not small, and when may we expect this to be the case?"

This question can be answered, for simply supported beams, by an extension of Timoshenko's theory.[6] Using the symbol ψ to designate the slope of the center line when shearing deformation is neglected and the symbol y to designate the actual center-line deflection, Timoshenko has derived equations of motion of the form

$$\psi_{xx} + (G/E\alpha r^2)(y_x - \psi) = (\rho/E)\psi_{tt} \quad [2a]$$

$$y_{tt} = (G/\rho\alpha)(y_{xx} - \psi_x) \quad [2b]$$

Here $\rho = \gamma/g$ is the mass density of the bar.

These equations, as well as the boundary conditions, are satisfied by solutions of the form

$$y = C \sin(n_i\pi x/l)\cos(2\pi f_i t) \quad [3a]$$

$$\psi = C[(n_i\pi/l) - (4\pi^2 f_i^2)(l/n_i\pi)(\rho\alpha/G)]\cos(n_i\pi x/l)\cos(2\pi f_i t) \quad [3b]$$

provided f_i satisfies the algebraic equation

$$f_i/f_{ei} = (l/n_i r)[B - (B^2 - K)^{1/2}]^{1/2} \quad [4a]$$

where

$$2B = 1/\pi^2 + K[\pi^2 + (l/n_i r)^2] \quad [4b]$$

$$K = (G/\pi^2 E\alpha) \quad [4c]$$

and, of course

$$f_{ei} = (n_i^2\pi/2l^2)(Er^2/\rho)^{1/2} \quad [4d]$$

The expression on the right-hand side of Equation [4a] is the full correction factor for rotatory inertia and shear. Equation [1] is a limiting form of this expression, valid for small $n_i r/l$ (i.e., for waves of long wave length).

The only ambiguity in the foregoing correction factor is the proper choice of the shear-deflection coefficient, α. It is known from the exact solution of the general equations of the linear theory of elasticity[7] that the wave velocity in thin rectangular beams must approach that of Rayleigh surface waves for motions whose wave length is small compared with the radius of gyration. Mindlin has shown how to adjust a similar shear correction coefficient in the case of the vibration of plates.[8] Proceeding in a like manner, introducing the half wave length $\lambda = l/n_i$, the wave velocity $c = 2\lambda/f_i$, and the velocity of shear waves $c_s = (G/\rho)^{1/2}$, we have directly from Equations [4]

$$c/c_s = \pi(E/G)^{1/2}[B - (B^2 - K)^{1/2}]^{1/2} \quad [5]$$

Taking the limit of this expression as the wave length decreases, we have

$$\lim_{\lambda/r \to 0} (c/c_s) = \alpha^{-1/2} \quad [6]$$

---

[1] By R. S. Ayre and L. S. Jacobsen, published in the December, 1950, issue of the JOURNAL OF APPLIED MECHANICS, Trans. ASME, vol. 72, pp. 391–395.

[2] Assistant Professor, Department of Civil Engineering, Carnegie Institute of Technology, Schenley Park, Pittsburgh, Pa.

[3] "Vibration Frequencies of Continuous Beams," by E. Saibel, *Journal of the Aeronautical Sciences*, vol. 11, 1944, p. 88.

[4] Department of Civil Engineering, University of Illinois, Urbana, Ill.

[5] "Vibration Problems in Engineering," by S. Timoshenko, second edition, D. Van Nostrand Company, Inc., New York, N. Y., Equation 150, p. 342.

[6] "On the Correction for Shear of the Differential Equation for Transverse Vibrations of Prismatic Bars," by S. Timoshenko, *Philosophical Magazine*, series 6, vol. 41, 1921, pp. 744–746.

[7] "On the Transverse Vibrations of Bars of Uniform Cross Section," by S. Timoshenko, *Philosophical Magazine*, series 6, vol. 43, 1922, pp. 125–131.

[8] "Influence of Rotatory Inertia and Shear on Flexural Motions of Isotropic, Elastic Plates," by R. D. Mindlin, JOURNAL OF APPLIED MECHANICS, Trans. ASME, vol. 73, 1951, pp. 31–38.

Since the ratio of the velocity of Rayleigh surface waves to the velocity of shear waves is given by the roots of the expression

$$(c_R/c_S)^6 - 8(c_R/c_S)^4 + 8(3 - 2\nu)(c_R/c_S)^2 - 16(1 - \nu) = 0 \quad [7a]$$

where ν is related to Poisson's ratio by the expression

$$\nu = (1 - 2\mu)/2(1 - \mu) \quad [7b]$$

it follows that to secure agreement between the approximate and the exact theories for the higher modes, α must be taken to satisfy the cubic equation

$$16(1 - \nu)\alpha^3 - 8(3 - 2\nu)\alpha^2 + 8\alpha - 1 = 0 \quad [8]$$

In the example given by the authors, E/G was taken at $^8/_3$ or, what is equivalent, Poisson's ratio was taken at $^1/_4$. For this case, the pertinent root of Equation [8], herewith, is $\alpha = 1.1500$. Using this value of α in the correction factor (Equations [4]), Fig. 4 of this discussion has been plotted. This figure is in good agreement with the theory of elasticity over the entire range of

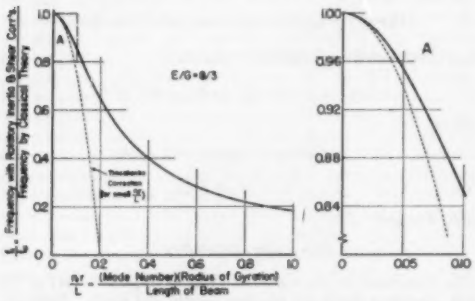

FIG. 1 INFLUENCE OF ROTATORY INERTIA AND SHEAR ON NATURAL FREQUENCIES OF SIMPLY SUPPORTED BEAMS

wave lengths, approaching the exact values at each extreme and differing at intermediate points by a very small per cent. The Timoshenko correction for the lower modes given by Equation [1] is also plotted. It agrees with Equations [4] over a useful range, differing from it by less than 5 per cent when $(n_i r/l)$ is less than about 0.08. In the example quoted by the authors, $d/l = {}^1/_{20}$ or $r/l = 0.0144$. The correction factor for the fundamental mode in this case is 0.995, in agreement with the value obtained from Equation [1]; for modes having $n_i = 2$, it is 0.983 instead of 0.980. On the other hand, referring to Fig. 4, it can be seen that for $n_i = 5$, the correction factor will be 0.910 (instead of 0.872), and for $n_i = 10$ it will be 0.753 (instead of 0.487). For stubbier beams the differences would be more striking.

This correction to the classical theory is probably not of much importance in connection with the vibration of large structural elements. Apart from other obvious considerations, uncertainty as to the precise nature of the restraint exerted by the supports, as well as the influence of damping, may be expected to have a much greater influence on the higher modes. In spite of this, the correction for rotatory inertia and shear is not academic. It is the essence of questions which arise in the design of vibrating elements used to control electronic circuits.[9]

There is another solution of the equations of motion (Equations [2] of this discussion) which is of a form entirely different from that of Equations [3], and which also satisfies the boundary conditions of the problem. This solution corresponds to the thickness-shear mode of vibration. If in Equation [2b] y be taken to vanish identically, $\psi = \psi(t)$, and in this event the quantity ψ has a simple physical interpretation. It is the negative of the angle through which is rotated a small line element situated at the center of the bar and originally perpendicular to the line $y = 0$. Substituting $\psi = \psi(t)$, $y = 0$ in Equation [2a] we have

$$\psi = A \cos [c_s t/r\alpha^{1/2} + \delta] \quad [9]$$

A and δ being constants of integration.

It is known that the exact value of the circular frequency of the thickness-shear mode for thin rectangular bars is $\pi c_s/r \sqrt{12}$. The circular frequency of the motion defined by Equation [9] is $c_s/r\ \alpha^{1/2}$. In order to make the two expressions agree, α must have the value $12/\pi^2 = 1.216$. This value is not (except for a particular value of Poisson's ratio) exactly the same as that given by Equation [8]. Since the two modes of motion coexist, α must be chosen according to the relative importance of the "flexural" and thickness-shear motions. In the case of the paper under discussion this choice is unequivocal.

The type of motion represented by the solution given in Equations [3] and which we have in the previous paragraph termed flexural, in contrast to the thickness-shear mode of motion, actually contains both flexural and shear deflection. If we set the bracketed coefficient of ψ in Equation [3b] equal to zero we have

$$f_s/f_\alpha = \pi\ (l/n_i r)\ \sqrt{K}$$

This expression is asymptotic to the correction curve in Fig. 3 for large values of $n_i r/l$. Since, therefore, $\psi \to 0$ as $n_i r/l \to \infty$, and since ψ represents the slope of the part of the deflection due to pure flexure, it is clear that the frequency of the higher modes is controlled by the shear deflection. Therefore it is not to be expected that the uncorrected Bernoulli-Euler theory, which ignores shear deflection, will give accurate values of the frequencies of the higher modes.

AUTHORS' CLOSURE

The authors wish to express their appreciation for the discussion by Prof. E. D'Appolonia, and particularly for the very comprehensive analysis of the effects of shear distortion and rotatory inertia submitted by Professors Goodman and Sutherland. The contribution made by Goodman and Sutherland extends the usefulness of the paper considerably since their discussion includes not only a lucid analysis of the rotatory inertia and shear distortion correction, but also a complete numerical example (their Fig. 1) in which they compare the exact correction with the approximate correction for small $n_i r/l$. We are in agreement with their statement that the correction for rotatory inertia and shear is not academic.

[9] "Thickness Shear and Flexural Vibrations of Crystal Plates," by R. D. Mindlin, *Journal of Applied Physics*, vol. 22, March, 1951, (to be published).

Momentum and Mass Transfer in Coaxial Gas Jets[1]

M. Z. v. Krzywoblocki.[2] The extensive bibliography given by authors of that very interesting investigation does not cover the recently published papers and notes (undoubtedly it was caused by the fact that the manuscript was sent in 1949), in which the simple cases considered by Bickley, Schlichting, (8, 58, 59) etc., are extended to satisfy the conditions more applicable to physical phenomena occurring in wakes and jets. These conditions are compressibility phenomena in both laminar and turbulent flows, coefficients of viscosity and heat conductivity as functions of temperature (and possibly pressure). The recent considerations include not only equation of motion but also energy equation, thus giving certain possibilities of presenting more precise distributions of all the simple variables like velocity, temperature, density, etc., as well as composite variables like momentum, etc., although the amount of calculations may be very extensive.

Extension of S. Goldstein method to a wake behind a solid symmetrical body in a compressible, heat-conducting fluid is given in the following:

"On the Two-Dimensional Steady Flow of a Compressible Viscous Fluid Far Behind a Solid Symmetrical Body," by M. Z. Krzywoblocki, *Journal of The Franklin Institute*, vol. 243, 1947, pp. 471–486.

Extension of Schlichting's paper (authors' Bibliography 58) to compressible, heat-conducting turbulent wake is given in the following:

"On the Two-Dimensional Steady Turbulent Flow of a Compressible Fluid Far Behind a Solid Symmetrical Body," by M. Z. Krzywoblocki, "I—Momentum Transfer Theory," *Journal of The Franklin Institute*, vol. 247, 1949, pp. 31–61; "II—Vorticity Transfer Theory," *Journal of The Franklin Institute*, vol. 247, 1949, pp. 137–154.

Extension of Schlichting's paper (authors' Bibliography 59) to compressible, heat-conducting flow is given in the following:

"On Steady, Laminar, Round Jets in Compressible Viscous Gases Far Behind the Mouth," by M. Z. Krzywoblocki, *Oesterreichisches Ingenieur-Archiv*, vol. 3, 1949, pp. 373–383.

Extension of Bickley's paper (authors' Bibliography 8) to compressible, heat-conducting flow is given in the following:

"On Steady, Laminar Two-Dimensional Jets in Compressible Viscous Gases Far Behind the Slit," by M. Z. Krzywoblocki, *Quarterly of Applied Mathematics*, vol. 7, 1949, pp. 313–323.

A general method of asymptotic expansion applicable to jets and wakes in three-dimensional flow is given in the following:

"On the Asymptotic Expansion in Three-Dimensional Compressible Viscous Flow," by M. Z. Krzywoblocki, *Journal of The Franklin Institute*, vol. 250, 1950, pp. 213–217.

From papers published in previous years, one may mention the interesting work of H. G. Drickamer, "Mixing of Fluid Streams," Engineering Experiment Station, University of Illinois, Quarterly Progress Report No. 1, June–August 31, 1946, Contract N6-ORI-71, Task Order No. 11, ONR, Navy Department. From papers published recently one may add the following:

"Note on Free Turbulent Flows, With Special Reference to the Two-Dimensional Wake," by G. K. Batchelor, *Journal of the Aeronautical Sciences*, vol. 17, 1950, pp. 441–445.

"L'Étude des Jets et la Mécanique Théorique des Fluides," by A. Oudart, France, Ministere de l'Air, *Publications Scientifiques et Techniques*, No. 234, 1949.

"The Eddy Viscosity in Turbulent Shear Flow," by A. A. Townsend, *Philosophical Magazine*, vol. 41, 1950, pp. 890–906.

"Spectrums and Diffusion in a Round Turbulent Jet," by S. Corrsin and M. S. Uberoi, NACA Technical Note No. 2124, 1950.

"Free Boundaries and Jets in the Theory of Cavitation," by D. Gilbarg and J. Serrin, *Journal of Mathematical Physics*, vol. 29, 1950, pp. 1–12.

"Jet Flow and Its Effects on Aircraft," by H. B. Squire, *Aircraft Engineering*, vol. 22, 1950, pp. 62–67.

"Penetration of Air Jets Issuing From Circular, Square and Elliptical Orifices Directed Perpendicularly to an Air Stream," by R. S. Ruggeri, E. E. Callaghan, and D. T. Bowden, NACA Technical Note No. 2019, 1950.

One may cite the literature on supersonic jets, such as the following:

"A Note on Prandtl's Formula for the Wave-Length of a Supersonic Gas Jet," by D. C. Pack, *Quarterly Journal of Mechanics and Applied Mathematics*, vol. 3, 1950, part 2, pp. 273–281; "On the Formation of Shock-Waves in Supersonic Gas Jets (Two-Dimensional Flow)," by D. C. Pack, *Quarterly Journal of Mechanics and Applied Mathematics*, vol. 1, 1948, part 1, pp. 1–17; "Axially-Symmetrical Supersonic Flow Near the Centre of an Expansion," by N. J. Johannesen, *Aeronautical Quarterly*, vol. 2, 1950, part 2, pp. 127–142.

The writer does not pretend to maintain that the references cited herewith exhaust the literature published recently on the subject in question.

Maurice Spielman.[3] The authors have presented a clear and useful summary of much previous work in the field but apparently have not considered the problem of a jet discharged parallel to a bounding surface in such a way that entrainment could not occur around the entire circumference of the jet. This problem has practical importance, for example, in windshield defrosting.

The writer has done some work in this field, and has also searched the literature for analytical and experimental work concerned with jet investigations in general. He would like to append the following additional Bibliography[4] in order to make more complete the comprehensive listing given by the authors. References 92, 93, 110, 114, 134, 135, 139, 146 deal with the subject of an air jet directed parallel to a surface.

The authors' experimental result that concentration diffuses more rapidly than momentum verifies the previously published data of Voorheis and Howe (144), Keagy and Weller (111), and some others. In this connection, it is sometimes convenient to define an "apparent jet origin" by extrapolating to zero the half-boundary radius r_{u_0} or $r_{u_0^2}$ on a $r - x$ plot (see authors' Fig. 1). Zerbe and Selna (146) made good use of this method.

ADDITIONAL BIBLIOGRAPHY

90 "Velocity Distribution in a Liquid-into-Liquid Jet," by E. N. da C. Andrade and L. C. Tsien, Proceedings of the Physical Society, vol. 49, 1937, p. 381.

91 "Velocity Distribution in a Liquid-into-Liquid Jet. Part II—The Plane Jet," by E. N. da C. Andrade, Proceedings of the Physical Society, vol. 51, 1939, p. 784.

92 "Heat Transfer and Velocity Distribution Characteristics of a Free Air Jet Discharged From a Narrow Slot and Directed Parallel to a Horizontal Plate," by R. C. Bergh, H. Wittner, M. Martin, and F. Donally, Report ERF-3 of the Republic Aviation Corporation, Farmingdale, N. Y., 1945.

93 "Heat Transfer and Velocity Distribution Characteristics of a Free Air Jet Discharged From Individual Nozzles and Directed Parallel to a Horizontal Plate," by R. C. Bergh, H. Wittner, M. Martin, and F. Donally, Report ERF-9 of the Republic Aviation Corporation, Farmingdale, N. Y., 1946.

94 "Application of the Theory of Free Jets," by A. Betz and E. Petersohn, *Ingenieur-Archiv*, May, 1931. Translated as NACA TM 667, 1932.

[1] By W. Forstall, Jr., and A. H. Shapiro, published in the December, 1950, issue of the Journal of Applied Mechanics, Trans. ASME, vol. 72, pp. 399–408.

[2] Professor of Gasdynamics and Theoretical Aerodynamics; Secretary, Fluid Dynamics Panel, University of Illinois, Urbana, Ill.

[3] Associate Research Engineer, Heat Transfer Laboratory, Illinois Institute of Technology, Chicago, Ill. Jun. ASME.

[4] Numbers in parentheses refer to the Bibliography at the end of this discussion. These numbers are an extension of those in the original paper in order that they will not be confused with the authors' sequence.

95 "Eddy Diffusion and Evaporation in Flow Over Aerodynamically Smooth and Rough Surfaces," by K. L. Calder, *Journal of Mechanics and Applied Mathematics*, vol. 2, part 2, 1949, p. 153.

96 "Investigation of the Penetration of an Air Jet Directed Perpendicularly to an Air Stream," by E. E. Callaghan and R. S. Ruggeri, NACA TN 1615, 1948.

97 "The Impact Tube in a Viscous Compressible Gas," by T. L. Chambre and H. R. Smith, Heat Transfer and Fluid Mechanics Institute, 1949, p. 271. Published by the ASME.

98 "On Gas Jets," by S. A. Chaplygins, Moscow University Scientific Memoirs, 1902, p. 1. Translated in NACA TM 1063, 1944.

99 "Temperature Gradients in Turbulent Gas Streams," by W. H. Corcoran, B. Roudebush, and B. H. Sage, *Chemical Engineering Progress*, vol. 43, 1947, p. 135.

100 "A Note on Three Dimensional Turbulence and Evaporation in the Lower Atmosphere," by D. R. Davies, Proceedings of the Royal Society of London, England, series A, vol. 202, 1950, p. 96.

101 "The Mechanics of Flames and Air Jets," by R. F. Davis, Proceedings of The Institution of Mechanical Engineers, vol. 137, 1937, p. 11.

102 "Turbulence and Diffusion," by H. L. Dryden, *Industrial and Engineering Chemistry*, vol. 31, 1939, p. 415.

103 "A Review of the Statistical Theory of Turbulence," by H. L. Dryden, *Quarterly of Applied Mathematics*, vol. 1, 1943, p. 7.

104 "Similitude of Phenomena of Entrainment of Air by Water in Motion," by L. Escande, Comptes Rendus, vol. 209, 1939, p. 626.

105 "Mixing of Parallel Flowing Streams in a Pressure Gradient," by C. K. Ferguson, Heat Transfer and Fluid Mechanics Institute, 1949, p. 77. Published by the ASME.

106 "Flow States in Emergent Gas Streams," by J. E. Garside, A. R. Hall, and D. T. A. Townend, *Nature*, London, England, vol. 152, 1943, p. 748.

107 "Heat Transfer to Liquid Metals Flowing in Asymmetrically Heated Channels," by W. B. Harrison and J. R. Menke, Trans. ASME, vol. 71, 1949, p. 797.

108 "Downward Projection of Heated Air," by L. Helander and C. V. Jakowatz, *Heating, Piping, and Air Conditioning*, vol. 20, No. 3, 1948, p. 129.

109 "Theoretical Calculation of the Diffuser Efficiency of Supersonic Wind Tunnels With Free Jet Test Section," by R. Herman, Heat Transfer and Fluid Mechanics Institute, 1949, p. 255. Published by the ASME.

110 "Heat Transfer From an Air Jet to a Plane Plate With Entrainment of Water Vapor From the Environment," by M. Jakob, R. L. Rose, and M. Spielman, Trans. ASME, vol. 72, 1950, p. 859.

111 "A Study of Freely Expanding Inhomogeneous Jets," by W. R. Keagy and A. E. Weller, Heat Transfer and Fluid Mechanics Institute, 1949, p. 89. Published by the ASME.

112 "The Discharge of Air From a Long Slot," by A. Koestel and G. L. Tuve, *Heating, Piping, and Air Conditioning*, vol. 20, No. 1, 1948, p. 153.

113 "Technique for the Optical Measurement of Turbulence in High Speed Flow," by L. S. G. Kovasznay, Heat Transfer and Fluid Mechanics Institute, 1949, p. 211. Published by the ASME.

114 "Jet Diffusion in Proximity of a Wall," by D. Kuchemann, NACA TM 1214, 1949.

115 "Heat Transfer in a Turbulent Liquid or Gas Stream," by H. Latsko, *Zeitschrift für angewandte Mathematik und Mechanik*, vol. 1, 1921, p. 268. Translated in NACA TM 1068, 1944.

116 "Some Basic Laws of Isotropic Turbulent Flow," by L. G. Loitsianskii, Report 440 of the Central Aero-Hydrodynamical Institute, Moscow, U 1939. Translated in NACA TM 1079, 1945.

117 "Evaporation of Liquids into Turbulent Gas Streams," by D. S. Maisel and T. K. Sherwood, *Chemical Engineering Progress*, vol. 46, 1950, p. 131.

118 "Effect of Air Turbulence on Rate of Evaporation of Water," by D. S. Maisel and T. K. Sherwood, *Chemical Engineering Progress*, vol 46, 1950, p. 172.

119 "How Far Can Air Be Thrown From Side Wall Grille With Given Velocity," by A. McGonagle, Heating, Piping, and Air Conditioning Contractors National Association Official Bulletin, vol. 48, No. 4, 1941, p. 30.

120 "Photographing an Air Jet," by A. J. Nicholas, *Power*, vol. 61, 1925, p. 603.

121 "Turbulence—A Fundamental Frontier in Air Distribution," by H. B. Nottage, *Heating, Piping, and Air Conditioning*, vol. 21, No. 4, 1949, p. 115.

122 "Velocity Distribution in Plane Jet," by T. Okaya and M. Hasegawa, Proceedings of the Physical-Mathematical Society of Japan, vol. 22, 1940, p. 771.

123 "Two-Dimensional Jet Mixing of a Compressible Fluid," by S. I. Pai, *Journal of the Aeronautical Sciences*, vol. 16, 1949, p. 463.

124 "Evaporation From a Plane Free Surface Into a Turbulent Air Stream," by F. Pasquill, Proceedings of the Royal Society of London, England, series A, vol. 182, 1943, p. 75.

125 "Eddy Diffusion of Water Vapor and Heat Near the Ground," by F. Pasquill, Proceedings of the Royal Society of London, England, series A, vol. 198, 1949, p. 116.

126 "Theory of Gaseous Jets," by D. Riabouchinsky, Comptes Rendus, vol. 202, 1936, p. 889.

127 "Gas Jets From Rectangular Orifices," by D. Riabouchinsky, Comptes Rendus, vol. 208, 1939, p. 1765.

128 "Study of Turbulent Diffusion of a Jet by Determination of Radon Concentration," by J. Roquet, Comptes Rendus, vol. 208, 1939, p. 2011.

129 "Gravitational Diffusion From a Boundary Source in Two-Dimensional Flow," by H. Rouse, JOURNAL OF APPLIED MECHANICS, Trans. ASME, vol. 69, 1947, p. A-225.

130 "Air Distribution and Draft," by J. Rydberg and P. Norback, *Heating, Piping, and Air Conditioning*, vol. 21, No. 7, 1949, p. 167.

131 "Heat Transfer to a Fluid Flowing Turbulently Between Parallel Walls With Asymmetric Wall Temperatures," by R. A. Seban, Trans. ASME, vol. 72, 1950, pp. 789–795.

132 "Heat Transfer, Mass Transfer, and Fluid Friction," by T. K. Sherwood, *Industrial and Engineering Chemistry*, vol. 42, 1950, p. 2077.

133 "Investigation of the Distance of Flow of a Fountain of Hot Air," by V. Slessaryoff, *The Journal*, ASME, vol. 36, 1914, pp. 0118–0119.

134 "Diffusion of Water Vapor From the Atmosphere Through a Jet of Less Humid Air," by M. Spielman, unpublished MS thesis, Illinois Institute of Technology, 1947.

135 "Local Coefficients of Mass Transfer by Evaporation of Water Into an Air Jet," by M. Spielman, unpublished PhD thesis, Illinois Institute of Technology, 1951.

136 "Air Discharge From Narrow Slots," by F. F. Stevenson, *Heating, Piping, and Air Conditioning*, vol. 13, 1941, pp. 308, 368, 558, 690; vol. 14, 1942, p. 23.

137 "The Equation of Diffusion in a Turbulent Medium," by W. G. L. Sutton, Proceedings of the Royal Society of London, England, series A, vol. 182, 1943, p. 48.

138 "Wind Structure and Evaporation in a Turbulent Atmosphere," by O. G. Sutton, Proceedings of the Royal Society of London, England, series A, vol. 146, 1934, p. 701.

139 "Laminar Flow of a Slightly Viscous Incompressible Fluid That Issues From a Slot and Passes Over a Flat Plate," by N. Tetervin, NACA TN 1644, 1948.

140 "The Discharge of Air Through Small Orifices, and the Entrainment of Air by the Issuing Jet," by J. S. G. Thomas, *Philosophical Magazine*, vol. 44, 1922, p. 969.

141 "Entrainment of Air by a Jet of Gas Issuing From a Small Orifice in a Thin Plate," by J. S. G. Thomas, *Philosophical Magazine*, vol. 47, 1924, p. 1048.

142 "Air Entrainment in Gas Burners," by G. von Elbe and J. Grumer, *Industrial and Engineering Chemistry*, vol. 40, 1948, p. 1123.

143 "Entrainment and Jet-Pump Action of Air Streams," by G. L. Tuve, G. B. Priester, and D. K. Wright, *Heating, Piping, and Air Conditioning*, vol. 13, No. 11, 1941, p. 708.

144 "The Entrainment of Air by a Cylindrical Jet," by T. S. Voorhees and E. D. Howe, Proceedings of the Pacific Coast Gas Association, vol. 30, 1939, p. 198.

145 "On the Velocity Distribution of Turbulent Flow in Pipes and Channels of Constant Cross Section," by Chi-Teh Wang, JOURNAL OF APPLIED MECHANICS, Trans. ASME, vol. 68, 1946, p. A-85.

146 "An Empirical Equation for the Coefficient of Heat Transfer to a Flat Surface From a Plane Heated-Air Jet Directed Tangentially to the Surface," by J. Zerbe and J. Selna, NACA TN 1070, 1946.

AUTHORS' CLOSURE

The authors wish to thank Messrs. Krzywoblocki and Spielman for their contributions in making the Bibliography more complete.

Plastic Biaxial Stress-Strain Relations for Alcoa 24S-T Subjected to Variable-Stress Ratios[1]

D. C. Drucker.[2] As the authors state, the data available on stress-strain relations under combined stress are meager indeed. Therefore it is important to analyze all new results carefully and obtain as much basic information of theoretical and of practical value as possible. Also, interpretation in terms of preconceived notions should not be permitted to obscure the real meaning of the data.

A point of great interest at present is how close an approximation simple deformation theory provides in practical problems. Deformation theory, in general, postulates that the existing state of stress determines the state of strain. The simplest form is based upon octahedral shearing stress τ_0

$$\epsilon_1 = \frac{1}{C(\tau_0)} [\sigma_1 - \nu'(\sigma_2 + \sigma_3)]$$

$$\epsilon_2 = \frac{1}{C(\tau_0)} [\sigma_2 - \nu'(\sigma_3 + \sigma_1)]$$

where the usual notation is followed, and $C(\tau_0)$ is a plastic Young's modulus, and ν' a plastic Poisson's ratio. In particular, therefore, the theory supposes that if σ_1 and σ_2 are given, and σ_3 is zero, ϵ_1 and ϵ_2 are determined regardless of the path of loading.

What do the authors' data prove? Their Figs. 5 and 11 are especially significant. Fig. 5 shows that when $\sigma_1/\sigma_2 = 1$ at all times $\epsilon_3 = 0.011 = \epsilon_2$ (approx.) at $\sigma_1 = \sigma_2 = 51{,}000$ psi. On the other hand, Fig. 11, which has a path of 5000-psi internal pressure followed by axial tension at constant pressure, gives $\epsilon_1 = 0.007$, and $\epsilon_2 = 0.016$ at $\sigma_1 = \sigma_2 = 51{,}000$. As the elastic-strain components are over 0.003, it is clear that the plastic-strain components of 0.004 and 0.013 are predicted very badly at this value of stress. Instead of being equal as deformation theory postulates, they are in the ratio of more than 3 to 1.

As another example, take the loading path of 3000 psi internal pressure followed by tension. Fig. 11 gives $\epsilon_1 = +0.0025$, $\epsilon_2 = -0.002$ at $\sigma_1 = \sigma_2 = 32{,}000$ psi, which means plastic strains of about 0.0005 and -0.004, respectively, which are again far from equal.

Obviously, the authors' statement that deformation theory is adequate does not hold for small but appreciable plastic strains when the path of loading changes abruptly. Clearly, it will not be adequate either for large deformations if the loading path is frequently varied appreciably. It is, however, a sufficiently good engineering approximation when the major part of the plastic deformation occurs over the portion of the loading path which is fairly close to a path with constant value of σ_1/σ_2.

In conclusion, it should be pointed out that if octahedral shearing stress or any isotropic function of shearing stress is the governing criterion,[3] the proper significant strain variable to plot against is proportional to $\int \sqrt{(d\epsilon_1^p)^2 + (d\epsilon_2^p)^2 + (d\epsilon_3^p)^2}$ where the $d\epsilon^p$ are the principal plastic-strain increments. Again, if the major part of the plastic deformation occurs when the loading path is not too far from $\sigma_1/\sigma_2 = \text{const}$, the integral is closely a constant times the octahedral shearing strain.

[1] By Joseph Marin and B. J. Kotalik, published in the December, 1950, issue of the Journal of Applied Mechanics, Trans. ASME, vol. 72, pp. 372–376.

[2] Professor of Engineering, Brown University, Providence, R. I. Mem. ASME.

[3] "Effective Stress and Effective Strain in Relation to Stress Theories of Plasticity," by G. N. White, Jr., and D. C. Drucker, *Journal of Applied Physics*, vol. 21, 1950, pp. 1013–1021.

Authors' Closure

The authors' statement that the deformation theory is adequate was intended to apply for the specific material tested, for large plastic strains for the stress condition used. They agree in general with the statements made by Mr. Drucker regarding the limitations of the deformation theory.

The Uniform Distribution of a Fluid Flowing Through a Perforated Pipe[1]

J. D. Keller.[2] This paper presents a worth-while extension of the theory of pipe burners, although the taking into account of the variation of the pipe friction coefficient with velocity which forms its chief claim to novelty has not the great importance seemingly attributed to it by the author (somewhat reminiscent of Maupertuis and the polar flattening of the earth).

The author wrongly assumes that previous investigators did not recognize this variation. Actually, it was well known but was judged to be of only minor importance; in the writer's opinion, the author has failed to show that this judgment was incorrect for the great majority of commercially usable pipe burners, although beyond question it was so in some special cases. Furthermore, except in the laminar-flow ranges, it is by no means certain that in pipe burners the friction coefficient decreases appreciably with increasing Reynolds number, as required by the author's Equation [8], since it is well known that in very rough pipes the coefficient remains almost constant; see, for example, the curves representing the experimental results of Nikuradse and of Fromm.[3] It seems very probable that the disturbance of flow produced by the diversion of fluid into the successive outlet ports along the pipe length is equivalent in effect to great roughness of the pipe wall.

Again, the author's assumption that the flow changes abruptly from turbulent to laminar at some point in the pipe length is directly contrary to experience. Long ago, Osborne Reynolds showed conclusively that turbulence once started tends to persist, and that a quieting section of considerable length is required to cause it to die out. This is also shown by the difference between the higher and lower critical velocities.

Of the four photographs cited by the author as proving his point, Figs. 3(*b*) and 6(*c*), which according to the author's Table 1 were obtained with burners having a ratio of total port area to pipe cross-sectional area greater than 1, evidently correspond to operation in the laminar-flow range. Figs. 5(*a* and *b*) were obtained with a burner having an area ratio less than 1 (actually, about 0.72 according to Table 1) and therefore are not pertinent to the argument; in these, again, the flow evidently was in the laminar and not in the turbulent range. Hence any conclusions drawn from these four photographs could apply only in the laminar-flow range.

In the writer's opinion, where fairly uniform gas distribution and flame heights are obtained along the length of pipe burners having port area/pipe area ratios considerably in excess of 1, this result is not due (or at least, not chiefly due) to variation of the friction coefficient, but to a factor hitherto overlooked by investigators, including Keller as well as Dow, namely, the increase of pressure below the flame, due to the expansion of volume caused by combustion and the acceleration of the gas par-

[1] By W. M. Dow, published in the December, 1950, issue of the Journal of Applied Mechanics, Trans. ASME, vol. 72, pp. 431–438.

[2] Associated Engineer, Pittsburgh, Pa. Mem. ASME.

[3] "Industrial Furnaces," by W. Trinks, third edition, John Wiley & Sons, Inc., New York, N. Y., 1934, Fig. 310.

ticles required thereby.[4,5] This effect, which is also responsible for the phenomenon of physical refraction at the flame front, means that the pressure against which the gas issues from the burner ports is higher than atmospheric; and, since the excess pressure thus produced is independent (within limits) of the velocity of flow through the ports, while the pressure required to produce the flow in the burner decreases as the square of the velocity, it is evident that at low turn down of the burners, as, for example, in the author's Fig. 6(*c*), deceleration pressure, friction loss, and port pressure drop all must become negligible compared to the nearly constant flame pressure, and the flame heights will thereby be equalized along the burner length. In other words, the effect of the flame pressure, at low turn down, is equivalent to greatly decreasing the ratio of total port area to pipe cross-sectional area.

In the writer's opinion, the author in his anxiety to adduce physical proof of the correctness of his mathematical derivations has done a disservice to engineers by laying stress on the fact that under a few exceptional conditions it is possible with care to produce nearly uniform flame heights in burners having A_p/A ratios greater than 1, while failing to emphasize at the same time the extremely erratic and unstable characteristics of such high-ratio burners.[6]

The theory of manifolds and pipe burners cannot be considered to have reached a reasonably complete and satisfactory stage of development until at least the following additional factors, up to the present neglected or not adequately treated by any investigator, shall have been taken into account:

1 The difference between the conservation-of-energy theory and the conservation-of-momentum theory where there are separate discharge ports instead of a continuous slot.[7]

2 The effect of residual velocity parallel to the pipe axis, in the fluid leaving the ports.

3 The effect of nonuniform velocity distribution across the pipe.

4 Effect of variation of port discharge coefficient with discharge pressure or velocity, and satisfactory experimental determination of the actual values of the coefficient applicable to pipe burners having various types of ports.

5 Experimental determination of the effect of flow disturbance at entrance to ports on the friction or turbulence loss along the pipe.

6 Especially in burners, the effect of buoyancy of the combustible mixture in the pipe and of the flames above it.

7 In burners, the effect of flame pressure, just mentioned.

8 In burners, the effect of heat transfer from the pipe to the gas flowing in it.[8]

R. E. Peck.[9] It was interesting to see that the optimum flow dimensions could be given by Fig. 1 of the paper.

The parameter $Q_0/\nu L$ can be written as

$$\frac{\pi}{4}\left(\frac{D_0}{L}\right)\left(\frac{D_0\, up}{\mu}\right)$$

Similarly, Equation [17] can be written as

$$\frac{L}{D} = \frac{R\, e_0}{16}$$

The range of applicability of a given burner would be a function of the Reynolds number. The burner that would be usable over the greatest range of gas flow, would be case 4, or the infinite reservoir. If $L/D = 70$ is a limiting case as given by Keller, the R_e would be 1120 and probably would fall into case 4 if there were an appreciable pressure drop through the parts.

The methods outlined in this paper would make it possible to obtain uniform distribution at high Reynolds numbers, but they still could be used only over a limited range of flow.

If pressure taps were made along a burner, it would be possible to check this range of applicability for a given pressure drop across the ports. However, Figs. 3 to 8, inclusive, do much the same thing in a qualitative way.

E. A. Richardson.[9] This paper constitutes a valuable addition to the literature dealing with manifold behavior. It is assumed the fluid is incompressible, while the differential equation used assumes variations in pressure, kinetic energy, and in friction loss. For the purposes of the author of the paper, the disregard of terms in the basic equation[10] involving change of level, heat addition, work done, and compressibility or changes in density, is of no importance. His burners are on a relatively small scale, heat additions may not be of importance, no energy is added as work, and the burner axis is horizontal. His test results show that the omissions are of negligible effect. Within these limitations, the equations and deductions are extremely useful.

The writer deals with a form of heat insulation[11] or furnace lining,[12] or retort chemical furnace,[13] involving a fluid-permeable wall with the surfaces thereof at different temperatures, through which wall a fluid is caused to permeate for any of a variety of purposes. Such a permeable wall is essentially a pipe with a very large number of holes, which are not quite uniform, so the pressure drop for a given rate of flow varies by, say, ±10 per cent over the surface. The law of flow through the holes is substantially that for laminar flow. The pressure drop for a given rate of flow tends to be relatively large. It is often required that the rate of flow shall be substantially uniform over the surface.

For small-scale apparatus, a manifold comprising an annular space (or spaces) covering the surface (or surfaces) of the permeable body is adequate, the criterion of effectively infinite manifold capacity being sufficient. This presumes, also, not too great differences of temperature and fluid density between the regions separated by the permeable body. Where lack of uniform flow may tend to occur due to the thinness of the annulus, a reduction of porosity of the permeable body may raise the drop of pressure to the point where the annulus becomes again effectively an infinite reservoir.

This is not true in the case of large-scale apparatus and may not be true in the case of high-pressure catalyst chambers whose walls are insulated by such means so as to operate at atmospheric temperature irrespective of the process temperature, for in such cases the space available is at a premium and must be used most

[4] "Combustion, Flames and Explosions of Gases," by B. Lewis and G. v. Elbe, Cambridge, 1938, chapter on Stationary Flames.

[5] "Explosion and Combustion Processes in Gases," by W. Jost, translated by H. O. Croft, McGraw-Hill Book Company, Inc., New York, N. Y., 1946, p. 80.

[6] Discussion by R. H. Solem, and author's closure, of paper by J. D. Keller, Trans. ASME, vol. 71, 1949, pp. 320–322.

[7] Discussion by R. W. Powell, ibid., p. 320.

[8] Associate Professor, Department of Chemical Engineering, Illinois Institute of Technology, Chicago, Ill.

[9] Partner, Edward, (Nellie), and George Richardson, RD2, Bethlehem, Pa. Mem. ASME.

[10] "Heat Transmission," by W. H. McAdams, second edition, McGraw-Hill Book Company, Inc., New York, and London, England, 1942, p. 114.

[11] U. S. Patent no. 2,215,532.

[12] U. S. Patent no. 2,311,350.

[13] U. S. Patent no. 2,235,644.

effectively. Furthermore, with high pressures and temperatures, so-called "chimney effects" arise.

The nature of the problem may be appreciated from two examples, and means for reducing the importance of such a chimney effect may be shown. Consider a furnace 40 ft high, the outer surface of the permeable wall being fed by air at about 68 F, while the inner surface is open to the furnace chamber containing gases at, say, 2400 F. The pressure head of air in the outer annulus is 3 psf, while that for the furnace gases is about 0.53 psf. The maximum chimney effect in 40 ft is then 2.47 psf, or about 0.48 in. H_2O. To secure uniformity of flow within ±10 per cent, the pressure drop through the wall at moderate rates of operation should exceed 5 in. H_2O, a figure which may be excessive from the standpoint of efficient supply of air.

Consider also a cracking chamber 40 ft high which operates at 850 F and 700 psi, in which the fluids being treated are near their critical point as vapors so that the density is subject to moderately rapid change with pressure, the mean density being about 10 lb per cu ft. First, let a gas such as hydrogen at 0.26 lb per cu ft; second, a liquid (a portion of the reacting material which has not been heated) of about 58 lb per cu ft density be used as permeating fluids. (The purpose of the permeable layer is to keep the pressure shell at atmospheric temperature, thereby avoiding creep, and substantially avoiding temperature stresses. It also recovers heat, normally lost through the walls, as preheat in the permeating fluid.) The pressure due to a 40-ft height of the hydrogen is 10.4 psf; that for the 58-lb liquid is 2320 fps, while that for the contents is 400 psf. Then the chimney effect with hydrogen is 390 psf or 2.71 psi. With pressure balance at the top, the contents tend to flow out at the bottom. The chimney effect with 58-lb liquid is 1920 pfs, so that if the pressure is balanced at the top, the liquid tends to flow in at the bottom. The chimney effect amounts to 13.3 psi.

Now in the hydrogen-cooled cracking chamber, the pressure drop through the permeable wall at normal rates of operation must be of the order of 27 psi to limit variations due to this cause to ±5 per cent of the mean rate of flow. This pressure must be supported by the permeable-body structure and the permeability must be made suitably low to secure the desired fluid flow. In the case of the liquid-cooled chamber, the pressure drop through the permeable body must become 133 psi (a large fraction of the 700-psi process pressure) which must also be carried by the outer shell.

It is still possible to secure an effectively infinite annular space and reduce the required pressure drop therefore by dividing the height into n sections, each separated from the next by a horizontal partition extending through the annular space and permeable body. The chimney effect in each section is $1/n$ part of what it was before and so is the required pressure drop for effectively infinite reservoir behavior. It is now sufficient to insure equal rates of flow to each section on a square foot of permeable body surface basis. Actually, such subdivision may be required to secure the proper balance between the permeability of available materials, the conductivity thereof, and their available strength to take the unbalanced pressure between annular space and contents.

In some cases involving varying rates of flow with height, chimney effect may prove helpful. In some cases it may be possible to vary the thickness of permeable wall. In some cases the wall may be made in two layers, one primarily for insulation, the other primarily for low permeability and strength.

If the burners used by the author were to be placed vertically, and if heat entered the pipe faster, or the burners were made longer, considerations such as these might become of importance. It seems well to call attention to them in view of the wide range of manifold problems which occur in practice.

In passing, it is noted that uniform distribution is securable in the burner case only at one rate of flow. It might be of interest to investigate the possibility of using a rotatable insert in the pipe, adapted to controlling the transfer of gas between the top and bottom portions of such pipe according to variations in the total rate of flow, whereby the rate of flow along the length might be kept constant. If desirable, it should be possible to do this.

Author's Closure

The interest shown in the author's paper and the comments and contributions of the discussers are appreciated.

The author does not agree with Mr. Keller that the variation of the friction factor along the length of the pipe burner is of minor importance. In any pipe burner the Reynolds number of the gas flow varies from a maximum at the inlet end to zero at the dead end. That the friction factor remains constant over a range of Reynolds numbers from zero to a value of several thousand is an untenable assumption. With commercially usable pipe burners the decrease of the Reynolds number with distance is rapid, a decrease from 2000 to 1000 over a distance of a few inches. This rapid decrease serves as a very effective quieting influence in establishing laminar flow. Obviously, the flow does not change abruptly from fully developed turbulent to fully developed laminar; however, in the particular cases treated by the author the change occurred over a distance of a few inches, and an attempt to account for a transition region of flow would have had a negligible influence on the over-all design of the pipe burner. There is nothing in the author's analysis to preclude the application of a friction-factor relationship for a transition region of flow, if one so desires.

The author wrote Equation [8] in a general form, namely $f = b/(N_{Re})^n$, so it would represent various empirical relationships for the friction factor in the turbulent-flow region, which will extend over only part of the total burner length. The final design equation for the turbulent region, Equation [10a], was also given in terms of the arbitrary constants b and n. If one chooses $n = 0$, then the friction factor will be constant in the turbulent region as desired by Mr. Keller. In the experiments conducted by the author, the Blasius relationship for the friction factor was found to be applicable for the turbulent-flow region.

Mr. Keller[14] had previously concluded (by assuming that the friction factor was constant over the entire length of the pipe burner) that there are two dimensionless ratios which define the operating characteristics of such a manifold, namely, the ratio of active length to diameter L/D, and the area ratio Ap/A. His theoretical reasoning led him to conclude that the variation of discharge is uniquely defined by these two ratios, and that only for the conditions of $L/D \cong 70$ and $Ap/A = 1$ is the distribution sufficiently uniform to meet practical requirements. He stated that for values of Ap/A greater than one it would be impossible to obtain a uniform flame height with a constant-diameter pipe burner. These conclusions are not in accord with the author's analysis, and consequently the critical experiment represented by Figs. 3(a), 3(b), and 3(c), was conducted. This experiment demonstrated that a pipe burner with an area ratio much larger than the value of one as given by Keller could produce a uniform flame, Fig. 3(b); and that the variation of discharge was not uniquely defined by Keller's two dimensionless ratios but was also a function of the total gas flow, Figs. 3(a), 3(b), and 3(c). In addition, this test gave experimental verification of the optimum flow rate for uniform fluid distribution as predicted by the author's Equation [17]. Mr. Keller may feel that the variation of the friction factor is of minor importance, but in the author's opinion this fact

[14] "The Manifold Problem," by J. D. Keller, JOURNAL OF APPLIED MECHANICS, Trans. ASME, vol. 71, 1949, pp. 77–85.

has completely invalidated Keller's general conclusions concerning the flow distribution in a pipe burner.

The author's analysis is not intended to apply to all manifold systems. As stated in the paper, the present results obviously could not be applied to any manifold system regardless of size and number of discharge ports. The author agrees with Mr. Keller that the theory of manifolds in general cannot be considered complete until various other factors have been taken into account. Dr. Streeter[15] discusses the application of the conservation-of-energy theory and the conservation-of-momentum theory to a manifold with separate discharge ports. He also gives some experimental results which indicate that the energy losses due to the fluid discharge through the ports of systems physically similar to pipe burners are negligible, a tacit assumption made in the author's analysis.

Mr. Keller's discussion of increase of pressure below the flame is interesting; however, it is difficult for the author to ascribe the uniform gas distribution shown in Fig. 6(*c*) to the effect of this phenomenon. This would mean that the pressure phenomenon caused uniform gas distribution at only one flow rate, which happened to coincide with the optimum flow rate predicted by Equation [17], and that it failed to produce uniform distribution at higher and lower flow rates.

The author disagrees with Mr. Keller that a disservice has been done to engineers by laying stress on the fact that it is possible to obtain a uniform distribution of heat and flame height with pipe burners having an area ratio greater than one. This makes possible the construction of a simple, drilled port pipe burner with a capacity as much as ten times greater than the capacity of the present commercially available pipe burner. The conventional pipe burner is now designed to perform as case 4, and its capacity and utility are limited by the conditions imposed by Equations [14], [15], and [16]. A tapered-bore pipe burner constructed in accordance with the author's analysis has very stable and desirable characteristics. The linear gas velocity in the manifold of such a burner is higher than the escape velocities through the ports. This tends to prevent flash back and to produce a stable flame, in contrast to the loping flame of the constant-diameter, low-area-ratio burner. Several tapered-bore, high-area-ratio pipe burners, which have capacities many times greater than conventional pipe burners, have been constructed for industrial heating applications. They have performed very satisfactorily. In every installation it would have been physically impossible to install enough conventional, constant-diameter, low-area-ratio burners to furnish the necessary heating requirements. These industrial applications are:

1 A 70-hp 125-psi, steam boiler in a commercial laundry.
2 A 50-hp, low-pressure, hot-water heating boiler in an office building.
3 Two 125-hp 125-psi, steam boilers in an office building.
4 A cane-syrup pan evaporator, 2 million Btu per hr.
5 A diaphram oil heater.

The production of a uniform flame height in a burner having an area ratio greater than one has made possible the construction of a pipe burner equivalent to ten conventional pipe burners. The author's concept of a disservice to engineers does not coincide with Mr. Keller's concept of a disservice.

Dr. Peck's comment that the range of applicability of a given burner would be the greatest for case 4 is certainly correct. For some manifold applications this large degree of flexibility may be desirable. The range of applicability of a tapered-bore pipe burner is a function of its dimensions and capacity. This can be easily seen by reference to Fig. 2. There is only a slight difference between curves 5 and 6 for a threefold variation in flow rate, while there is a rather large difference between curves 1 and 2 for the same variation in flow rate. Fortunately the most useful pipe burners are of such dimensions that they can be operated at turndown ratios of 4 to 1 or greater and still have satisfactory flame characteristics. In many applications it is necessary for a pipe burner to operate at only one flow rate.

Mr. Richardson's comments concerning flow through a fluid-permeable furnace lining are interesting. An appreciable addition of heat to the fluid flowing through the manifold would alter the solution. The necessary condition for a uniform distribution of the fluid through the ports is a constant pressure along the length of the manifold; consequently the solution is valid for compressible and incompressible fluids. The present solution is also valid for a burner placed vertically, because then the necessary condition for a uniform distribution of the fluid is a constant piezometric head along the length of the burner. This condition reduces the energy balance to the same differential equation as treated in the paper.

[15] "Engineering Hydraulics," edited by Hunter Rouse, John Wiley & Sons, Inc., New York, N. Y., 1950, pp. 436–437.

Beam Vibrations With Time-Dependent Boundary Conditions[1]

E. H. Lee.[2] Since the method developed in this paper has been presented in an entirely mathematical form, it may be of interest to mention the method of moving axes of reference, which can be used to handle certain types of this class of problems. The axes of reference are taken to move with the time-dependent boundary conditions, so that the usual type of boundary-value problem with fixed boundary conditions is obtained in terms of the moving axes. The change of axes calls for a time-dependent force distribution on the body, which leads to a forced-vibration type of problem. The resulting analysis is substantially the same as that given in the paper, but it may be helpful to some engineers, who are required to solve such problems, to have a physical picture of the force distribution on the system which replaces the time-dependent conditions, and to work directly with the familiar problem of forced oscillation. A simple example of this method is given by von Kármán and Biot.[3]

W. H. Hoppmann, 2nd.[4] The authors of this paper have presented concisely a method for determining the deflection of a vibrating beam having time-dependent boundary conditions. Work of this kind in the basic theory should be welcomed by those who may be faced with such problems in engineering. Unfortunately, textbooks such as that by S. Timoshenko[5] contain no specific treatment of this type of problem and the work by Duhamel and Phillips mentioned by the authors are inaccessible from the standpoint of the texts themselves or the unsystematic presentation of the subject.

With regard to the specific content of the paper, there is a generality of solution implied in the introduction which is not contained in the derived equations. For example, Equations

[1] By R. D. Mindlin and L. E. Goodman, published in the December 1950, issue of the Journal of Applied Mechanics, Trans. ASME, vol. 72, pp. 377–380.

[2] Associate Professor of Applied Mathematics, Brown University, Providence, R. I. Mem. ASME.

[3] "Mathematical Methods in Engineering," by Th. von Kármán and M. A. Biot, McGraw-Hill Book Company, Inc., New York, N. Y.

[4] Associate Professor of Mechanical Engineering, The Johns Hopkins University, Baltimore, Md. Mem. ASME.

[5] "Vibration Problems in Engineering," by S. Timoshenko, D. Van Nostrand Company, Inc., New York, N. Y., second edition, 1937.

[17] for A_n and B_n require that the shape functions X_n form an orthogonal set. This obviously is a rather severe restriction on the type of problem that can be solved. Investigations in which one structural element interacts with another seem to fall outside of the scope of the formulation in the paper, although the authors apparently say in their introduction that they are included as special cases. In order to pursue this point a bit further the effect of one structural element on another will now be examined somewhat in detail.

For the purpose consider the case of a cantilever which has a simple mass-spring system attached to the free end and which is driven by a harmonic force, as shown in Fig. 1 herewith.

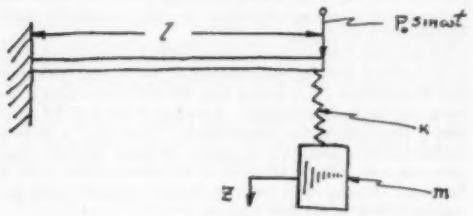

FIG. 1

The two simultaneous differential equations for the structure will be written

$$EI\,\frac{\partial^4 w}{\partial x^4} + \rho A\,\frac{\partial^2 w}{\partial t^2} = 0$$

and

$$m\ddot{z} + k(z - w_l) = 0$$

The boundary conditions for the beam are

$$w(0,t) = \frac{\partial w}{\partial x}\Big]_{x=0} = \frac{\partial^2 w}{\partial x^2}\Big]_{x=l} = 0$$

and

$$EI\,\frac{\partial^2 w}{\partial x^2}\Big]_{x=l} = k[w(l,t) - z(t)] + P_0 \sin \omega t$$

Using the differential equation for the mass m this latter boundary condition becomes

$$\left[\frac{mEI}{R}\,\frac{\partial^4 w}{\partial t^2 \partial x^2} + EI\,\frac{\partial^2 w}{\partial x^2}\right]_{x=l} = m\,\frac{\partial^2 w}{\partial t^2}\Big]_{x=l} + P_0\left(1 - \frac{m\omega^2}{k}\right)\sin \omega t$$

It may be noted that this boundary condition contains explicitly a time derivative. No such derivative occurs in the boundary conditions given by the authors.

Assuming the driving force to be absent, we may try as a solution of the differential equation of motion of the beam

$$w = \sum w_n(x) T_n(t)$$

Then we find

$$w = \sum w_n(x)(A_n \sin p_n t + B_n \cos p_n t)$$

where

$$p_n^2 = \frac{a^2 m_n^4}{l^4} = \frac{EI}{\rho A}\,\frac{m_n^4}{l^4}$$

and

$$w_n(x) = C_n \sin m_n \frac{x}{l} + D_n \cos m_n \frac{x}{l} + E_n \sinh m_n \frac{x}{l} + F_n \cosh m_n \frac{x}{l}$$

Satisfying the boundary conditions with $w(x,t)$ the frequency equation is

$$\frac{1 + \cos m_n \cosh m_n}{\sin m_n \cosh m_n - \cos m_n \sinh m_n} = \lambda m_n$$

where

$$\frac{1}{\lambda} = \left(1 - p_n^2\,\frac{m}{k}\right)\frac{M}{m} = \left(1 - \frac{a^2 m_n^4}{l^4}\,\frac{m}{k}\right)\frac{M}{m}$$

and where M = mass of the beam. The solution for free vibrations is then

$$w_1 = \sum\left[\sin m_n \frac{x}{l} - \frac{(\sin m_n + \sinh m_n)}{(\cos m_n + \cosh m_n)}\cos m_n \frac{x}{l} - \sinh m_n \frac{x}{l} + \frac{(\sin m_n + \sinh m_n)}{(\cos m_n + \cosh m_n)}\cosh m_n \frac{x}{l}\right]\times [A_n \sin p_n t + B_n \cos p_n t]$$

Now if the force $P_0 \sin \omega t$ acts on the end of the beam, we may use w_1 in the solution and choose an auxiliary function w_2, in accordance with the suggestion of the authors, so that

$$w_2 = \left(1 - \frac{m}{k}\,\omega^2\right) P_0 \sin \omega t\, F(x)$$

w_2 satisfies the differential equation of the beam and is such as to satisfy all of the boundary conditions. Then we may write the complete solution

$$w(x,t) = w_1 + w_2$$

$$= \frac{\left(1 - \frac{m\omega^2}{k}\right)}{2m\omega^2} P_0 \sin \omega t \left\{\frac{(\cos jl + \cosh jl)\sin jx - (\sin jl + \sinh jl)\cos jx - (\cos jl + \cosh jl)\sinh jx + (\sin jl + \sinh jl)\cosh jx}{\sin jl \cosh jl - \cos jl \sinh jl - \alpha j^3(1 + \cos jl \cosh jl)}\right\}$$

$$+ \sum_1^\infty \left[\sin m_n \frac{x}{l} - \frac{(\sin m_n + \sinh m_n)}{(\cos m_n + \cosh m_n)}\cos m_n \frac{x}{l} - \sinh m_n \frac{x}{l} + \frac{(\sin m_n + \sinh m_n)}{(\cos m_n + \cosh m_n)}\cosh m_n \frac{x}{l}\right][A_n \sin p_n t + B_n \cos p_n t]$$

$$j^4 = \frac{\omega^2}{a^2} \quad \text{and} \quad \alpha = \left(\frac{EI}{m\omega^2} - \frac{EI}{k}\right)$$

The constants A_n and B_n can be obtained so that the initial conditions are satisfied.

Suppose

$$w(x,0) = w_0$$

and

$$\dot{w}(x,0) = \dot{w}^0$$

Writing $w(x,t) = w_2 + \sum w_n [A_n \sin p_n t + B_n \cos p_n t]$

For the initial condition

$$w(x,0) = w_0$$

we may write

$$\int_0^s w_0 w_m dx = \sum B_n \int_0^s w_n w_m dx$$

Then observing that

$$\left.\frac{\partial^3 w_n}{\partial x^3}\right]_{x=l} = -\left.\frac{m p_n^2}{\left(EI - \dfrac{mEI}{k}\right)} w_n\right]_{x=l}$$

and using equations given by Timoshenko[6] the values of B_n can thereby be obtained in closed form. In a similar manner A_n may be obtained.

This brief investigation indicates that some problems of beam vibrations with time-dependent boundary conditions outside of the scope of the specific formulation of the authors may be solved but they really become special cases requiring individual treatment.

N. O. Myklestad.[7] It should be pointed out that the general problem solved by the authors is not always physically realizable. This is best illustrated in Example 1 of the paper in which the free end of a cantilever beam is given an arbitrary displacement $f_1(t)$, while at $t = 0$ the beam is at rest in its neutral position. Physically this is only possible if $f_1(0) = f_1(0) = 0$, since otherwise the beam will have a discontinuity of $f_1(0)$ in displacement and $f_1(0)$ in velocity at the free end. Since the mathematical solution was obtained for the general case in terms of an infinite series, this discontinuity is not immediately apparent. However, it is easily verified from Equation [20] of the paper that at $x = 0$ and $t = 0$, the deflection is $w = f_1(0)$ while the slope $\partial w/\partial x = -\infty$, so that a discontinuity does exist if $f_1(0) \neq 0$.

Similarly, it is not possible to prescribe an arbitrary end velocity $f_2(t)$ without having $f_2(0) = 0$. However, forces, moments, and accelerations may be prescribed in a perfectly arbitary manner without anything being said about their initial values.

G. A. Nothmann.[8] The authors should be complimented for making a useful contribution to the theory of beam vibrations. The method which they present furnishes solutions to an important class of problems and should be of great help to engineers, particularly those who prefer the "classical" approach of separation of variables. It is especially interesting that the boundary functions $f_i(t)$ are carried through, with only mild restrictions, to the final solution; the results thus appear in very general form, and these functions need not be specified until the solution is established.

The functions $g_i(x)$, which are used to convert the boundary conditions to the stationary type, possess a physical significance which permits an interesting interpretation of the solution. This may be seen by consideration of a static problem, with the beam loaded by (at most) a linearly varying distributed load, in which, for the particular $g_i(x)$ considered, the corresponding boundary condition $f_i(t)$ is made equal to 1 (with appropriate units), and the other three zero. Then $1 \cdot g_i(x)$ becomes the static deflection curve. Thus the deflection of the beam under consideration would be equal to $\sum_{i=1}^{4} f_i(t)\, g_i(t)$ if the quantities (ρA) and $q(x)$ were equal to zero. The afore-mentioned linearly varying distributed load has to be added in certain problems, where end moments and shears are prescribed, in order to maintain static equilibrium of the beam.

On this basis, the actual dynamic deflection may be thought of as resulting from the superposition of this "static" deflection and the deflection $\xi(x,t)$ arising from the distributed mass of the beam and the loading $q(x)p(t)$. Examples 1 and 2 of the paper readily demonstrate this superposition. Even with a physical interpretation of this type, of course, the same algebraic equations ordinarily have to be solved in the determination of the g_i functions. In some cases, however, this interpretation lends special significance to the final solution.

With regard to the authors' statement concerning the applicability of transformation methods to solutions of this type, it may be pointed out that the requirements for the existence of Laplace transforms in vibration problems are not severe. Beam loading and boundary functions are usually bounded and sectionally continuous, conditions which are sufficient to assure the existence of the required transforms. Boundedness and continuity of the deflection function also assure the convergence of the inversion integral, though its evaluation may be laborious in some instances. In problems where the transformation methods are applicable, the time-dependent boundary conditions transform directly and do not necessitate any significant revision in the method of solution of the transformed (ordinary) differential equation.

Bending of an Elliptical Plate by Edge Loading[1]

C. L. Perry.[9] In addition to the papers mentioned in the introduction, the following papers should be cited:

"Calculation of the Bending of Freely Supported Elliptical Plates," by B. G. Galerkin, *Zeitschrift für angewandte Mathematik und Mechanik*, vol. 2, 1923, pp. 113–117.

"On the Equilibrium of Elliptic Plates," by H. Happel, *Mathematische Zeitschrift*, vol. 11, 1921, pp. 194–223.

"On the Bending of an Elliptic Plate Under Certain Distribution of Load, Parts II and III," by H. Sengupta, Bulletin of the Calcutta Mathematical Society, 1948.

"Strength of a Flat Elliptic Plate Loaded Uniformly and Supported at the Perimeter," by T. Matsumura, *Journal of the Society of Mechanical Engineers*, Tokyo, Japan, vol. 24, 1921, pp. 31–40.

"Thin Plates of Elliptic Contour," by M. N. Nichols, *Annales des Ponts et Chaussées*, vol. 2, 1937, pp. 160–166.

"Deflection of Elliptic and Top Formed Plates of Variable

[6] "Vibration Problems in Engineering," by S. Timoshenko, second edition, D. Van Nostrand Company, Inc., New York, N. Y., 1937, Eq. 132, p. 334, and Eq. *K*, p. 336.

[7] University of Illinois, Urbana, Ill. Mem. ASME.

[8] Research Engineer, Armour Research Foundation of Illinois Institute of Technology, Chicago, Ill. Jun. ASME.

[1] By W. A. Nash, published in the September, 1950, issue of the Journal of Applied Mechanics, Trans. ASME, vol. 72, pp. 269–274.

[9] Mathematician, Oak Ridge National Laboratory, Oak Ridge, Tenn.; Assistant Professor of Mathematics, University of Arkansas, Fayetteville, Ark. (on leave of absence).

Thickness by Hydrostatic Pressure," by R. G. Olsson, *Ingenieur-Archiv*, vol. 9, 1938, pp. 108–115.

"Exact Solutions for Bending of Elliptic Plates," by L. N. Persen, Norske, Vid. Selsk. Forh, Trondjem, vol. 18, 1945, pp. 1–4.

"On a Particular Solution of the Biharmonic Problem for the Exterior of the Ellipse," by T. Pöschl, *Mathematische Zeitschrift*, vol. 11, 1921, p. 80.

"Applied Elasticity," by J. Prescott, Longmans, Green & Company, New York, N. Y., 1924, p. 469.

"Recherches sur les Problèmes aux Limites Relatifs à l'Equations de l'Élasticité à Deux Dimensions," by N. I. Muscheliŝvili, *Mathematische Annalen*, vol. 107, 1932, pp. 282–312.

Author's Closure

The author would like to thank Dr. Perry for suggesting additional references to papers treating elasticity problems involving elliptical boundaries. Since the publication of the author's paper, the following additional work on elliptical plates has been published:

"Bending of an Elliptic Plate With a Confocal Hole," by B. R. Seth, *Quarterly Journal of Mechanics and Applied Mathematics*, Oxford, vol. 2, part 2, 1949, pp. 177–181.

Matrix Solution for the Vibration of Nonuniform Beams[1]

H. W. Pope.[2] For obtaining frequencies only of simple beams such as treated by the author,[3] the method appears to involve less labor than Myklestad's tabular method.[3]

In flutter and dynamic load investigations of airplanes, the trend is to use complete airplane modes. Examining the aforementioned paper from the view of extending the results to obtain complete airplane modes and frequencies, it appears that it would be more cumbersome than an extension of Myklestad's method.

R. M. Rosenberg.[4] The author has given a concise formulation of Myklestad's method[4] of computing natural bending frequencies and modes which discloses the principles underlying this method perhaps more clearly than does the original paper by Myklestad. The compact notation of matrix algebra and the attendant ease with which details can be omitted lends itself, therefore, particularly well to classroom instructions. Thus the author's contribution lies primarily in the area of pedagogy.

Some of the points made by the author may be considered from a different point of view. For instance, any method treating correctly the problem at hand may be used successfully on "airplane wings and fuselages, bridges, critical speeds of shafts, and so forth," provided only that the structure under consideration behaves essentially like a long elastic beam. This applicability is not a characteristic peculiar to Myklestad's method only.

Also, while it is true that the uniqueness of Myklestad's method (and of similar methods in torsional vibration analysis) lies in the fact "that the shape of the vibration curve need not be assumed, and higher modes of vibration are obtained readily," it might be a formidable task requiring a great deal of experience on the part of the computer to determine the seventh frequency and mode, for instance, for it is necessary to assume a frequency which lies in the neighborhood of the seventh natural frequency and not the fifth, say.

To paraphrase the author's statement, but made with regard to the sweeping method,[5] it may be said "the uniqueness of the sweeping method (and other related methods) lies in the fact that natural frequencies need not be assumed, and the first and kth frequency and mode of a beam having k-sections may be obtained at once." Modes and frequencies between these extremes are obtained in a straightforward manner leaving no doubt as to which mode is being computed.

E. H. Bateman.[6] *Suggested Emendation.* The order of the vector components, and the rows of the matrix, in the last equation under "Computation Procedure," might be reversed to conform with the arrangement of Equation [6].

Suggested Modification of First Example. If the fixed and free ends of the cantilever were reversed, Equation [7] would read

$$\begin{vmatrix} A_{11} & A_{12} \\ A_{21} & A_{22} \end{vmatrix} = 0$$

which gives a determinate result for the case $n = 1$, i.e., $1 + mw^2(a_1 l - d_1) - mw^2 l(a_m l - d_m) = 0$ leading at once to the result $w^2 = 3EI/ml^3$, for a cantilever of uniform section with the mass m, concentrated at one end.

Suggested Extension of Final Illustration. At first sight the method of treating stepped beams looks formidable, and a few additional examples would complete the picture without marring the elegance of the paper. Thus (after adopting the first suggestion)

Uniform Cantilever:

Equation [7] of the paper gives $a^2 - bd = 0$, from which follows

$$\cosh \beta l + \sec \beta l = 0$$

Thus

$$\beta l = 1.88, 4.70, 5\pi/2, \text{ etc.}$$

Uniform Beam With Hinged Ends:

Equation [8] gives $b^2 - d^2 = 0$

that is

$$(\sinh \beta l)(\sin \beta l) = 0$$

which is satisfied by $\beta l = \pi, 2\pi, 3\pi \ldots$ etc. These are the well-known coefficients in the formula for frequency

$$w^2 = (\beta l)^4 EI/ml^4$$

General Comment. The regular method of finding natural frequencies of nonuniform beams is based on the Rayleigh approximation which gives results of sufficient accuracy for engineering design, with probably considerably less arithmetic than the formation of continued matrix products. The writer has recently completed a short set of tables by means of which the fundamental frequencies of simple cantilevers of nonuniform section can be estimated rapidly for stepped sections, as shown in Fig. 3 of the paper, and for sections in which the variation in stiffness can be expressed as a polynomial function of length. These tables, which it is hoped will be ready for publication before long, might be used to obtain preliminary estimates of the frequency for substitution in the author's matrix equations.

For the elementary problems of the beam and cantilever the matrix solution may possibly not show much advantage over an

---

[1] By W. T. Thomson, published in the September, 1950, issue of the Journal of Applied Mechanics, Trans. ASME, vol. 72, pp. 337–339.

[2] Project Engineer, Convair, San Diego, Calif.

[3] "New Method of Calculating Natural Modes of Uncoupled Bending Vibrations," by N. O. Myklestad, *Journal of the Aeronautical Sciences*, vol. 11, April, 1944, pp. 153–162.

[4] Associate Professor of Aeronautical Engineering, University of Washington, Seattle, Wash.

[5] "Higher Modes of Vibration by a Method of Sweeping, by L. Beskin and R. M. Rosenberg, *Journal of the Aeronautical Sciences*, vol. 13, November, 1946, pp. 597–604.

[6] Design Superintendent, Ministry of Supply, Highlands, Kent, England.

organized system of Rayleigh approximations, except in the determination of higher frequencies. Moreover, the failure of the matrix method to give any form of result in the author's examples shows that it may be necessary to take a large number of stations in order to compare with the accuracy obtained by the Rayleigh approximation.

The matrix method of solving this problem is, however, extremely powerful as witnessed by the ease with which standard results such as those in the foregoing comments can be pulled out. For this reason the matrix solution may well be found to be capable of reducing problems of greater complexity, where attempted solutions by existing methods quickly become unmanageable. One of the principal difficulties in such problems is that the preservation of continuity, at the boundaries of connected systems, greatly complicates the algebra. With the matrix solution, it appears that this preservation of continuity becomes automatic and the results depend upon straightforward matrix arithmetic.

Author's Closure

A requirement essential to a logical discussion of a problem is clear formulation, and in that respect the matrix method is well suited. However, the problem of the engineer seldom ends with formulation, the formidable part of vibration analysis generally being the computational task. This is especially true for high-mode calculations. Regardless of the method used, such analysis requires the attention of experienced personnel. The author well remembers an experience of his in attempting to calculate the higher modes of a vibrational system by the method of sweeping. No success was achieved until the effect of the order of significant figures involved in the calculation was recognized.

Dr. Bateman's deductions for simple beams from the matrix equation are of interest, and the author has since deduced results for other boundary conditions with equal ease.

The author has had an opportunity of discussing the computational procedure with Professor Myklestad, who states that the amount of time required for the numerical work is almost directly related to the number of figures one must write down. In that respect, if one wishes to do so, Equation [5]-may be computed by a table of the form shown herewith, where station 1 is a free end.

i	$m\omega^2$	S	M	θ	y
1		$m_1\,\omega^2$	0	φ	1
2					
3					
–					
–					
–					
–					
–					
n					

This table requires the writing down of a number of figures equal to that of the tabular scheme devised by Professor Myklestad.

It may be worth mentioning that the square matrix of Equation [5] can be expressed in an alternative form

$$[A_i] = [B_i] + m_{i+1}\omega^2[C_i]$$

where

$$[B_i] = \begin{bmatrix} 1 & 0 & 0 & 0 \\ l_i & 1 & 0 & 0 \\ -\alpha_{si} & -\alpha_{mi} & 1 & 0 \\ (\alpha_{si}l_i - d_{si}) & (\alpha_{mi}l_i - d_{mi}) & -l_i & 1 \end{bmatrix}$$

$$[C_i] = \begin{bmatrix} (\alpha_{si}l_i - d_{si}) & (\alpha_{mi}l_i - d_{mi}) & -l_i & 1 \\ 0 & 0 & 0 & 0 \\ 0 & 0 & 0 & 0 \\ 0 & 0 & 0 & 0 \end{bmatrix}$$

This form separates the inertia components from the elastic components.

Temperature Distribution in a Steady, Laminar, Preheated Air Jet[1]

M. Z. v. Krzywoblocki.[2] The author presented an elegant—mathematically—solution of the temperature distribution in a simplified case of a jet: The fluid is assumed to be incompressible, coefficients of viscosity and heat conductivity are assumed to be constant, and the dissipation function is completely neglected. For this reason, it is highly questionable whether the title. ". . . Air Jet" is correct unless we assume the presented solution to be the first approximation only. The assumptions refer rather to a liquid. The flow conditions of gases justify the following assumptions: Compressibility phenomena are taken into account, coefficients of viscosity and heat conductivity are functions of temperature and pressure (the second dependence may be omitted) since their variations are of the order of density variation, and the dissipation function is taken into account. The author did not mention that such solutions of both types of jets lately appeared in the literature.

Author's Closure

The present writer wants to thank Professor Krzywoblocki for his pertinent remarks and for the information of related papers that recently appeared in the literature. In the paper under discussion, it has been tacitly assumed that the temperature difference is small enough for the physical properties to be considered as practically constant, and yet large enough for the dissipation function to be neglected. Noteworthy also is the fact that for diffusion of one gas into another with approximately the same kinematic viscosity, the assumption that the kinematic viscosity and the diffusivity are constant is valid if the concentration difference is not excessively large. As to compressibility, the author feels that if the velocity is so large that compressibility cannot be neglected at large distances from the opening, the flow will probably not remain laminar there.

In recent papers by Professor Krzywoblocki dealing with laminar jets the temperature and velocity fields have been treated as interdependent, but the effect of gravitational force was not considered. It seems that when such interdependence is maintained, free convection due to variation of specific weight can be considered without introducing too much additional labor. A complete and rigorous treatment of the problems presented in the paper under discussion would be obtained only when the interdependence of velocity and temperature fields, a superimposed temperature difference, and free convection are all considered. For such a treatment, however, a simple solution in closed form has to be sacrificed.

The author would like to utilize this occasion to correct a few mistakes in his paper. In the introduction, it was wrongly stated that in 1937 Bickley gave a closed solution for the axial-symmetry case. It should have been the two-dimensional case. Also, following Equation [4], c_p (specific heat at constant pressure) in-

[1] By Chia-Shun Yih, published in the December, 1950, issue of the Journal of Applied Mechanics, Trans. ASME, vol. 72, pp. 381–382.

[2] Professor of Gasdynamics and Theoretical Aerodynamics, Secretary, Fluid Dynamics Panel, University of Illinois, Urbana, Ill.

stead of c_v (specific heat at constant volume) should have been used in defining the thermometric conductivity (or thermal diffusivity) if the fluid under consideration is a gas. In case the fluid considered is a liquid, c_v can remain unchanged.

Vibration of Rectangular Plates by the Ritz Method[1]

J. N. Goodier[2] and K. T. Chang.[3] The paper makes a notable addition to the list of results on record for the modes and frequencies of the square plate. As in the applications of the Ritz method to plates which Ritz himself made, the author employs series in which each term is a product of normal functions of a beam.

When the edges of the plate are clamped, the appropriateness of the normal functions of the clamped beam is apparent. Each term of the series will satisfy the boundary conditions of the plate and the determination of coefficients by the minimization process brings about an approach to satisfaction of the differential equation.

When the edges of the plate are free, the normal functions of a beam with free ends do not give terms in the series which each satisfy the free-edge boundary conditions of the plate. The beam functions will have vanishing second and third derivatives. The satisfaction of the free-edge plate conditions will require nonzero values of the corresponding derivatives. The plate-boundary conditions thus remain to be satisfied by the series as a sum. It appears that the minimization process is relied on for this, as bringing about an approach to the satisfaction of "natural" boundary conditions. The situation thus appears to resemble the representation of a constant as a Fourier sine series in the interval 0–π. The fact that as $x \to 0$ or π the constant must be the sum of a series of terms, each tending to zero, has its consequences in a slow rate of convergence. Is it then the case in the author's calculations that there is a similar disadvantage, but that it is offset by advantages such as orthogonality and simplicity of the beam functions? The result of the author's experience would be of value to us in calculations we have undertaken on the critical loads of rectangular plates.

A. Weinstein.[4] The author states that there appears to be little published data for the vibration of rectangular plates by Ritz's method and gives in Table 7 of his paper upper bounds for six frequencies of vibration of clamped square plates.

The writer wishes to draw attention to the following publications:

(*a*) Alexander Weinstein Memorial des Sciences Mathematiques, No. 88, 1937.

(*b*) N. Aronszajn, "The Rayleigh-Ritz and the Weinstein Methods for Approximation of Eigenvalues," Technical Report 3, ONR Project 041 090, in which the same problem has been discussed. These publications contain numerical upper and lower bounds for the first ten eigenvalues. In this way the accuracy of the results can be estimated with certainty, the errors ranging from 0.39 to 6.1 per cent. The numerical results obtained in the papers (*a*) and (*b*) will be submitted to the Applied Mechanics Division as soon as they are recomputed in the same units as the author's paper.

Author's Closure

As pointed out by Professor Goodier and Mr. Chang, the functions used in the paper for plates with free edges do not satisfy exactly the boundary conditions at the free edges. However, the so-called artificial or essential boundary conditions are satisfied and therefore, as shown in a number of the references in the paper, the functions used are valid ones for the Ritz method. The minimizing process assures the convergence of the quotient of the energy integrals to the true characteristic value. The question of the convergence of w to the exact mode shapes is more involved as has been discussed by R. Courant in reference (7) and related papers.

The reason for the choice of the beam functions is essentially the same as given by Goodier and Chang. For these functions it is found that diagonal terms in the determinant of Equation [13] are large compared to the other terms and, what is equally important from the point of view of ease of calculation, is that the characteristic value λ occurs only in the main diagonal term. As a consequence, by using a simple iteration procedure, a high-order determinant can be solved with moderate labor and thus a large number of terms may be used in the approximate series.

The author wishes to thank Professor Weinstein for calling attention to two additional publications dealing with the vibration of clamped square plates. These papers, which give data on both upper and lower bounds for the frequencies, constitute a major contribution.

Prof. Eric Reissner has very kindly sent the author two other papers which treat the problem of the clamped square plate. These are:

"The Transverse Vibration of a Square Plate Clamped at Four Edges," by S. Tomotika, *Philosophical Magazine*, series 7, vol. 21, 1945, pp. 745–760.

"On the Transverse Vibration of a Square Plate With Four Clamped Edges," by S. Tomotika, Report of the Aeronautical Research Institute, Tokyo Imperial University, Report No. 129, September, 1935.

The Stresses Around a Small Opening in a Beam Subjected to Pure Bending[1]

Lieut. Commander R. L. Karl, U.S.N.; Lieut. S. R. Heller, Jr., U.S.N., and Lieut. (jg) W. R. Gerich, U.S.N. It should be of interest to engineers, in general, to know that there is, at this time, some experimental verification of their theoretical work. The following discussion is the result of experimental work undertaken at the Massachusetts Institute of Technology for incorporation into a thesis:

Fig. 1 of this discussion shows the nomenclature used when referring to the opening. Table 1, herewith, represents the compilation of stress-concentration factors obtained photoelastically both at the boundary of the opening and at the free edge of the beam. These results are plotted in Fig. 2 against the ratio of depth of opening to depth of beam b/C, in contours of the ratio of length of opening to depth of opening a/b. It should be noted that values for direct comparison with the authors' work were obtained by extrapolation back to a ratio of $b/C = 0$. Fig. 3 shows the cross-fairing of these data with stress-concentration factor at the edge of the opening plotted against the ratio a/b in contours of b/C with the theoretical solution superimposed.

[1] By Dana Young, published in the December, 1950, issue of the Journal of Applied Mechanics, Trans. ASME, vol. 72, pp. 448–453.

[2] Professor of Engineering Mechanics, Division of Engineering Mechanics, Stanford University, Stanford, Calif. Mem. ASME.

[3] Division of Engineering Mechanics, Stanford University, Stanford, Calif.

[4] Research Professor, Institute for Fluid Dynamics and Applied Mathematics, University of Maryland, College Park, Md.

[1] By J. A. Joseph and J. S. Brock, published in the December, 1950, issue of the Journal of Applied Mechanics, Trans. ASME, vol. 72, pp. 353–358.

TABLE 1 SUMMARY OF EXPERIMENTAL DATA OBTAINED PHOTOELASTICALLY

Ratio of length to depth of opening a/b	Ratio of depth of opening to depth of beam b/C	Stress-concentration factor (SCF) Edge of hole	Edge of beam
	0.1115	2.067	1.060
	0.239	2.027	1.033
1.0	0.364	2.060	1.024
	0.485	2.180	1.040
	0.600	...	1.100
	0.100	1.430	1.045
	0.200	1.440	1.016
1.5	0.300	1.520	1.045
	0.400	1.648	1.124
	0.500	1.910	...
	0.100	1.320	1.026
	0.200	1.322	1.035
2.0	0.300	1.320	1.012
	0.400	1.410	1.072
	0.500	1.672	1.162
	0.100	1.160	1.077
	0.200	1.176	1.026
2.5	0.300	1.300	1.054
	0.400	1.280	1.087
	0.500	1.235	1.138

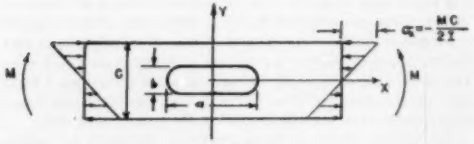

FIG. 1

Figs. 4 and 5 are similar to Figs. 2 and 3, except that the stress-concentration factors are those at the edge of the beam. It should be noted that the curve of stress-concentration factor for $a/b = 1$ (circle) coincides with that determined by Howland and Stevenson.[2]

Fig. 2 indicates that an opening approximately $^1/_4$ to $^1/_3$ of the depth of the beam may be made without fear of increasing materially the stress-concentration factor at the edge of the opening over that existing at $b/C = 0$, or that the stress at the edge of the opening will exceed that existing at the edge of the beam. Fig. 5 indicates that a definite maximum value of the stress-concentration factor at the edge of the beam exists in the region of $a/b = 1.5$. At this writing no satisfactory explanation for this has been found, but it is suspected that the radius of curvature at the ends is a major contributing factor.

Evaluation of Parameters. Neither the authors or Greenspan give any methods for the determination of s, t, and r—those parameters necessary for the evaluation of the tangential stress at the boundary. Many conditions may be imposed on Equations [10] of the paper with $\alpha = 0$ for their evaluation such as

(*a*) $s + t + r = {}^1/_2$ length $= {}^1/_2 a$
(*b*) $s - t + r = {}^1/_2$ depth $= {}^1/_2 b$
(*c*) Area of opening $= \int y\, dx$
(*d*) Radius of curvature at $\beta = 0$ = radius of semicircle $= {}^1/_2 b$

Using the Greenspan notation of p, q, and r and by substituting in Equations [10] with $\alpha = 0$, these become

For $a > b$	For $a < b$
(*a*) $p + r = {}^1/_2 a$	(*a*) $p + r = {}^1/_2 a$
(*b*) $q + r = {}^1/_2 b$	(*b*) $q + r = {}^1/_2 b$
(*c*) $pq - 3r^2 = \frac{b}{\pi}(a-b) + {}^1/_4 b^2$	(*c*) $pq - 3r^2 = \frac{a}{\pi}(b-a) + {}^1/_4 a^2$
(*d*) $\frac{(q-3r)^2}{p+9r} = {}^1/_2 b$	(*d*) $\frac{(p-3r)^2}{q+9r} = {}^1/_2 a$

} ... [1]

[2] "Biharmonic Analysis in a Perforated Strip," by R. C. J. Howland and A. C. Stevenson, Philosophical Transactions of the Royal Society of London, series A, vol. 232, 1933, pp. 155–222.

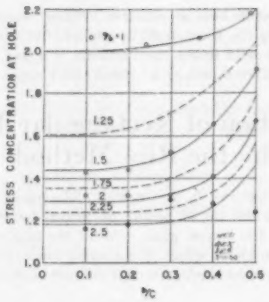

FIG. 2

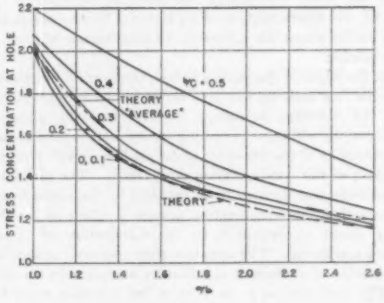

FIG. 3

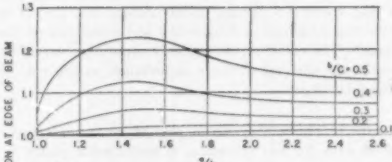

FIG. 5

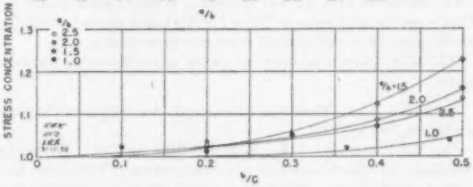

FIG. 4

Dealing with the case of $a > b$ only, and choosing b arbitrarily as 2, Equations [1] of this discussion become

$$\left.\begin{aligned} &(a)\ p + r = a/b \\ &(b)\ q + r = 1 \\ &(c)\ pq - 3r^2 = \frac{4}{\pi}(a/b - 1) + 1 \\ &(d)\ \frac{(q - 3r)^2}{p + 9r} = 1 \end{aligned}\right\} \quad \ldots\ldots\ldots [2]$$

This is a system of equations with one more equation than there is unknown, which is inconsistent. Accordingly, the four combinations of Equations [2] taken three at a time were solved, and the resulting values of p, q, r, and stress-concentration factor at the minor axis calculated. These results are summarized in Table 2, herewith, together with that of Case 1 of the paper.

TABLE 2 CALCULATED VALUES OF PARAMETERS OF OPENING

Properties held constant	Parameters	1.0	Values of a/b 1.5	2.0	2.5
Depth	p	1.0	1.586	2.1243	2.6871
Area	q	1.0	1.0334	1.0636	1.0914
Radius	r	0	—.0334	—.0636	—.0914
	SCF	2.0	1.524	1.327	1.212
Length	p	1.0	1.5303	2.059	2.5863
Depth	q	1.0	1.0303	1.059	1.0863
Radius	r	0	—.0303	—.059	—.0863
	SCF	2.0	1.547	1.346	1.196
Length	p	1.0	1.557	2.098	2.625
Depth	q	1.0	1.057	1.098	1.125
Area	r	0	—.057	—.098	—.125
Theory	SCF	2.0	1.450	1.264	1.164
Length	p	1.0	1.5234	2.0505	2.578
Area	q	1.0	1.0756	1.1115	1.135
Radius	r	0	—.0234	—.0505	—.078
	SCF	2.0	1.604	1.400	1.266
Case 1	p			2.064	
	q			1.108	
	r			—.079	
	SCF			1.304	
Average	p	1.0	1.5492	2.083	2.6191
	q	1.0	1.0491	1.1083	1.1094
	r	0	—.038	—.0678	—.0952
	SCF	2.0	1.515	1.322	1.218

NOTE: Stress-concentration factor = SCF.

Also included in this table are the values of the arithmetic averages of the four previous calculations. This latter set of values is included because it was found, quite by accident, to agree quite closely with the experimental values obtained for $b/C = 0.3$, a fairly average practical condition.

The stress-concentration factors plotted as "theory" in Fig. 3 are those obtained using the values from Table 2 listed while holding length, depth, and area constant. This particular set was used because it is the opinion of the writers that this represents the closest fit to the actual hole. On a very large-scale plot of one quadrant of an opening with $a/b = 2$ (Case 1 in the paper), curves representing those of the four calculated values and that of the paper were plotted and studied quite carefully for discrepancies. Figs. 6 and 7, herewith, are plots of the values of parameters versus a/b for theory and "average," respectively.

Finally, Equation [27] of the paper has been put into a slightly more usable form by expressing it as the maximum stress-concentration factor (at the vertical diameter, $\beta = 90$ deg) and eliminating the parameter T

$$\frac{(\sigma_\beta)_{\alpha=0}}{-\frac{M}{I}y_0} = \frac{\frac{2s}{y_0}\left[(s - 2r)(s + r) - (t - 2r)^2 - \frac{rt}{s}(t - 3r)\right]}{(s + t - 3r)^2} \quad \ldots [3]$$

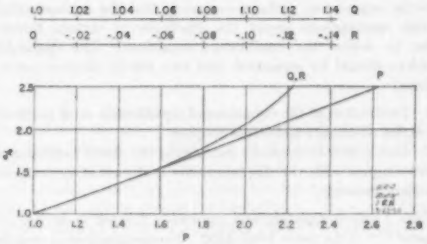

FIG. 6

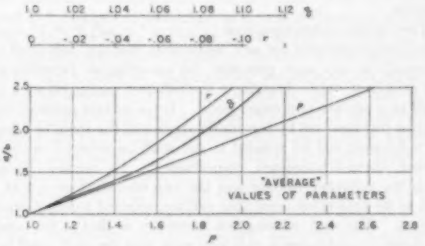

FIG. 7

The writers wish to extend their gratitude to the ASME Applied Mechanics Division for granting them the privilege of participation in their Semi-Annual Meeting and to the authors for an excellent paper.

AUTHORS' CLOSURE

The authors wish to thank the contributors of the valuable discussion of the paper. It is gratifying to observe that the difference between their experimental results and our theoretical analysis is very small and probably within the accuracy of the experiment. This is rather remarkable when one considers the fact that the equations used in the paper gave only an approximation to the true opening. An experimental curve of the stress distribution around the boundary of the opening would be of additional interest.

It should be pointed out that the thesis[2] from which the discussion was extracted contains more detailed information both on experimental procedure and evaluation of the parameters of the opening.

On the General Theory of Thin Shells[1]

C. TRUESDELL.[2] The literature attempting to derive correct equations for thin elastic shells has become extensive and repetitious. A thorough, accurate, and critical review of this subject is desirable. The paper under discussion is among the many which

[2] "The Effect of Small Holes on the Stress Distribution in Webs Subjected to Pure Bending," by R. L. Karl, S. R. Heller, Jr., and W. R. Gerich, submitted as a thesis for the degree of Naval Engineer, Massachusetts Institute of Technology, May 1950.

[1] By W. R. Osgood and J. A. Joseph, published in the December, 1950, issue of the JOURNAL OF APPLIED MECHANICS, Trans. ASME, vol. 72, pp. 396–398.

[2] Professor of Mathematics, Graduate Institute for Applied Mathematics, Indiana University, Bloomington, Ind.

give the impression, perhaps incorrect, that the authors employ certain assumptions about the smallness of certain terms in order to derive the equilibrium equations. The elastic shell problem should be separated into two wholly distinct parts as follows:

1 Derivation of the equations of equilibrium or of motion for the stress resultants and stress couples.

2 Derivation of relations connecting the stress resultants and stress couples with the displacements and partial derivatives of the displacements.

Part 1 was completely and rigorously treated in at least four papers[5,6,7,8] in the years 1942–1950. No assumptions of smallness of any kind are needed to derive the differential equations and boundary conditions in terms of stress resultants and stress couples.

The Cauchy stress equations ($t^{ij}{}_{,j} + \rho f^i = \rho \ddot{x}^i$, $t^{ij} = t^{ji}$, $t_{(n)}{}^i = t^i{}_j n^j$) hold rigorously for any continuous medium deformed continuously in any way, provided the co-ordinates be referred to the deformed state. Imagine a shell-shaped region, either a shell itself or a portion of a larger body. Let a certain surface, which may be but need not be the middle surface of the shell, be selected for reference, and let a point in the shell be referred to the following three-dimensional co-ordinates: its normal distance from the reference surface and the two co-ordinates u, v of the foot of its projection upon that surface, referred to any Gaussian system. The only assumption necessary is that it be possible to choose co-ordinates in this way such that the shell itself is the region bounded by the two surfaces $z = \delta_1(u, v)$, $z = \delta_2(u, v)$, which two surfaces are supposed to cut neither themselves nor each other at any point, and the thickness of the shell is thus $|\delta_2 - \delta_1|$, not necessarily constant. Let the general three-dimensional Cauchy stress equations be referred to this co-ordinate system. Now define stress resultants and stress couples in the usual way. By integrating the general equations from $z = \delta_1$ to $z = \delta_2$, precisely the ordinary equations of equilibrium or motion for shell theory are obtained. The only points at which approximations may occur are as follows:

1 When the displacement gradients are small, derivatives with respect to the co-ordinates in the deformed state may be replaced by derivatives with respect to the initial co-ordinates: $\partial/\partial u \approx \partial/\partial u_0$, etc.

2 When the displacements are small, each term in the equations may be evaluated at the corresponding initial point: $f(u, v, z) \approx f(u_0, v_0, z_0)$.

3 When the shell is thin the various load terms, which in the exact shell equations are fairly complicated functions of the body forces and of the loads (or stresses) on the inner and outer surfaces of the shell, may be replaced by the components of resultant force and moment per unit area of the reference surface.

Assumptions 1 and 2 are always made in the three-dimensional linear theory of elasticity. Assumption 3 is peculiar to shell theory, but it is not strictly necessary (nor does it effect any marked simplification), and for the case of a thick shell it should not be used.

Since part 1 is wholly settled, discussions of the foundations of shell theory should be limited to part 2, where remain the real difficulties and points still at issue.

[5] "On an Error in a Hypothesis of the Theory of Shells," by V. V. Novojilov, C. R. (Doklady) Academy of Sciences, URSS, vol. 2, 1943, pp. 160–164.

[6] "The Membrane Theory of Shells of Revolution," by C. Truesdell, Trans. American Mathematical Society, vol. 58, 1945, pp. 96–166. See §§ 4, 5, 8.

[7] "Derivation of the Equations of Equilibrium of an Elastic Shell From the General Theory of Elasticity," by W. Z. Chien, Science Reports, National Tsing Hua University, series A, vol. 5, 1948, pp. 240–251. Material in this paper understood extracted from the author's 1942 Toronto dissertation.

[8] "The Equilibrium of Thin Elastic Shells," by A. E. Green and W. Zerna, *Quarterly Journal of Mechanics and Applied Mathematics*, vol. 3, 1950, pp. 9–22.

Closure by J. A. Joseph

The author sincerely agrees with Professor Truesdell's comment that "a thorough, accurate, and critical review of this subject is desirable." The paper under discussion was, it was thought, a step in this direction. We started with one generally accepted system of approach (Love's General Theory of Thin Shells, which many engineers find applicable to their problems) and pointed out the errors that Love had made.

It was not our intention to present a new theory or to change any of Love's hypotheses or to extend the theory to any higher order of accuracy. Rather it was to be certain that all terms of the established order of accuracy were retained under the hypotheses and mathematical method of approach that Love had established.

The author disagrees with Professor Truesdell's comment that "Part 1 was completely and rigorously treated in at least four papers in the years 1942–1950." In fact, the latest of these four papers (Professor Truesdell's Reference 6) says, in March, 1950, "It appears that it is still desirable to attempt to develop a theory of thin shells which can be used for practical applications and which is, as far as possible, a systematic first approximation."

Of the four references given by Professor Truesdell: (*a*) References 5 and 6 seem to be excellent treatments in tensor notation of the subject. No doubt some may find the solutions practical and systematic. (*b*) There seems to be some mistake in the footnote detailing Reference 3. The journal specified did not contain (in the Library of Congress copy) any article by Novojilov or on this subject. (*c*) Reference 4 treats a special case.

The remainder of Professor Truesdell's comments are of interest but refer to matters outside the objectives of the paper under discussion.

In a recent publication by T. Au, L. E. Goodman, and N. M. Newmark, "A Numerical Procedure for the Analysis of Pressure Vessel Heads," Technical Report to ONR, department of civil engineering, University of Illinois, Urbana, Ill., Feb. 15, 1951, there is an excellent annotated bibliography, pp. 89–105. It contains a discussion of our paper that sums up our own feelings on the subject: "(the paper) pointed out inconsistencies in Love's equations of equilibrium and presented a new set of equations. However, these equations reduce to Love's equations when the deformations of the middle surface is inextensional and irrotational. While these comments on Love's theory are in general sound and indeed convincing, it may also be noted that such modifications and corrections may be of little practical importance. In particular, the case of pressure vessels, the extension and rotation of the middle surface are small." But, the big point is that one does not know in general whether the modifications and corrections are of practical importance except by considering each special case on its own merits.

Book Reviews

Elasticity

ELASTICITY. Volume III. Proceedings of the Third Symposium in Applied Mathematics of the American Mathematical Society. Held at the University of Michigan, June 14–16, 1949. Cosponsored by The Applied Mechanics Division of The American Society of Mechanical Engineers. Editorial Committee R. V. Churchill, Eric Reissner, A. H. Taub. McGraw-Hill Book Company, New York, N. Y., 1950. Cloth, 6½ × 10 in., illus., v and 233 pp., $5.

REVIEWED BY S. TIMOSHENKO[1]

THIS book is a collection of papers on the mathematical theory of elasticity and its applications. These papers were presented at the joint meeting of the American Mathematical Society and the Applied Mechanics Division of the American Society of Mechanical Engineers which was held at the University of Michigan in June, 1949. Collaboration of this sort is especially important nowadays since engineers are constantly calling for greater accuracy in the solution of stress-analysis problems. While research engineers can contribute much toward the mathematic formulation of practical problems, they will gain a great deal of help toward solving them by coming into contact with mathematicians who are interested in the application of their subject to the theory of elasticity.

In the early days of the theory there was no such need for collaboration. The originators of the theory of elasticity, Navier, Cauchy, Poisson, were graduated from the famous École Polytechnique and were given a combined mathematical and engineering training. Again, later workers (e.g., Lamé and Saint Venant) not only received a complete training, but also practiced engineering for considerable periods. However, in more modern times, the great mathematician Felix Klein advocated a much closer liaison between mathematicians and engineers and it is largely due to his influence that societies of applied mathematics and mechanics were organized first in Germany and later on in other countries. As an example of progress in engineering mechanics accomplished by the combined activity of mathematicians and engineers we can take the case of Russia. At the beginning of the twentieth century a better contact between mathematics and engineering was established under the influence of such men as N. E. Joukowski, A. N. Krylov, and S. A. Chaplygin, and the use of mathematics in engineering research was further developed by their pupils. As a result of this, now Russia occupies a strong position in such fields as theory of elasticity, plasticity, and nonlinear mechanics. Some of the papers in the book under review are closely related to Russian publications.

The contents of the book can be divided into three parts: (*a*) papers on theory of elasticity proper, (*b*) papers on plates and shells, and (*c*) papers on plasticity. Starting with the first group we find I. S. Sokolnikoff's paper dealing with two-dimensional problems in anisotropic elasticity. This kind of work is of great practical importance especially in airplane structures where materials are sometimes used whose elastic properties are quite different in different directions. The theory of anisotropic elasticity has seen rapid advances recently, especially in Russia. In a recent review[2] of this field, 88 Russian publications are mentioned and the principal results obtained in them are given in the book "Anisotropic Plates by S. G. Lechnitsky.[3] Sokolnikoff, in his paper, limits himself to the case where the material has only slight anisotropy, and describes the method of solution developed for such problems by Lechnitsky. He also refers to the work which is going on at present under his direction at the University of California (Los Angeles).

The next paper, "Beams Under Concentrated Loading" by G. E. Hay, has a somewhat misleading title. Hay is not concerned with beams but considers, as a two-dimensional problem, a ring bounded by two confocal ellipses and compressed by two equal and opposite forces applied at the ends of the major axis. He uses the method of Muschelisvili and derives the required solution in series form. For one shape of ring he also made numerical calculations, but as the results of these are not given we cannot make a comparison of the rigorous solution with the results of the elementary theory (which assumes that cross sections of the ring during bending remain plane).

In the paper by B. R. Seth the theory of finite elastic deformation is briefly discussed and its application in such cases as simple tension, compression, pure bending and Lamé's problem is shown. A long list of new publications on finite deformations is given in the conclusion.

The paper by A. Weinstein is of a more mathematical character. It gives a review of some recent investigation on inequalities and estimates for torsional rigidity.

H. Poritsky discusses the problems of torsion of a shaft of variable diameter and also of a shaft of uniform cross section twisted by forces distributed over a lateral surface. For the latter problem some particular cases are considered and results are presented in the form of charts.

From the second group of papers the work of Eric Reissner is of special interest to engineers. Forty years ago, Hans Reissner showed how the deformation of a spherical shell can be analyzed when the displacements are small. Here his son makes the next step and discusses axisymmetrical deformations of shells of revolution involving finite displacements. He does not limit himself to the derivation of general equations of equilibrium, but applies these equations to the particular cases of spherical and cylindrical shells and shows that the range of applicability of the small-deflection theory is in some respects greater than that of the small-deflection theory of bending of flat plates. He also makes a more detailed study of the shallow spherical shell and shows the limits beyond which both bending and membrane action must be taken into account.

The paper by F. B. Hildebrand deals with asymptotic integration in shell theory. This method has not found wide application in engineering. Designers usually apply the so-called "Geckeler" method[4] and an investigation of the accuracy of this and a comparison of the two methods (having regard to the time required for arriving at a sufficiently accurate result) would be of great use.

In the interesting paper by K. O. Friedrichs, a discussion of Kirchhoff's boundary conditions and the edge effect for elastic plates is given. The method applied yields a justification of Kirchhoff's boundary conditions.

[1] Professor of Engineering Mechanics, Stanford University, Stanford, Calif. Fellow ASME.

[2] "Mathematical Theory of The Elasticity of Anisotropic Media," by M. M. Fridman, *Prikladnaya Matematika i Mekhanika*, Russian, 1950, vol. 14, no. 3, pp. 321–340.

[3] "Anisotropic Plates," by S. G. Lechnitsky, Moscow, 1947, 355 pp.

[4] See "Handbuch der Physik," 1928, vol. 6, p. 246.

The paper by D. L. Holl discusses dynamic loads on thin plates on elastic foundations. Neglecting the mass of the moving load and of the foundation and assuming that the reaction of the foundation is normal to the plate and proportional at each point to the deflection at that point, a transform solution of the problem is obtained. This is applied to the particular cases of a simply supported rectangular plate and a plate with circular symmetry. In the latter case, the problem of a pulsating concentrated force acting on an infinite plate is discussed.

Among the papers on plasticity we have an abstract of R. V. Southwell's Symposium address. In that address Southwell showed how his "relaxation method" can be applied in investigating elastic-plastic straining in two-dimensional and torsional problems.

In conclusion, the reviewer would like to make the two following remarks: (1) In the papers on elasticity, each author uses his own notation. Reading would be greatly simplified by the use of some standardized symbols. (2) In references to Russian publications, we must not only keep the language difficulty in mind but also the difficulty of getting the necessary publication in many instances. The use of Russian work would be greatly simplified, if some of the important books were translated into English. The Russian literature on anisotropic elasticity is very completely presented in the afore-mentioned book by S. G. Lechnitzky. That of plasticity is presented in Sokolovsky's book[5] and the numerous publications of N. I. Muschelisvili and of his pupils are very completely covered in the new edition of Muschelisvili's book on elasticity.[6]

Maschinenelemente

MASCHINENELEMENTE. By G. Niemann. Volume I. Springer-Verlag, Berlin, Göttingen, Heidelberg, Germany, 1950. Cloth, 7½ × 11 in., viii and 308 pp., 795 figs., tables, bibliography, index, Dm 28.50.

REVIEWED BY L. M. TICHVINSKY[7]

AS USUAL Julius Springer books are well edited and contain numerous expertly drawn sketches and graphs. This book is no exception from these general standards; perhaps some lower quality of the paper and of the binding may be noticed. This volume is made up of the following four main parts; fundamentals, elements for connection, bearings, and shafting. Fundamentals are presented on the first 60 pages and begin with a short note on the art of construction of machine elements followed by considerations of economy, service, and safety. General remarks are made with regard to the technology associated with welding, casting, pressing, as well as with various basic types of machining. Considerable space is devoted to the problems of wear and corrosion, this being a rather new and welcome addition to textbooks on machine design. Elementary strength of materials is reviewed and supplemented with a discussion of failures due to fatigue, vibration, and impact. One chapter is on lightweight constructions incorporating lightweight materials and lightweight designs such as used in aviation industry. Concluding the first part is a chapter on engineering materials, describing the main physical and chemical properties of ferrous, nonferrous, and nonmetallic materials. The second part of the book describes various methods of connections such as obtained by welding, soldering, and by the use of rivets and bolts. A comprehensive discussion of all practical types of springs, with a short description of elements employing rolling and sliding contacts concludes the second part of the book. The two last parts of the book are devoted to bearings and shafting. Ball and roller bearings are discussed with special reference to loading and life limits. The performance of journal bearings is described as based on the hydrodynamic theory of lubrication together with a review of bearing materials and lubricants used. Shafting and shaft connections conclude the last part of the book.

The book is well illustrated and is supplemented with numerous tables and graphs all of which will be of value to students and to designers of actual machine elements. There are few, not too many, working examples. Each chapter is supplemented with a rather impressive bibliography which is abundant with references of the last ten to fifteen-year period. However, among the many German references (over 650) there are only eleven American references.

[5] "Theory of Plasticity," by W. W. Sokolovsky, Moscow, 1946.

[6] "Some Fundamental Problems of the Mathematical Theory of Elasticity, by N. I. Muschelisvili, Moscow, 1949, 635 pp.

[7] Professor of Mechanical Engineering, University of California, Berkeley, Calif. Mem. ASME.

Classical Mechanics

CLASSICAL MECHANICS. By H. C. Corben and Philip Stehle. John Wiley and Sons, Inc., New York, N. Y., Chapman and Hall, Ltd., London, England, 1950. Cloth, 5½ × 8½ in., diagrams, bibliography, index, xvii and 388 pp., $6.50.

REVIEWED BY E. H. LEE[8]

THIS is a book on advanced dynamics written primarily for physics students, and it emphasizes the carry-over of the concepts of classical dynamics to the quantum theory and relativity theory of modern theoretical physics. Examples are taken mainly from physics, for example, particle-scattering theory and the vibrations of molecules.

Thus the emphasis differs from that usual in applied-mechanics courses, but the reviewer, who has been trained mainly in the field of applied mechanics, found this difference of outlook stimulating. However, for course work in an applied-mechanics department this book would probably be found to overemphasize the theoretical physics aspects of dynamics and to carry general theory further than is usual.

The book is carefully written from an advanced standpoint. A novel feature is a set of introductory exercises which the reader should be able to solve easily before studying the main text. These comprise problems of motion in one dimension, trajectories with and without air resistance, and rigid-body problems of rolling cylinders connected by ideal weightless threads.

A careful notation is used, the distinction between covariant and contravariant tensors being introduced with the discussion of co-ordinate systems, and carried through the book. After these preliminaries, systems of particles are discussed, and in chapter 5 Lagrange's equations. Applications follow, including chapters on linear vector spaces and application to small oscillations of conservative systems. A chapter on rigid-body motion completes the first half of the book. The second half is concerned with Hamiltonian theory, contact transformations and their developments. There is a chapter on special relativity theory, and a final chapter (chapter 18) on the motion of particles in high energy accelerators.

In spite of the care with which the book is written the reviewer noticed one or two errors. The discussion of the theory of normal modes of vibration is based on the statement that the dynamic matrix is symmetric. This is true only in very special circumstances when the product of symmetric matrixes gives a symmetric matrix. However, this shortcoming of the general discussion in this chapter does not appear in the examples, for this matrix product is not used in the detail treatment.

[8] Associate Professor of Applied Mathematics, Graduate Division of Applied Mathematics, Brown University, Providence, R. I. Mem. ASME.

To sum up, this book will be of particular value to workers in the field of applied mechanics who wish to carry over into the field of theoretical physics. With the development of nuclear engineering, there will presumably be an increasing number of such people.

The Variational Principles of Mechanics

THE VARIATIONAL PRINCIPLES OF MECHANICS. By Cornelius Lanczos. Mathematical Expositions, No. 4. University of Toronto Press, Toronto, Ont., Can., 1949. Cloth, 5 1/2 × 8 1/4 in., 22 figs., bibliography, index, xxv and 307 pp., $4.

REVIEWED BY ERIC REISSNER[9]

THE present text is a basic treatment of particle mechanics. It does not, as the title might lead one to expect, include such matters as variational principles and methods in elasticity, plasticity, and hydromechanics. The scope of the book may be indicated by the headings of the various chapters: (1) Basic concepts of analytical mechanics; (2) the calculus of variations; (3) the principle of virtual work; (4) d'Alembert's principle; (5) the Lagrangian equations of motion; (6) the canonical equations of motion; (7) canonical transformations; (8) the partial differential equation of Hamilton-Jacobi; (9) historical survey. The author's aim is not to teach the solving of problems but rather to help gain insight into the structure and significance of the body of classical mechanics. While the presentation appears to be leisurely and penetrating, this reader, at least, soon found out that it required considerable effort and concentration on his part to follow the latter portions of the work. It is clear, however, that this book is an eminently serious piece of work, worthy of study by those who are teachers of applied mechanics.

Engineering Mechanics

ENGINEERING MECHANICS. By S. Timoshenko and D. H. Young. McGraw-Hill Book Company, Inc., New York, N. Y., Third edition, 1951. Cloth, 6 × 9 in., 736 figs., problems, appendixes, index, xiv and 517 pp., $5.50.

REVIEWED BY N. O. MYKLESTAD[10]

THE make-up of the third edition is similar to that of the second edition but many details of the text have been improved by the revision. The entire book has 195 examples and 650 problems divided about equally between the statics and dynamics parts, while the second edition had 567 problems some of which were in the nature of illustrative examples. The main change in the third edition, therefore, is the addition of a large number of illustrative examples and many excellent problems.

Part 1, dealing with statics, starts with the introduction of force systems and proceeds logically through concurrent forces in a plane, parallel forces in a plane, general case of forces in a plane, forces in space, and finally ends with a chapter on virtual displacements.

Part 2, dealing with dynamics, starts with the principles of dynamics and proceeds through rectilinear and curvilinear translation, rotation about an axis, plane motion, and relative motion. There are also two appendixes on moments of inertia of plane figures and solid bodies.

In the statics part the inclusion of a chapter on virtual displacements with its many excellent examples and problems is particularly gratifying; while in the dynamics part d'Alembert's principle is used extensively and to good advantage.

Another feature of the book is that the sections on momentum, angular momentum, and energy are scattered all through the dynamics part of the book whenever it is appropriate to discuss these topics rather than having them collected in separate chapters.

In the opinion of the reviewer the book is well balanced as to contents and its clear and rigorous style puts it in the forefront among undergraduate textbooks on engineering mechanics. The only criticism that occurs to the reviewer is that free-body diagrams could have been used more freely in setting up the equations of equilibrium.

International Association for Bridge and Structural Engineering

FINAL REPORT OF THE THIRD CONGRESS OF THE INTERNATIONAL ASSOCIATION FOR BRIDGE AND STRUCTURAL ENGINEERING, edited by F. Stüssi and P. Lardy. Swiss Federal Polytechnic Institute, Zurich, Switzerland, 1950. Cloth, 7 × 9 1/2 in., illus., 736 pp., 450 Belgian fr.

REVIEWED BY N. J. HOFF[11]

THIS volume is a follow-up of the preliminary publication reviewed earlier in this Journal.[12] It contains a general description of the activities of the Congress, the opening and closing addresses of the officers and honorary officers, and the conclusions and suggestions of the five panels of the Congress as well as a total of 70 original technical contributions. Thirty-five of the technical papers are in French, 24 in English, and 11 in German. All of them have summaries in all the three languages and the conclusions of the panels as well as the tables of contents are printed in the three official languages of the Congress.

As the Congress made important contributions to the theory and art of structural engineering, it is regrettable that American engineers participated so little in its activities. Of the members of the Congress, 98 were Belgian, 49 French, 38 Swiss, 32 English, 32 Dutch, 32 Swedish, 15 Danish, 10 Italian, 10 Czechoslovakian, 7 Norwegian, 7 Portuguese, 7 Finnish, 6 Luxemburger, 4 Austrian, 4 Yugoslavian, 3 Hungarian, 3 Turkish, 3 Egyptian, 3 Spanish, 1 Canadian, and only 5 were from the United States.

The only American contributions in this final report are a paper by Prof. L. E. Grinter of the Illinois Institute of Technology entitled "Stresses in Gusset Plates by Use of an Analogous Grid," a supplement to the general report on "Developments in Long-Span Steel Bridges" by Dr. O. H. Ammann, consulting engineer, New York, N. Y., and a paper by E. E. Howard of Kansas City, Mo., on the "Erection of the Main Span of the Mississippi River Bridge in Dubuque (Iowa)." Professor Grinter applied his method of numerical analysis developed earlier in "Numerical Methods of Analysis in Engineering," (The Macmillan Co., New York, N. Y., 1949) to the problem of the stresses in gusset plates. Dr. Ammann makes a few short additions to his original report presented in the preliminary publication and Mr. Howard gives details of the erection procedure of the Julien Dubuque highway traffic bridge. Of the other papers, only those which the reviewer

[9] Professor of Mathematics, Massachusetts Institute of Technology, Cambridge, Mass. Jun. ASME.

[10] Professor of Theoretical and Applied Mechanics, University of Illinois, Urbana, Ill. Mem. ASME.

[11] Head of Department of Aeronautical Engineering and Applied Mechanics, Polytechnic Institute of Brooklyn, Brooklyn, N. Y. Mem. ASME.

[12] JOURNAL OF APPLIED MECHANICS, Trans. ASME, vol. 71, 1949, pp. 325–326.

found particularly interesting will be mentioned by title or name of the author.

The technical papers are presented in five chapters. The first deals with "Assembling Devices and Structural Details in Steel Structures" and contains 21 original contributions. A good portion of this chapter treats of the problems of the failure of welded structures. Although some authors present investigations of the weldability of various alloys, the main effort is directed toward measurement and calculation of the stresses caused by shrinkage. In particular, Belgian and French engineers have contributed much to the clarification of these problems. The most prominent names to be mentioned in this connection are those of Prof. F. Campus of the University of Liége and H. Louis, director of the Department of Highways and Bridges in Liége, Belgium. Details of welded bridge structures are discussed by these two men as well as by Prof. F. Faltus of Prague, Czechoslovakia, and Dr. Szechy of Budapest, Hungary. The latter gives an impressive account of the unusual solutions necessitated by the shortages in materials, equipment, and skilled labor in Hungary after the war when the long-span bridges, dynamited by the retreating Germans, had to be reconstructed. Dr. C. Massonnet of the University of Liége presents a method for the calculation of the stresses in the nodes of Vierendeel girders and by means of the large-deflection theory gives an interesting demonstration of the difficulties involved in determining the buckling loads of plates which are not completely plane. Dr. C. F. Kollbrunner of the Polytechnic Institute of Zurich, Switzerland, reports on tests in which good agreement was obtained with the theory of the buckling of rectangular plates having various edge conditions. Prof. H. Nylander of the Polytechnic Institute of Stockholm, Sweden, describes a method by which the resistance of I-beams to lateral buckling was increased.

Chapter 2 is entitled "Developments in Building Structures in Concrete and Masonry." Most of the 18 papers in this chapter are devoted to the significant improvements in the efficiency of reinforced-concrete structures attained through the prestressing method originated by E. Freyssinet of Paris, France. Mr. Freyssinet describes a number of bridges designed and constructed according to this method. Prof. K. Hofacker of Zurich, Switzerland, discusses a beautiful arch bridge originally designed by Prof. N. Ritter; Kurt Billig of London, England, shows pictures of the modern Dublin airport terminal; Dr. H. Gottfeldt of London, England tells about an unusual floating horizontal arch bridge across the Derwent River near Hobart in Tasmania.

A new method of introducing prestressing by means of expanding cements is presented by Henry Lossier of Paris, France; Prof. E. Friedrich of the Polytechnic Institute of Graz, Austria, reports on recent research results on prestressed concrete; and Kurt Billig of London, England, describes the efforts of the Ministry of Works of Great Britain to develop prestressed concrete as a substitute for timber and steel for transmission poles, telegraph poles, structural beams, and floor units. Dr. P. W. Abeles of London, England gives some conclusions on the behavior of prestressed concrete at cracking. The welding of steel rods in reinforced concrete is discussed by A. Hormidas and H. Louis, directors of the Department of Highways and Bridges of Belgium, while Michel Fahmy of Cairo, Egypt, describes an interesting warehouse construction having mushroom floor slabs.

The subject of "Developments in Long-Span Steel Bridges," treated in chapter 3 of the volume, is introduced by Dr. O. H. Ammann. Prof. F. Stüssi of the Polytechnic Institute of Zurich, Switzerland, presents theoretical considerations for the choice of the system of long-span bridges and develops a rather simple new method of analysis for suspension bridges. This chapter contains seven articles.

Chapter 4, consisting of 14 contributions, deals with "Slabs and Various Curved Structures in Reinforced Concrete." A number of structures utilizing mushroom slabs are described by C. F. Casado of Madrid, Spain, and an unusual thin shell roof construction in reinforced concrete is presented by Prof. E. Torroja, also of Madrid. Interesting contributions to the theory are made by Dr. A. M. Haas of The Hague, Holland, who calculates the stresses in mushroom slabs; by L. Broglio of Rome, Italy, who develops a new analysis of thin-wall shells in the form of ruled surfaces; and by Dr. K. W. Johansen of the Polytechnic Institute of Denmark in Copenhagen who deals with the theory of failure of reinforced-concrete slabs, the integration of the differential equations of the membrane theory of shells and with the design of cylindrical shells.

Chapter 5, containing 10 contributions, is entitled "Analysis of Safety and Effect of Dynamic Forces." Although some interesting ideas on the use of probability calculations in determining the safety of structures are presented by F. V. Costa of Lisbon, Portugal, and by Prof. E. Torroja of Madrid, Spain, the French team consisting of engineers of the Department of Highways and Bridges, the Department of Buildings and Public Works, and the National Society of French Railroads still carries the ball most of the time. Following up the fundamental work printed in the preliminary publication more data are given on the dispersion of strength test results. M. Cassé of the National Society of French Railroads shows that the minimum failing stress of mild steel is considerably smaller than generally assumed. For instance in a batch of 512 test specimens cut out of a single sheet of steel the minimum failing stress was found to be 35.6 kg per sq mm (50,600 psi) when the maximum failing stress was 46.3 kg per sq mm (66,000 psi). Dr. Marcel Prot, chief engineer of the department of highways and bridges, reports on tests carried out with specimens of concrete and mortar. He found that one has to test 350 to 400 specimens with a great deal of care in order to obtain an average that is accurate within 1 per cent. One hundred and fifty specimens result in an average that may be off by as much as 3 per cent. If only five or six specimens are tested, as is usual in practical work, the results must be considered entirely unreliable.

The editing and printing of this book and the reproduction of the figures are excellent. It would be well for the Congress for Theoretical and Applied Mechanics to use this volume as a standard for their future publications.

Mathematical Engineering Analysis

MATHEMATICAL ENGINEERING ANALYSIS. By Rufus Oldenburger. The Macmillan Company, New York, N. Y., 1950. Cloth, 6¼ × 9¼ in., 220 figs., appendix, index, xiv and 426 pp., $6.

REVIEWED BY WALTER W. SOROKA[13]

THE author states, and this reviewer concurs, that one of the most difficult tasks in industrial research is that of expressing physical situations in terms of equivalent mathematical relations. This book, which is an outgrowth of courses on the subject at the Illinois Institute of Technology and De Paul University, seeks to help the engineering research worker formulate physical problems mathematically. Once a mathematical formulation has been established, various methods of obtaining numerical answers become available from other sources, hence the book concentrates on the primary problem of setting up the governing equations and logically avoids, for the most part, becoming involved in methods of solution.

The book is divided into five parts, each part being concerned with a broad engineering field, as follows: Part 1, mechanics of

[13] Associate Professor of Engineering Design, University of California, Berkeley, Calif.

rigid bodies; Part 2, electricity and magnetism; Part 3, heat; Part 4, elasticity; Part 5, fluid mechanics. A set of problems at the end of each part enables the reader to evaluate his grasp of the principles set forth in the preceding pages. Answers and hints given at the end of the book provide a check and help prevent possible frustration.

The book does require a good background of advanced calculus and vector analysis. The author makes this clear in his preface, and it becomes evident as one reads the book. It is not a book that can be read easily by the usual research engineer, and yet the subject matter itself, for the most part, is rather elementary such as that usully covered in undergraduate courses in physics and engineering. The difficulty perhaps arises from the book's point of view, namely, that of an active researcher in pure mathematics turned to applied mathematics and the engineering field.

The material is presented in a highly compressed form. Thus, the entire field of rigid-body mechanics, including basic concepts of dimensions, forces, gravitation, momentum, energy, collision, vibration in one and two-degrees of freedom, dynamics of rockets and airplane flight, is covered in a matter of sixty-five pages (Part 1). Obviously, only the barest fundamentals can be touched upon, so that the engineer is still left facing the formidable task of applying these fundamentals to the highly complex problems of vibration, impact, and stability with which he is more likely to be concerned.

Part 2 takes up 109 pages. Here the fundamentals of electricity and magnetism are developed, leading to a discussion of electric circuits, d-c and a-c motors, generators, transmission lines, a brief section on electronics, electromagnetic fields, light, and radiation pressure.

Part 3, comprising 82 pages, introduces the usual thermodynamic concepts, with applications to flow in nozzles, gas turbines, rockets, reciprocating engines, the Carnot cycle, the refrigeration cycle. The principles of heat conduction, convection, and radiation are applied to gas-turbine blades, stirring rod, and steam pipes. A brief section is devoted to dimensional analysis of free convection.

Part 4, in 60 pages, brings in the relations between stresses and strains (with a paragraph on plastic flow and creep), bending of beams, buckling of columns, continuous beams, biaxial stress, shaft torsion, membranes, pure bending of plates, and thermal stresses.

Part 5, in 52 pages, discusses fundamental fluid theory with applications among other things, to emptying a reservoir, water-jet impact, impulse wheel, pipe flow with viscosity, open channel flow, water hammer, pipe friction, sound, and ideal aerodynamics of the airplane wing.

Handbook of Experimental Stress Analysis

HANDBOOK OF EXPERIMENTAL STRESS ANALYSIS. M. Hetényi, Editor-in-Chief. John Wiley and Sons, Inc., New York, N. Y., 1950. Cloth, 6 × 9¼ in., tables, bibliography, index, xii and 1077 pp., 820 illus., $15.

REVIEWED BY A. M. WAHL[14]

IN THE past, the subject of stress analysis has on occasion been interpreted rather narrowly to mean simply the determination of stress distribution in structures or machine parts. At present, however, there is a growing tendency among engineers to regard this subject as a branch of engineering which deals not only with the determination of stresses but also with the evaluation of the effects of such stresses on the operation and service life of the machine or part, with a view toward making a better or more economical design. If this broader definition be accepted, it follows that the stress analyst must not only be familiar with a wide variety of techniques and experimental methods for determining stress but must also be acquainted with methods for appraising the effects of such stresses on the basis of the properties of the materials used. However, the acquiring of such a broad field of knowledge is a difficult task at best, and it is in this connection that the recently forthcoming "Handbook of Experimental Stress Analysis" can be of great help.

This handbook, edited by Prof. M. Hetényi and sponsored by the Society for Experimental Stress Analysis represents the work of some thirty engineers or scientists, each an authority in his own field. It consists of eighteen chapters dealing with various branches of experimental stress analysis together with three appendixes on related subjects. As indicated in the preface, many of these chapters constitute the first systematic treatment of their particular fields.

Perhaps the most important of the available experimental-stress-analysis techniques is the determination of stress by means of direct strain measurement. Such measurements may, however, be carried out by a variety of methods utilizing, for example, mechanical extensometers, wire resistance gages, electric-inductance gages, etc. In the handbook a major amount of space is quite properly devoted to chapters dealing with such methods. For instance, the chapter on mechanical gages by Donnell and Savage treats not only the fundamentals involved in the design of such gages and the sources of errors, but also gives an interesting history of the development of mechanical extensometers as well as descriptions of modern instruments. The important subject of wire resistance (SR-4) gages and associated electrical equipment and circuits is comprehensively treated by Dohrenwend and Mehaffey. On reading this chapter, and also the authoritative treatment of electric-inductance gages by Langer, one is struck by the knowledge of electrical engineering and circuit theory which must be possessed by the experimental stress analyst working in these fields. This is also true of the chapter on electric-capacitance gages by Carter, Forshaw, and Shannon. Optical methods of strain measurement are covered by Maulbetsch and x-ray methods by Barrett.

Measurement of strain is only part of the stress-analysis problem, however, and the determination of stress from the measured strains is often not a simple procedure. This subject is adequately covered by Meier in the section on strain rosettes.

The use of brittle coatings (Stresscoat) has recently become an important tool for the experimental stress analyst; this subject is treated together with the use of brittle models in a chapter by Hetényi. Another section dealing with models is that on structural model analysis by Wilbur and Norris which should be of particular interest to structural engineers.

Since photoelasticity is one of the best-known stress-analysis techniques no handbook of this type would be complete without a comprehensive treatment of this subject; in this respect the present work is not lacking. The subjects of fundamentals and two-dimensional applications of photoelasticity are well covered by Dolan and Murray while the comparatively unexplored field of three-dimensional photoelasticity is treated by Drucker.

With the present trend toward increasing use of shot-peening, nitriding, carburizing and other techniques for improving fatigue durability and service life of machine or structural parts, the subject of effects produced by such processes becomes increasingly important. In the chapter on residual stresses by Horger the measurement, production, and effects of residual stress are treated in a very comprehensive manner. This chapter also contains a

[14] Advisory Engineer, Westinghouse Research Laboratories, East Pittsburgh, Pa. Mem. ASME.

great deal of related metallurgical information of value not only to stress analysts but also to designers and metallurgists.

As an indication of the tendency to broaden the stress-analysis field, the presence in this volume of an extensive treatment of the subject of vibration or motion measurement by Ormondroyd, Allnutt, Mintz, and Specht may be cited. This chapter deals largely with vibration instruments and measurements, including displacements produced by shock as well as steady-state motions. Although the stress analyst is not usually concerned with vibration problems as such, yet in many cases vibration tests on models or on machines in the field may enable him to improve his methods of calculation or his knowledge of operating conditions. For example, many large structures (aircraft frames, for example) which are subject to periodic forces are of such complicated shape that an exact calculation of natural frequencies or a mathematical determination of natural modes of vibration is practically impossible; yet such frequencies and modes must be known if a rational design is to be had. Vibration tests on such structures can thus become an important aid for the stress analyst. Again in many cases operating loads are not known or cannot be calculated with any degree of accuracy; in such cases vibration or motion measurements in the field may yield the necessary information.

A feature of this handbook is the comprehensive treatment of analogies by Mindlin and Salvadori. The usefulness of such a discussion is apparent when it is considered that in many practical structures, both theoretical analysis and direct strain measurements are either impractical or impossible in the present state of our knowledge. In certain cases, however, measurements or tests made on an analog of the actual system may be perfectly feasible. For example, the determination of thermal stresses in structural or machine parts by direct measurement of strains under operating conditions is often difficult or impossible; however, by using the analogy between thermal and dislocation stresses the problem, in certain cases, may be solved by photoelastic measurements of dislocation stresses on a model.

Another important aid which may be available to the stress analyst comprises the information obtainable from service experience. This subject is authoritatively covered in the chapter on interpretation of service fractures by Peterson. As pointed out by this author, a study of actual service fractures can often do much toward guiding an experimental stress-analysis program by giving the designer information concerning actual operating loads and conditions, which information may be very difficult to obtain otherwise. It is at times surprising to an engineer or designer to find that, by examining a fatigue fracture of a shaft in bending, for example, he can often predict approximately the percentage reduction in stress required for satisfactory operation.

The subject of working stress (treated by Soderberg) and that of mechanical properties of materials (MacGregor) may appear to some to be out of place in a handbook of this type. However, the first subject is important from the standpoint of rationalizing design procedure and improving design methods while the second is required in evaluating the effects of stresses determined by stress-analysis techniques. Thus from a broad viewpoint, the inclusion of these subjects is logical.

Three appendixes are also provided as follows: 1, Fundamentals of the Theory of Elasticity by Timoshenko; 2, Dimensional Analysis by Goodier; and 3, Precision of Measurements by Hetényi. In the first of these, enough elasticity theory is given so that the experimental stress analyst will have a better understanding of the fundamentals involved in stress determination by strain measurements or other techniques. The second appendix is of particular interest where models are used in solving stress problems while the third is of fundamental importance where experimental techniques are employed.

Other chapters include: methods of crack detection by Lipson and testing machines by Marin.

One of the most useful features of this handbook, in the writer's opinion, comprises the extensive bibliographies provided at the end of each chapter. A novel feature of these is the listing, with most of the references, of a sentence or two describing the contents. This enables the reader to get a much better idea of the reference than that given by a mere listing of the title.

It should be noted that this handbook deals largely with experimental stress-analysis methods for cases involving *elastic* strains or stresses. Unfortunately, with the present trend toward higher temperatures in many fields, i.e., gas and steam turbines, jet engines, refinery equipment, etc., where creep and relaxation effects occur, in many cases such methods based on elastic conditions are no longer sufficient. One could wish that the subject of stress analysis involving plastic flow, creep, or relaxation effects particularly at elevated temperatures could be developed as comprehensively as is the elastic case exemplified by the present handbook.

In conclusion, it is the reviewer's opinion that ownership or ready availability of this book is a must not only for stress analysts but also for designers and engineers concerned with the application of stress analysis procedures. It may also be useful to workers in related fields, e.g., metallurgists, vibration experts, testing engineers, and others.

Engineering Hydraulics

ENGINEERING HYDRAULICS.[15] Proceedings of the Fourth Hydraulics Conference, Iowa Institute of Hydraulic Research, June 12–15, 1949. Edited by Hunter Rouse. John Wiley and Sons, Inc., New York, N. Y., 1950. Cloth, 6 × 9 in., figs., tables, references, appendix, indexes, xiii and 1039 pp., illustrated, $15.

REVIEWED BY ANDRE L. JORISSEN[16]

THIS book contains a comprehensive review of principles and applications of mechanics of incompressible fluids as developed in the last fifty years. It constitutes the Proceedings of the Fourth Hydraulics Conference held at the Iowa Institute of Hydraulic Research in June, 1949, and is edited by Dr. Hunter Rouse, director of the Institute.

In the first chapter Dr. Rouse reviews the fundamental principles of flow. Much of this material was already available in his "Fluid Mechanics for Hydraulic Engineers," but this condensed presentation serves as an introduction to the volume, stressing definitions, properties, methods of analysis, and fundamental equations.

The second chapter, prepared by the late G. E. Warnock of the Bureau of Reclamation, perfects this purpose by discussing basic laws of hydraulic similitude and their application to model studies. Practical information is made available and several examples are given such as flow in closed conduits, including cavitation, flow in open channels, tidal and wave models, and hydraulic machinery. In chapter 3, Prof. J. W. Howe of the State University of Iowa, presents various methods of measurement: Measurement of fundamental quantities (distances, elevations, times, forces), of derived quantities (pressures, velocities), and discharge measurements in closed conduits and in open channels.

Hydrology is the subject of chapter 4, written by G. R. Williams of Knappen Tippetts Abbetts Engineering Company. Emphasis is laid on the principles of this science but numerous applications

[15] Reprinted from *Applied Mechanics Reviews*, vol. 4, March, 1951, p. 170.

[16] Professor, Department of Civil Engineering, The Pennsylvania State College, State College, Pa. Mem. ASME.

are given. Meteorological principles, climatology, runoff, ground water, storm rainfall, storm runoff, relation between storm rainfall and storm runoff, theory of surface runoff for drainage design are the topics studied in the various paragraphs.

In chapter 5, flow of ground water, Prof. C. E. Jacob of the University of Utah, after deriving the fundamental equations based on a generalization of Darcy's law, studies their application to the problem of confined flows, both steady and unsteady. Numerous problems on well systems are treated.

Steady flow in pipes and conduits is analyzed in chapter 6 by Prof. V. L. Streeter of the Illinois Institute of Technology. The modern concepts on velocity distribution and energy loss are reviewed. Information is given on surface and form resistance in various cases and compound and complex systems of pipe lines are studied, including a solution of pipe-network problems by the Hardy Cross method.

Unsteady flow problems in closed conduits are treated in chapter 7. Prof. J. S. MacNown, of the State University of Iowa, discusses water hammer in simple and complex conduits and analyzes the function of surge tanks. Effect of pipe resistance is taken into consideration and attention is given to the hydraulic design and to the consequences of water hammer in pumping systems.

Chapter 8, written by Prof. A. T. Ippen of the Massachusetts Institute of Technology, contains considerations on the design and operation of transitions and controls for open-channel flow in the subcritical and supercritical flow stages. This is probably one of the newest and lesser known aspects of engineering hydraulics. This chaper also contains information on stilling basins.

In chapter 9, Prof. C. J. Posey of the State University of Iowa, reviews the problem of gradually varied flow in open channels, giving the various methods used to compute and plot backwater curves both in uniform and nonuniform channels. This chapter also includes a study of the hydraulic jump.

The complex problem of flood routing is analyzed mathematically in chapter 10 by B. R. Gilcrest of the Ohio River Division, Corps of Engineers, U. S. Army. This is followed by studies of routing of floods through reservoirs and through open channels.

G. H. Keulegan of the National Hydraulic Laboratory, Bureau of Standards, is the author of chapter 11 on wave motion. Shallow-water waves, deep-water waves, oscillatory waves in shallow water, transformation of waves, open-channel surges, and internal waves are the various topics included in this chapter.

Chapter 12, prepared by Mr. C. B. Brown of the Soil Conservation Service, U. S. Department of Agriculture, deals with the mechanics of sediment transportation. After a review of sediment properties, it is indicated how the information obtained is used to design canals and desilting works, as well as in the stabilization and improvement of rivers. Other problems include sedimentation in reservoirs and coastal-sediment problems.

The last chapter, on hydraulic machinery, was prepared by Prof. James W. Daily of the Massachusetts Institute of Technology. The theory of hydraulic machinery, based on the methods of modern fluid mechanics, is explained with application to centrifugal and axial-flow pumps, propulsion machinery, hydraulic turbines, hydrodynamic transmissions, and positive-displacement machinery.

The appendix includes: (*a*) A list of symbols which will prove to be very useful in uniformising notations, (*b*) dimensional analysis considerations, and (*c*) information on the properties of common fluids.

This volume, which is the only one of its kind in the English language, has been prepared with extreme care. Each chapter has been written by one of the foremost specialists in the field. Rather than to present new information, a successful attempt has been made to prepare a comprehensive synopsis of the methods involved and to discuss typical applications.

In this respect, "Engineering Hydraulics" will be of invaluable assistance. Although not a textbook, it will undoubtedly be used as a reference in many graduate courses. Although not a handbook, it contains a wealth of information for the practicing engineer. Primarily, however, it constitutes a true encyclopedia of modern hydraulics.

Photoelasticity

PHOTOELASTICITY: Principles and methods. By H. T. Jessop and F. C. Harris. Dover Publications, Inc., New York, N. Y., 1950. Cloth, $6^1/_2 \times 9^1/_4$ in., 164 illus., 5 tables, viii and 184 pp., $3.75.

REVIEWED by W. M. MURRAY[17]

THIS book is a refreshing and readable small volume on photoelasticity. The authors have made no attempt (as they say) to go deeply into the underlying theory but they have presented enough of it to enable a novice to obtain a good grasp of the subject. An interesting feature of the book is the separation of certain physical explanations from detailed mathematical derivations. This arrangement has made the volume easy to read. For those who need the mathematical derivations the appendixes will provide the necessary information.

The book contains ten chapters dealing with stresses, strains, and their relations, elementary optics, polarization and double refraction, the theory of photoelasticity and interpretation of the observations which one makes with it. A short discussion of the "frozen-stress" method for three-dimensional problems has been included, and also a chapter dealing with the details of the optical bench and loading devices. Two chapters have been devoted to photoelastic material, laboratory procedures, and numerical examples. In addition there are appendixes dealing with the mathematical relationships and proofs corresponding to subjects taken up earlier in the book.

This book should be a welcome addition to any library dealing with experimental stress analysis. Its price is within the range of college textbooks and the manner in which the material has been arranged should make it attractive to students taking a first course in photoelasticity.

Introduction to Servomechanisms

INTRODUCTION TO SERVOMECHANISMS. By A. Porter. John Wiley & Sons, Inc., New York, N. Y., 1951. Methuen's Monographs on Physical Subjects. Cloth, $4 \times 6^1/_2$ in., 70 diagrams, references, bibliography, index, vi and 154 pp., $1.75.

REVIEWED BY JOHN A. HRONES[18]

THIS book is another one in a series of Methuen's Monographs which in terms of the publisher is "Intended to supply readers of average scientific attainment with a compact statement of the modern position in each subject." In 154 pages the author covers the following material listed below by chapter title: Closed-Sequence Control Systems, Basic Equations of Linear Servo Systems, Transient and Steady-State Behavior, Harmonic Response Diagrams, Lag Correction and Stabilization, and Notes on Some Nonlinear Problems.

This material is presented briefly but competently. A minimum of mathematics is used being presented essentially from a

[17] Associate Professor of Mechanical Engineering, Massachusetts Institute of Technology, Cambridge, Mass. Mem. ASME.

[18] Professor of Mechanical Engineering, Massachusetts Institute of Technology, Cambridge, Mass. Mem. ASME.

"classical" viewpoint without resorting to the Laplace transformation method.

There are included some 70 diagrams to graphically present the material covered in the text. The differential analyzer is often used as an example of applications of the theory presented. There is also an ample bibliography somewhat heavy on the English side. Many of the components referred to are the English equivalents of American products.

The book is worth while and has an extremely broad coverage considering its size. It is recommended for the library of all having interest in this field.

Hydrodynamics

HYDRODYNAMICS—A Study in Logic, Fact, and Similitude. By Garrett Birkhoff. Princeton University Press, Princeton, N. J., 1950. Cloth, 5½ × 8½ in., xiii and 186 pp., illus., $3.50.

REVIEWED BY KENNETH S. M. DAVIDSON[18]

THIS book is frankly philosophic. In effect it is a reappraisal of the old problem of narrowing the gap between theory and experiment in the field of hydrodynamics, where important difficulties have long been recognized. It is less a textbook than a study for the mature mind. It needs to be read carefully, and it presupposes a comprehensive background. But the author has a pleasant way of taking the reader into his confidence, and the book is unusual and interesting.

The general point of view is taken that a principal defect of present-day theoretical hydrodynamics is a lack of mathematical rigor in carrying through the consequences of well-defined physical assumptions. The first chapter introduces this concept by discussing a number of paradoxes, in which theoretical conclusions are at variance with experiment. The rest of the book considers various theoretical advances and their relation to certain mathematical methods, notably dimensional analysis, inspectional analysis, and group theory.

Most of the paradoxes are convincing. A few are less so, and one or two seem rather forced. Moreover, it is not always clear whether the theoretical difficulties lie with the physics or the mathematics. Long association with the individual problems is needed to decide this distinction, as the demonstrations are for the most part quite condensed.

The mathematical treatment is ingenious and stimulating. Broadly, it is argued that the purely mathematical difficulties of solving rigorous analytical expressions such as, for instance, the Navier-Stokes equations, have too often led to abandoning the analytical approach in favor of a simple dimensional analysis, with a consequent tendency to rely blindly on the latter. Inspectional analysis, whereby all analytical expressions that have a bearing on a physical situation are examined dimensionally, is then put forward as a means of utilizing such analytical expressions to test the dimensional analysis and to insure that pertinent factors have not been lost. This step is important in assessing the validity of model testing procedures. Finally group theory, of which inspectional analysis is an offshoot, is considered more generally, and its use developed as a means of testing the validity of mathematical theories of hydrodynamics in some instances, when it is impossible to integrate the partial differential equations. Interesting examples are given of the latter process, and its generality in solving the partial differential equations of mathematical physics through the search for symmetric solutions is clearly described.

The main thesis of the book is controversial: that physical reasoning must be viewed with suspicion when the mathematical analysis is complicated. This thesis is not likely to be universally accepted, at least for some time to come. It is nonetheless an intriguing thesis, and one that is bound to have an increasing influence on our understanding of the relations of theory to experiment in the field of hydrodynamics.

There is an excellent bibliography, with separate lists of references for collateral study on each chapter. The book deserves serious attention.

[18] Director, Experimental Towing Tank, Stevens Institute of Technology, Hoboken, N. J. Mem. ASME.

Thermodynamics

AN INTRODUCTION TO THERMODYNAMICS: The Kinetic Theory of Gases and Statistical Mechanics. By Francis Weston Sears. Addison-Wesley Press, Inc., Cambridge, Mass. (Principles of Physics Series), 1950. Cloth, 6 × 9 in., illus., x and 348 pp., $6.

REVIEWED BY NEWMAN A. HALL[19]

THE field of thermodynamics is not only difficult to define in view of many tacit associations but any description is strongly affected by the viewpoint of the writer. There are found in the current literature three fairly sharply distinguishable patterns. These correspond to and aim to meet the needs of the physicist, chemist, and engineer. It is doubtful whether a unified treatment is possible or even desirable. Many texts have been written from the engineering viewpoint and a number from that of chemistry. However, treatments devoted specifically to thermodynamics by physicists have been few, though most of these have been of excellent caliber.

This tradition of quality and physical rigor in thermodynamics has been admirably maintained by F. W. Sears in this latest edition. While ostensibly prepared as a basic course for electrical engineers, this book is suitable for the broadest range of application. It will be found useful not only to those whose interest is exclusively in physics but also to any who believe that the thermodynamic training of engineers should be firmly grounded in physics.

The first nine chapters treat the fundamentals of thermodynamics as contained in the equation of state, the first and second law, and associated energy functions. Equations of state of any variety are presented only briefly. However, the thermodynamics of phase relations is developed in extensive detail. In this respect the emphasis is on the fundamental thermodynamic analysis rather than on application to specific substances or processes. Thus the Maxwell equations and associated partial differential relations are developed and applied not only to systems involving mechanical but also electrical and magnetic work. Entropy is introduced conventionally by reference to the Carnot cycle and the Clausius inequality.

Chapter 10 referring to engineering applications of thermodynamics is devoted almost exclusively to vapor cycles. In no place in the text are the Otto, Diesel, or Brayton cycles mentioned.

The last eight chapters are specifically concerned with the microscopic thermodynamic aspect of substances. These involve primarily the essentials of kinetic theory and statistical mechanics as applied to thermodynamic systems. The treatment would be advanced for the average engineering undergraduate, but represents a compact and coherent introduction for the physicist or graduate engineer.

For the theoretical physicist, this material is on an elementary level; for the engineer, it presents clearly the basic tools required for a physicial interpretation of thermodynamic phenomena. In general, it represents a major addition to the literature in the field.

[19] Professor of Mechanical Engineering, Institute of Technology, University of Minnesota, Minneapolis, Minn. Mem. ASME.